THE UNIVERSITY
of EDINBURGH

How is an ant navigation algorithm affected by visual parameters and ego-motion?

Paul Björn Ardin

Doctor of Philosophy
Institute of Perception, Action and Behaviour
School of Informatics
University of Edinburgh
2017

Abstract

Ants typically use path integration and vision for navigation when the environment precludes the use of pheromones for trails. Recent simulations have been able to accurately mimic the retinotopic navigation behaviour of these ants using simple models of movement and memory of unprocessed visual images. Naturally it is interesting to test these navigation algorithms in more realistic circumstances, particularly with actual route data from the ant, in an accurate facsimile of the ant world and with visual input that draws on the characteristics of the animal. While increasing the complexity of the visual processing to include skyline extraction, inhomogeneous sampling and motion processing was conjectured to improve the performance of the simulations, the reverse appears to be the case. Examining closely the assumptions about motion, analysis of ants in the field shows that they experience considerable displacement of the head which when applied to the simulation leads to significant degradation in performance. The family of simulations rely upon continuous visual monitoring of the scene to determine heading and it was decided to test whether the animals were similarly dependent on this input. A field study demonstrated that ants with only visual navigation cues can return the nest when largely facing away from the direction of travel (moving backwards) and so it appears that ant visual navigation is not a process of continuous retinotopic image matching. We conclude ants may use vision to determine an initial heading by image matching and then continue to follow this direction using their celestial compass, or they may use a rotationally invariant form of the visual world for continuous course correction.

Acknowledgements

Many people have helped me along the path to this thesis, many more than I can recognise in this acknowledgement. Without doubt the greatest thanks are reserved for Barbara Webb who took on an interesting student and did her utmost to make him an effective researcher. Without her guidance and support this work would not have been possible.

Professors Holger Krapp, Eric Warrant, Xim Cerda and Jochen Zeil all deserve special recognition. Holger helped set me on the right trajectory in the early stages of my work giving me the confidence to push ahead. Eric kindly offered the facilities of his lab as well as his enduring enthusiasm. Xim's hospitality to the field researchers from Edinburgh was extraordinary, stretching remarkably to the use of his Samurai Jeep. Jochen was the perfect academic host giving me the opportunity to develop as an independent scientist and make my own critical discoveries.

Many researchers at earlier stages of their careers aided my work but particular thanks are due to my co-authors Kostas Lagogiannis, Antoine Wystrach and Fei Peng without whom my own research would have been so much less rich. Beyond their scientific insights they are all good people who deserve success in their own fields. But my most heartfelt thanks are to Michael Mangan who gave me resources, direction and support without hesitation and always with good humour.

My fellow students and office mates have made this an exciting journey and I particularly need to thank Ksenia Kuzenotsova, Wioleta Kijewska, Marzena Bihun, Nathalie Dupuy and Katharina Heil for making the whole experience so much fun.

And to Elena who has kept my eyes focused on the end of this adventure and the start of the next.

Declaration

I declare that this thesis was composed by myself, that the work contained herein is my own except where explicitly stated otherwise in the text, and that this work has not been submitted for any other degree or professional qualification except as specified.

(*Paul Björn Ardin*)

The papers used as the basis for chapters 3 and 4 (“How variation in head pitch could affect image matching algorithms for ant navigation” and “Ant Homing Ability is not Diminished when Travelling Backwards”) and as appendix A (“Using and Insect Mushroom Body Circuit to Encode Route Memory in Complex Natural Environments”) are reproduced in this thesis with the permission of the authors.

My contribution to “How variation in head pitch could affect image matching algorithms for ant navigation” was the formation of the original experimental question, design of the data capture, analysis of the field research, conversion of the data into a simulation of head pitch, modification of the visual model to allow for roll and pitch, implementation of a model of navigation including the head pitch simulation, authorship of sections on Head Pitch Analysis, The Simulated Ant World, Effect on Simulated Navigation in the Ant’s World, and The Effect of Error on Route Following, production of figures 1 and 4 and elements of figures 2 and 3, commenting on and editing of the paper and submitting the paper.

My contribution to “Ant Homing Ability is not Diminished when Travelling Backwards” was the formulation of the original experimental question, piloting the original design in Sevilla, development of the experimental paradigm in Canberra, all of analysis with the exception of heading correction after forward look (figure 3(D)), authorship of sections on Materials and Methods and Results, contribution to all other sections of the paper, commenting on and editing of the paper and submission of the paper.

Table of Contents

1 Introduction **1**

1.1 Overview of ant navigation 2

1.2 Ant navigation without visual learning 2

1.2.1 Systematic search 3

1.2.2 Path integration 3

1.2.3 Other navigation senses 5

1.3 Visual ant navigation 5

1.3.1 The zero vector ant 6

1.3.2 Visual navigation and environmental geometry 6

1.3.3 Interaction of path integration and visual navigation 7

1.3.4 The nature of the input into visual navigation 9

1.4 Visual navigation models 10

1.4.1 Visual homing 10

1.4.2 Route following with waypoints 11

1.4.3 Route following using continuous image matching 12

1.4.4 Limitations of current approaches 15

1.5 The visual world of the moving ant 15

1.5.1 Overview 15

1.5.2 The sampling properties of the apposition compound eye . . . 16

1.5.3 The desert ant eye 18

1.5.4 Visual processing beyond the eye 19

1.6 Ant motion 21

1.7 Summary 22

2 Low level visual processing and ant navigation **25**

2.1 Introduction 25

2.1.1 Resolution and visual sampling 27

2.1.2 Colour sensitivity 28
2.1.3 Motion processing 29
2.1.4 Summary 30
2.2 Materials and Methods 30
2.2.1 Simulated world 30
2.2.2 Navigation algorithm 32
2.2.3 Modelling the visual input 34
2.3 Results 41
2.3.1 Random results 41
2.3.2 Route errors and segment length 41
2.3.3 Resolution and image separation 42
2.3.4 Skyline extraction 45
2.3.5 Centre-weighting 47
2.3.6 Motion processing with an EMD 48
2.3.7 Input correlations 52
2.3.8 Relevance of error locations 53
2.3.9 Variable training step sizes 57
2.3.10 Specific error states in real ant routes 58
2.4 Discussion 64

3 How variation in head pitch could affect image matching algorithms for ant navigation 66
3.1 Introduction to the paper 66

4 Ant Homing Ability is not diminished when travelling backwards 82
4.1 Introduction to the paper 82
4.2 Additional analysis 92
4.2.1 Using rotational and translational IDF to navigate in a symmetrical environment 92
4.2.2 Do ants use polarised light patterns to stabilise heading directions? 96

5 Discussion 100
5.1 Key Contributions 100
5.2 Future Work 103
5.2.1 Visual processing in ant navigation simulations 103

5.2.2 Continuous or vector-based visual navigation 104
5.2.3 Integrating visual navigation and path integration 106
5.2.4 Analysis with more sophisticated motion metrics 107
5.3 Concluding Remarks 109

A Glossary **110**
A.1 Glossary 110

B Using an Insect Mushroom Body Circuit to Encode Route Memory in Complex Natural Environments **112**
B.1 Introduction to the paper 112

Bibliography **135**

Chapter 1

Introduction

How the interplay of the sensory world and the environment produces the of an animal can be a productive means not only to understand biology but also to develop artificial intelligence (Dennett, 1978; Braitenberg, 1986; Webb, 2002; Gibson, 2014). Hymenoptera display some of the most sophisticated behaviour of insects. In particular central place foraging in bees, wasps and ants has been the focus of extensive research, perhaps in part motivated by the inevitable parallels that can be drawn with the navigational abilities of vertebrates (Menzel, 2012). In the case of the visual navigation of desert ants, sufficient behavioural data has been collected to allow models to be constructed which can in turn produce ant-like behaviour (Lambrinos et al., 2000; Baddeley et al., 2011). Our understanding has been most recently advanced by combining these algorithms with a more sophisticated world simulation and comparing the results with an accurate model of a part of the ant brain implicated in visual learning (Ardin et al., 2016a). Closing the loop between the observation of the animal, the neural structure and reproduction in silico is exciting, and drives us towards adding greater realism to allow refinement of our understanding and to direct further research. Taking Gibson's stance, this thesis explores the interaction of the desert ant's perceptual world and ego motion using these new models.

Self evidently context is important and the following sections attempt to rehearse and draw together the various relevant research strands. The nature of desert ant navigation, particularly using vision, is described, and the models which have attempted to replicate this behaviour are then explored. An overview is given of insect vision with detailed descriptions of the optical properties of compound eyes as they relate to desert ants. The later stages of processing are discussed, in particular motion detection, leading to a summary of what is known about the small scale motion of the ant.

1.1 Overview of ant navigation

Desert ants have become a model system for the exploration of navigation in central place foraging animals. Their navigation ability is not unique but the two dimensional constraint of the environment allows closer examination of some of the behaviour than is possible in the ant's flying relatives. Compared to its body size, large distances are covered at high speed by the desert ant, following circuitous paths in the search for food items scattered in their home environment. The behaviour is interesting due to a number of key features. The foraging behaviour normally occurs when ground surface temperatures are reaching a peak during the late morning and early afternoon, which reduces the risk of predation while increasing the chance of finding undiscovered prey overcome by heat (e.g. Cerdá et al. (1998)), but this strategy brings other consequences, critically for this research the surface temperature precludes the use of the pheromone trails widely used by other ant species (e.g. Van Oudenhove et al. (2012)). A further consequence is that very efficient return paths are required to minimise the exposure to the extreme heat. Thus the inward path to the nest of these animals is characteristically very direct with seemingly no relationship to the complexity of the outward route. The nest entrance itself is a small and inconspicuous hole offering no obvious visual cues which could be used as a beacon. The wider visual environment for desert ant species varies from flat and featureless such as the salt pan habitat of *Cataglyphis bicolor*, to complex with visual obstructions as in the case of the scrubland of *Melophorus bagoti*.

Retinotopic images have long been suspected as playing a key role in allowing both ants and the other hymenoptera to reach goal locations (Cartwright and Collett, 1982), but other senses are also at work.

1.2 Ant navigation without visual learning

Before exploring retinotopic navigation it is worth reviewing the various other mechanisms of desert ant navigation to understand the complexity of the behaviour and what may be confounding factors. Some of the systems are known to interact and at various stages in this thesis we will need to consider whether these interactions are critical to our understanding of visual navigation.

1.2.1 Systematic search

In a location close to the nest entrance desert ants will perform what is commonly known as a systematic search. This behaviour consists of a sequence of growing loops which can be formally described as following a spiral pattern with periodic return to the expected goal location (Müller and Wehner, 1994). This is underpinned by the path integration system described next, demonstrating the key role this sense plays in many aspects of the navigational toolkit. By itself systematic search does not allow for efficient return to the nest and it is combined with a suite of other mechanisms which allow long routes to be followed.

1.2.2 Path integration

Path integration is one of the most well-established features of desert ant navigation. As it searches on the outward path for a food item, the animal records the distance it travels at every orientation. These variables are continually summed so that when the food is located the reverse vector provides the straightline location of the nest for the inward journey. It is a commonly applied navigation strategy for both animals and robots but without accurate odometry and critically an external compass sense, it will rapidly accumulate error unless correction is applied using other sensory information (Benhamou et al., 1990; Cheung et al., 2007). The astonishing feature of the desert ant is that it uses path integration over very long complex outward paths and then returns with very high accuracy, an observation which has excited considerable research into the processes at work.

The ant must sense distance and orientation to create outward and inward vectors and of these senses determining direction appears the least contentious. The ant visual system typically possesses at least three relevant adaptations: 3 low resolution eyes on the dorsal plane of the head (the ocelli) which detect polarised light (Mote and Wehner, 1980), photoreceptors in the dorsal visual field of the compound eyes have a higher density of ultraviolet receptors allowing for greater sensitivity to spectral gradients in the sky (Labhart, 1986) and specialisations of ommatidia in the dorsal rim area (DRA) which detect polarisation across a wide range of orientations (Labhart, 1986). While the role of the latter two adaptations in determining direction independent has not yet been conclusively proven, the role of the ocelli has been demonstrated (Fent and Wehner, 1985; Schwarz et al., 2011a). It is speculated that either together or independently these adaptations provide the ant with a direction sense which is not based on

the immediate environment, widely described as the sky or celestial compass (Wehner et al., 2014). Even limited access to the sky can allow a heading to be determined (Fent and Wehner, 1985) and receptor tuning to detect polarisation in UV wavelengths may overcome the effects of cloud cover (Barta and Horváth, 2004) neverthless other environmental cues may also be used to provide heading cues (e.g. wind direction - Müller and Wehner (2007)).

The distance travelled can be measured by counting the steps the animal takes provided that the step length has a reasonably narrow statistical distribution. Experimental manipulation has shown that increasing or decreasing the leg length, and hence the stride, leads to predictable changes in the distance the animal covers before searching for the nest entrance (Wittlinger et al., 2006). However there is also evidence that the optic flow in the ventral visual field can be used to estimate distance (Ronacher and Wehner, 1995) and self-induced optic flow in honeybees has been shown to be used both while walking (Schöne, 1996) and flying (Srinivasan and Gregory, 1992). The advantage of optic flow is that it is derived from the environment and is therefore more robust to noise than a proprioceptive sense, but how the two modalities are combined is still a matter for conjecture (Wittlinger and Wolf, 2013). The spread of the systematic search for the nest entrance increases with the length of the inward route (Merkle et al., 2006; Schultheiss and Cheng, 2011) which can be taken as evidence of compensation by the animal for the accumulation of errors.

Path integration is impressive in the ant, but it has limitations. If the view of the sky is occluded on the outward route, the odometer is switched off leading to systematically shorter searching than the actual distance travelled (Ronacher et al., 2006). Displacement of the ant off the home route by wind, or by a zealous experimenter before the home vector has run down, will cause the animal to continue on this vector until the predicted distance is exhausted (Wehner et al., 1996). However the reliance on the home vector is species dependent, with *M. bagoti* much more willing to abandon it compared to *C. fortis* (Bühlmann et al., 2011). One explanation for this phenomena is that the more visually rich environment of *M. bagoti* allows for the use of more cues than the barren world of *C. fortis*. Equally, while the path integrator runs continuously and is only reset on entry to the nest (e.g. Knaden and Wehner (2006)), the structure of the environment of *M. bagoti* provides more obstructions causing a more tortuous inward path. These additional deviations may increase the error in the path integration requiring *M. bagoti* to adopt a different model of the reliability of both visual and proprioceptive cues.

1.2.3 Other navigation senses

In order to mitigate these problems with path integration there is evidence of the use of various navigation cues although due to the different physical scales at which they operate they probably serve different purposes in the overall animal behaviour. Surface vibration, such as that produced by the underground activity of a colony, can identify the nest entrance (Buehlmann et al., 2012) but it is improbable that this is functional except over short distances due competing signals from other nests. The authors also demonstrate that magnetic fields can help identify the nest entrance but note that it is unlikely that enough unique magnetic cues exist in the natural environment to work effectively as landmarks. Despite the lack of pheromone following, desert ants make extensive use of odour to locate both food sources (Wolf and Wehner, 2000) or to learn the location of the nest entrance (Steck et al., 2010). Olfaction can override path integration on the outward route to a feeder site to allow the selection of closer food items on the previously learnt path (Buehlmann et al., 2013) but on the inward route path integration gates the use of the nest's odour plume to ensure that the ant does not attempt to enter another colony (Buehlmann et al., 2015). It is possible that other sensory cues, such as the texture of substrate are also used by the animal (Seidl and Wehner, 2006), altogether providing a rich, multi-modal dataset which can reduce uncertainty over location. It is also worth noting that desert ants also appear to be able to recruit conspecifics to follow them to food locations although the exact mechanisms are unknown (Schultheiss and Nooten, 2013). However while this confounds observations about the formation of outward routes, it is much less relevant to the study of inward routes which form the basis of this research.

1.3 Visual ant navigation

Despite the sophistication of these senses the ant can and does make extensive use of vision to find its way around the environment. In the following sections we will be introduced to a fundamental experimental paradigm of the field in the zero vector ant, consider the effect of environmental geometry on visual navigation, explore how path integration and vision may interact before examining what the visual input for way finding might be.

1.3.1 The zero vector ant

Once the food is found the ant will return to the nest, automatically switching to the path integration home vector it has stored. An in-bound desert ant returning from a foraging trip approaching the nest entrance has exhausted this vector and if it is relocated back on its route can no longer rely upon the integrated proprioceptive and orientation data. Under experimental conditions ants at the point of leaving the feeder can be described as full vector while those at the nest entrance are zero vector. A zero vector ant relocated onto any part of its route will reacquire this path and return to the nest, following closely the original trajectory (Wehner et al., 1996; Kohler and Wehner, 2005; Bühlmann et al., 2011; Mangan, 2011). The distances over which this is conducted are the same as for path integration, for example 30 metres or more for *Cataglyphis* (Wehner et al., 1996). This occurs in both featureless and cluttered environment species and the observation that it is the original path that is followed, rather than the heading to the nest, confirms that the ant is not using one of the many possible beacon senses. Experimental manipulation shows that the desert ant has the ability to learn visual sequences in an artificial maze, the laboratory analog of a visually occluded world (Chameron et al., 1998).

1.3.2 Visual navigation and environmental geometry

Ants which are taken to a new site will perform a systematic search for the nest entrance, but if they have been previously trained with striking visual artificial landmarks they will search in accordance with these features (Wehner et al., 1996). A paradigmatic result is that maintaining the position of these landmarks but altering their size reliably causes the systematic search to be distorted in accordance with the retinal projection of the feature (Wehner et al., 1996). In more natural circumstances, ants which are displaced to another site which shows the same broad visual characteristics as the home nest location, will search in the area that the nest should be (Wehner et al., 1996). When displacement is several metres to the side of the learnt route in a cluttered environment, zero vector ants will initiate what appears to be a systematic search, but once the learnt path is encountered have no difficult in returning to the nest (Collett et al., 1992; Kohler and Wehner, 2005).

Further manipulation has shown that it is the dorsal-lateral field which is particularly important in detecting visual landmarks (Wehner et al., 1996) leading to investigation of role that the panorama may play. An approximation of the panorama

replicating scene heights at every 15 degrees around the nest will reliably cause ants to search in the direction indicated by the artificial skyline (Graham and Cheng, 2009a) but also a 17 degree vertical field of view is sufficient to induce accurate visual guidance (Graham and Cheng, 2009b). However experimentation and examination of the optical properties of the eye have shown that it is not the case that large scale visual features are exclusively important for navigation (Seidl and Wehner, 2006; Wystrach et al., 2011b). Consistent with observations in the field (Wystrach et al., 2011a) it has been shown that when the panorama is not available local features become important through different combinations of near, intermediate and far objects in a simulated world (Dewar et al., 2014).

Specific landmarks appear to trigger particular motor actions (Judd and Collett, 1998; Collett et al., 1998; Legge et al., 2010); the ant's path follows a "local vector" when faced with a familiar view, but the complexity required to describe this behaviour formally (Smith et al., 2007) means that it remains controversial (Wystrach et al., 2013a).

The visual geometry of the environment also affects the accuracy with which the nest entrance is relocated (Wehner and Müller, 2010) and search times are very substantially reduced by scenes where the effect of translational optic flow is maximised. Ants that approach the feeder at an acute angle to two landmarks create significantly greater change in the angular position and angular width than an orthogonal approach either through or towards the same landmarks, maximising the change in the image.

The ability to use visual landmarks has inevitably drawn parallels with the cognitive map hypothesis in vertebrates where it is assumed that the relative spatial location of landmarks is stored in an abstract structure allowing the ability to generate novel routes and reasoning about the relationships between locations. There is evidence that honeybees can undertake short-cutting (for a review see Menzel (2012)) and therefore have abstracted the spatial relationship between landmarks. However no such behaviour has yet been demonstrated in ants.

1.3.3 Interaction of path integration and visual navigation

While ants may not build maps of the environment there are interactions between their visual world and home vector created by path integration. Ants construct their visual guidance using path integration (Müller and Wehner, 2010). When leaving the nest on a learning walk *Ocymyrmex rubistor* align multiple times directly with the visually

concealed entrance, a feat which is only possible using path integration. The path integration system was thought to dominate visual navigation based on the results from *Cataglyphis* (Wehner et al., 1996), but inter-species research has shown that the relationship is more complex than thought (Bühlmann et al., 2011). By subjecting *C. fortis* and *M. bagoti* to identical training and testing conditions the differing thresholds for interaction between the systems has been uncovered. As might be predicted by its visual environment *M. bagoti* is less likely to rely upon path integration and will more readily abandon its home vector if it encounters a visual landmark which it has been trained to associate with the nest entrance. In contrast *C. fortis* adheres closely to the home vector and is more reluctant to accept visual landmarks typically activating visual navigation only when the home vector is almost exhausted. While path integration is essential to create the route, visual navigation and path integration are used flexibly with evidence that visual memories are used to provide more accurate targeting or to fully replace path integration when compass information is not available (Collett, 2012). Idiosyncratic routes for individual *M. bagoti* and *C. velox* foragers are clear evidence that visual cues dominates path integration once a route is learnt (Kohler and Wehner, 2005; Mangan and Webb, 2012).

What is the architecture of this system? Experimentation comparing zero and full vector ants has suggested that there is a combination of global and local path integration vectors active which are switched when the animal uses either visual landmarks or the celestial compass for guidance (Collett et al., 1998). Full vector ants trained along a corridor will follow an untrained diagonal route to the nest if the corridor is shortened, but if zero vector ants are released in the same corridor they will initially follow a vector predicted by a visual memory. Some research suggests visual memories may be tagged against the celestial compass, but will also be used preferentially to direct search patterns when the cues are placed in conflict (Åkesson and Wehner, 2002).

How path integration and visual cues are combined has become an increasingly popular topic in the field (Legge et al., 2010; Reid et al., 2011; Collett, 2012; Legge et al., 2014; Wystrach et al., 2015). Evidence has been sought for Bayesian cue integration, an established phenomena in vertebrates (Cheng et al., 2007), with the most recent research contending that the path integration vector length is used as a proxy measure of path integration certainty (Wystrach et al., 2015).

1.3.4 The nature of the input into visual navigation

Although the scene may operate as a strong navigational cue, occlusion of parts of the eye and hence the visual field appears to show that there is no interocular transfer, that is a landmark seen in one eye forms part of different sensory representation than the same landmark seen in the other eye (Wehner and Müller, 1985). The treatment of each eye as a separate cue would indicate that if there is an abstract representation of the scene or the route it is not based on a unified visual input. Wood and desert ants form separate and distinct outward and inward paths from nest to feeder which cannot be interchanged (Harris et al., 2005; Wehner et al., 2006; Mangan and Webb, 2012). A zero vector ant transported from the inward route to the outward path does not recognise the landmarks on the outward path and cannot either retrace its steps along the outward path back to the nest or follow the outward path to the feeder and then reacquire the inward path. If it crosses the inward path it can recognise it and return home, but if not it will tend to search in the area predicted by the home vector (Wehner et al., 2006). However in a panorama-rich environment when ants are displaced sufficient from the learnt route they appear to be able to switch to guidance based on the skyline height rather than relying on visual memories alone (Wystrach et al., 2012). These findings could be considered antithetic to abstract reasoning about space, suggesting that complex procedural knowledge may be coupled with uncertainty measures and multi-modal sensing to produce a robust navigation system.

The ant does not appear to create a 3 dimensional representation of space. While motion parallax can be used by insects to determine depth and environmental structure (Collett, 1978), the absence of interocular transfer, the results from altering landmark sizes and separation of inward and outward routes suggest that the ant relies upon the 2 dimensional pattern across the eye for landmark navigation. Returning briefly to honeybees, the combination of the natural observation of learning flights coupled with experimental data and simulation lead to the snapshot hypothesis (Cartwright and Collett, 1982). Bees on foraging flights circle around the nest, slowing at certain points and looking back in the direction they came, strongly suggesting that a sequence of static memories is stored which guide the journey home. Localisation is performed simply by matching the stored snapshot against the current retinal image and minimising the difference between the view and memory creates visual homing. This hypothesis has been supported in ants by evidence of learning walks in ants (e.g. Müller and Wehner (2010)) and further experimentation (e.g. Judd and Collett (1998)). Further research

in bees has provided more insights. By camouflaging landmarks against the background in such a way that they are only visible under self motion, it has been shown that honeybees do not rely on static images alone (Dittmar et al., 2010) and therefore the retinal image may be subject to further sensory processing in order to produce a distinctive visual memory. It is a persuasive assumption that the periods of fixation on the goal location are indicative of a memory consolidation process, but if the snapshot is integrated over time then the animal's trajectory becomes important rather than the terminal locations of the path. While comparisons of learning and return flights show similarities in orientation they are not identical with the return flights showing a tighter distribution (de Ibarra et al., 2009). This could be interpreted as the bee performing some kind of integration of the visual information, for example derivation of optic flow, rather than relying on a series of specific and independent views and it is worth considering whether a close relative such as the ant may also use integration over time rather than static snapshots.

1.4 Visual navigation models

The depth of knowledge about visual navigation in the ant and its close relatives motivates the creation of synthetic models. At a simplest level we will encounter visual homing before considering the more complex case of route following and the solution provided by continuous image matching.

1.4.1 Visual homing

Visual homing is the ability to return to a single goal location using only visual cues. The simplicity of the snapshot model has attracted modellers and robotics researchers eager both to explore the behaviour of the animal and to provide simple but robust methods for artificial navigation. A multitude of visual homing models have emerged of which the original snapshot model of Cartwright and Collett (1982) is only one. These have been helpfully categorised by Möller and Vardy (2006).

At the most general level holistic methods perform analysis across the entire image, for example, calculating the image difference function (IDF), such as the root mean square (RMS) difference between every pixel in the current view and the snapshot and then seeking to minimise this value (Zeil et al., 2003). In contrast the correspondence approach identifies areas within the scene which are then matched against the snapshot

to determine an average vector which can reliably point to the goal (Lambrinos et al., 2000; Möller et al., 2001). While there has been a proliferation of working algorithms surprisingly few have attempted to recreate the ant's behaviour in the actual or a similar environment (e.g. *Cataglyphis*, Lambrinos et al. (2000), *Melophorus*, Basten and Mallot (2010), Baddeley et al. (2011), *Velox*, Mangan (2011), Ardin et al. (2016a)). The results from Zeil et al. (2003) are significant in that they show that the RMS difference gradient tends to be sharply peaked as the current view approaches the reference image. It is unknown whether ants seek to minimise the RMS difference but if they do a prediction would be that a zero vector ant reacquiring a route would travel on the trajectory matching the RMS gradient before orientating back to the stored path. If the RMS is not minimised this suggests that a threshold is used to judge when sufficient similarity exists for the route to be followed and the generally slow rate of RMS change might make selecting such a threshold difficult. Notwithstanding these difficulties the image difference gradient from the real environment and in simulation closely maps onto the paths taken by displaced *Myrmecia crosslandi* foragers (Narendra et al., 2013; Stürzl et al., 2015).

Basten and Mallot (2010) compared directly performance of average landmark vector (ALV) (Lambrinos et al., 2000) and gradient ascent (Zeil et al., 2003) algorithms, demonstrating that the parametric approach produces larger catchment areas over which visual homing can operate. The results were obtained by calculating the homing vector fields for each algorithm at points along an actual ant route in a simulation of that specific ant's environment. Of secondary interest, the ambiguity in location was lowest when the vertical field of view was restricted between 0 to 10 degrees and 0 to -10 degrees, the sections of the visual field which are least homogeneous.

1.4.2 Route following with waypoints

De facto the models described above can all achieve visual homing around a single goal location but what is rather more problematic is creating and using a series of waypoints to form a reliable route. This was explored by testing the performance of a comprehensive range of models (ALV, Centre of Mass ALV (COMALV), image difference functions and optic flow first and second order) for route formation by Mangan (2011). By creating new waypoints where the ant route crossed the boundary of a catchment area as defined by Basten and Mallot (2010), the total number of waypoints gave an indication of the efficiency of the homing technique. The best performing

algorithms were first and second order optic flow, and image difference function. A critical technical step was to attempt to use the visual homing models to predict the locations at which memories would be formed. A simple approach to waypoint creation is to use a threshold to determine whether the current view is sufficiently different for a new place memory to be required, and, when route following, conversely once a threshold is reached for a particular waypoint, the next waypoint is triggered (Smith et al., 2007). However, the use of thresholds is inherently problematic as the values can vary not only between environments but in different areas of the same environment. An alternative is the linked local navigation (LLN) method which uses ALV to generate local homing and triggers a new waypoint when the number of visible landmarks changes (Smith et al., 2007). Through this approach the difficulties in determining thresholds are avoided but the model, at least in the simple environment in which it has been tested, can fail when there is simultaneous occlusion and appearance of landmarks. Experiments where the order of landmarks are altered have shown that both the individual landmark and the context provided by the panorama are important when navigating back to the nest (Wystrach et al., 2011b). Ants will sometimes use individual landmarks, and on other occasions either an array of landmarks or the panorama. Therefore, the snapshot approach is not trivially easier to simulate in a way which replicates accurately the behaviour of the animal.

1.4.3 Route following using continuous image matching

Most recently a series of simulations have attempted to avoid these complications by moving away from discrete landmark memories to more continuous representations of routes (Baddeley et al., 2011). In the simplest case storing every image, or more correctly an image generated at relatively short intervals, along an ant route allows retrieval of a location by calculating the IDF between the current scene and all the stored images. Two other useful properties emerge from this methodology; the IDF provides a gradient between a location displaced from the route allowing error correction when deviations occur (Zeil et al., 2003), and by comparing images while rotating on a single location the lowest value should provide the orientation of the route (Baddeley et al., 2011). Rotational scanning is an observed behaviour in desert ants using visual navigation (Wystrach et al., 2014; Zeil et al., 2014), and it is plausible to combine this behaviour with a complete memory of route images in a simulation of route recapitulation. This is the so-called “perfect memory” model and it has been successfully applied

to modelling aspects of ant navigation (Wystrach et al., 2016; Ardin et al., 2016b).

Such a model is only a step along the way in our understanding; the storage of every route image seems biologically unlikely and biologically inspired models of signal processing and learning hold more promise. Infomax (Bell and Sejnowski, 1997) has been suggested as model of the perirhinal cortex, an area of the vertebrate brain which is involved in discriminating between familiar and unfamiliar stimuli, but which also appears to continuously update the representation as unfamiliar stimuli are presented (Lulham et al., 2011). By applying the Infomax algorithm to route learning in a simulated but realistically complex environment it has been possible to recreate ant-like paths without the need for the explicit storage of every snapshot (Baddeley et al., 2012). Instead a route is learnt by altering the weights of the neural net with the presentation of a sequence of images and route following performed by undertaking a rotational scan of the entire panorama at each movement step. Convolving the set of images from the rotational scan with the learnt weights produces a range of familiarity values, the minimum being the most familiar view and hence the direction to be followed. The approach has been extended to the data from Wehner et al. (1996) and Judd and Collett (1998), demonstrating that this approach can replicate accurately the behaviour of the animal without using specific snapshots (Wystrach et al., 2013a). Crucially this algorithm requires no knowledge of location or abstract reasoning about space in order to perform the task, but demonstrates that simple continuous processes can account for complex behaviour.

The preliminary research with Infomax (Baddeley et al., 2012) used an entirely synthetic ant environment; ant routes were generated by avoiding obstacles in an artificial world with a density of vegetation much below that of the cluttered environments of some ant species, arguably creating a visual input which had much less complexity than the real world. The visual input relied on a simple projection from the 3d artificial world onto the "retina" and was reduced to binary in order to present the network only with the skyline. Ardin et al. (2016a) remedied these deficits using data from real ant routes (Mangan and Webb, 2012) in an accurate in silico recreation of that world, a more sophisticated model of the eye and gray scale images with a distribution of shades corresponding to the reflectance of the foliage at the original field site. The actual ant routes pass close to and through a much denser virtual environment which frequently obscures the distant panorama or causes abrupt changes in the view. The model is not only robust to these changes but also can learn routes from a single exposure to the images, a behaviour which has been surmised in ants although not yet proven.

In parallel, the neural basis for the integration of sensory information and learning has been developing with strong evidence for the involvement both of the mushroom bodies based on morphological and synaptic changes associated with sensory experience (e.g. Kühn-Bühlmann and Wehner (2006); Stieb et al. (2010)), and the central complex based on electrophysiology and modelling (Webb and Wystrach, 2016). An implementation the olfactory associative learning model of the mushroom body in *Drosophila melanogaster* (Wessnitzer et al., 2012) for visual route following has shown that it is capable of the ant navigation task at a level comparable with the Infomax variant (Ardin et al. (2016a)). Analysis of the mushroom body model has shown that it can be characterised as a Willshaw net (Willshaw et al., 1969) allowing the memory capacity of the ant to be calculated which in turn seems to confirm that the very extensive routes observed in some cases (Wehner et al., 1996) could be stored by learning a continuous visual input.

All the algorithms described so far require that the view is scanned to determine the correct heading at every step along the path during recapitulation. This is problematic for a number of reasons. Firstly the animal does not possess fully panoramic vision and the experiments with partially blinded ants have shown that interocular transfer appears not to be possible with the image falling on each eye treated as an independent cue to location (Wehner and Müller, 1985). Therefore it seems unlikely that the visual pathway produces a percept which could be mentally rotated by the animal. There is evidence of the animal being able to predict motion (Lent et al., 2010) which could suggest some ability to model or abstract visual input. However the findings are similar to those from optomotor responses (the ability to track global movement of the environment) which are considered a reflexive response. On this basis if scanning is used as part of a continuous process to determine heading it must be a physical process involving re-orientation of the eyes.

While scanning is seen periodically there is no evidence of a continuous rotational scanning behaviour, nor an increase in yaw rotation where part of the horizontal field of view is occluded which would be expected if the ant is trying to generate a panorama. However Kodzhabashev and Mangan (2015) showed that during restricted yaw motion between translational steps it is possible to detect the “familiarity valley” and keep on a previously learnt route, a technique described as route-following by klinokinesis. Essentially the natural side to side movement caused by locomotion could detect changes in a visual familiarity gradient sufficiently to avoid the ant moving away from a known trajectory.

1.4.4 Limitations of current approaches

Considering the potential for a subtle interplay between the sensory input and navigation processes it is perhaps a surprising characteristic that virtually all of the robot or virtual simulations use extreme generalisations of the visual and motor systems. Approaches vary between the use of untransformed camera input containing detail at a much higher spatial frequency than the animal can detect (e.g. Zeil et al. (2003)) to uniform down-sampling typically based on one metric from the range that describe the optical properties of the eye (e.g. Baddeley et al. (2012)). Notable exceptions are Basten and Mallot (2010) and Ardin et al. (2016a) who make a principled attempt to generate a more realistic visual input to test respectively the COMALV and IDF, and Infomax and Mushroom Body models. Equally, despite the animals high speed, little consideration is given to the physical trajectory through the environment: either how this might alter sensory processing, or how the visual and motor systems may be connected to produce embodied behaviour. If considered at all in these models, motion is likely to be treated as a source of noise. As noted the separation of signal from noise can be somewhat subjective (Bell and Sejnowski, 1997) and it may be more appropriate to see motion as either a constraint or even an essential component of the visual system.

1.5 The visual world of the moving ant

1.5.1 Overview

We have established that ants can use vision alone for route navigation and that there is an algorithm which can use just a simulated visual input to reproduce ant-like routes. In the pursuit of greater realism the requirement for rotational scanning at every step in the original formulation of the model can be overcome using klinokinesis. The ability to follow routes with an uncomplicated optical model leads to the proposition that incorporating greater accuracy into the sensory processing should improve the performance of the model, but in order to explore this possibility we need a deeper understanding of what the ant's eye tells the ant's brain.

Vision is adapted to the behaviour and environment of the animal (Land and Nilsson, 2012). It is a common modality and uses a substantial proportion of neural resources (e.g. for the ant see Gronenberg and Hölldobler (1999)) indicating that it provides significant evolutionary advantage. It is also far from a general sense and

the diversity and sophistication of eyes is astonishing (for a review see Land and Nilsson (2012)). In this section the general properties of the anatomy of the apposition compound eye found in ants is described and the relationship between optical design, neural processing and behaviour is discussed. The adaptations of the desert ant eye are outlined including the possible effect of motion on the optical system and finally the collateral effect of the motion processing in the visual pathway is considered.

1.5.2 The sampling properties of the apposition compound eye

Ants in common with the other hymenoptera possess a specific eye design, the apposition compound eye. The main distinguishing feature compared to the other common compound eyes (optical superposition and neural superposition) is that each facet lens guides light to a single rhabdom, and thus each optical cartridge can be considered an individual signal producing unit. However the image forming properties of compound eyes are relatively similar, well-explored and the mathematical properties are explicit. The general design of the compound eye is a series of columnar optical structures, the ommatidia, each providing a separate signal to a change in light stimulus. While each ommatidium shares some optical properties with traditional camera-like lens systems, it does not form a detailed image onto a distal imaging surface. Instead the external surface of the eye is analogous to the the retina of a camera eye with each ommatidium acting as a point detector. The ommatidium itself comprises a facet lens which focuses light into a crystalline cone that acts as a light-guide to the rhabdom, a structure containing up to 8 photoreceptors. The function of the lens is to concentrate light into the ommatidium balancing requirements for contrast against the area of the scene from which light is sampled. In simple terms, the smaller the area the lens samples from, the greater the contrast at the detector enhancing the ability to measure small changes in light. The refractive properties of the ommatidium scramble the light entering the structure and the rhabdom responds to the effect of all light focused through the lens. Some excellent papers cover in detail how the structure of the eye relates to the ability to resolve detail in the external world (Land, 1997; Stavenga, 2003). Without resorting to a full description some key principles are important to understanding the ant's visual world.

A key limit on the ability to resolve detail is the maximum sampling frequency of

the eye mosaic, defined as ((Land, 1997)):

$$v_s = \frac{1}{2\Delta\varphi} \tag{1.1}$$

where $\Delta\varphi$ is the interommatidial angle which in turn is the diameter of the facet lens divided by the local radius of the surface of the eye. The eye is not able to optically sample at frequencies more than the number of ommatidia that can be fitted into the arc of the eye. However as facet size increases so the area sampled decreases; this is defined as the acceptance angle ((Land, 1997)):

$$\Delta\rho = \sqrt{\left(\frac{\lambda}{D}\right)^2 + \left(\frac{d}{f}\right)^2} \tag{1.2}$$

where λ = wavelength of light, D = facet lens diameter, d = rhabdom diameter and f = focal length.

The consequence of the relationship between these equations is that it is possible for the acceptance angle of the ommatidium to be either greater or smaller than what might be predicted from the interommatidial angle. A natural assumption is that maximum sampling frequency is equal to the reciprocal of the acceptance angle ((Land, 1997)):

$$\frac{1}{\Delta\rho} = \frac{1}{2\Delta\varphi} \tag{1.3}$$

In this case each ommatidium would cover exactly enough of the scene to ensure that the field of view was entirely covered or matched and indeed in the equivalent calculation for humans this is the case. However it is possible for the ratio to be larger than 2, over-sampled, or smaller, under-sampled, and while the former has been recorded in some circumstances (e.g. dark-adapted eyes where photon capture becomes the critical requirement), it is much more common for the scene to be under-sampled, sometimes quite dramatically (e.g. the blowfly, *Calliphora*, has front light-adapted visual field sampling ratio of 0.68 ((Land, 1997))).

What we can conclude is that the sampling pattern of the compound eye is a balancing act of optical resolution and the detection of changes in illumination which we can assume is driven by environmental and behavioural requirements. The result for the desert ant has implications for how its navigation can operate.

1.5.3 The desert ant eye

The nature of ant vision has been explored across species and using different methodologies (e.g. anatomy in *Myrmecia* inter-species and caste (Narendra et al., 2010), psychophysics in *Myrmica sabuleti* and *Myrmica ruginodis* (Cammaerts, 2004, 2012) but with detailed optical information about both *Cataglyphis* (Labhart, 1986; Zollikofer et al., 1995) and *Melophorous bagoti* (Schwarz et al., 2011b).

Cataglyphis displays a distinctive horizontal regionalisation with more tightly packed ommatidia in a foveal belt but unfortunately the local radius of the eye nor the facet diameters are reported and it is not possible to infer what the image producing qualities will be (Zollikofer et al., 1995). Notwithstanding it is worth noting there is both a reduced inter-ommatidial angle in the very centre of the anterior visual field (pointing in the straight ahead direction) and a pronounced area of binocular overlap covering the anterior and dorsal visual field. It has been assumed that the equatorial pattern reflects the flat and featureless nature of the *Cataglyphis* environment but the exact features being extracted are unknown.

M. bagoti shows a distribution of interommatidial angles which is quite different and full data for facet sizes is available (Schwarz et al., 2011b). There is a pronounced bias towards large facets in the anterior and ventral visual fields with much smaller facets in the dorsal field. The horizontal cross-section of the eye shows a flattening orthogonal to the direction of travel, with more ommatidia pointing in the direction of travel than in other axes. The optical properties show that the interommatidial angle varies from 6.4 degrees anterior to 4.9 degrees medial to 3.0 degrees posterior, while acceptance angles vary from 1.6 degrees anterior to 2.6 degrees posterior. These results show that the eye is arranged in such a way that there is dramatic undersampling in the anterior visual field (ratio 0.25) but with higher contrast discrimination (Schwarz et al., 2011b).

Description of the optical resolution of the static eye neglects the effect of animal motion on the formation of the image on the retina. High walking speed is a feature of desert ants, a requirement of the thermophilic lifestyle. A cruising *Cataglyphis* at 50cm/s (Ronacher, 2008) may be significantly slower than flying insects but it is at the highest end of the terrestrial animal speed scale (i.e. 52km/h is the human scale speed for the normal walking speed of *Cataglyphis*) and it would then be prudent to consider the effect of motion on the image-forming properties of the eye. The angular velocity

of an image (v) across the retina can be readily calculated ((Land, 1997)):

$$v = \frac{U sin\alpha}{b} \tag{1.4}$$

where U = insects linear velocity, α = angle between the object and insect heading, and b = the distance to the object.

The effective acceptance angle of the ommatidia is then given by ((Land, 1997)):

$$\Delta\rho_v^2 = \Delta\rho^2 + (v\Delta t)^2 \tag{1.5}$$

where $\Delta\rho$ = acceptance angle of the ommatidia, v = angular velocity across the retina and Δt = temporal response to a light flash.[1]

The net effect of translational motion is to exaggerate the size of the acceptance angle (exponentially in the near field) and is thought to account in part for the patterns of regionalisation in some species, for example horizontal under-sampling in Apis ((Land, 1997)). In the case of the desert ant high speed will cause substantial motion blur in the lateral visual field for near objects perhaps making them invisible when at full speed, but objects at a distance of 10m or more will be largely unaffected. Such an observation provides support for the use of the panorama for continuous homing (Graham and Cheng, 2009a; Baddeley et al., 2011), but is not readily compatible with the salience that smaller, closer objects seem to take (Wehner et al., 1996; Seidl and Wehner, 2006; Wystrach et al., 2011b). A conundrum appears here: how do both distant and close objects contribute to visual navigation? The subsequent processing of retinotopic information in the visual pathway to extract motion and features may provide some insights.

1.5.4 Visual processing beyond the eye

All visual systems operate on the basis of being able to detect the amount of or change in luminance from the environment, for example to allow the motion of either the viewer or of the environment to be detected. Motion processing in the compound eye has been very extensively researched since the discovery of the Hassenstein-Reichardt, or Elementary Motion Detector (EMD) (for a review see Borst et al. (2010)). The

[1]There is little research on the critical duration of the ant ommatidia, which we will assume is synonymous with temporal response to the light flash, but a relationship with diameter of the rhabdom has been demonstrated experimentally by de Souza and Ventura (1989):

$$\text{critical duration} = (1.47 \text{ x rhabdhomal area}) + 10.63 \tag{1.6}$$

model has been shown to have very wide application but operates on a simple conceptual basis: signals from adjacent photoreceptors are delayed and compared (typically multiplied) with the undelayed signal from the neighbour. The addition of the results gives the direction in which the stimulus is moving between the photoreceptors with characteristics such as a non-linear speed response which have been experimentally demonstrated across species and is computationally well-characterised (Higgins et al., 2004). More elaborate models include high-pass filtering to remove sustained light levels, low-pass filtering for the delay between the signals, direct signal transmission and rectification with offset (e.g. Eichner et al. (2011)) .

The time constants have been shown to be of the order of 100ms (*Drosophila*) and 50ms (*Calliphora*) but less is known about the dynamics of terrestrial insects. Results from the crab, *Carcinus maenas*, suggested that there may be more than one channel operating with different optokinetic tuning (Nalbach, 1989) and although perhaps a specific adaptation for nocturnal vision, the hawkmoth, *Deilephila elpenor*, may have two parallel delay lines (O'Carroll and Warrant, 2011). Even the time constants for flying insects in daylight are surprisingly long. The blowfly will travel 8.25cm over the period that the motion detection system integrates but this is an oversimplification for the sake of illustration (*Calliphora* velocity from Nachtigall and Roth (1983)). The visual system may integrate over these periods but this may be different from the sampling frequency and further into the processing pathway there is integration of the individual motion signals.

The anatomy of this pathway is complex but well-mapped (e.g. Fischbach and Dittrich (1989)). The rhabdom contains 8 receptor cells (R1-8) of which R1-6 respond to the different wavelengths of light entering the structure and project in a columnar manner into the lamina. From the lamina there is projection into the medulla and subsequently into the third neuropil, the lobula, where aggregated motion signals can be detected in the lobula plate tangential cells (LPTC). Thus the evidence points to the EMD location in the medulla and although the exact structures remain elusive anatomical evidence (Takemura et al., 2008) and neurophysiology (Joesch et al., 2010) appear to confirm this assumption. Within the LPTC, horizontally selective (HS) and vertically selective (VS) cells code for patterns of EMD input representing specific, complex flow patterns with both translation and rotation components (Krapp et al., 1998). The response of a range of VS neurons has been shown to be comparable with what is predicted by a matched filter model using some assumptions about the motion and structure of the animal's environment (Franz and Krapp, 2000). Therefore motion

coding at the third neuropil appears to reflect the behaviour and environment of the species being studied.

Beyond the LPTC the motion pathway has been traced through the protocerebrum eventually reaching the mushroom bodies, which are thought to act as a multimodal integration centre and the basis of learning in the insect brain. However the visual system does not only respond to motion; pathways have been found for colour, combined colour and motion, achromatic shape and other feature extraction alongside independent inputs for polarisation information from the dorsal rim area and ocelli (Paulk et al., 2009). While it tempting to focus exclusively on the role of motion perception in route finding the additional pathways of colour and polarised light cannot be ignored. *Cataglyphis bicolor* has at least two identified colour receptors tuned respectively for green (510nm) and ultraviolet (350nm) light (Mote and Wehner, 1980; Labhart, 1986) and in combination these can produce discrimination across the range 320nm to 627nm (Kretz, 1979). Both receptors are distributed across the eye although UV cells are more common in the DRA and also demonstrate significantly greater polarisation sensitivity. The colour pathway shows some similarity to motion detection in that chromatic information is coded in a complex arrangement of broadband and narrowband receptive fields in the medulla (Kien and Menzel, 1977).

1.6 Ant motion

While ant navigation has been the subject of intense study there is considerably less information about the exact trajectories the ant and, most importantly, the ant's head take through the environment. If there is motion of the head while moving the retinal pattern may be different when the ant learns and subsequently attempts to follow the route, but little is known either about this phenomenon or the means by which correction might be applied. Absence of interocular transfer suggests that visual input is not abstracted and there is very little published data about the micro-movement of the animal. Duelli (1975) found that the head angle of running *C. bicolor* was 44.1 degrees +/-4.1 degrees which suggests a degree of stabilization when moving on a flat plane. More recently Weihmann and Blickhan (2009) found that the caput angle increased significantly as *C. fortis* and a tree dwelling species, *Formica pratensis*, climbed an incline but that the caput angle (the angle between the substrate and the axis of the mandibles and the neck joint) was more stable on falling slope. It is possible that the animal disambiguates the effect of the change in angle on the visual scene either through proprioception, by

using the polarisation pattern in the sky or another stable feature in the environment (Graham and Collett, 2002) as a reference point, or a combination of these cues.

At the level of the interaction of the ant's small scale body movement relative to the environment some additional features have been observed. Desert ants perform visual centring, but in contrast to optic flow methods seen in flying hymenoptera, the geometric structure of the environment, and specifically the height of landmarks, appears to be important (Heusser and Wehner, 2002). Given the specialisation of the *Cataglyphis* eye and the effects of speed on resolution it may be difficult to generalise this result to the scrub-dwelling species. A series of saccade-like behaviours have been observed: in the case of *Formica rufa*, a fixation-like turn can be produced experimentally (Lent et al., 2010) but in *Ocymyrmex robustior*, a natural scanning behaviour where the body is aligned with the nest through fast pirouettes has been observed (Müller and Wehner, 2010; Wehner and Müller, 2010). Finally as noted earlier the trajectory the ant chooses appears to be designed to maximise self-motion generated optic flow associated with prominent landmarks (Wehner and Müller, 2010).

The overall interaction of the visual environment and locomotion has been illustrated in *Myrmecia pyriformis* where walking speed decreases at light levels and visual contrasts fall, probably due to increased temporal summation in the visual system (Narendra et al., 2010). There is greater variability in the tracks produced suggesting less ability to discriminate the path possibly due to the effect visual integration over longer time periods.

1.7 Summary

This section has shown the current appreciation of visually guided ant navigation and clearly many questions remain unanswered. It is still not clear exactly which features of the visual world are relevant to the ant: the assumption of the snapshot models is that an individual retinotopic pattern is sufficient but given the limitations of the model and the behavioural evidence from the animal this does not seem in any way certain. The optical properties of the eye and subsequent visual processing may have evolved to generate these features but there is no research relating how these attributes may contribute to navigation. While the observation of scanning behaviour can be seen as a method of acquiring and comparing views, in general the animal moves at high speed: is visual navigation used during locomotion and is it combined with path integration?

The basis of ant vision is a small eye with features for resolving detail which ap-

pear to be environment specific and there is general evidence for the interaction of the optical properties of the eye not just with the environment but in combination with the animal's motion. The field research undertaken with C. velox provides a rich data source which allows comparison with more accurate simulations of the animal's perceptual world and motion (Mangan, 2011; Mangan and Webb, 2012). By demonstrating that a model of the Mushroom Body can reproduce ant routes as well as Infomax, the evidence for continuous visual navigation by these means seems irresistible (Ardin et al., 2016a), but how does the complex processing of visual information when the animal is in motion affect this finding?

This thesis attempts to answer this question over the subsequent chapters. In chapter 2 the RSInfomax model of Ardin et al. (2016a) is tested with image processing approximating aspects of the ant's visual pathway, which suggests that more sophisticated versions of the retinotopic image do not benefit navigation. The interaction of the specific algorithm in relation to the qualities of the input is considered alongside the effect on the images of the animal's trajectory through the environment. In combination the results create questions about whether the navigation is strictly continuous image matching. The relative position of the ant's head as it moves across the substrate of its home environment can help us explore this further. In chapter 3 we show how the ant's head moves under a variety of locomotion conditions in the natural environment, and critically how this range of motion will disrupt image matching. By this stage we can be fairly certain that a process of image matching which uses very small sampling steps is not possible but observation in the field of ants walking backwards to the nest suggests that facing towards the nest, and thus in the direction of the retinal stored image, could be infrequent. Chapter 4 describes field research of this phenomena and subsequent investigation of which visual mechanisms might be at work. We can conclude that ant visual navigation is not a process where there is continuous comparison of a stored retinal images. The evidence allows two alternative explanations for ant visual navigation; that it is a process with using a sensory input which is independent of rotation generated at small and regular time intervals, or it consists of visual sampling on an irregular basis followed by periods of heading stabilised locomotion. Further research which may help disambiguate these hypotheses is described in the discussion.

Overall this research provides some new insights into the processes which are at work during ant visual navigation. The relationship between visual processing, the environment and route recapitulation is not as straightforward as might be hoped: adding

additional sophistication does not improve route fidelity and we are still at a loss to explain both the visual salience of the correct path or why errors occur. What is more certain are the parameters under which navigation must occur. Any new theory or model must be able to accomodate the effect on the visual scene of head movements, and to account for the ability to reach the nest without having a continuous view of the goal.

Chapter 2

Low level visual processing and ant navigation

2.1 Introduction

Research using the Infomax algorithm has shown considerable promise in simulating ant visual navigation (Baddeley et al., 2012; Ardin et al., 2016a) but the models of the visual system have used a number of simplifying assumptions and in this chapter we will examine the effect of increasing the realism of the visual environment and visual processing. Introducing biologically inspired processing steps and a more faithful version of the experimental world was hypothesised to improve the fidelity of route recapitulation, but across a variety of simulations no substantial improvement was found. These results provided the inspiration for undertaking more detailed examination of the animal's behaviour and further in silico experiments.

A major corpus of research on the navigational feats of non-pheromone laying ants has been published (see Wehner (2009) for a review) but until recently there was little understanding of how the process of navigation occurs. A key behaviour is the ability to relocate the nest entrance relying on visual cues alone with the retinal image providing sufficient input to explain the navigation. This observation is interesting as the visual pathway includes additional processing steps before finally reaching the areas of the brain thought to be responsible for navigation.

A variety of theories had been advanced to explain this type of visual navigation but none have been able to fully reproduce the complex routes taken through the environment (Cartwright and Collett, 1982; Lambrinos et al., 2000; Basten and Mallot, 2010) until Baddeley et al. (2011) provided a major advance through training an In-

fomax network with a series of retinotopic images from a simulated ant environment. Routes could then be recapitulated by scanning across a range of views and picking the direction which yielded the highest ”familiarity when the retinotopic input was convolved with the network. This algorithm, rotational scanning with a trained Infomax network, is referred here as RSInfomax to differentiate it from the general properties of the algorithm. Although Infomax is thought to be a valid approach to modelling neural circuits (Bogacz and Brown, 2003), Ardin et al. (2016a) demonstrated that a model of the mushroom bodies of the insect brain could also reproduce ant routes with good fidelity and that the mushroom body model could be reasonably represented as a Willshaw net (Willshaw et al., 1969). Although simpler to implement than the Mushroom Body model, no results have yet been published on the Willshaw net's performance on the navigation challenge. Therefore Infomax remains an attractive workbench for testing aspects of the retinotopic input on navigation as it is computationally tractable and can make use of dense retinotopic patterns for learning.

Motivated by the behavioural data showing the importance of the retinal image (e.g. Wehner and Räber (1979); Judd and Collett (1998)) the input into RSInfomax has been an untransformed input, typically at a spatial resolution of 4 degrees and across a field of view of approximately 300 degrees (Baddeley et al., 2012; Ardin et al., 2016a), values obtained from anatomical analysis of desert ant species (Zollikofer et al., 1995; Schwarz et al., 2011b). It is likely that either the mushroom bodies (Stieb et al., 2010; Ardin et al., 2016a) or the central complex (Webb and Wystrach, 2016) are the neural circuits responsible for insect navigation but the projections they receive are likely to have been processed by the complete visual pathway (Paulk et al., 2009). Assuming an untransformed retinal input into RSInfomax is unrealistic and we now need to understand how this model performs when processing is added which begins to reproduce elements of the visual pathway. As with other machine learning techniques, the input characteristics have a significant effect on the performance of Infomax, particularly the degree of correlation, and we can anticipate that processing which reduces image similarity will assist RSInfomax navigation.

In the introduction what is known about the visual processing of the ant was outlined, and even with the limited information it is obvious that the visual input into a continuous navigation model may be very different from the sequence of images currently used. This chapter serves as an exploration of how certain types of processing affect navigation and thus which aspects may be important, or indeed may reveal features of the model which were previously unknown. 8 aspects are investigated. The

simulations are all based on the ant world and real ant paths used in Ardin et al. (2016a) and more detailed consideration is given to what the nature of the "visual landscape" along the routes says about navigation. Resolution and the effect of changing the step size between training images is explored; low resolution features may be lost in reducing photoreceptor density, but this may be compensated by using a larger number of training images. In either case the learning algorithm may not be able to discriminate between locations if images are too similar. Altering the sampling distribution may allow areas of the environment which contain more useful information for navigation to be more heavily weighted, improving the performance of the simulation. The initial work with Infomax used binary images, but from an environment where these were particularly effective; the effect of skyline extraction should be tested in the more biologically realistic version. Finally if navigation is genuinely continuous the input should not be a series of static images, but the optic flow pattern generated by ego motion; in the absence of small-scale motion trajectories or neurophysiological data, an EMD is tested across a range of values to observe the effect on the task.

2.1.1 Resolution and visual sampling

Creating a visual sensory experience with an apposition compound eye consists of a number of complex processing steps some of which are as yet only partially understood. Transformation of the world starts at the surface of the eye, where sampling is determined by the distribution of the ommatidia facets. Larger facets sample a smaller section of the environment increasing resolution and contrast but physical constraints mean that in order to have a high resolution image either the diameter of the eye must increase or the surface must be shaped in such a way to pack in a greater number of large facets in a zone of interest.

Large facet diameters can also lead to undersampling of the visual scene due to the interaction of the curvature of the eye surface with the acceptance angle of the ommatidia. If the acceptance angle is less than the neighbouring inter-ommatidial angles, light will be received only from certain parts of the scene. The compromises caused by physical space interact with the ecological and behavioural requirements of the animal to produce different sampling patterns which concentrate image forming on the most salient parts of the scene (for a review see Land (1997)). Stereotypical patterns of ant motion may interact with the pattern of sampling to produce a percept different from the image produced by the static eye (Seidl and Wehner, 2006).

The relationship between resolution and field of view in a simulated ant environment has been thoroughly explored in the context of perfect memory navigation (Wystrach et al., 2016) demonstrating that both extremely high (<1 degrees) and low (>10 degrees) resolution images are less optimal than those in between and intuitively that a wider field of view improves direction selection. As the authors note, such findings tend to generalise to other navigational models, but as Infomax is both learning the input and performing independent component analysis (Lulham et al., 2011) it is conceivable that changes in resolution may affect it in an unpredictable manner. Correlation between input images will be a function of the resolution of the eye and the structure of the environment, and as suggested by Wystrach et al. (2016) this relationship may not be monotonic. Values of resolution which increase image correlation in a simulated environment should lead to a greater number of errors with RSInfomax.

The optical sampling patterns of species of non-pheromone laying ants in different habitats is known to be different and thought to reflect the areas of the scene that contain the most valuable information for navigation (Zollikofer et al., 1995; Schwarz et al., 2011b). In the visually-rich habitat of *M. bagoti* masking the vertical extent of the visual panorama confirms that the area between 9 and 17 degrees is not only sufficient but produces the best navigation performance compared to other sections (Graham and Cheng, 2009a). *M. bagoti* and *C. velox* inhabit similar environments so will weighting the visual field in different dimensions affect the navigation performance of the RSInfomax model? Certain parts of the scene such as the ground and sky contain less contextual information about location and it seems not unreasonable that inhomogeneous sampling can produce images which are less correlated than the full view.

2.1.2 Colour sensitivity

Ant eyes contain at least 2 photoreceptors known to be sensitive to wavelengths of light in the region of approximately 510nm and 350nm respectively (Mote and Wehner, 1980), roughly corresponding to green and UV light. In order to extract skyline either the difference between UV and green response of these photoreceptors (Möller, 2002) or the UV response alone (Stone et al., 2014) has been shown to be useful. The skyline is known to be an effective cue for navigation (Reid et al., 2011; Stone et al., 2014) and then extracting it from the panorama using UV has been shown to be critical for correct orientation of ants displaced from learnt routes (Schultheiss et al., 2016b). The

original RSInfomax model used a black and white image of the areas of sky and not-sky as the input to the network (Baddeley et al., 2011) but with an environment with greater visibility of distant landmarks due to a lower density of vegetation and the addition of prominent features. In the circumstance where there is less stability in distal features can the navigation model perform as well using an input of binary values representing the regions of sky and not-sky as opposed to a gray-scale image based on green wavelength reflectance?

2.1.3 Motion processing

The green channel of the hymenopteran eye is processed for motion (Lehrer et al., 1988) most probably with the elementary motion detector (EMD), a common characterisation of motion vision (Borst and Egelhaaf, 1989). The circuit in its simplest form detects the change in luminance falling on adjacent ommatidia from which a vector field or optic flow pattern across the retina can be derived. The optic flow pattern is retinotopic but contains information about the 3 dimensional structure of the world which can allow the motion of the animal to be accurately controlled (Srinivasan and Gregory, 1992) and optic flow been shown in ants to play a slight role in measuring distance travelled alongside more conventional means such as step-counting (Ronacher and Wehner, 1995). Bio-inspired models of navigation have employed optic flow (Franz and Krapp, 2000) and have been tested for the ant navigation task (Mangan, 2011).

Optic flow processing can be interpreted as feature extraction, with the effect of translation through the environment identifying the physical location of objects relative to the path. Vegetation which is close to the path will generate horizontal vectors substantially greater than that which is further away and due to the change in vertical angle subtended on the retina the vector components in the vertical direction of near objects will also be higher. By comparison the far horizon along the direction of translation may be effectively invisible as pixel by pixel changes on the retina in this area may be limited by the resolution of the eye. This distant structure may become apparent only under rotation, when the animal turns to face another direction. This presents a visual environment very different from the unprocessed retinal image, and one which closely ties the motion of the animal to the percept. The various species of ants under study are very fast moving along the path to the nest (Ronacher and Wehner, 1995) which will generate rich translational optic flow, but also undertake rotational

scanning as part of their navigational behaviour (Wystrach et al., 2014).

Optic flow might make the visual input into navigation more robust to changes in the scene resulting from minor displacements from the learnt path (Mangan and Webb, 2012) or the disturbance in the visual field caused by locomotion (Raderschall et al., 2016; Ardin et al., 2015). There is evidence from other hymenoptera to support this speculation. Where landmarks are camouflaged from a static viewpoint Apis appears to use optic flow snapshots, leading to speculation that the learnt images are motion processed (Dittmar et al., 2010). Of specific relevance to this research desert ants take more direct routes to the nest in situations where optic flow is maximised implicating the extraction of features through motion processing during navigation (Wehner and Müller, 2010). For these reasons we might assume that introducing motion processing might reduce errors during simulated route recapitulation.

2.1.4 Summary

A range of biologically relevant processing steps have been outlined which could improve RSInfomax and thus provide new insights into visual navigation of the ant. What effects do they have when applied to the model?

2.2 Materials and Methods

Introducing steps into the simulation of the eye which mimic aspects of the animal's visual pathway should improve route fidelity, particularly when the world has features, such as shading, which are drawn from the animal's habitat. Ardin et al. (2016a) had already demonstrated that an Infomax network could learn ant routes from a single trial in a simulation of the real ant environment. Extending the experiments to include variation of optical resolution, changes in sampling homogeneity, skyline extraction and elementary motion detection were hypothesised to improve performance, specifically a reduction in the number of errors during route recapitulation.

2.2.1 Simulated world

The methodology used in Ardin et al. (2016a) provided the basis for this research. A 3d reconstruction of an ant environment was created in silico by mapping in detail the topography of the foraging area for a colony of *Cataglyphis velox* at a field site close to Seville (37.332211N, -5.989751W). The site was used by Mangan and Webb (2012)

who allowed animals to discover a feeder approximately 8m from the nest and after returning home displaced them back to the feeder location allowing the recording of multiple routes under a zero vector condition. The combination of the detailed routes and the 3d world allows the visual experience of the ant during visual navigation to be reproduced.

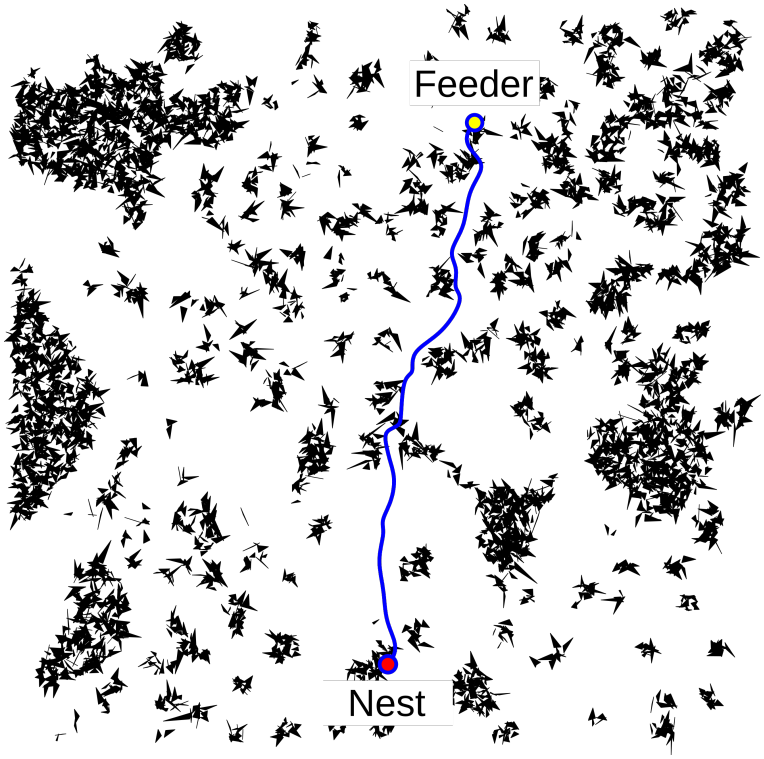

Figure 2.1: The ant world model aerial view. An example ant route between the feeder and the nest is marked in blue. Black triangles show the location of foliage used to create the images along the route.

The simulated world was augmented by adding colour values to the ground, sky and vegetation, with the latter determined from sample photographs of the field site (Nikon D6000 with Novoflexar 35mm F2.5 lens) and the frequency distribution of values for foliage in the green channel in RGB space used to shade the polygons. Photographs of the site using a specially adapted camera (Stone et al., 2014) established that vegetation and sky could be segmented using UV wavelengths which confirmed that the skyline could be reliably extracted in this environment.

2.2.2 Navigation algorithm

The Infomax algorithm uses a network comprising an input and an output layer which are fully connected with a set of random weights (figure 2.2). For these experiments the network was trained separately for each ant with images generated with a constant training step of either 1cm or 10cm along routes taken by 15 ants on the first zero vector run from the feeder to the nest (figure 2.4) (Mangan and Webb, 2012). The input to the network was the processed image from the current route location converted to vector form. The different types of processing are described later but in all cases except motion processing it retained a structure of pixel values across the simulated retina: in the case of motion processing a vector field was created yielding two values for every pixel leading to a doubling of the input vector length. The input layer was scaled according to the size of the chosen visual processing with the network size symmetrical up to an upper bound of 2000 nodes in order to make the simulation run at a reasonable speed. The size and values of the visual processing changed sufficiently to require simple adaptation of the learning rate ensuring that an optimal value would be selected for every run. The same series of random numbers was used to initialise the network weights on every run to ensure reproducibility of the results.

A single presentation of the images was presented sequentially and the weights in the network were changed using the Infomax learning rule. The image is presented to the network:

$$h_i = \sum_{j=1}^{N} w_{ij} x_j \tag{2.1}$$

where h_i is the activation of unit i of the output layer resulting from the weight of the connection between nodes i and j, w_{ij}, and input image x_j. To conform with requirement that the input into the network is supergaussian (Bell and Sejnowski, 1995) the activation values are converted using the sigmoid function:

$$y_i = tanh(h_i) \tag{2.2}$$

In order to store the image the network weights are then adjusted, where η is the learning rate.

$$\Delta w_{ij} = \frac{\eta}{N}(w_{ij} - (y_i + h_i) \sum_{k=1}^{N} h_k w_{kj}) \tag{2.3}$$

Familiarity of a test image is calculated by summing activation of h:

$$d(\overrightarrow{x}) = \sum_{i=1}^{M} |h_i| \tag{2.4}$$

During route recapitulation the visual input was reproduced along a -/+60 degree sweep centred on the current heading direction. Multiplying the visual input at each position along a 121 degree scan with the trained weights gives a vector, the lowest value of which corresponds to the most familiar view (figure 2.3). Identifying the position of the minimum allows a heading to be selected which corresponds most closely with a trained image.

The simulation then takes a step forward 10cm on this bearing at which point a new scan is initiated. The simulation is considered to have successfully found the nest if it reaches a point within 20cm of the end of the route, and if at any point a position more than 20cm from the route is selected, an error is recorded and the simulation placed on the next point on the route. Similarly, if the simulation picks a point which it has already traversed it is considered to have looped back and an error condition is also triggered.

A simulation set was run where the heading direction was selected on the basis of the previous heading plus a new bearing selected from a uniform random distribution in the range -/+60 degrees. This generates a random walk where the selection of the next heading is equally likely to be any position in a 121 degree scan from the current direction and thus corresponds to the methodology used in the RSInfomax simulations where heading selection is a Markov process. This simulation provides what should be a worst-case baseline for route-following against which the RSInfomax models can be compared.

The number of errors was recorded for each recapitulated track, but by itself this statistic was considered potentially unhelpful. While a low number of errors is suggestive of a successful combination of parameters, a high number of errors might be the result of localised problems on the route with relatively long sections of correct path in other areas. In order to address this the number of steps taken between errors, segment length, was calculated for each set of simulations. Finally specific locations of the simulated world may present issues for the different processing steps and to explore this further the original ant routes were plotted alongside the position of errors on the world map.

2.2.3 Modelling the visual input

At the most fundamental level, modelling the visual input involves projection of the 3d structure of the world onto a 3d sphere representing the surface of a compound eye resulting in a 2d image when unwrapped. This falls into the class of problems associated with map projection with the attendant compromises different approaches take. The preferred solution was to use an equidistant cylindrical projection as it accurately reflects the area on the sphere close to the equator which has the highest density of information in the images used in the simulation.

The eye resolution was varied between 1, 4 and 8 degrees reflecting the resolutions of various ant species as well as a lower resolution comparator (Narendra et al., 2010; Schwarz et al., 2011b). Example images created by the different resolutions are given in figure 2.4. The step size between images along the route was varied between 1cm and 10cm, giving approximately 800 or 80 inputs across a typical path. Examples of the difference between 1cm and 10cm step size are given in figure 2.4 C) and D). From the results of these simulations an optimal combination of step size and resolution was selected as the basis for further comparison.

By reducing all values either to 0 for ground and foliage, or raising to 1 for the sky, an approximation of skyline extraction using ultraviolet frequencies could be made. An example of the skyline extraction is given in figure 2.4.

The homogeneity of the visual field was altered by applying a mask varying continuously between 0 and 1. The mask was defined by a minimum value, and lower and upper bounds for the vertical and horizontal visual field. Figure 2.5 gives some examples of the masks used in the experiments. The different configurations of the mask allowed testing of both the general effect of a non-homogeneous input as well as the specific effect of altering the visual field 2.6 (Graham and Cheng, 2009b; Wystrach et al., 2016).

A Fast Fourier Transform of route images shows some harmonics in the vertical direction but with less in the horizontal dimension across resolutions (figure 2.7). Harmonics suggest some redundancy in the image and in this case weighting in the vertical dimension may have less effect on navigation than in the horizontal dimension.

An EMD array was simulated using the model originally described by Hassenstein and Reichardt (1956) (figure 2.8). The EMD used two images generated in the simulated world from which a vector field in polar coordinates is produced for every location on the retina. The input is generated by spatial rather than temporal sampling

as there is no data on the time constant for the EMD circuit of the ant. The two images are taken at the prescribed distance apart along the heading determined at the current location on the route and with very long separations this is an acknowledged deficit as second image may fall outwith the route. An example of the vector field is given in figure 2.4, row F.

Given the potential for a conflict between image similarity and capacity to emerge a technique used in Ardin et al. (2016a) was applied to the visual input in an attempt to decorrelate the input. A network with random connections from an input stage to a larger output stage was applied as processing to the image and by adjusting a threshold value the sparsity of the transformed input can be controlled. This allows the degree of similarity between inputs to be altered systematically. This projection network has biological validity (Tsodyks, 1990), but the input for navigation is a transformed version of the pattern at the eye and is no longer strictly retinotopic.

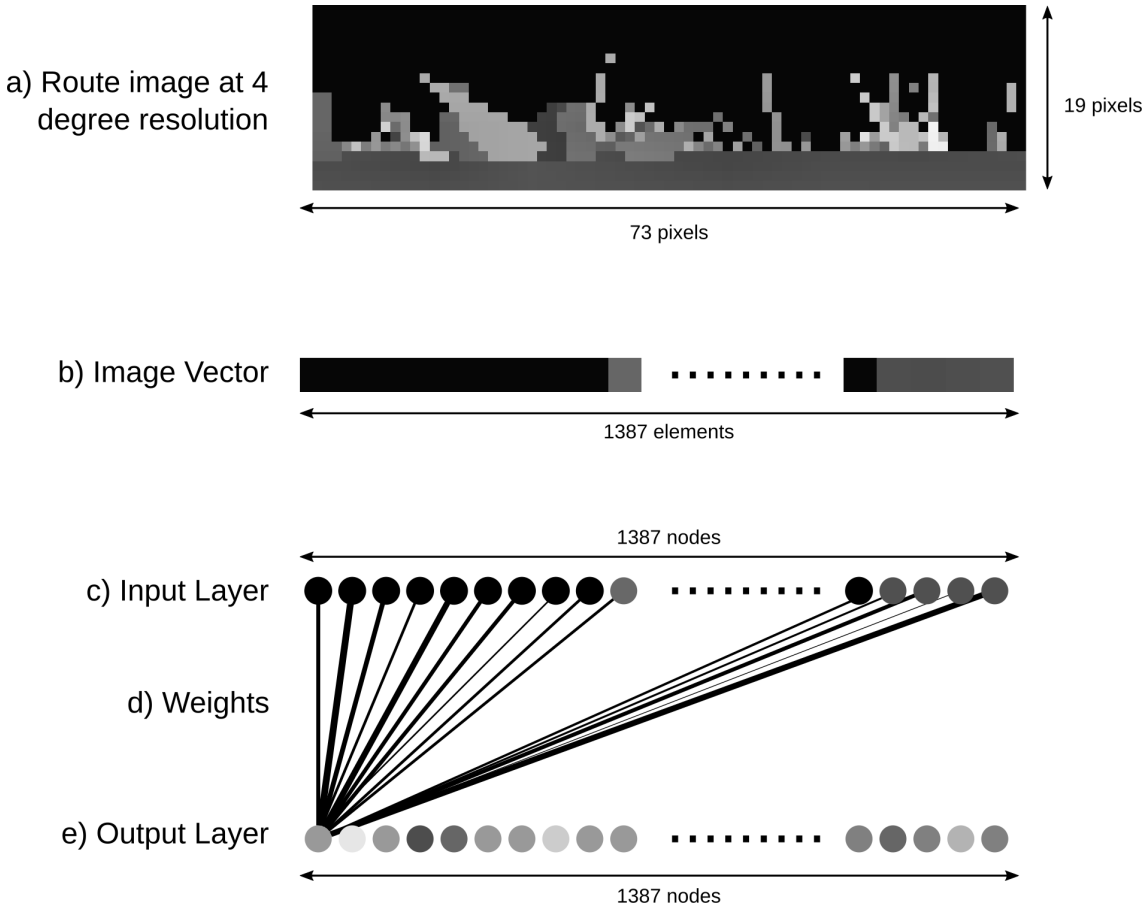

Figure 2.2: The Infomax Algorithm: During training; a) images are taken at regular intervals along the route, in this example using 4 degree resolution, creating a 73 pixel by 19 pixel output. b) the image is then converted into vector form yielding a 1387 element vector. c) the vector is presented to the input layer of the network which corresponds in size to the vector. d) the network topology is a fully connected set of input and output nodes, with the weights of the connections initially set to a random value but each image presentation alters the weights according to the learning rules given in the text. e) where the input vector is less than 2000 elements the network is symmetrical with the same number of input and output nodes, but where this number is exceeded the size of the output layer is gated to ensure the simulation runs quickly. During testing; images are presented at the input layer c) and convolved with the weights d). The sum of the values at the output layer e) indicates the familiarity of the image. Values of familiarity are relative to network size and trained weights.

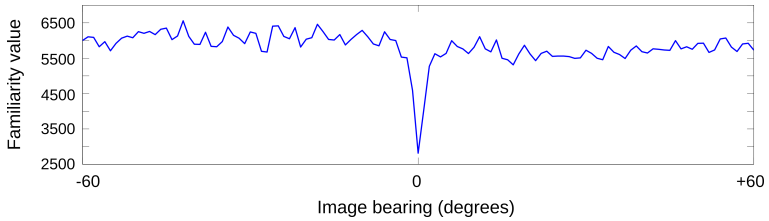

Figure 2.3: Example Infomax values across a 121 degree scan. The trained network is convolved with an image generated at each one of a 121 headings (+/-60 degrees) in this example centred around a previously learnt location. The values give an indication of the degree of familiarity of each direction and during route recapitulation selecting the minimum value is likely to correspond to a bearing which will keep close to the learnt route. Note that in this example with a perfect position on the stored location the values form a stereotypical ”valley” and undertaking a scan at an untrained location produces a less distinctive signal.

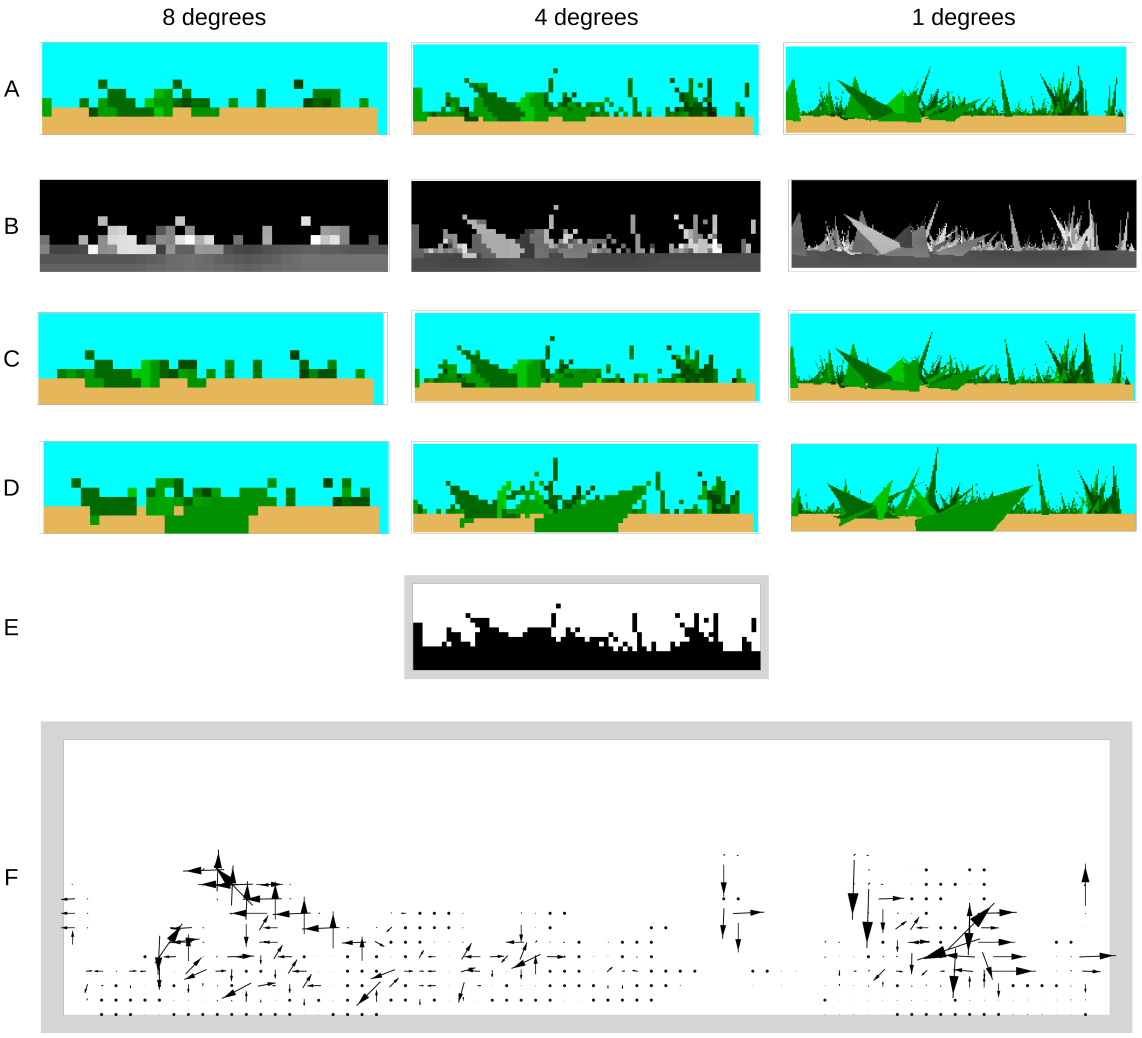

Figure 2.4: Examples of the visual inputs. The images are generated from the same starting location and then transformed according to the various processing steps used in the experiments. Rows: A) Raw images generated at 8, 4 and 1 degree resolutions. B) Images processed for input into the Infomax network. C) and D) Raw images at locations +1cm and +10cm from the original location, illustrating the effect of different training step sizes on the image content. E) Skyline extraction at 4 degree resolution. F) Vector field output from EMD model at 4 degree resolution (scale increased for clarity).

Vertical mask | Combined horizontal and vertical mask | Horizontal mask

Figure 2.5: Example centre weighting masks. The mask on the left reduces the effect of the image in the extremes of the vertical dimension, while the mask on the right works in the horizontal dimension. The middle mask is a combination of the vertical and horizontal dimensions.

Figure 2.6: The effect of centre weighted masks on input images. Using the same test location as used in figure 2.4 the effect is shown of applying the range of masks used in the experiments. Rows show changes in the vertical fader of the mask while columns the horizontal fader. The top left image is the most restricted version while the bottom right is the complete image.

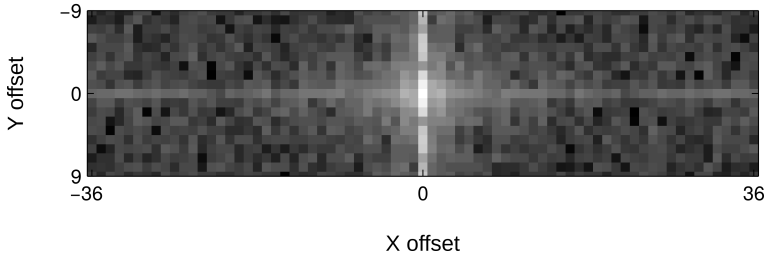

Figure 2.7: Fast fourier transform of input images. The axes show the degree of offset across the image of harmonic components when subject to FFT. The analysis shows stronger components in the vertical rather than horizontal dimension implying that more information may be present in this direction.

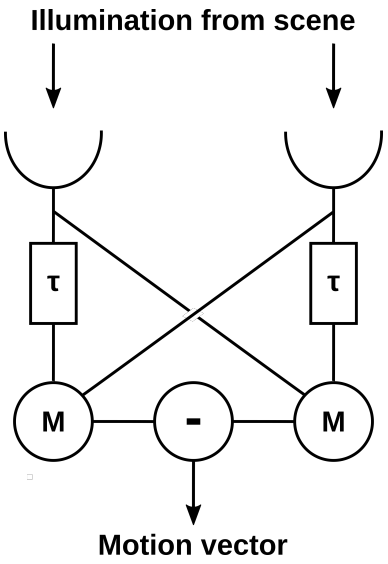

Figure 2.8: EMD model used for motion processed input. The figure shows the typical reduced form of adjacent receptors isolated from a larger array. Light hitting the left receptor is delayed time constant τ before multiplication with the undelayed signal from the right receptor. The resulting outputs are subtracted to give a value which across an array of 3 or more tessellated receptors generates a motion vector in 2d.

2.3 Results

2.3.1 Random results

The random heading direction selection simulation was used as a comparator demonstrating what should be the worst case performance under the same test and error regime as the Infomax models (figure 2.10, first column). The mean performance was 20.0% +/-2.3% errors per route, with a mean segment length of 50.8cm +/-27.7cm, and errors scattered uniformly on the routes. While the principal purpose was to demonstrate that the Infomax simulations were improvements on random heading selection, conceivably the combinations of input and network could result in worse performance, for example if there was over-training on a particular view which would then be preferentially selected as the correct heading in the wrong location.

2.3.2 Route errors and segment length

A preliminary analysis of the mean number of route errors for each simulation against the mean segment length demonstrated a close relationship between the two variables (figure 2.9). For brevity for the rest of this section the focus is on the number of route errors although the segment length information is provided in the figures.

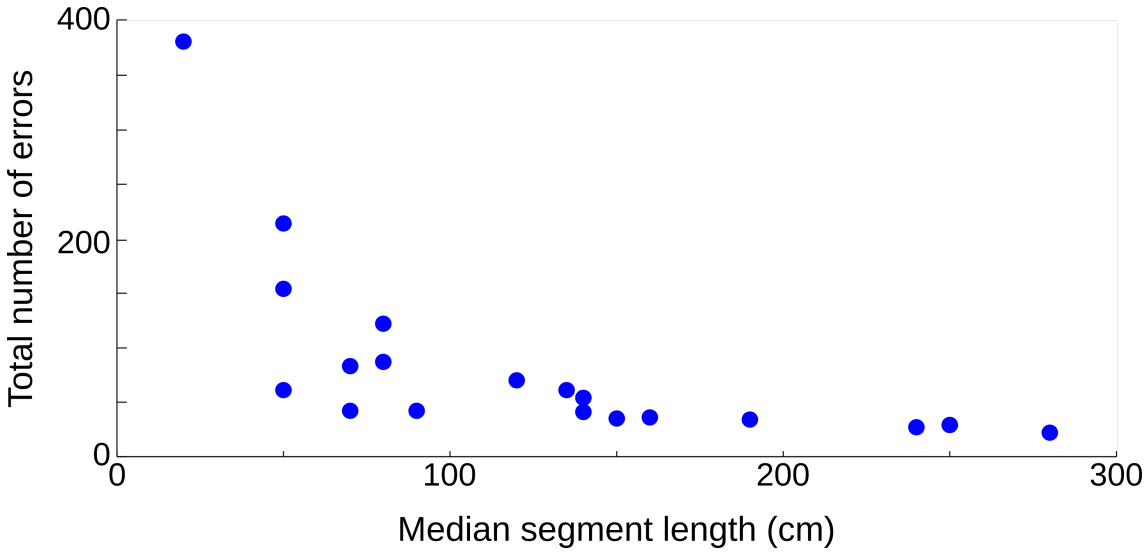

Figure 2.9: Error rate and segment lengths are closely related. Summarising the results across all simulations the total number of errors is closely related to the median segment lengths, confirming that the number of errors along the route length will provide a consistent measure of performance across the simulations.

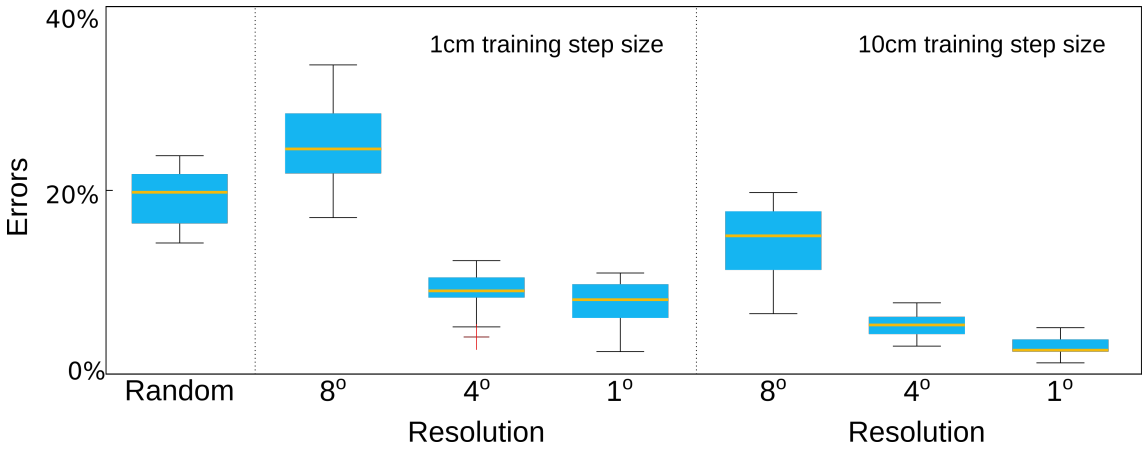

Figure 2.10: Effect of resolution and training step size on navigation errors. Columns 2 and 5, 8 degree resolution in the input image, columns 3 and 6, 4 degrees and columns 4 and 7, 1 degree. Columns 2 to 4, 1cm training step size and columns 5 to 7, 10cm step size. The first column gives the result from the random navigation simulation for comparison against the combination of resolution and step size. Low image resolution and a high number of inputs produces a result similar to random heading selection suggesting that the images are too closely correlated to allow the network to determine familiarity reliably. Increasing resolution above 4 degrees does not appear to significantly improve performance consistent with the results of Wystrach et al. (2016), but increasing the number of memories (1cm step size) does appear to have an effect probably due to interaction between the correlation in the training images. The 10cm step size and 4 degree resolution was selected due to the combination of performance and close relationship with the resolution of the ant eye.

2.3.3 Resolution and image separation

The effect of resolution and image separation were combined due to an anticipated interaction of image similarity and capacity of the Infomax network (figures 2.10, 2.11 and 2.12). In all cases the shorter training step (1cm) performed less well at the same resolution than the longer step (10cm). The combination of 8 degree resolution and 1cm step size performed worse than the random baseline implying that a bottleneck of image similarity and capacity had been reached. Increasing resolution to 4 degrees substantially improved performance, but the further increase to 1 degrees did not reduce the number of errors despite the fourfold increase in the size of the input.

Analysis of image similarity goes some way to explaining this finding: at 8 degrees the average correlation between an image and all other images on the route was

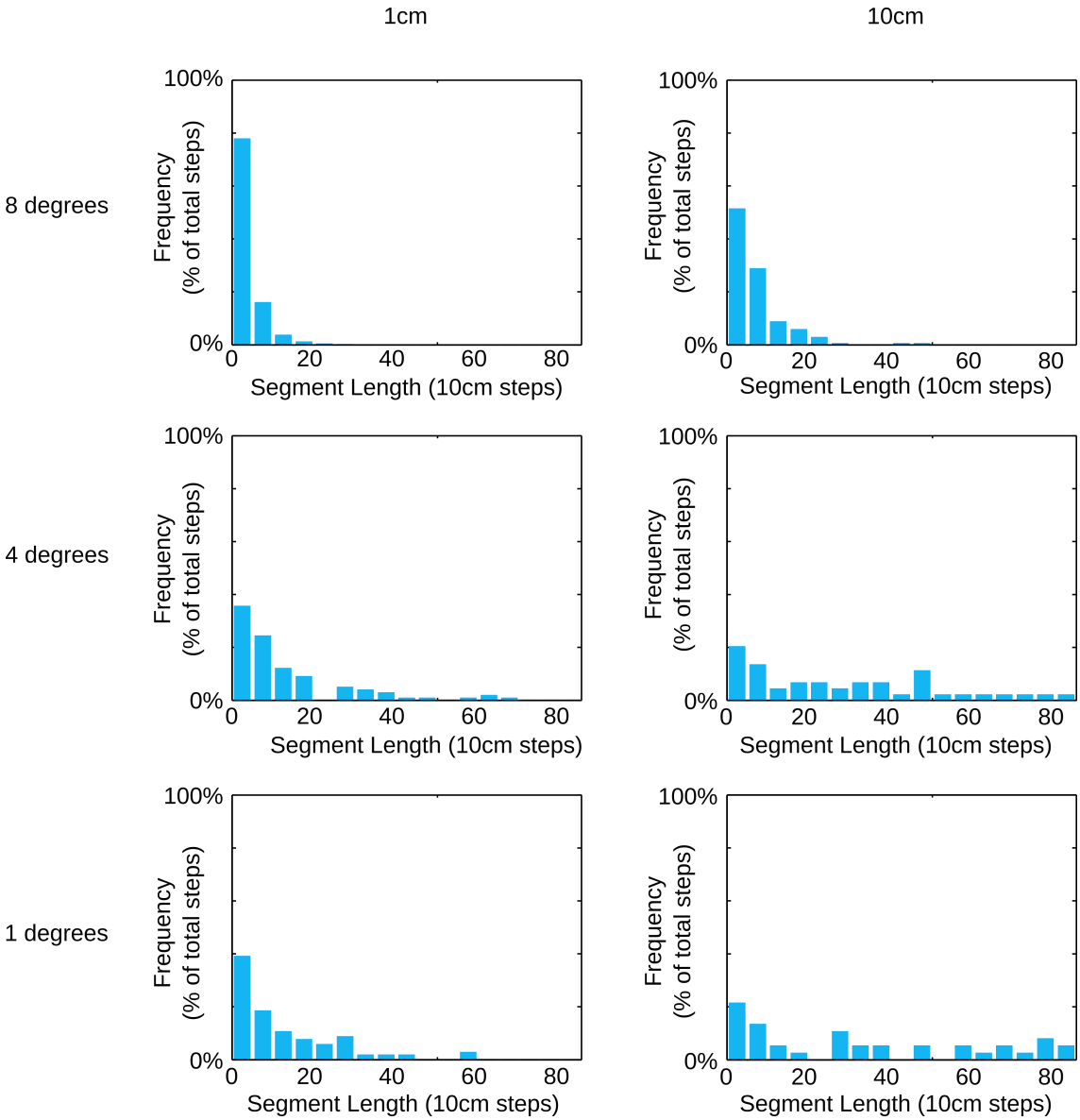

Figure 2.11: Effect of resolution and training step size on segment length. Each histogram shows the frequency of the segment lengths (in 10cm bins) for that combination of resolution and training step size. At 8 degree resolution consistent with the high error rate, segment lengths are small and improve where the number of training images reduce. For both 4 and 1 degree resolutions the notable feature is the extent to which much longer segments appear as the number of training images reduces, while very short segments decrease.

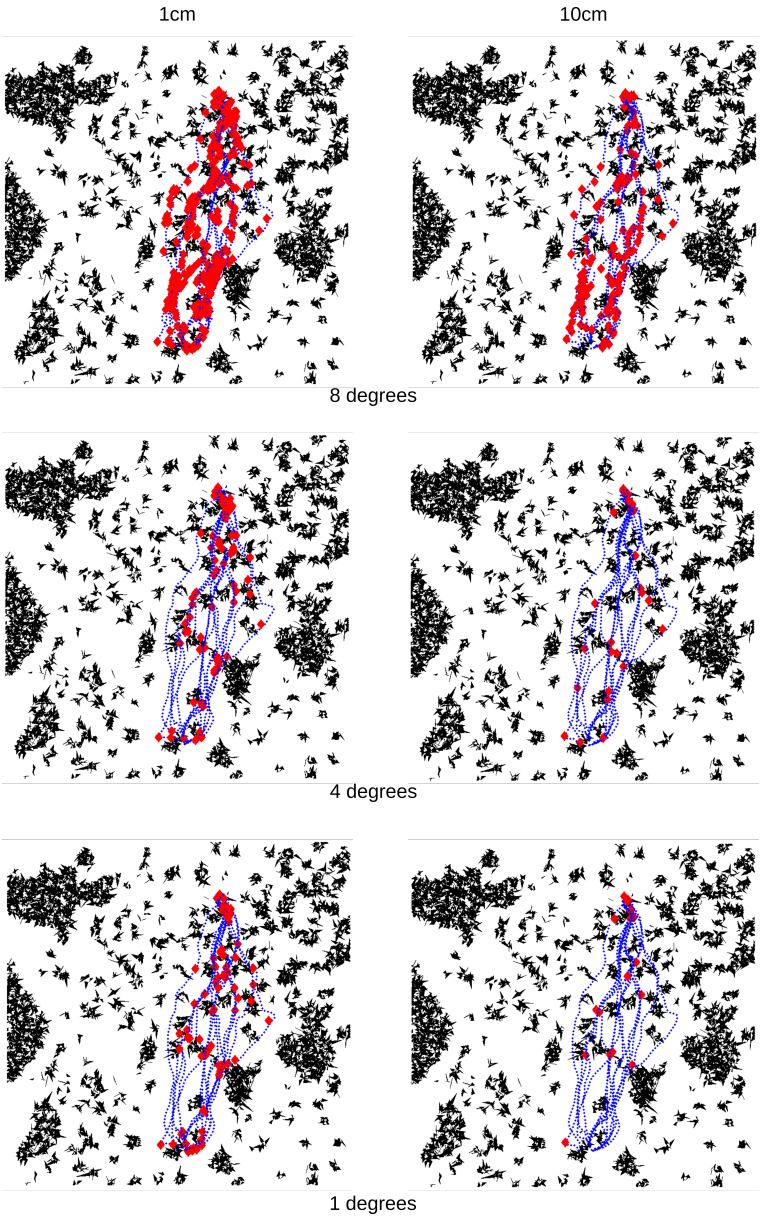

Figure 2.12: Error locations with different combinations of resolution and training step size. For location of the nest and feeder see figure 2.1. The original ant routes are marked in blue and errors in red. The concentration of errors in particular areas indicates interaction between image similarity and the capacity of the network. At 8 degree resolution and 10cm image separation (top right) errors are concentrated in the open area in the lower third of the routes, where the distance from foliage creates near indistinguishable images. As resolution increases this problem decreases substantially although the small changes between 4 and 1 degrees indicate that an optimal level of resolvable detail has been reached.

r^2=0.48 but at 4 and 1 degrees the correlation falls to r^2=0.41 and =0.43 respectively. The negligible difference in the performance of the network for the higher resolutions appears to be closely related to the input similarity, and the increase in errors when the number of images increases from 80 to 800 is similar for 4 and 1 degrees strongly suggesting that resolution no longer has a strong effect in this range.

A resolution of 4 degrees has been used in previous research (Baddeley et al., 2011; Ardin et al., 2016a) and is consistent with the known resolution of *M. bagoti* which inhabits an environmental niche similar to *C. velox* (Schwarz et al., 2011b). Wystrach et al. (2016) showed that values in this range were optimal using the perfect memory test and as the higher resolution did not appear to significantly improve the results using Infomax, 4 degrees was selected as the resolution for subsequent simulations. Given that at this level of image similarity 1cm training steps produced higher errors, the 10cm step size was selected for this resolution. This was the parameter combination used for the subsequent simulations.

The 8 degree resolution results have a potentially interesting implication. Capacity of an Infomax network does not scale linearly with increasing size (Lulham et al., 2011) and for the level of image similarity at 8 degrees it is not safe to assume that a larger set of nodes would resolve the problem. Indeed a classification test using the same size network for all 3 resolutions did not produce dramatically different results (figure 2.13, first column). However a further possibility is that increasing the sparsity of the input through a projection network could allow the images to become sufficiently decorrelated for reliable discrimination to occur. This approach was used in Ardin et al. (2016a) to provide an input of 2% sparsity for a Willshaw network, but testing with Infomax showed that an activation level of around 60% after projection was required before reliable route learning could be achieved. The network was trained with route images and then tested with the images from another ant route or the training set. The resulting values from the Infomax network are shown in figure 2.13, second column: a clear decision boundary can be seen for 8 degree resolution once the input is processed through the projection network. It is possible that decorrelation of inputs by projection is a neural tactic employed in order to achieve greater reliability in this task.

2.3.4 Skyline extraction

When the input is reduced to just a binary image representing the ground and vegetation against the sky, the network performs less well than with the grayscale image

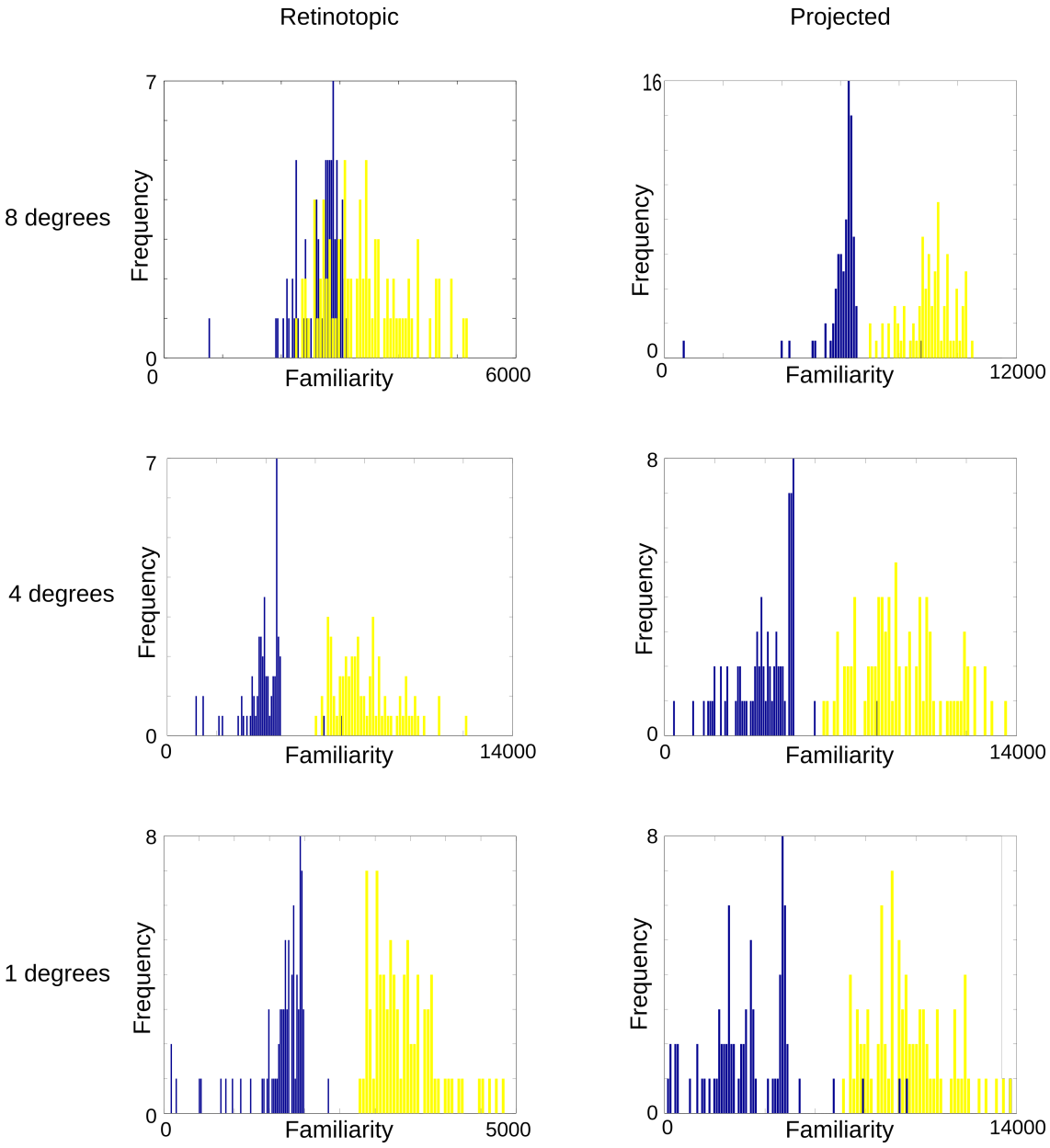

Figure 2.13: Using a projection network to decorrelate inputs into the network. First column, the network is tested when trained with untransformed input using the training data (blue bars) and images from another ant route (yellow bars). At 8 degree resolution the network has difficulty discriminating between the training and test images (top left chart). Second column, when the inputs are passed through a projection network, all resolutions allow discrimination between the training and test data. Note: familiarity values are relative to the network size and trained weights.

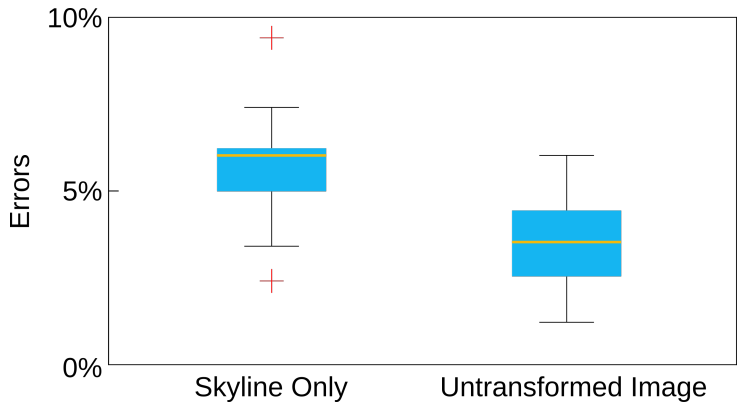

Figure 2.14: Effect of skyline extraction on navigation errors. Using just the binary image of the skyline provides performance which is similar to the results at this resolution and image separation for the grayscale image.

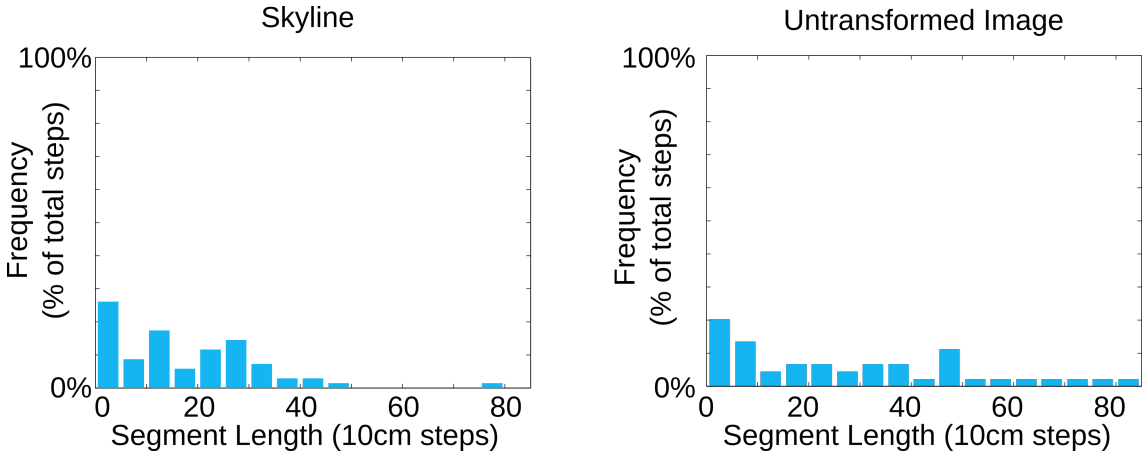

Figure 2.15: Effect of skyline extraction on segment length. The ability to follow long sections of path error-free is reduced over using the gray scale images, but one almost error free route is recorded.

(figure 2.14). Notably the ability to follow long (>40cm) segments reduces although one almost error free route is reproduced. It is impressive that with such a dramatically reduced input reasonable navigation is still possible, but it also indicates that while the skyline alone may be sufficient in some circumstances for continuous navigation, it is not as effective as the full image in this environment.

2.3.5 Centre-weighting

The results for each image mask are shown in figures 2.17, 2.18 and 2.19. Contrary to expectations changing the fade start point in the horizontal dimension did not affect

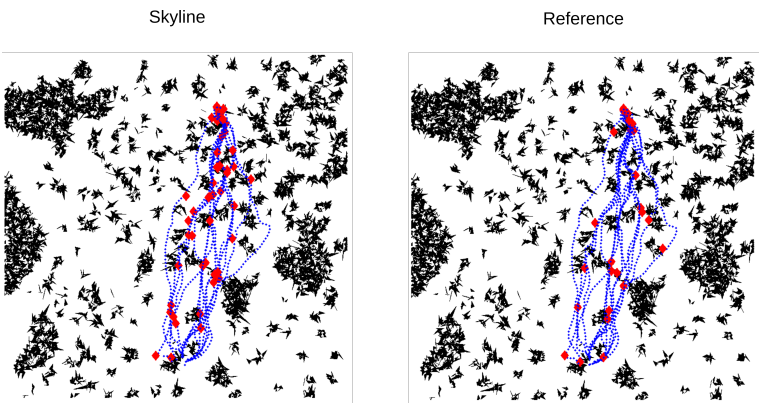

Figure 2.16: Error locations with skyline extraction. While the number of errors increases over the reference simulation, they are in similar locations close to vegetation.

navigation errors (figure 2.17, C and F against I) and similarly the lowest value of the fade start for the vertical dimension had no discernible effect on navigation errors (figure 2.17, B, E and H against I). However when the fader start point was increased for the horizontal dimension navigation errors increased significantly (figure 2.17, A, D and G against I).

2.3.6 Motion processing with an EMD

The low 3d complexity of the world combined with a 4 degree optical resolution meant that small spatial separations between images produced very small changes in the flow field, leading to sparse inputs (Figure 2.20).

Lower values for image separation, 0.5cm and 1cm, gave results consistent with the sparsity of the input for the network (figures 2.21, 2.22 and 2.23), with the lowest value performing at a level similar to random navigation. As the separation between images increased the number of errors decreases substantially (5cm and 10cm) but is still worse than the route learning without motion processing.

Tests of correlation of the motion-processed input show a range of r^2=0.65 to =0.79. This is much higher than that for the non motion processed images (r^2=0.41 for 4 degrees) and the conclusion is that the input sparsity is insufficient to allow the Infomax network to learn the patterns. The rate at which sparsity reduces as the separation between images grows (figure 2.20) shows that the activation level of the input is unlikely to increase substantially even if the images moved even further apart. At a gap of 10cm the spacing of the images is already higher than that estimated in the Introduction for the faster moving *Calliphora*. It is an interesting finding that the RSInfomax model

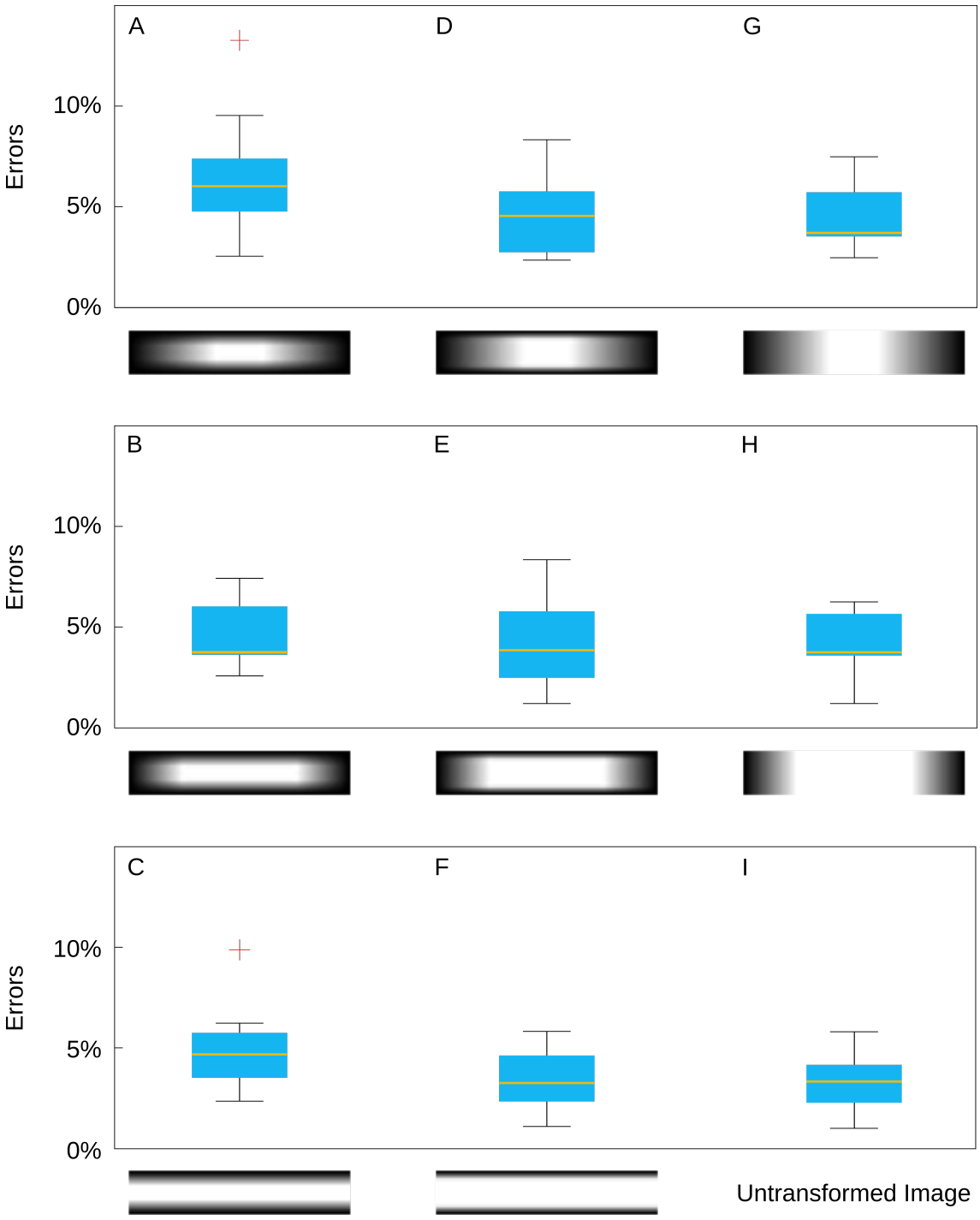

Figure 2.17: Effect of centre weighting on navigation errors. The boxplots are shown with the corresponding centre-weighting mask below: from left to right across columns the vertical fader increases, while the horizontal fader increases from top to bottom. The bottom right hand plot provides the reference simulation. Values in the first column A), D) and G) are noticeably different from the reference simulation I) indicating the extent of the vertical panorama is significant. Other masks do not have such an effect on the number of errors.

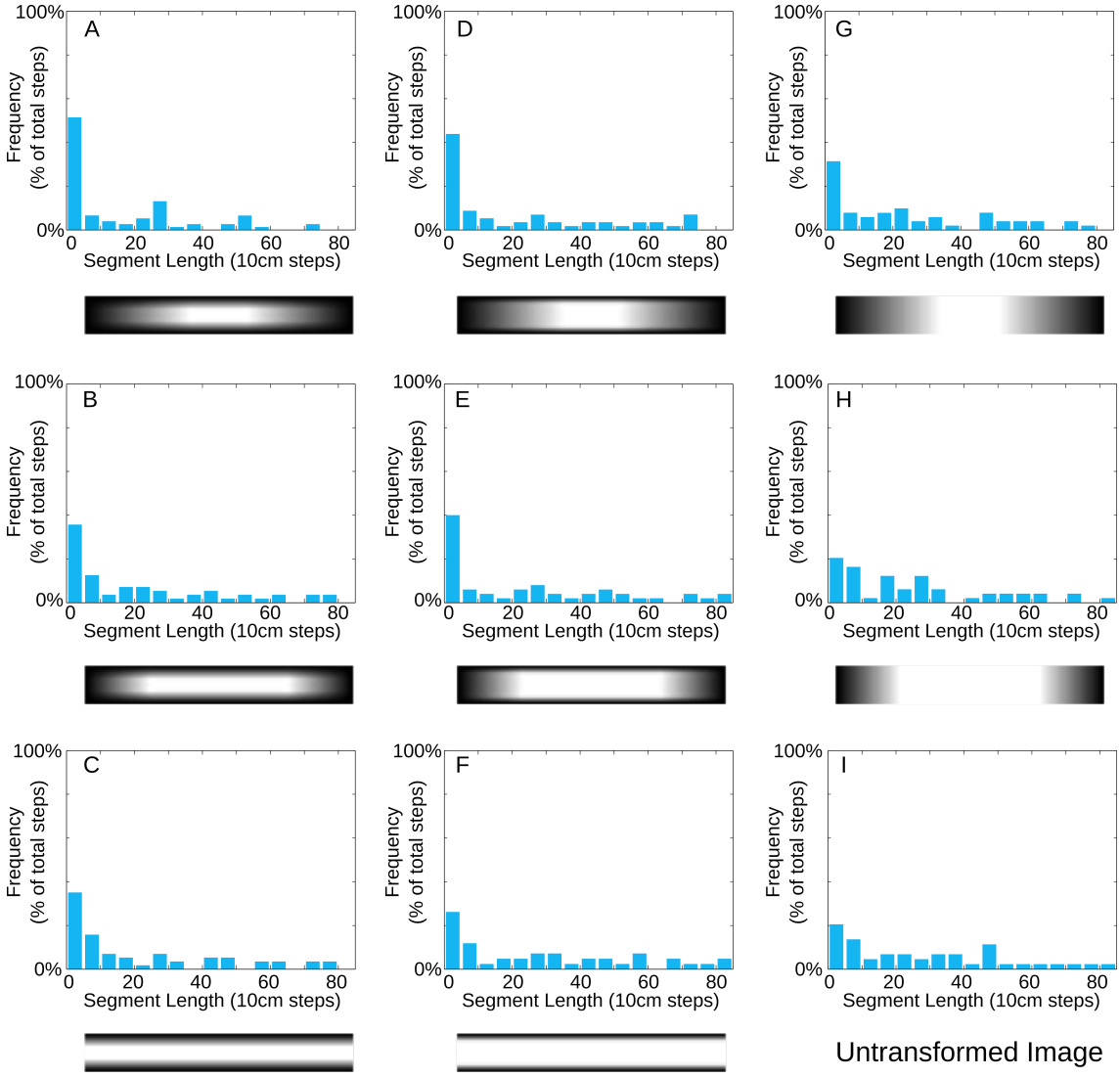

Figure 2.18: Effect of centre weighting on segment length. The number of short segments (<10cm) typically increases where a mask is applied, but in all cases some individual simulations can still reproduce long segments (<400cm). In C), F) and I) the effect of reducing the visual field becomes apparent: the distribution of segments is similar in F) and I) while the narrower field of view in C) produces notably more short segments (<10cm).

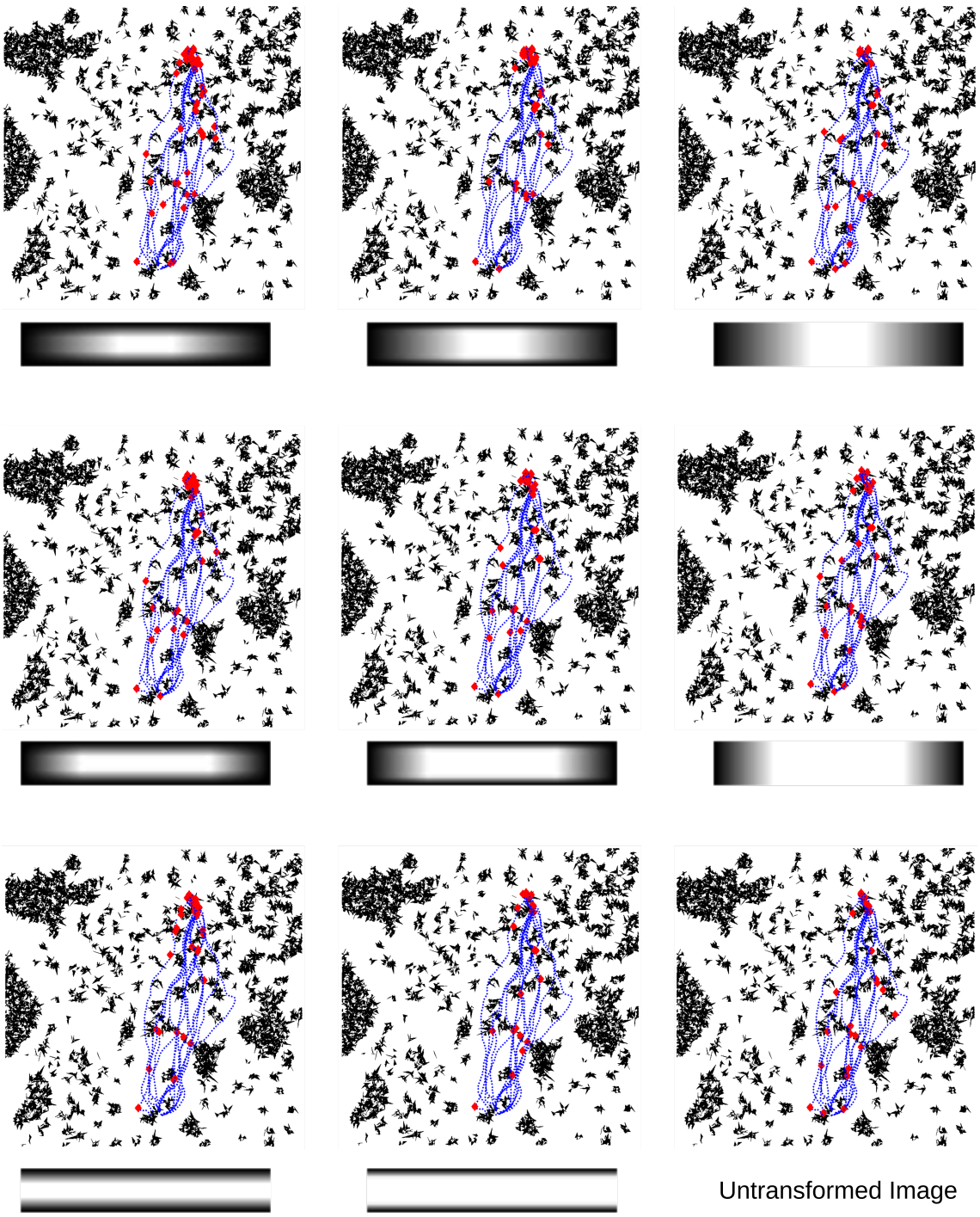

Figure 2.19: Location of errors with centre weighting. While masks affect the general performance of the simulations where errors occur is largely consistent with the reference.

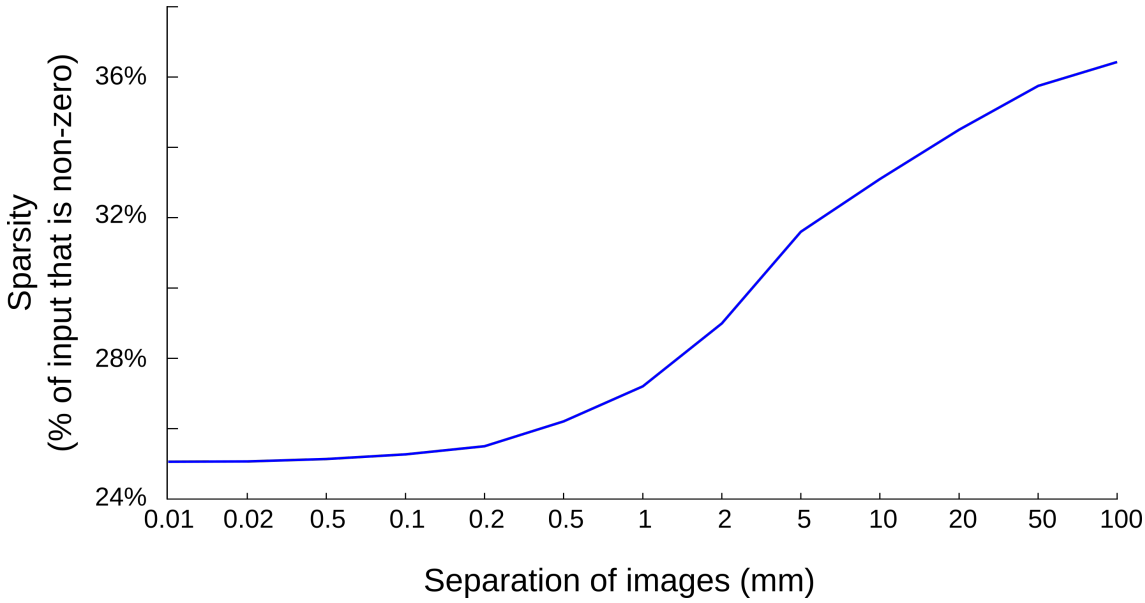

Figure 2.20: Sparsity of input by separation of images for motion processing. Over a wider range of image separation values than those used in the navigation task the relationship with input sparsity (the % of the input which is non zero) becomes clear. In the simulated world small changes in position yield negligible changes in the image generating few motion vectors, but as image separation approaches 100mm the change is maximised in the inputs giving a larger vector field. However this vector field is still only 36% of the activation of the full image.

requires dense inputs as motion processing is a key component of the visual pathway.

2.3.7 Input correlations

Correlation in the inputs presents an issue to all machine learning algorithms, and we have seen that by using a projection network to reduce correlation the performance of the RSInfomax can be restored (figure 2.13). The extent to which the input correlation is affecting the simulation is shown in figure 2.24 where the similarity of the processed images is plotted against the mean error rate. For the set of resolution and image separation tests and EMD the relationship is quite clear - increasing image similarity is a factor in performance although clearly not the only one. Where images are centre-weighted, similarity and error rates are relatively consistent. However the skyline simulation shows that while the input may be highly correlated, as would be expected in a binary image of the horizon, it can still be used effectively for navigation.

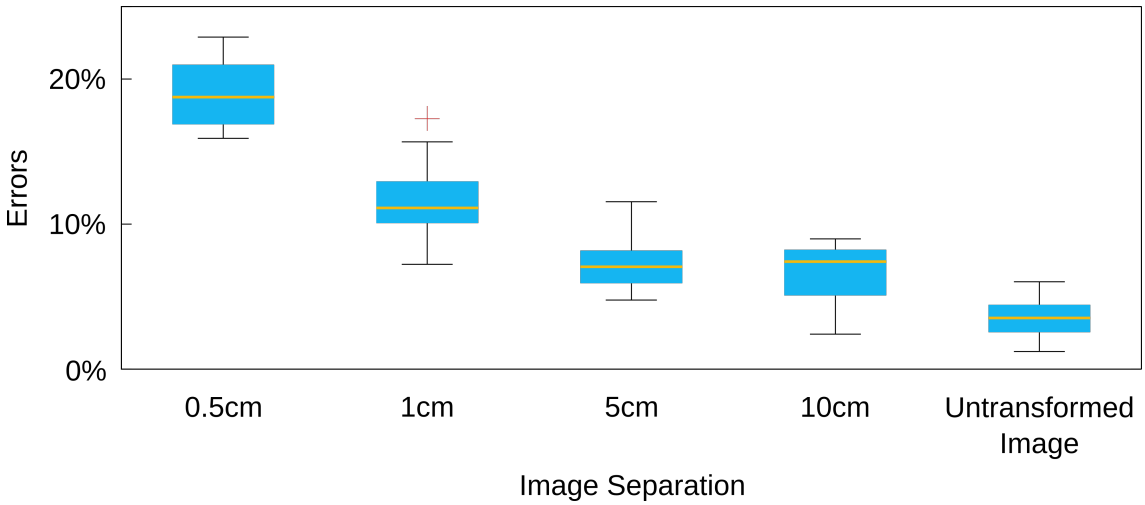

Figure 2.21: Effect of motion processing on navigation errors. Closely spaced input images into the EMD model give substantially more errors than the reference, a result of the sparsity in the input (figure 2.20).

2.3.8 Relevance of error locations

Failures in route following did not appear to be randomly distributed across the routes irrespective of the model of visual processing. Calculation of the RSInfomax values for a trained network where each scan is performed on the route is uninformative (figure 2.25 gives an example) - some features of the route are visible such as the presence of the more open area in the last third of the routes, but it is not possible to directly relate the relative values to error locations. However a more prosaic analysis is helpful. All ant routes pass through foliage in the vicinity of 10 to 20 cm of the feeder and small changes in position in this area of the environment will naturally lead to extensive changes in the visual scene, with the corollary observation that no simulation performs well in the early stage of the navigation. A further common feature is that few errors tend to occur in the last third of the ant routes where the density of vegetation is substantially less. Where errors do occur in this region they tend to be close to an isolated tussock located half-way through the section (e.g. figure 2.10, resolution 4 degrees, training step size 10cm). This is found in the majority of processing variants but very notably not for the 8 degree resolution eye (figure 2.10, resolution 8 degrees, training step size 10cm). In this case there are a higher number of errors in this region and it seems likely that these are the result of the inability of the low resolution eye to resolve enough detail in mid to far visual range to reliably select a direction. It is self-evident that eye resolution may be more important for orientation where features in the visual

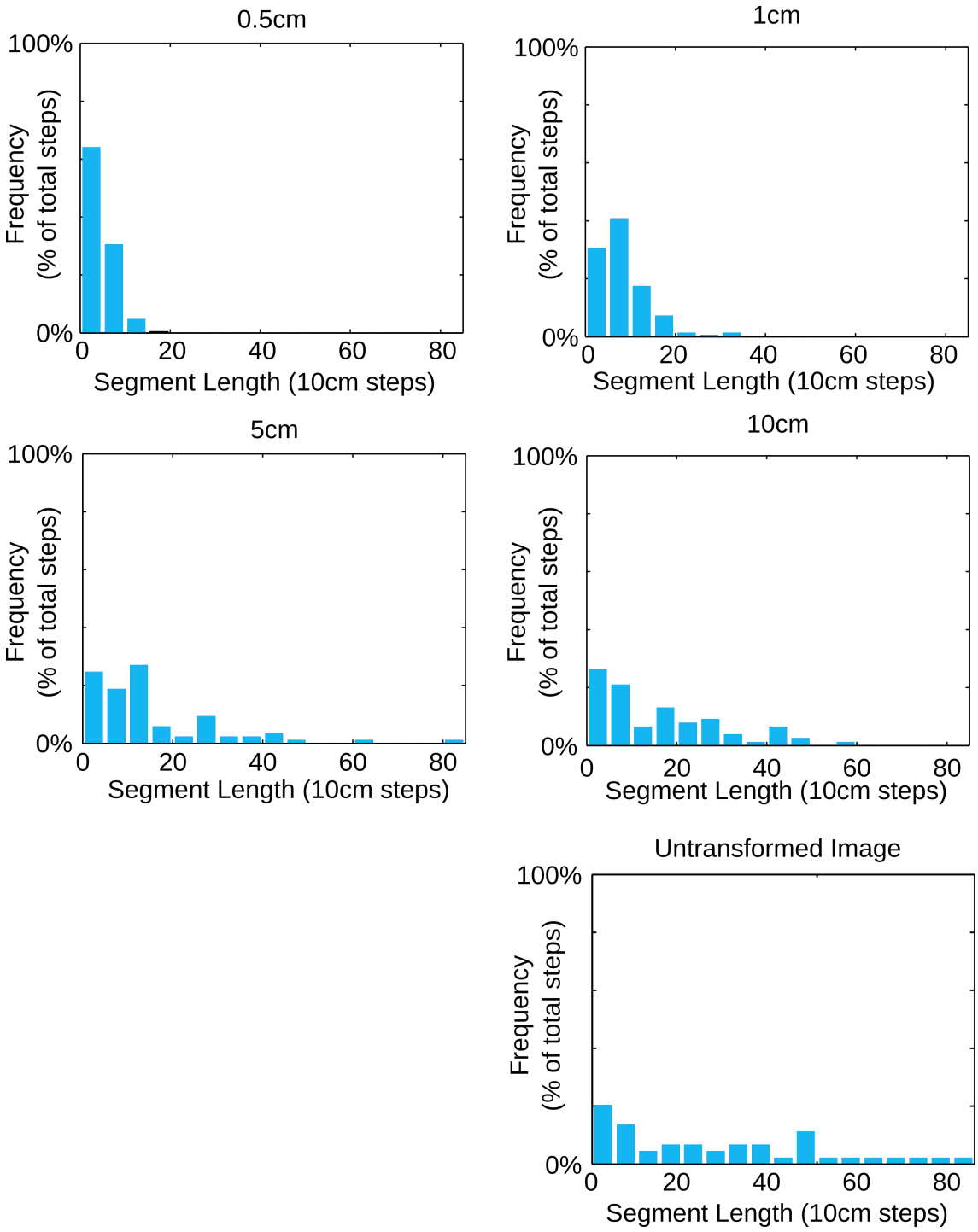

Figure 2.22: Effect of motion processing on segment length. Consistent with the number of errors the distribution of segment lengths grows as image separation increases in a predictable fashion.

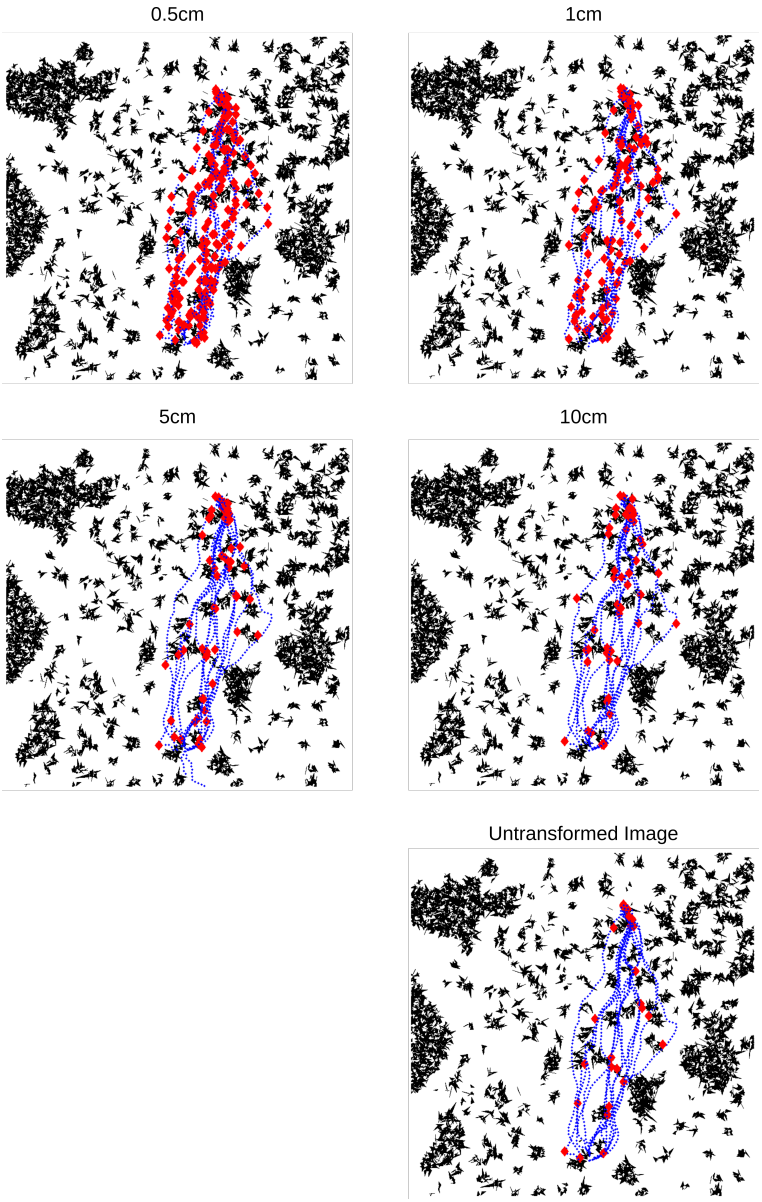

Figure 2.23: Error locations with motion processing. At the shortest image separation errors are distributed uniformly but as separation increases the pattern becomes closer to the reference with locations clustered at particular points in the environment.

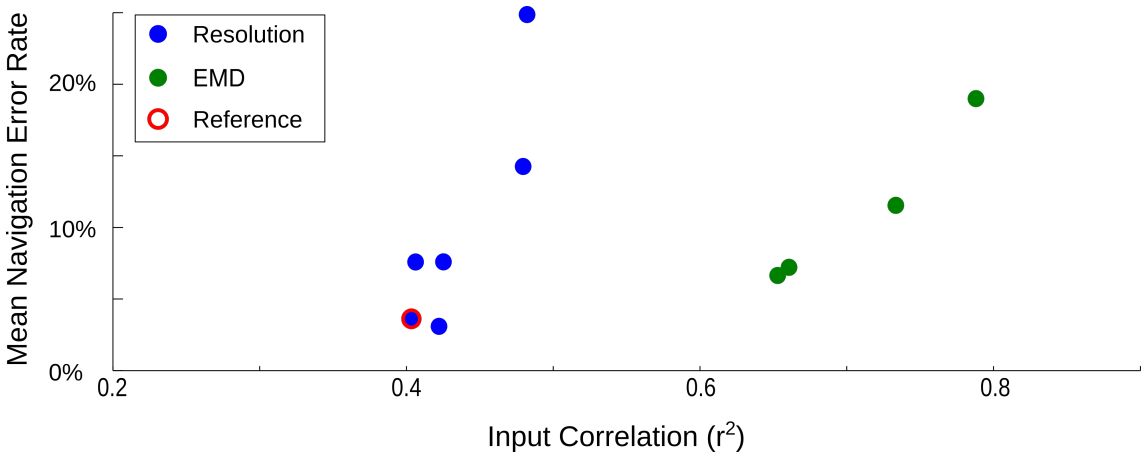

Figure 2.24: Relationship between input correlation and error rate. Error rates for resolution and EMD image processing are shown alongside the correlation of the input. The selected reference combination of 4 degree resolution and 10cm image separation is shown with a red circle. Different image processing is not directly comparable due to the difference in sparsity of the input but the relationship within processing simulations for resolution and EMD is quite clear - increasing input correlation increases the error rate.

scene are further away. In general errors seem to occur in proximity to vegetation and where there are the most substantial changes in visual scene. This is perhaps a little counter-intuitive in a continuous visual process where clear visual landmarks should make localisation simpler but may reflect more on assumptions about the input. The passage close to vegetation leads to substantial changes in the retinotopic pattern, and small deviations from the route will lead to equally large changes in the pattern. If the ant is using just this pattern and is not extracting features or landmarks from the environment, unless there is a strong correlation between the route image and one which is slightly displaced, there is no reason why the presence of nearby vegetation would be of benefit. Figure 2.26 shows the values of r^2 for a reference image marked by a blue star against images at the same orientation in a surrounding 21cm grid at locations in the simulated ant environment which are either far from or close to foliage.

This points to a conundrum at the heart of the continuous image matching approach in this environment. Locations in the world which produce more dissimilar (less correlated) inputs should be easier to learn and recall, but accurate recall is dependent on being able to closely match the viewing location and heading of the stored image. In practice the animal wants to have distinctive enough images to allow robust learning occur, but sufficient tolerance to allow for deviations in the route which still allow the

nest to be recovered.

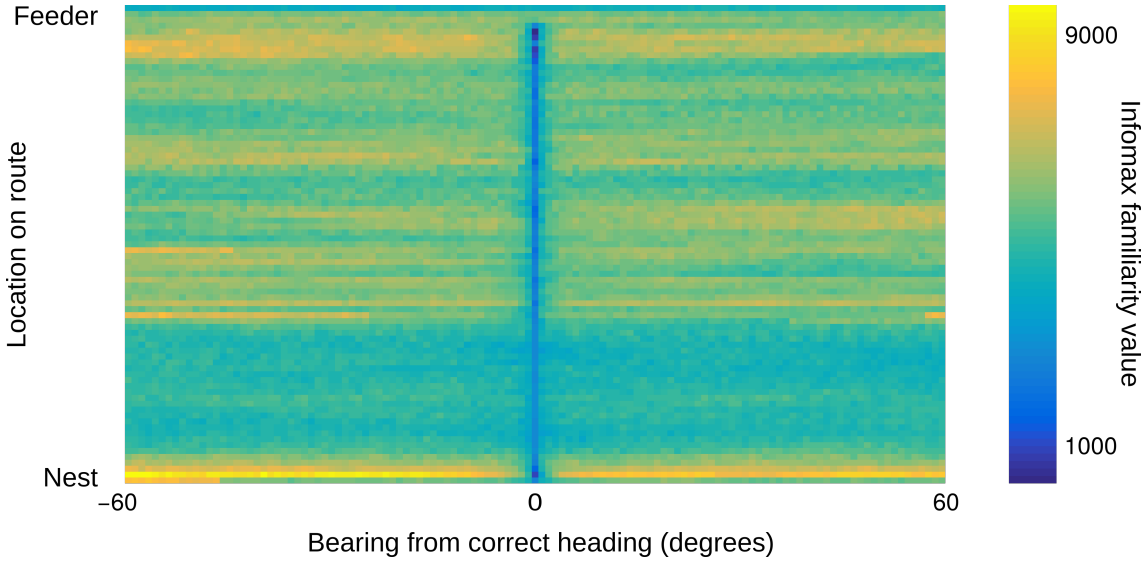

Figure 2.25: Infomax values along an entire ant route. The plot shows the familiarity score for a trained network scanning across +/-60 degrees along the learnt route of the ant from figure 2.1. The most familiar heading is clearly seen at 0 degrees along the route. Comparing with the reference simulation map (figure 2.12) areas where familiarity is generally low correspond to the more open area in the final third of the ant routes. However errors seldom occur in this area, and instead appear more frequently in areas where the RSInfomax algorithm should more reliably determine direction.

2.3.9 Variable training step sizes

Increasing the training step size in RSInfomax improves performance (figure 2.10) which we noted may be due to the interaction of the input correlation with the capacity of the network (figures 2.24 and 2.26). Decreasing the number of memories and specially selecting those which have particular salience could improve navigation performance and could be seen to be consistent with the use of local vectors and tagging of memories (Collett et al., 1998; Åkesson and Wehner, 2002). By implication this is a move away from continuous image matching towards a mediated approach the mechanism for which remains elusive (Smith et al., 2007) but it is still interesting to consider whether such a mechanism could operate efficiently in the simulated ant world.

In order to test the practicality of this theory an example ant route was decomposed into 13 segments using 12 locations, determined by the points at which a turn greater than 20 degrees had occurred (figure 2.27).

An Infomax network was trained with the 12 locations and then tested with images from scans of +/-60 degrees at 2cm points on a 41cm grid around the trained locations. On the assumption that the ant aims to get to a target zone defined as an area of an arbitrary 5cm radius of a trained location, a path must be followed which falls within a triangle defined by the distance that must be travelled from the current location to the next location and this arbitrary radius. In this case the maximum allowable deviation in the trajectory is given simply by:

$$r_{ij} = arctan\left(\frac{c}{H_{ij}}\right) \tag{2.5}$$

where r is the maximum allowable deviation, c is the radius (5cm) around the trained location and H is the Euclidean distance from the origin i to the target j. Figure 2.28 shows the results from this simulation. Where the Infomax network selects a heading which exceeds the correct heading by a value greater than the maximum allowable deviation, the area is coloured white, while values which will lead to the area around the next trained location are shaded in values of grey to black scaled according to maximum allowable deviation. Where the stored locations are close, the deviation in the trajectory can be large but as distances increase catchments become smaller suggesting there may be an optimal distance between locations which maximises recognition and the ability to reach the next waypoint.

Such an account is interesting in that it is consistent a wide range of the observed behaviours including normal route following, route deviations (as location to location paths are guided by PI) and intermittent scanning behaviours along the route, but in the movement away from continuous image matching it raises the substantial problem of managing the transition between stored locations.

2.3.10 Specific error states in real ant routes

Reviewing the ant routes recorded by Mangan and Webb (2012) the hypotheses we have considered so far may have difficulty reproducing some of the unique errors observed. Multiple inward routes were recorded for the same ant showing path development from what one must assume is the initial trajectory, and source of the visual memory, through various alternates and highly specific error patterns (figure 2.29). Of these closed loops occur in 3 ants, with a total of 4 examples across 133 routes (3% of the total) - they are rare but distinctive comprising a deviation from the normal path followed by an almost circular segment until the path is re-encountered. Crucially they

are not like either backtracking (Wystrach et al., 2013b) or systematic search (Müller and Wehner, 1994) which seem to invoke more stereotyped behaviours. An example is given in figure 2.29, showing routes 1, 2, 7 and 9 of ant 1. In route 2 there is an error at the location marked 1 where the animal deviates to the right instead of the left of a tussock, which under the variable step size model would quite easily be explained as obstacle avoidance and then reacquisition of the route under PI correction. However for routes 7 and 9 this is not plausible - in both cases the animal deviates to the wrong side of a tussock at location 2/3 which then appears to disrupt the heading following. If PI was being used to correct these deviations then as in route 2 then there would be a correction after the tussock bringing the ant back to the path. A form of celestial navigation does appear to be in operation as the animal seems to be able to form a perfect circle in a novel area, a feat which is easy to accomplish when using a compass. Routes 7 and 9 can also be interpreted to give evidence that visual navigation is not continuous. We might expect that the visual memory is updated by the error at location 2 on route 7, but route 9 follows a different direction which is not predicted by either the route 1 or route 7. Subtle changes in placement around location 2 may lead to a different heading being selected, but this would indicate a surprising level of fragility in direction finding which is not consistent with the variation seen in across repetitions of the other ant routes (Mangan and Webb, 2012).

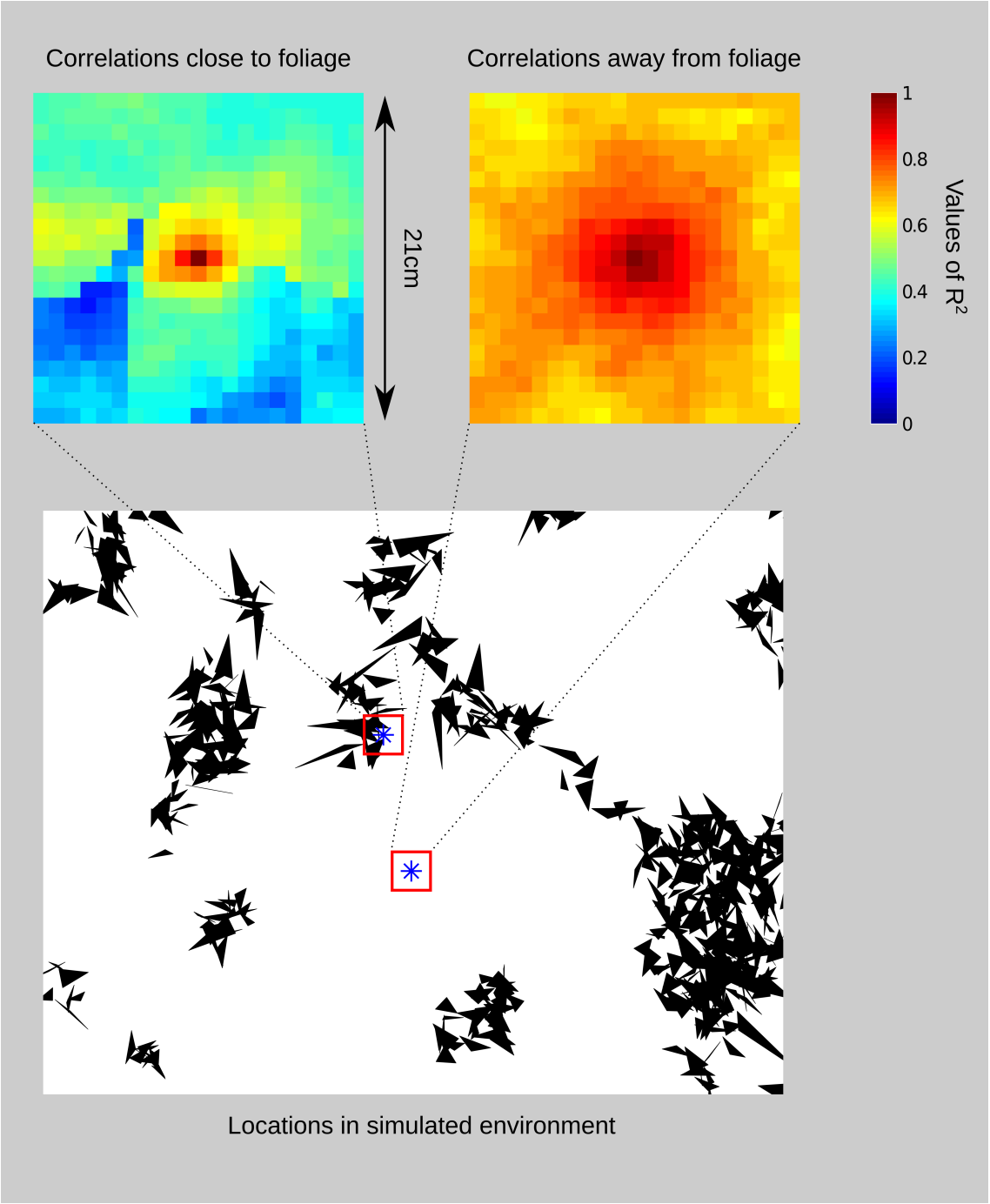

Figure 2.26: Input correlations in open and highly vegetated areas. The infomax values in figure 2.25 become more intelligible with examination of the change in images around locations close or far away from vegetation. The two upper plots give the values for r^2 for reference images against images in a surrounding 21cm grid. The lower plot indicates the location of the reference images with a blue star and the catchment of the comparison images is soon with a red box, with one location far away from foliage while the other is placed in a dense area. Being close to vegetation gives high specificity of a location but only if close to the reference point. If repositioning onto the learnt route is not exact distance from the landmarks gives greater tolerance in the match.

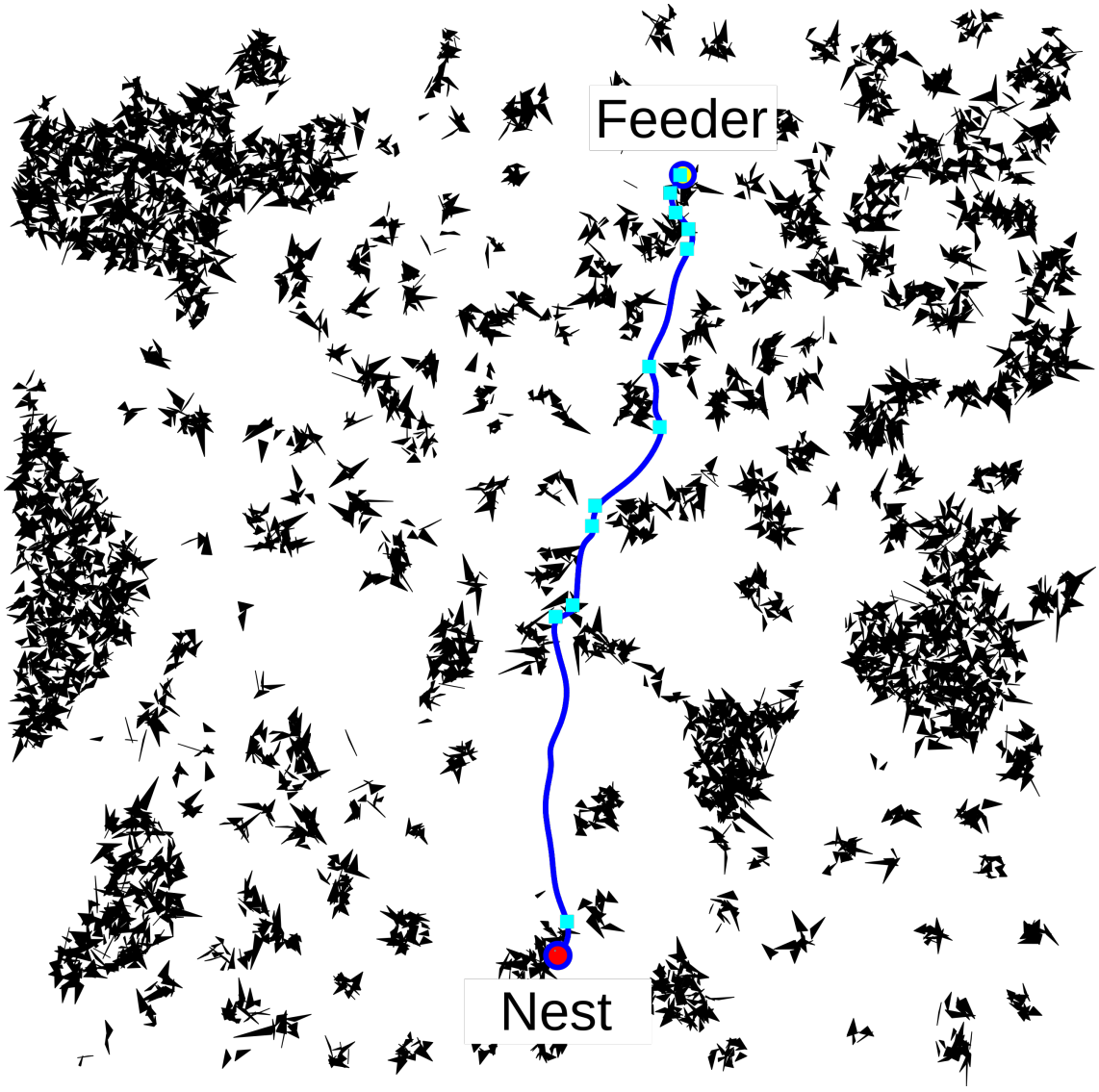

Figure 2.27: An ant route is split into 13 segments using the points at which a turn of greater than 20 degrees has occurred, indicating significant reorientation. Blue boxes show the location of the 12 turning points which largely appear in areas of dense vegetation.

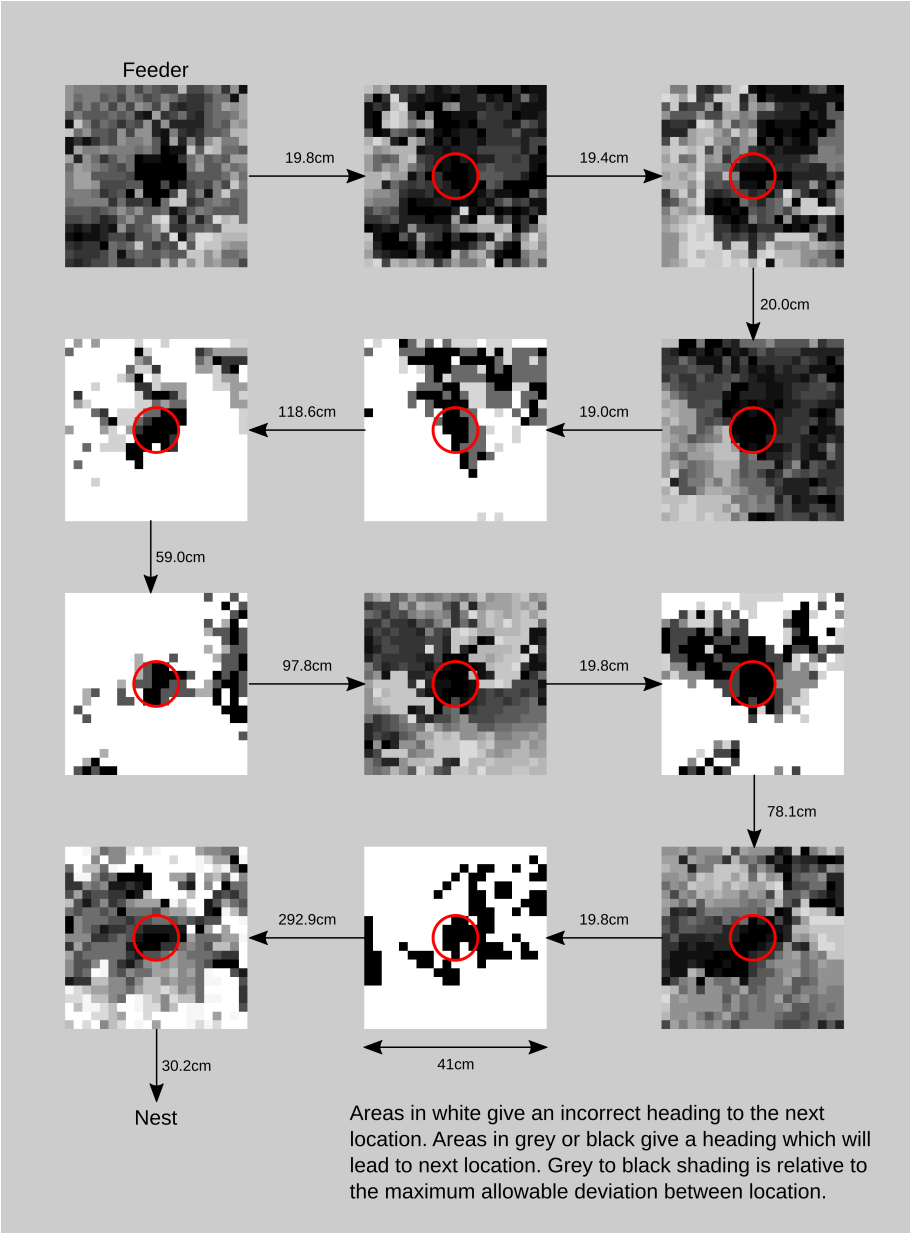

Figure 2.28: Can familiarity catchments provide accurate way-finding with variable step sizes? The ability to select a correct heading to the next stored location was tested across 12 selected locations along an ant route. At each trained location the network was tested across a scan of +/-60 degrees on a 2cm grid in a 41cm catchment areas, and the preferred heading angle recorded. The preferred heading angle was then compared to the correct heading to the next location plus or minus the maximum allowable deviation to get to the 5cm target radius around that location. Areas in grey to black give a heading which should lead to the next target zone (see text), while the white areas will not provide a sufficiently accurate heading. Target zones are marked by the red circles and in most cases the overlap appears to be sufficient for familiarity-based way-finding to be successful.

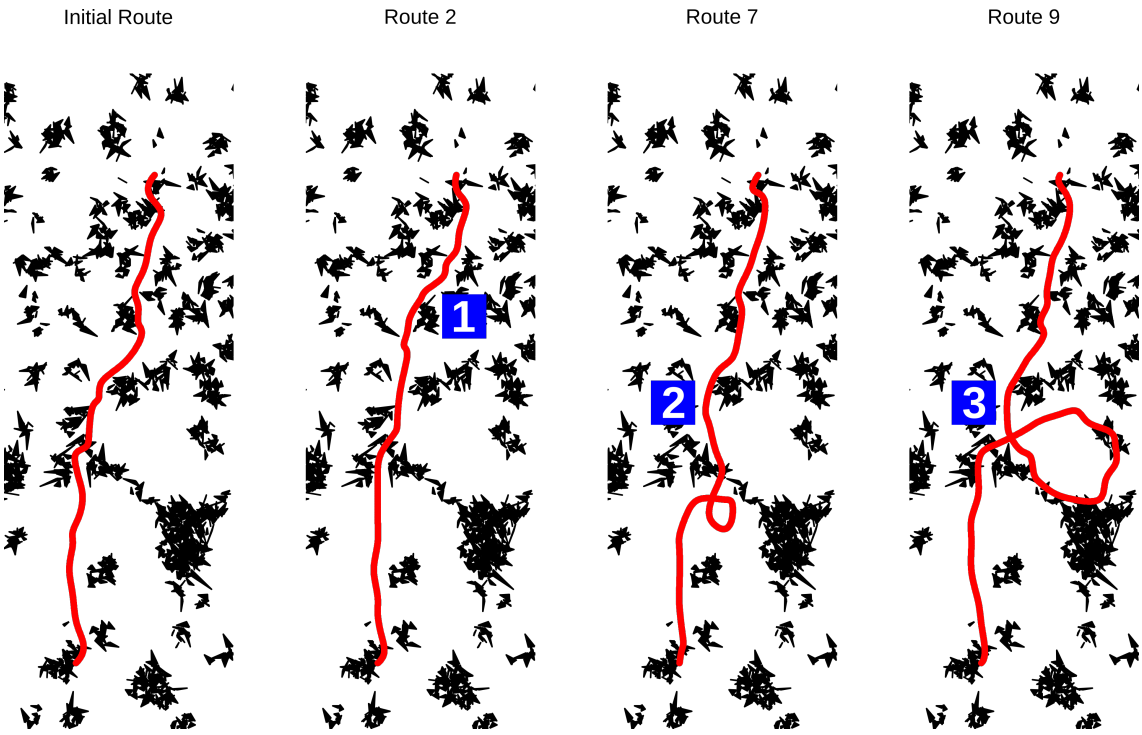

Figure 2.29: Variability and errors in a single ant route. The same ant was followed over numerous zero vector recapitulations between the feeder and the nest (Mangan and Webb, 2012) and displays variations which are difficult to account for with exclusively visual navigation. In Route 2 an error occurs at location 1 but once this has been recovered the rest of the path is successfully followed. But for Route 7 a deviation at location 2 causes the animal to emerge into an open area at the wrong point resulting in a carefully executed loop. Route 9 suffers from a deviation at the same point as Route 7 but results in a wider loop.

2.4 Discussion

RSInfomax in this simulated environment performs at least as well using the untransformed retinal input compared to any of the other tested processing variants. This is an interesting result as this algorithm has been shown (in the case of direct retinal input) to be effective at recapitulating routes, and the simulated processing steps are consistent with additional processing that occurs in the visual pathway before the putative neural structures of navigation.

Understanding the reasons why this additional processing does not improve performance with a model of continuous navigation can shed some light on the direction for further research. Analysing the failures draws us into some areas which are revealing.

The RSInfomax model is a machine learning technique which has the common interaction of input similarity, classification performance and capacity (Lulham et al., 2011). Simply put as the input becomes more correlated, discrimination will become worse and/or capacity will be reduced. Figure 2.3 shows the correlations for the inputs created by the various processing steps against the mean errors during navigation and we can also note that performance reduced when the memory load increased with a smaller step size (figure 2.10). If navigation is truly continuous it places considerable pressure on the visual pathway to generate dissimilar images which can then be used to reliably determine heading. But is this necessary or would it be simpler to store fewer images?

Observation of ant routes shows that there is a reasonable degree of tolerance in position even though the routes clearly follow the same general path through the environment. Image difference function gradients might explain how the animal can relocate the route after displacement using a previously stored view (Zeil et al., 2003) and RSInfomax alongside other models has been shown to exploit these gradients to allow recovery of minor deviations (Ardin et al., 2016a). It may be the case that the animal does not store a fully continuous memory but rather a series of points separated by a distance below the level where the navigation process can reliably extract a heading. Certainly having a system which is built around a certain level of noise is beneficial and this suggests that alongside high levels of visual resolution (Wystrach et al., 2016) high levels of sampling resolution may not be advantageous.

Indeed ant route following is not exact, and not only in that it allows deviations within a visually similar route corridor, but also divergence along visually distinct paths in the same general heading (figure 2.29, routes 1 and 2). This phenomena is

widely displayed in the routes recorded by Mangan and Webb (2012) although the causes are not clear. It is tempting to suggest that they reflect periods where visual homing is subordinated to the celestial compass, but further experiments would be needed to explore this proposition.

As a sidelight we should consider the effect of sparsity in the input on RSInfomax. Optic flow fields generated with a biologically inspired EMD produce sparse images as little changes over small spatial displacements. Wider image separation has the effect of producing substantial changes across the visual field, but the vector field no longer accurately reflects the 3d structure of the environment. Figure 2.20 shows the relationship between input sparsity and image separation, plotted against the errors from the navigation simulation, demonstrating a close relationship between these variables. If visual input into navigation is in the form of sparse activation, the current RSInfomax model is unlikely to produce good results.

What then should we conclude about the effect of low-level visual processing? The demonstration that additional processing does not improve the results for RSInfomax could just be exposing the limitations of this algorithm in describing continuous visual navigation, or perhaps it reopens the question of whether visual route following is a process of continuous image-matching. As ants move through the environment they are subject to considerable displacement by the interaction of locomotion with the substrate. If at each step of movement the ant is comparing the current view with a stored memory it will need to be able to accommodate this disturbance, either by employing mechanisms to control the “noise”, or by being sufficiently tolerant to the effects of ego-motion.

Chapter 3

How variation in head pitch could affect image matching algorithms for ant navigation

3.1 Introduction to the paper

This chapter explores the degree of head movement in ants moving in their natural environment and examines how this could affect current simulations of visual navigation. Video recordings in the field site revealed that the pitch of the ant's head could vary across a range of up to 20 degrees without a load and by 60 degrees when carrying a food item. This range of head pitch distorts the visual input sufficiently to make image-matching difficult or impossible and can disrupt a continuous image-matching navigation algorithm.

In the previous chapter the effect of processing of the retinotopic image was examined to test the effect on simulated ant navigation. Motion processing performed much worse than denser representations, an important result as the desert ant typically moves at high speed and it is natural to assume, as with the flying hymenoptera, that it would routinely use optic flow in visual navigation (Ronacher and Wehner, 1995). While it is not possible from the results to decide whether the relatively weaker performance of optic flow was due to the features of the RSInfomax algorithm or simply does not feature in the ant's navigational toolkit, the results from related species support the conjecture that the character of the animal's motion could be relevant to how it undertakes navigation (Dittmar et al., 2010).

Preliminary investigations showed that the simulated ant-world images become

quickly dissimilar as roll and pitch angles were changed. Yaw was discounted from this analysis as image rotation in this axis is used as the means to determine heading for rotational scanning visual compass algorithms and is a known behaviour of the ant (Graham and Cheng, 2009b). An example is given in figure 3.1: the RMS IDF was calculated between a level image and images at +/-45 degrees of roll and pitch using the antworld from (Ardin et al., 2016a) with the dotted line box showing the range of +/-10 degrees. In the area outside the box the IDF gradient is weak or non-existent and by implication matching to a reference view would be difficult.

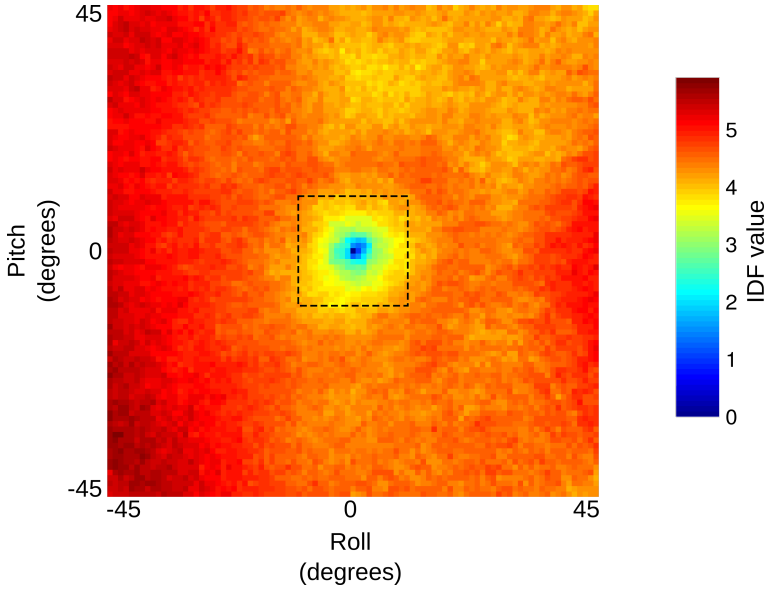

Figure 3.1: Example of the effect of roll and pitch on image similarity at the non-vegetated location in figure 2.26: the view direction in a simulation was changed across both +/-45 degrees of pitch and roll with the dotted line box showing the area of +/-10 degrees. Even moderate displacements of the head show that retinotopic image matching will be extremely difficult.

With this information it was deemed significant to know if ants were subject to changes in the position of the head while walking or if there was mechanical stabilisation of the head to avoid disruption of the visual input. Limited information was available from previous research in a natural environment and was based on the species native to the flat and relatively featureless salt pans of Tunisia where visual disruption might have been attenuated (Duelli, 1975). Therefore primary research was undertaken at the field site in Sevilla with *C. velox* the data from which could then be incorporated without qualification into the simulated ant-world based on the same species and environment.

Incorporating any observed change in the orientation of the ant's head allowed models to be validated with natural motion, but also provided insights into broader issues in visual navigation such as the need for continuous visual processing or sensory abstraction. The attached paper reports the results from the field work and consequently various simulations. It is highly significant to this thesis as it shows that there is substantial variation in head pitch which if used as the input to continuous visual image matching can disrupt navigation.

J Comp Physiol A (2015) 201:585–597
DOI 10.1007/s00359-015-1005-8

ORIGINAL PAPER

How variation in head pitch could affect image matching algorithms for ant navigation

Paul Ardin · Michael Mangan · Antoine Wystrach · Barbara Webb

Received: 28 October 2014 / Revised: 19 March 2015 / Accepted: 21 March 2015 / Published online: 21 April 2015

Abstract Desert ants are a model system for animal navigation, using visual memory to follow long routes across both sparse and cluttered environments. Most accounts of this behaviour assume retinotopic image matching, e.g. recovering heading direction by finding a minimum in the image difference function as the viewpoint rotates. But most models neglect the potential image distortion that could result from unstable head motion. We report that for ants running across a short section of natural substrate, the head pitch varies substantially: by over 20 degrees with no load; and 60 degrees when carrying a large food item. There is no evidence of head stabilisation. Using a realistic simulation of the ant's visual world, we demonstrate that this range of head pitch significantly degrades image matching. The effect of pitch variation can be ameliorated by a memory bank of densely sampled along a route so that an image sufficiently similar in pitch and location is available for comparison. However, with large pitch disturbance, inappropriate memories sampled at distant locations are often recalled and navigation along a route can be adversely affected. Ignoring images obtained at extreme pitches, or averaging images over several pitches, does not significantly improve performance.

Keywords Navigation · Route following · Ant · Pitch · Retinopic matching

Abbreviations

IQR Interquartile range. The difference between the 75 and 25 % percentiles of the data

rIDF Rotational image difference function. The resulting function produced after computing the image difference between a reference image and the current view across a defined rotational range

Introduction

The field of neuroethology owes a great debt to the pioneering work of Prof Rüdiger Wehner. Of particular note are his studies of navigation in desert ants, which have been fundamental in revealing how a 'toolbox' of simple mechanisms gives rise to complex guidance behaviour (see Wehner 2008 for review). His work also laid foundations for the emerging fields of computational biology and biorobotics by providing benchmark behavioural assays against which functional hypotheses, embodied as computer programmes, can be verified.

An example of his lasting legacy is found in the observation of visual homing behaviours in desert ants (Wehner and Räber 1979; also reported in bees by Cartwright and Collett 1982, 1983), which inspired the long-standing hypothesis that insects store visual memories retinotopically, allowing the animal to return to a location by moving so as to increase the retinotopic match between what they currently see and their memory. This concept inspired a family of computational models able to reproduce visual homing behaviour in various experimental scenarios (Cartwright and Collett 1983; Hafner 2001; Möller 2001; Stürzl and Mallot 2006; Vardy and Möller 2005; Zeil et al. 2003). The same retinotopic principle has been in used in the 'visual compass' or 'alignment image matching' hypothesis

Electronic supplementary material The online version of this article (doi:10.1007/s00359-015-1005-8) contains supplementary material, which is available to authorized users.

P. Ardin · M. Mangan (✉) · A. Wystrach · B. Webb
School of Informatics, University of Edinburgh, 10 Crichton St, Edinburgh EH8 9AB, UK
e-mail: mmangan@staffmail.ed.ac.uk

for recovery of heading direction (Zeil et al. 2003; Collett et al. 2013), i.e. that the heading direction when an image was stored can be recovered by physically rotating to find the minimum in the image difference. Coupled with dense storage of multiple images, this has recently been shown to be an effective method (Baddeley et al. 2012) for recapitulating routes in complex environments as observed in ants (Kohler and Wehner 2005; Mangan and Webb 2012; Wehner et al. 1996). The scanning behaviour that has been described in ants (Wystrach et al. 2014) is also consistent with the assumption that they are attempting to find a retinotopic match, rather than being able to recognise a rotated image.

These algorithms have been shown to work in simulation, and in some cases on robots, but are not always challenged with realistic stimuli as experienced by the ant in its natural habitat. For example, in our own field studies of *Cataglyphis velox* following routes through scrubby undergrowth, the highly cluttered environment lacks any distinctive or consistently visible landmarks (Mangan and Webb 2012). Algorithms are often tested with higher resolution than the eye of an ant (inter-ommatidial angle around 4 degrees), or with complete omnidirectional views, whereas the ant has a significant rear blindspot (Schwarz et al. 2011; Zollikofer et al. 1995). Additionally, few of these tests take into account the potential noise or alteration of the view due to the ant's movement over uneven terrain, which might invalidate the retinotopy-based methods outlined above. To quote Wehner '… the snapshot is fixed relative to retinal coordinates and does not rotate within the ant's head to compensate for changes in the orientation of the animal's longitudinal body axis… This has important implications. If the snapshot is retinotopically fixed, and if it should later be matched to a current retinal image, this match can be accomplished only if the animal assumes the same orientation of its body as it did while acquiring the snapshot' (Wehner et al. 1996). Note that this requires 'the same orientation' of the head in all three axes: yaw, pitch and roll.

If moving on uneven terrain causes the ant's head to experience pitch and roll, this could affect the projection of the view onto the retina and hence the crucial information available about yaw orientation. Early reports of head stabilisation in navigating ants (Duelli 1975; Wehner and Räber 1979; Wehner et al. 1992) lack detailed analysis. More recent data suggest that even when walking on flat terrain the ant's gait does not keep the head completely level (Reinhardt and Blickhan 2014). The latter result is for the wood ant *Formica polyctena*, but a similar range of movement can be measured for the desert ant *Cataglyphis fortis* running on flat ground (Steck et al. 2010; supplementary video). Desert ants inhabiting the extremely flat salt pans of North Africa might experience little additional substrate-induced disturbance, but many ants use visual memory in habitats with more uneven terrain, or even extreme conditions such as rough undergrowth and rainforest (Harrison et al. 1989), where walking up, down and along vegetation is necessary and will strongly affect posture. Ants have also been reported to successfully home (although possibly using path integration alone) when amputation of two legs leads to continuous stumbling (Steck et al. 2009). Head pitch is also influenced by the need to balance the load being carried (Moll et al. 2010); evidence that the posture is altered by the mass of a load is given in (Zollikofer et al. 1995) although the direct effect on head angle was not measured. Other studies have suggested that pitch compensation when walking on slopes is also far from complete, with a change in slope from −75 to +75 degrees inducing a change in the average caput-substrate angle of less than 40 degrees in *C. fortis* (Weihmann and Blickhan 2009). It is similarly reported in (Wohlgemuth et al. 2002) that 'during ascent and descent walks (for slopes of 54 or 24 degrees) the ants had their heads inclined (relative to the skylight pattern) at an angle that differed from the one kept on even ground' (p. 277).

These latter two studies show that the average head pitch relative to gravity or the horizon is substantially affected by the substrate for large-scale terrain features, but not the extent to which rapid variation in pitch might be induced by an uneven ground surface combined with the ant's gait, or whether the ant stabilises its head at this time scale (note Steck et al. 2009 find that regular corrugations in terrain at 12- to 25-mm spacing are not compensated by gait adjustment). In this paper, we observed variance in head pitch using high-speed close-up videos of ants running, with different loads, over natural terrain. As we report, there is substantial variation and little evidence of stabilisation. We then use realistic modelling, with 'ant-eye' filtering of images taken from a 3D reconstruction of our field site, to assess whether the observed degree of pitch variation would have a significant effect on the ability of ants to recover heading direction from image matching. We also assess the effect of the induced error on the ability to follow routes through cluttered natural environments, under the simplifying assumption that the ant's storage or matching of images is not directly linked to knowledge of its current head pitch. We revisit this assumption, and consider alternatives, in the discussion.

Materials and methods

Head pitch analysis

At a field site on the outskirts of Sevilla, Spain (37°20N, 5°59W), ants of the species *Cataglyphis velox* were trained to a trap feeder positioned approximately 2 m from the nest,

where they were provided with cookie crumbs of various sizes. The direct route back to the nest was through a channel made by embedding two white plastic boards approximately 10 cm apart in the ground. Consequently, the ants were still running over their natural (earth and gravel) terrain, but would reliably pass a specific point for close-up filming, approximately half way through their homing run. A small section was cut out of one side of the channel wall and replaced with clear Perspex to give a side view of the animals. Due to its absorption of ultraviolet light, the Perspex would appear opaque to the ants and we did not observe any significant deviation of ants within the channel when passing this section. Ants were filmed using a high-speed camera (Casio EX-F1) at 300 fps with a macro lens. The field of view covered approximately 4 cm of the ant's path.

Five videos were selected for analysis on the basis of video quality and variety of items being carried by the ants (see Fig. 1). The head and body pitch was measured by analysing the videos with a custom programme developed in MATLAB (Mathworks Inc, USA). For each frame where the complete head and body was visible, the centre of the mandible and the dorsal joint of the head and neck were manually labelled and the resulting angle with respect to the horizontal image frame was computed. Similarly, the body angle was measured from the dorsal joint of the neck to the ventral joint of the alitrunk and petiole. We define the angle relative to the horizontal such that 90° points downwards.

The simulated ant world

To test the effect of head pitch on the views experienced by ants, and the possible consequences for navigation, we created test scenarios in a 3D reconstruction of a natural environment, based on data from our study of route following in *Cataglyphis velox* (Mangan and Webb 2012). The field site used in that study was a flat semi-arid area covered in low scrub and grass tussocks. We mapped the tussock location and size and used panoramic pictures taken from ground level to estimate tussock height. From this, we generated a corresponding virtual environment, consisting of a 10 × 10 m area in which each tussock is represented as a collection of triangular grass blades of appropriate size and height, with a distribution of shading taken randomly from the intensity range in the panoramic pictures (Mangan 2011; Mangan et al. in preparation). Ground and sky have uniform intensities that differ from the grass blades. Within this virtual environment, the view from any position on the ground plane, facing in any direction, can be captured by a virtual panoramic camera. In particular, we can reconstruct the series of views along a path in this virtual environment that corresponds to the actual path we recorded for an ant in the real environment. The 3D world and image creation software are available at http://www.insectvision.org/.

A simulated ant eye was used to recreate the approximate retinotopic input that would be experienced by an ant. The eye model reproduces the projection of the visual world onto a uniformly curved retina (a spherical section) with a field of view (window in the sphere) that extends 296 degrees horizontally, and 76 degrees vertically, with 4 degree resolution. At zero pitch, the field of view is aligned such that the horizon runs through the centre of the image. Changing pitch rotates the field of view around the corresponding axis, so that the horizon line is changed and distorted as shown in Fig. 2a.

We used this virtual world in three ways in the following analysis.

- We first tested how, at any specific location, the ability of an ant to recover a heading direction using the visual compass method (see below) would be affected by the visual distortions produced by systematic alteration of the pitch of the head. This analysis was repeated for 81 different locations, which were taken at 10 cm intervals along a path corresponding to that of a real ant.
- We then used the distribution of pitches actually observed in the ant to investigate the directional error induced by pitch variation between the storing of visual memories and their use on a subsequent path traversal, under several different assumptions about how memories are stored and retrieved.
- Finally, to test whether the traversal of a whole route using repeated heading corrections is robust to the level of directional error caused by pitch variation, we test a simulated ant for its ability to follow the same route as a real ant under realistic levels of pitch variation.

Each of these analyses is now described in more detail.

Visual compass and the systematic effect of pitch

The visual compass method recovers a heading direction by calculating the difference between a reference image and the images obtained as the viewpoint is rotated around the yaw axis. The difference is typically calculated as the pixel-wise sum square intensity difference between the images, that is:

$$\text{Image difference} = \sum_i (I_i(x) - I_i^r)^2$$

The change in this value as the viewpoint is rotated is called the rotational image difference function (rIDF). The minimum in the rIDF, i.e. the best match to the reference, should occur when the viewing direction is the same as that of the reference image. The directional minimum

is generally robust to small displacements in location or changes in lighting etc. We tested whether it was robust to changes in pitch by calculating 360 degree rIDFs between a 0 pitch reference image and images generated at a pitch of −40, −20, −10, −5, 0, 5, 10, 20 or 40 degrees. This was repeated for 81 different images, which were generated in the simulated environment by taking images at 10-cm spaced locations along a route corresponding to that of a real ant.

We assess the effect of pitch firstly by directly visualising the rIDFs (Fig. 2a) and also using two measures of how distortion in the rIDF introduced by pitch could affect its use as a visual compass. The first measure is the absolute difference between the minimum in the rIDF, which a visual compass would select as the heading direction, and the actual heading direction for which the reference image was stored (Fig. 2b). We compare the median and interquartile range (IQR) of this error, for the 81 images, across different degrees of pitch alteration between the reference and test image. Second, if the rIDF is distorted (e.g. becomes noisier or flatter) due to pitch variation, detecting any minima could become more difficult. As an index of detectability, we use the ratio of the median rIDF to the minimum rIDF; if this is near 1, then the directional information available in the rIDF is low (Fig. 2c).

Modelling variable head pitch of the ant during learning and retracing of routes

For an ant to use the visual compass to follow a route, it needs to learn images along the route, and then on subsequent traversal, compare what it currently sees to the stored images to find the heading direction that corresponds to the minimum in the rIDF. In the following, we store an image every 1 cm along an 8.12 m route and use this memory to recover a heading direction. The absolute error between the selected heading and the correct direction along the route is used as performance metric and is calculated for 81 locations spaced at 10-cm intervals along the route. To avoid distortions caused by perfect matches, we assume a minimum 1 cm difference between the test location and the nearest stored location.

As discussed in the introduction, previous tests of this type of algorithm have assumed zero variation in pitch, in either learning or testing, so we include this condition (zero pitch) as a control. We compare this to the following more realistic situations:

Small pitch The stored images along a route are each pitched by a value randomly sampled from those observed for the ant carrying a small cookie (Fig. 1a, second row), with the mean shifted to 0º resulting in pitch values ranging from −20.6º to 12.99º. At test locations, the pitch is randomly varied using the same distribution. Note that this assumes that the variation in the pitch is due to the close interaction of the ant's stepping pattern and small-scale terrain rugosity, and hence, there is no significant correlation of the pitch between learning and test runs.

Fig. 1 Head movement in navigating ants. Ants were recorded walking across the normal substrate at the field site in Sevilla, under 5 load conditions (from *top* to *bottom row*): no load, small food item, medium food item, large food item and carrying another ant as shown by the images *inserts*. **a** The distribution of head angles over the entire recording. **b** The instantaneous head and body angle of the ant as it moved across the camera field of view (*blue line*—body angle and *red line*—head angle). Angle conventions used are shown by the *insert*. The head of the ant moves across a substantial pitch range and varies with load. The attitude of the head is only partially decoupled from the motion of the body indicating that there is no continuous stabilisation of gaze ▶

Large pitch More extreme pitch angles are simulated by randomly sampling from the pitch angles observed for the ant carrying a large cookie (Fig. 1a, fourth row), again following mean shifting to 0º. Head pitch values range from −40.4º to 21.69º, for both learning and test.

Small to large or *large to small* Ants may carry food items of different sizes on different traversals of the route, so we also test using small pitch variation on the stored images with large pitch variation on test and vice versa. The small and large distributions are as above. We do not include a difference in the mean of the variation, although it is possible that different size food items would also provide consistent bias in the pitch. We also do not represent the possibility that different food items might partially block the ants view in different ways.

For all five pitch variation possibilities, we test the directional error resulting from five alternative memory and visual processing assumptions:

(I) *Using spatially closest memory* Heading angles were recovered at every test location by computing the rIDF between current views and a memory 1 cm further along the route. Thus, images should be spatially well matched but are unlikely to be the same with regard to the pitch angle. Note this method makes the somewhat unlikely assumption that the ant knows where it is to within 1 cm and can recover the correct corresponding image from memory.

(II) *Using spatially near best matching memory* Simulated ants were allowed to search for the best rIDF score between current view and the visual memories taken at 1-cm intervals in the area 15 cm before and after the current location. Thus, they may potentially recover a more accurate heading direction by using a memory that has a more similar pitch but possibly greater displacement than 1 cm along the route. We omitted the memory at the current location to prevent perfect matching.

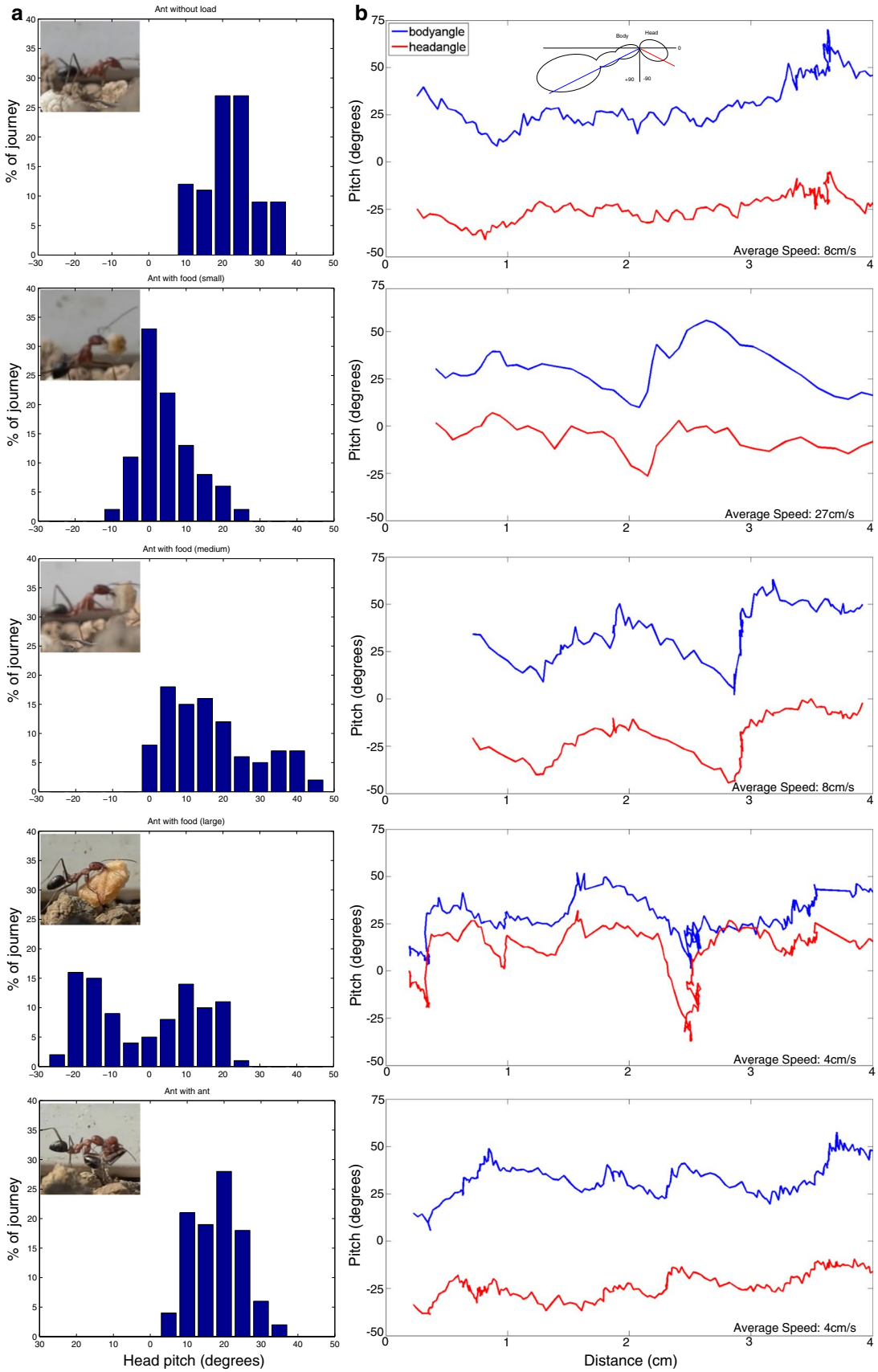
a
b
Ant without load
Ant with food (small)
Ant with food (medium)
Ant with food (large)
Ant with ant
% of journey
Head pitch (degrees)
Pitch (degrees)
Distance (cm)
bodyangle
headangle
Body
Head
Average Speed: 8cm/s
Average Speed: 27cm/s
Average Speed: 8cm/s
Average Speed: 4cm/s
Average Speed: 4cm/s

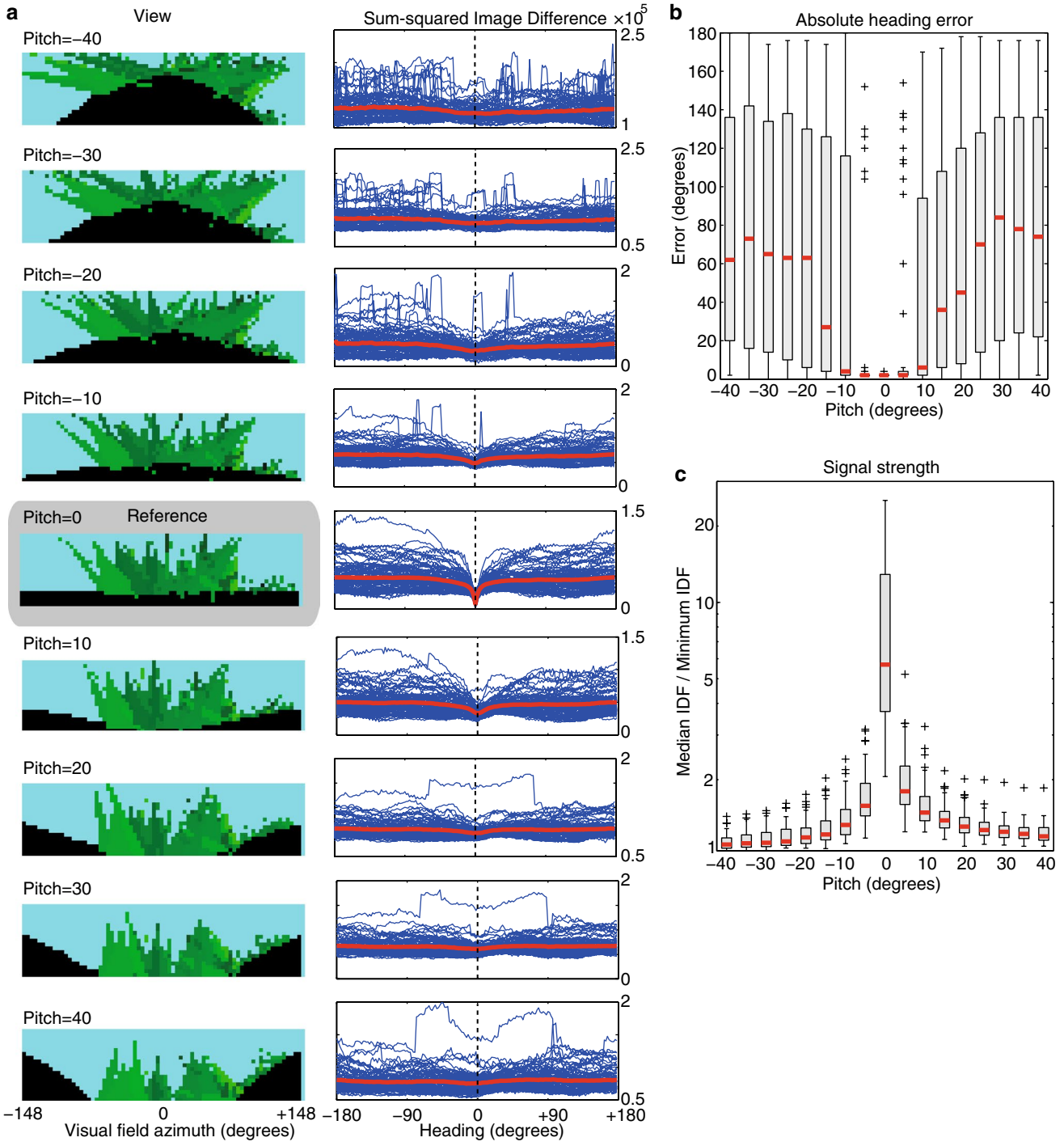

Fig. 2 The effect of pitch on the visual compass. **a** *Left column* shows an example of the panoramic views generated at the same location in our 3D world but with pitch angle varying from −40° to 40°, introducing substantial distortion of the view. **a** *Right column* shows the rIDFs calculated at 81 test when comparing the reference image (no pitch) to the same image at differing pitch angles (−40° to 40°). *Blue lines* are the individual rIDF values for each location (aligned so the correct direction is at 0°), while the *red line* shows the mean across all the locations tested. At 0° pitch, the reference heading (0°) is readily identified as a minimum, but as pitch increases it becomes increasingly difficult to reliably extract the correct heading. **b** Range of heading errors computed across 81 test locations under varying pitch (median are shown in *red*, and inter-quartile range by *box*). Error increases significantly when pitch exceeds ±15°. **c** Signal strength, i.e. the median rIDF value divided by the minimum rIDF, as pitch varies. The depth of the minimum, and hence its detectability, drops dramatically with head pitch

(III) *Using best matching memory across route* Simulated ants searched for the best rIDF score between current view and the visual memories taken at 1-cm intervals across the whole route (812 cm long). This is more consistent with current route following algorithms (Baddeley et al. 2012; Philippides et al. 2011) than the local search described above and does not require the ant to have indexed its memories by their location. Again, the memory of the current location was omitted.

(IV) *Disregard views at large pitch values* Ants may infer that they are viewing the world at a pitch angle not conducive to accurate heading recovery and opt to omit the view from memory, or not compute a new heading direction on test. This could improve matching but at the cost of potentially having gaps in the route in which correction does not occur. To simulate this selectivity, method III above was altered so that training images sampled at pitch greater than 10º or less than −10º (i.e. at the onset of visual compass degradation, Fig. 2c) were removed from the memory, and during test, any current image exceeding this pitch was ignored and the direction that was computed at the previous location selected instead.

(V) *Best matching memory of averaged images* Another means to overcome the influence of head pitch variation might be to store images not as instantaneous snapshots, but as averaged images taken over time. In this way, the stored view would contain information from a range of pitch angles and thus might more closely match the view from the same location regardless of pitch angle. 'Average images' were created every 1 cm by taking the mean of the current view and the previous four images separated at 1 cm. Method III was then used with these images as the memories to be compared to the current image.

Effect on simulated navigation in the ant's world

The above analysis will reveal the angular error caused by realistic pitch undulations at specific locations along a real ant route, and whether the error is reduced under certain processing assumptions. However, it is difficult to quantify whether the angular errors remaining would prevent an ant from retracing a learned path or not. In particular, the continuous nature of route following might offer robustness to instantaneous errors, by allowing correction in the next instant. We therefore tested the ability of a simulated ant to recapitulate the entire ant route in the simulated ant environment (see Fig. 4a for real ant route).

Images were again stored along the full ant route at 1 cm. The simulated ant would attempt to retrace the route from the starting point by first calculating the rIDF, for ±90º around the current heading, comparing against memories taken across the entire route (method III above). Once a global minimum was found, the ant would move 1 cm in that direction and the entire process was repeated until the ant reached home. In the case that the ant deviated from more than 1 m from the original route, or overshot the route length by 0.1 m (822 cm), the simulation was halted. The resulting path gives an indication of the robustness of navigation to disturbance of the visual input.

As above, we focus on five test scenarios: zero pitch training vs. zero pitch test as a control and all combinations of small and large pitch on both training and test, representing realistic situations of ants returning home with food of differing size.

Results

Do ants stabilise their head?

Homing ants were recorded with high-speed video as they ran over natural terrain. Five ants were selected for analysis as they carried a variety of objects that a homing ant is likely to possess while retracing her learned route: a small, medium or large piece of cookie (estimated mass and volume: 8 mg and 1 mm^3; 16 mg and 2 mm^3; 32 mg and 4 mm^3 respectively); another ant [approximately 7.1–27 mg (Kühn-Bühlmann and Wehner 2006; Cerdá and Retana 1997)]; or nothing. Ants were highly motivated and thus moved quickly nestward but the differing weights of their bounty meant they moved at different speeds through the 4 cm recording area (see Fig. 1b). Figure 1b shows the time course of head and body pitch angles, relative to horizontal location of the neck joint in the camera image (i.e. location in their travel from left to right side of the frame), and Fig. 1a displays the distribution of pitch angles of the head for each ant. We stress that this is a simple observational study to support the parameters of head pitch variation used in our modelling, and not an experimental study to determine the causes of that variation.

We see that the body pitch is altered by the combination of uneven terrain and step cycle or leg configuration (it is not possible in our recordings to separate these factors, as unevenness of terrain in the depth axis of the camera obscured detail of footfall locations). If ants were actively stabilising, the head pitch should remain relatively constant, or at least fluctuate substantially less than the body pitch, but it is clear that for the most part it follows the body pitch. In some cases (ant with small cookie), the head movement is somewhat reduced relative to the body, but in other cases (ant with large cookie), it is increased. It also appears that carrying different items affects the median of the pitch as well as the distribution, but we would need more examples to conclude that this is a consistent effect.

In every case, the ant experiences a wide range of pitches (at least 20–30 degrees) in this short time interval. There is also little consistency in the time/locations of higher or lower pitch from ant to ant as they encounter different small-scale undulations in the same terrain. We would consequently expect the same ant running repeatedly through the same part of a route, possibly carrying different food items, could be faced with the problem of matching images that are altered in pitch from one experience to the next by as much as ±30 degrees.

The systematic effect of pitch on image difference

The lack of head stabilisation and consequent range of pitch experienced by an ant may not be a problem for the visual compass algorithm if this amount of pitch variation does not substantially affect ability to find the best directional match. In Fig. 2, we show the image difference function is affected by pitch, by comparing a reference image with no pitch to test images at pitches from −40 to 40 degrees. Eighty-one ant-eye images, taken every 10 cm along a real ant route, were generated in our reconstructed ant world (see 'Methods'). For each, we calculated the rIDF as the viewing direction is rotated from 0° to 360° in 2° intervals. All rIDFs were then aligned so that the correct heading corresponded with 0°. As expected, at 0 degrees pitch of the test image, there is a perfect match at the correct direction (0°), surrounded by a monotonically increasing valley of image similarity. However, as a pitch difference between the test and reference view is introduced, the rIDF is clearly affected. The valley becomes much shallower as pitch difference increases, with additional local minima appearing at incorrect heading directions. Both factors would make a visual compass—which functions by selecting the minimum in the rIDF—less reliable. At each location, we also calculated the absolute difference between the selected direction (rIDF minimum) and the correct direction, and show the distribution of the errors as the pitch increases (Fig. 2b). Within the range of ±5° of pitch, the errors are relatively small (medians of 2° for both with 0° IQR for both), while at ±10° the median remains low (6° and 4° respectively) although the IQR increase significantly (92° and 114° respectively). For higher values of pitch mismatch, the median error increases substantially (e.g. 36° and 26° for ±15° respectively). Moreover, this assumes that the ant is able to detect a minimum (correct or incorrect), which should become increasingly difficult as the rIDF becomes flatter or noisier. As described in the methods, we take the ratio of the median rIDF to the minimum in the rIDF as an index of detectability; if this is near 1 then the directional information detectable in the rIDF is low. It is apparent in Fig. 2c that the detectability of the best match and thus the reliability or confidence in a directional choice also decreases substantially as the pitch difference is increased.

Errors induced by pitch variation during route learning and recapitulation

The previous analysis compares the rIDFs for different pitches against a zero pitch reference image at the same location. However, a navigating ant would presumably experience a range of pitches both when learning and recapitulating a route. We examine whether a visual memory of a route that includes dense sampling for both location and pitch can be used to improve the directional choice made by the visual compass mechanism. As described in the methods, we sample pitch angles directly from those observed in real ants (either the ant carrying small cookie or ant carrying large cookie) and use this to vary visual input experienced along a route. We use zero pitch variation on learning and test as a control. In training, images are stored every 1 cm along the route, generating 812 memories for the test route to potentially exploit (see supplementary material for videos of training route for the various pitch conditions).

We first assess the performance of the visual compass if the current view is compared with visual memory at the closest location (Fig. 3 box plots, orange filled boxes) and we use 1 cm further along the route to avoid the unrealistic accuracy that can occur if the exactly identical location is used. The data show the visual compass is accurate when tested with zero (Fig. 3a, median = 0.9º) or small pitch angles (Fig. 3d, m; medians = 1.9º and 7.9º, respectively). The worst performance is found when we test with large pitch regardless of the training condition (Fig. 3g, j; medians = 15.7º and 14.1º). Figure 3e, h, k, n shows that when using the nearest location, there can be significant mismatch in pitch, which in turn leads to the increased angular errors.

We then assessed performance when the visual compass is allowed to find the best matching image in the 30 training images closest to the current location, that is, 15 steps before and after the test location. In this case, the simulated ant may find a good match with the current image in terms of pitch while being constrained to only small spatial mismatches. The data (Fig. 3, green box plots) show that the visual compass combined with a local search through dense memories remains accurate across all memory and test scenarios (Fig. 3a, d, g, j, m; medians = 0.8º, 1.5º, 3.1º, 3.9º, 3.0º respectively). Figure 3e, h, k, n shows that by searching through nearby memories sampled across a range of pitch angles, the simulated ant can find an image stored at a similar pitch as the test image, and thus a better match than for the spatially closest image.

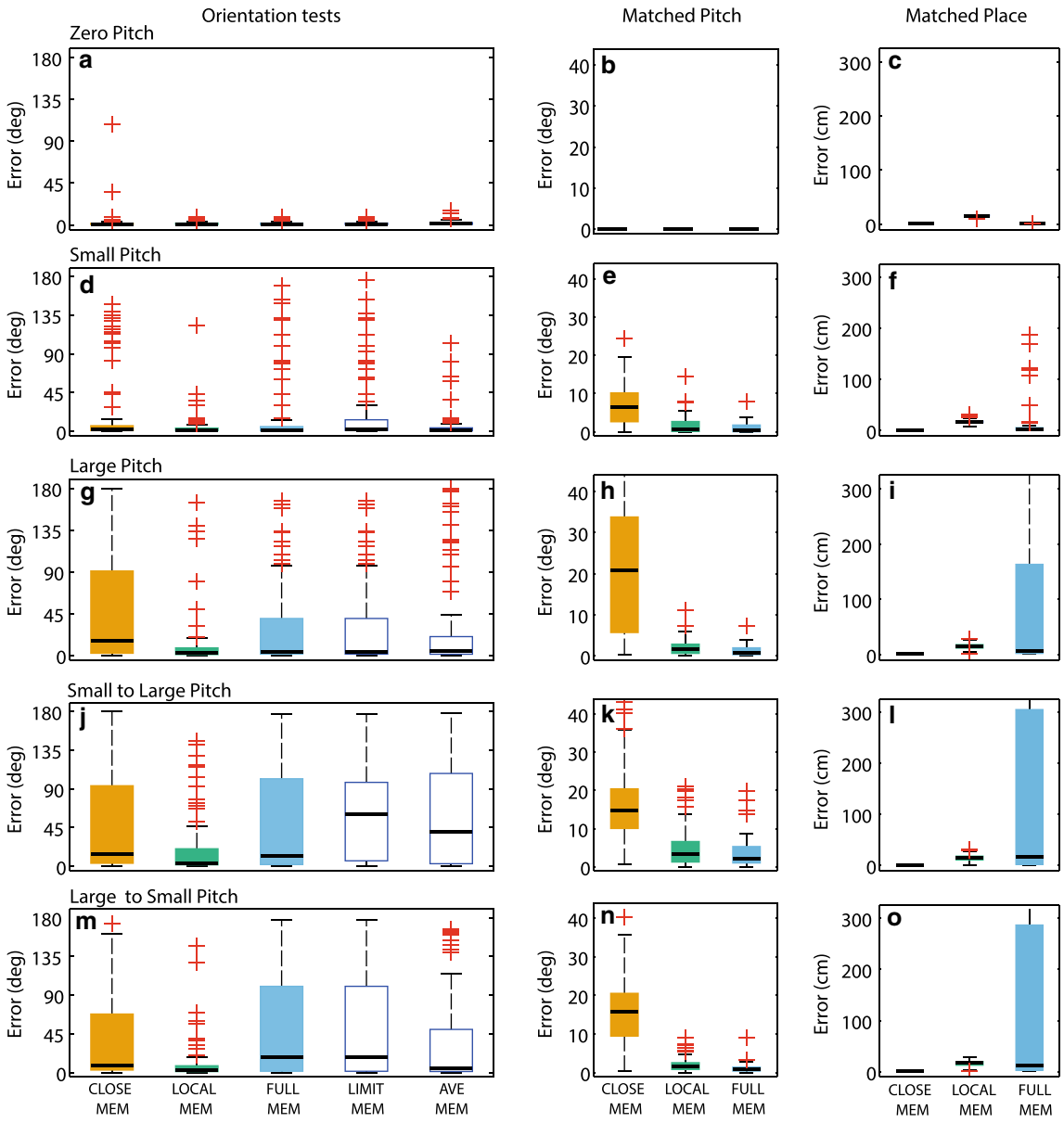

Fig. 3 Approaches to reducing the impact of head pitch on visual compass. *Left column* (**a**, **d**, **g**, **j**, **m**) angular difference between the ant path and the direction selected at 81 test locations along a real ant route using five different memory and visual processing techniques: Closest Memory (*orange boxes*); Local Memory (*green boxes*); Full Memory (*blue boxes*); Limited Memory; and Average Image. Medians are shown by the *black bar* and the IQR by the *box*. From *top* to *bottom* are the combinations of pitch in memory and test: zero, small and large pitch in memory and test; followed by small pitch memory and large in test and vice versa. *Middle column* (**b**, **e**, **h**, **k**, **n**) angular error between the pitch angle at which the test image was sampled and the best match found in memory using the Closest, Local and Full Memory methods, respectively. *Right column* (**c**, **f**, **i**, **l**, **o**) distance in cm between the location at which the test image was sampled and the best match found in memory using the Closest, Local and Full Memory methods, respectively. Searching in local memories only allows a spatially close image to be found at a correlated pitch angle, hence good performance. However, when searching over the entire route memory, pitch matching dominates, leading to spatial mismatches and poor performance. Learning only at small pitch values <10° and averaging memory do not improve performance

While the above data shows that dense memories can provide robustness to pitch disturbances, both methods assume that ants have indexed their memories by location and can recover the relevant memory (within 1 cm) or set of memories (within 15 cm). Behavioural data suggests ants can follow routes from arbitrary points along them, i.e. in ignorance of their spatial location (Kohler and Wehner 2005; Mangan and Webb 2012; Narendra 2007a, b), and recent algorithms have replicated this capability by assuming ants use the visual compass to find the best matching

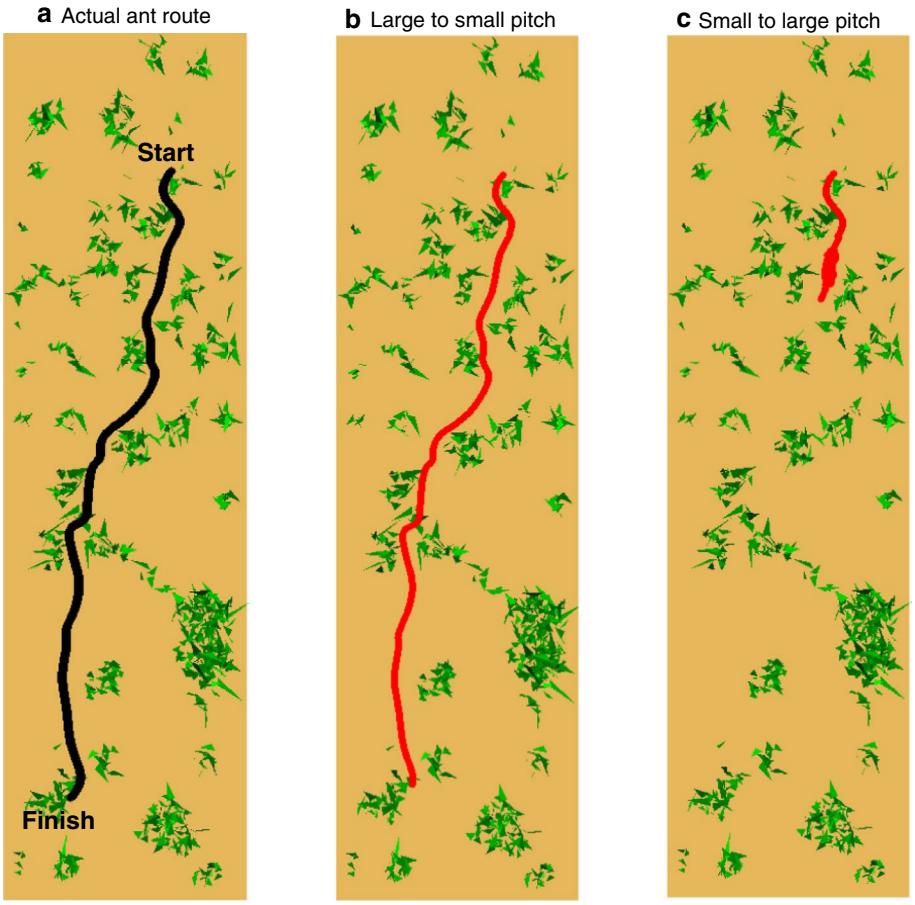

Fig. 4 Navigating real ant routes with realistic head movement. **a** Actual route followed by an ant through its cluttered environment in Sevilla, Spain, acting as ground truth. **b**, **c** Example paths followed by simulated ant following visual compass methodology and realistic head pitch for memory and route recapitulation (**b** large to small; **c** small to large). The iterative computation of direction can compensate for the errors introduced by pitch (**b**) but is still susceptible to failure (continuous loops in this case) (**c**)

memory across the entire route (Baddeley et al. 2012). We therefore assessed whether finding the best matching image across the entire 812 route memories (excluding the current location) was also robust against pitch variation. We find that performance using all route memories remains statistically indistinguishable from the local search except when large pitch is present in the memory ($p < 0.02$ using Wilcoxon rank-sum test) (Fig. 3a, d, g, j, m blue box plots, medians = 0.8º, 1.6º, 3.9º, 12.5º, 17.6º). The reason for the increase in angular error with a global search is clear when the position and pitch of the matched images are examined (Fig. 3h, i, n, o). When we allowed to search the entire route memory, best matches are found at similar pitch angles to that on the test, but this often leads to image matches with images far from the test location (upper IQR around 3 m from the test site). This aliasing of views leads to erroneous heading directions.

It is clear that most degradation in performance occurs when there are large pitch disturbances on the training or test set. Thus, if ants were able to detect the angle of pitch (see discussion), they may actively chose to omit learning views, or updating their home direction, until the head returns to a more suitable position. However, such a schema might be costly as it may produce gaps in the memory or lead to errors at key points when later navigating. We report that this method indeed leads to decreased performance when compared to perfect memory when trained with small pitch and tested with large pitch (Fig. 3j; medians = 60.8º, $p < 0.01$ Wilcoxon rank-sum test). Results in other conditions are similar to the full memory condition (Fig. 3 a, d, g, m; medians = 0.8º, 2.1, 3.9º and 17.6º, respectively). In summary, this approach does not improve performance.

Finally, we tested the performance of the visual compass when memories were converted from single snapshots to averaged images. That is, each stored memory is the mean of the last five steps and should therefore incorporate various head pitch angles. We test the heading error when comparing the current view with the averaged views stored across the entire route. We find that this also does not improve performance over the perfect memory of instantaneous images (Fig. 3a, d, g, j, m; medians = 1.3º, 1.5º, 4.5º, 40.4º, 4.9º).

The effect of error on route following

C. velox ants experience considerable variation in head pitch when running over moderate terrain (Fig. 1), and this could induce substantial error in the directional information

of a visual compass (Fig. 2). Large angular errors remain when matching memories across the entire route (Fig. 3, blue box plot). However, as route following with a visual compass involves successive re-orientations to the best matching direction, we would expect it to be somewhat robust against small or occasional directional errors. That is, if the ant deviates from the learned path due to an erroneous visual compass reading, it might still recover the route in the next step through a better match, and hence reach home.

To evaluate the error tolerance of route following with a visual compass, we simulated an ant driven by visual compass with perfect memory (at 1-cm intervals) to travel along our reconstructed real ant route, using either zero, small or large pitch variation as described above. For route recapitulation, the simulated ant scans ±90 degrees from the current heading direction, selecting the view with the lowest image difference from the entire bank of stored memories. The corresponding heading is then chosen for the next step. If the simulation deviates more than 1 m from the original ant route, or exceeds the route length by 0.1 m, it is stopped. These conditions mirror actual behaviour of the animal as substantial deviations from the route corridor are seldom observed and nest bound ant routes are not tortuous (Mangan and Webb 2012).

Under the conditions where the training and test pitch were drawn from the same distribution (i.e. zero, small and large pitch), the entire route could be followed with no errors despite the difference in the visual input (data not shown). Where the pitch angle varies (e.g. Small to Large and vice versa), errors were often encountered. However, the capacity to correct over successive steps appears to offer some robustness as shown in Fig. 4b, but does not offer complete robustness as demonstrated by the catastrophic error in Fig. 4c. In contrast, ants returning home rarely deviate from their path, even in the absence of path integration (Kohler and Wehner 2005; Mangan and Webb 2012; Wystrach et al. 2011) and thus may have developed strategies to deal with disturbances in visual input.

Discussion

The study of visual navigation in ants has led to the development of a number of algorithms that reproduce aspects of their behaviour (Cartwright and Collett 1982; Hafner 2001; Möller 2001; Stürzl and Mallot 2006; Wystrach et al. 2013; Zeil et al. 2003), including the ability to follow extended visual routes (Baddeley et al. 2011, 2012). In general, these models use some form of retinotopic image matching to recover a heading direction. It is increasingly argued that ants use essentially raw or whole image matching, with minimal image processing and no feature extraction. This means the potential distortions introduced by variability in head pitch or roll could have a significant effect, but most models assume stable visual input.

However, the evidence for head stabilisation is not clear. Ants running on flat ground, such as the Tunisian salt pans, may experience only small disturbances, although even here, as discussed in the introduction, some variation in head pitch during the step cycle is observed (Steck et al. 2010). Ants experiencing gradual or consistent change in body orientation due to a substrate slope show some ability to compensate their head position, but they do not fully compensate for substantial slopes (Wohlgemuth et al. 2002; Weihmann and Blickhan 2009). High-speed video provides the opportunity to examine whether there is rapid compensation for the fine-scale variation in body position caused by walking over moderate variations in terrain. Our results suggest that, at least for *C. velox* head pitch, no such compensation occurs. Rather, head position varies with body position as determined by the terrain combined with the gait and is also influenced by any object that the ant might be carrying. Consequently, we report rapidly varying head pitch: up to ±30 degrees. We note here that preliminary processing of high-speed video of a *C. fortis* ant running on flat terrain (supplementary data from Steck et al. 2010) also reveals substantial variation in head pitch (at least ±10 degrees) (see supplementary material). Experiments inducing roll in the body orientation of ants also show some, but not full, compensatory roll of their head (Raderschall et al. 2014) and ants under these conditions can be observed to experience a similar range of roll (i.e. ± 15 degrees) over a short timescale (C. Raderschall, personal communication). Note that this suggests our analyses of the effects of head motion on navigation are conservative, as roll would provide additional distortion.

We use simulation of the ant's visual input, based on a reconstruction of a real ant environment, to assess the effects of the observed variation in pitch on current navigational methods. It is clear that pitch differences have a significant effect on image matching algorithms such as the visual compass. For pitch differences of 15 degrees or more, the minimum in the rIDF is hard to detect and often falls in the wrong location, which would result in errors in directional choice. The accuracy of visual compass can be improved if ants have a dense memory of views around its current vicinity containing a large range of pitches similar to the pitch value current experienced. The ant would then potentially have available a 'nearby' memory at the same pitch as the current view and therefore be able to more accurately recover the correct direction than using nearest memory, which might be at the wrong pitch. However, such a local search in memories would require memory indexing which does not fit with behavioural data (Kohler and Wehner 2005; Mangan and Webb 2012; Narendra 2007a,

b). When tested with visual memories with large pitch from the entire route, performance degrades because pitch matching is favoured at the expense of proximity. We then tested in a full simulation of route following, to quantify the impact of instantaneous errors on a real navigation task. We conclude that while the iterative process of route following offers some tolerance to pitch induced heading errors, the variability of head pitch observed in ants is potentially problematic for the visual compass hypothesis, at least in its most straightforward form, and in our challenging environment comprising a dense array of proximal grass tussocks without any distal cues.

The ant visual system (eye and optic lobe) filters information directly reducing the computational load on the brain. We therefore investigated whether rudimentary visual averaging might restore visual matching without increasing memory load. Each image should encompass a range of pitches, and this may be more robust for image matching than the single snapshots used in current methods. However, we find the results were no better than for simple image memory.

Ants might be able to detect when their heads are at a level pitch and roll, or intermittently adopt a stereotyped pose with a levelled head, and only 'take snapshots' at these key moments. It is plausible that the ant has sensory mechanisms that could enable it to detect the pitch and roll of its head, for example through proprioception relative to gravity (Seidl and Wehner 2008), or visual information (possibly from the ocelli) about the horizon [as in locusts (Taylor 1981)]. However, using knowledge of the pitch to reject memories, and prevent comparisons, at pitches of more than 10 degrees did not significantly improve the performance in our tests.

Ants could also potentially use pitch information directly to make the required correction to the image, i.e. to perform mental rotation. Another possibility is that the mechanisms for visual navigation are not so strongly retinotopic as image matching algorithms suggest. Models of navigation that use landmark bearings may be less affected by pitch and roll, which principally distort height (Collett 1992). Yet such methods are known be ineffective in natural environments where landmarks can be hard to identify and do not fit well with behavioural studies of visual homing in insects (Mangan and Webb 2009).

A possibility is that other view matching strategies could reduce or compensate for such inaccuracies. The visual compass approach used here does not capture all aspects of ant visual guidance. For example, ants recapitulate routes without scanning at each step, and recover routes after a deviation (Collett 2010; Wystrach et al. 2012) suggestive of alternative visual strategies. Finally, sky compass may also be helpful. It is important to note, however, that variability in pitch and roll to the extent described here could also affect the sky compass. That is, the input to polarisation sensitive ommatidia in the dorsal rim of the ant eye depends on their orientation relative to the sky pattern of polarisation which in general is not a uniform across the entire sky; hence, pitch and roll of the head will alter the input. Again, it is possible that subsequent neural filtering could reduce the impact of this variation or that active correction from detection of the head position is used to compensate.

As computational models are developed that can account for increasingly complex behaviours, it is vitally important to introduce realistic constraints derived from animal observation. Here, we have challenged the assumption that ants stabilise their heads and introduced the constraint that navigation must be robust to pitch variation. Only through repeatedly and rigorously challenging assumptions can we hope to refine our hypotheses to reveal the secrets of these amazing navigators. 'By entertaining this kind of bottom–up approach to understanding the organization of behaviour, we might finally follow the routes originally taken by evolution in orchestrating the different guiding mechanisms and knitting them into what Fabre (1882) called "the insect's awe-inspiring system of navigation"' (Wehner et al. 1996).

References

Baddeley B, Graham P, Philippides A, Husbands P (2011) Holistic visual encoding of ant-like routes: navigation without waypoints. Adapt Behav 19:3–15. doi:10.1177/1059712310395410

Baddeley B, Graham P, Husbands P, Philippides A (2012) A model of ant route navigation driven by scene familiarity. PLoS Comput Biol 8:e1002336. doi:10.1371/journal.pcbi.1002336

Cartwright BA, Collett TS (1982) How honey bees use landmarks to guide their return to a food source. Nature 295:560–564

Cartwright BA, Collett TS (1983) Landmark learning in bees. J Comp Physiol A 151:521–543. doi:10.1007/BF00605469

Cerdá X, Retana J (1997) Links between worker polymorphism and thermal biology in a thermophilic ant species. OIKOS 78(3):467–474

Collett TS (1992) Landmark learning and guidance in insects. Philos Trans Biol Sci 337:295–303

Collett M (2010) How desert ants use a visual landmark for guidance along a habitual route. Proc Natl Acad Sci 107:11638

Collett M, Chittka L, Collett TS (2013) Spatial memory in insect navigation. Curr Biol 23:R789–R800. doi:10.1016/j.cub.2013.07.020

Duelli P (1975) A fovea for e-vector orientation in the eye of *Cataglyphis bicolor* (Formicidae: Hymenoptera). J Comp Physiol 56:43–56

Hafner VV (2001) Adaptive Homing—robotic exploration tours. Adapt Behav 9:131–141. doi:10.1177/10597123010093002

Harrison JF, Fewell JH, Stiller TM, Breed MD (1989) Effects of experience on use of orientation cues in the giant tropical ant. Anim Behav 37:869–871

Kohler M, Wehner R (2005) Idiosyncratic route-based memories in desert ants, *Melophorus bagoti*: how do they interact with path-integration vectors? Neurobiol Learn Mem 83:1–12. doi:10.1016/j.nlm.2004.05.011

Kühn-Bühlmann S, Wehner R (2006) Age-dependent and task-related volume changes in the mushroom bodies of visually guided desert ants, *Cataglyphis bicolor*. J Neurobiol 66:511–521. doi:10.1002/neu.20235

Mangan M (2011) Visual homing in field crickets and desert ants: a comparative behavioural and modelling study, PhD Thesis, University of Edinburgh

Mangan M, Webb B (2009) Modelling place memory in crickets. Biol Cybern 101:307–323. doi:10.1007/s00422-009-0338-1

Mangan M, Webb B (2012) Spontaneous formation of multiple routes in individual desert ants (*Cataglyphis velox*). Behav Ecol. doi:10.1093/beheco/ars051

Moll K, Roces F, Federle W (2010) Foraging grass-cutting ants (*Atta vollenweideri*) maintain stability by balancing their loads with controlled head movements. J Comp Physiol A Neuroethol Sensory Neural Behav Physiol 196:471–480. doi:10.1007/s00359-010-0535-3

Möller R (2001) Do insects use templates or parameters for landmark navigation? J Theor Biol 210:33–45. doi:10.1006/jtbi.2001.2295

Narendra A (2007a) Homing strategies of the Australian desert ant *Melophorus bagoti*. II. Interaction of the path integrator with visual cue information. J Exp Biol 210:1804–1812. doi:10.1242/jeb.02769

Narendra A (2007b) Homing strategies of the Australian desert ant *Melophorus bagoti*. II. Interaction of the path integrator with visual cue information. J Exp Biol 210:1804–1812. doi:10.1242/jeb.02769

Philippides A, Baddeley B, Cheng K, Graham P (2011) How might ants use panoramic views for route navigation? J Exp Biol 214:445–451. doi:10.1242/jeb.046755

Raderschall C, Narenda A, Zeil J (2014) Navigation at night a balancing act: head stabilisation in *Myrmecia* ants during twilight. International Congress for Neuroethology, Sapporo

Reinhardt L, Blickhan R (2014) Ultra-miniature force plate for measuring triaxial forces in the micronewton range. J Exp Biol 217:704–710. doi:10.1242/jeb.094177

Schwarz S, Narendra A, Zeil J (2011) Arthropod structure & development the properties of the visual system in the Australian desert ant *Melophorus bagoti*. Arthropod Struct Dev 40:128–134. doi:10.1016/j.asd.2010.10.003

Seidl T, Wehner R (2008) Walking on inclines: how do desert ants monitor slope and step length. Front Zool 5:8. doi:10.1186/1742-9994-5-8

Steck K, Wittlinger M, Wolf H (2009) Estimation of homing distance in desert ants, *Cataglyphis fortis*, remains unaffected by disturbance of walking behaviour. J Exp Biol 212:2893–2901. doi:10.1242/jeb.030403

Steck K, Knaden M, Hansson BS (2010) Do desert ants smell the scenery in stereo? Anim Behav 79:939–945. doi:10.1016/j.anbehav.2010.01.011

Sturzl W, Mallot H (2006) Efficient visual homing based on Fourier transformed panoramic images. Rob Auton Syst 54:300–313. doi:10.1016/j.robot.2005.12.001

Taylor CP (1981) Contribution of compound eyes and ocelli to steering of locusts in flight: II. Timing changes in flight motor units. J Exp Biol 93:19–31

Vardy A, Möller R (2005) Biologically plausible visual homing methods based on optical flow techniques. Connect Sci Spec Issue Navig 17:47–90. doi:10.1080/09540090500140958

Wehner R (2008) The architecture of the desert ant's navigational toolkit (Hymenoptera: Formicidae). Myrmecol News 12:85–96

Wehner R, Räber F (1979) Visual spatial memory in desert ants, *Cataglyphis bicolor* (Hymenoptera: Formicidae). Cell Mol Life Sci 35:1569–1571. doi:10.1007/BF01953197

Wehner R, Marsh A, Wehner S (1992) Desert ants on a thermal tightrope. Nature 357:586–587

Wehner R, Michel B, Antonsen P (1996) Visual navigation in insects: coupling of egocentric and geocentric information. J Exp Biol 199(Pt 1):129–140

Weihmann T, Blickhan R (2009) Comparing inclined locomotion in a ground-living and a climbing ant species: sagittal plane kinematics. J Comp Physiol A Neuroethol Sens Neural Behav Physiol 195:1011–1020. doi:10.1007/s00359-009-0475-y

Wohlgemuth S, Ronacher B, Wehner R (2002) Distance estimation in the third dimension in desert ants. J Comp Physiol A Neuroethol Sensory Neural Behav Physiol 188:273–281. doi:10.1007/s00359-002-0301-2

Wystrach A, Schwarz S, Schultheiss P et al (2011) Views, landmarks, and routes: how do desert ants negotiate an obstacle course? J Comp Physiol A Neuroethol Sens Neural Behav Physiol 197:167–179. doi:10.1007/s00359-010-0597-2

Wystrach A, Beugnon G, Cheng K (2012) Ants might use different view-matching strategies on and off the route. J Exp Biol 215:44–55. doi:10.1242/jeb.059584

Wystrach A, Mangan M, Philippides A, Graham P (2013) Snapshots in ants? New interpretations of paradigmatic experiments. J Exp Biol 216:1766–1770. doi:10.1242/jeb.082941

Wystrach A, Philippides A, Aurejac A et al (2014) Visual scanning behaviours and their role in the navigation of the Australian desert ant *Melophorus bagoti*. J Comp Physiol A Neuroethol Sens Neural Behav Physiol 200:615–626. doi:10.1007/s00359-014-0900-8

Zeil J, Hofmann M, Chahl J (2003) Catchment areas of panoramic snapshots in outdoor scenes. J Opt Soc Am A Opt Image Sci Vis 20:450–469

Zollikofer C, Wehner R, Fukushi T (1995) Optical scaling in conspecific *Cataglyphis* ants. J Exp Biol 198:1637–1646

Chapter 4

Ant Homing Ability is not diminished when travelling backwards

4.1 Introduction to the paper

In this chapter a new behaviour of the zero vector ant is described which has implications for models of visual navigation. Previous research had assumed that the animal's visual input was aligned to the direction of travel, an assumption which fits easily with continuous course correction using a previously learnt route. In this study a zero vector ant displaced to a novel location is shown to be able to navigate back to the nest while facing some or most of the time away from the direction of travel. The animal can do this with the same efficiency as an ant which is facing towards the direction of travel suggesting that a continuous view forwards is not necessary for visual navigation.

A process of continuous image matching for navigation was thrown into doubt by the results in Chapter 3: ants do not stabilise their heads when walking over the substrate of their home, and the range of movement of the head was sufficient to cause problems in matching images during simulated route recapitulation. If the head must be at a certain attitude to allow image matching then navigation cannot be a continuous process, or if it is a continuous process then a mechanism other than physical stabilisation must be used to attenuate the effects of ego-motion or create a pitch-invariant percept. It is normally assumed that temporal processing is confined to optic flow detection but in Chapter 3 we saw that the assumption of some form of averaging over time steps had little effect in improving location selection. Despite the inability to produce an adequate hypothesis to explain this level of visual disruption, there was reason to believe that the ant experienced even more radical transformation of the visual world

while successfully reacquiring the nest during zero vector navigation.

Observation of ants returning to the nest showed that they experienced extreme transformation of the visual environment: large food items could force the ant to drag them facing away from the nest. A pilot study was undertaken in Sevilla which aimed to place in conflict a previously learnt visual panorama with the path integration vector on the assumption that at least one of these two systems would be needed to get back to the nest. The protocol used ants with a path integration vector at 0 degrees in an arena at 90 degrees to the nest, with the visual panorama initially obscured. Once the initial movement of the ant was established the shader was removed allowing the animal to perform a visual correction. Ants were tested without food and with large items which required to be dragged backwards. The results were inconclusive and it was thought that the complexity of the experimental set-up was a significant factor.

Hibernation of the Spanish ant colonies required an experiment to be conducted in the Southern hemisphere and the well-studied Australian predatory ant *Myrmecia crosslandi* was selected. The hunting behaviour of these ants makes route-learning experiments difficult to design and instead the protocol placed in conflict the PI vector with visual homing from a novel location. The experiment demonstrated unequivocally that ants of this species could return to the nest while facing away from the direction of travel for significant periods. This finding confirms that a direct view of the nest is not necessary for visually guided navigation confirmed subsequently in other research (Pfeffer and Wittlinger, 2016).

There are some implications of this research which still need to be tested, notably:

- Visual navigation is not a continuous process but an interaction between vision for heading selection and path integration for route following; or,
- Visual navigation is a continuous or semi-continuous process made possible by using rotationally invariant processing of the panorama;

Additional data and analysis is included as an addendum to the paper which explores these hypotheses through a pilot study and simulations.

frontiers in Behavioral Neuroscience

ORIGINAL RESEARCH
published: 13 April 2016
doi: 10.3389/fnbeh.2016.00069

Ant Homing Ability Is Not Diminished When Traveling Backwards

*Paul B. Ardin *, Michael Mangan and Barbara Webb **

Insect Robotics Lab, School of Informatics, University of Edinburgh, Edinburgh, UK

Ants are known to be capable of homing to their nest after displacement to a novel location. This is widely assumed to involve some form of retinotopic matching between their current view and previously experienced views. One simple algorithm proposed to explain this behavior is continuous retinotopic alignment, in which the ant constantly adjusts its heading by rotating to minimize the pixel-wise difference of its current view from all views stored while facing the nest. However, ants with large prey items will often drag them home while facing backwards. We tested whether displaced ants (*Myrmecia croslandi*) dragging prey could still home despite experiencing an inverted view of their surroundings under these conditions. Ants moving backwards with food took similarly direct paths to the nest as ants moving forward without food, demonstrating that continuous retinotopic alignment is not a critical component of homing. It is possible that ants use initial or intermittent retinotopic alignment, coupled with some other direction stabilizing cue that they can utilize when moving backward. However, though most ants dragging prey would occasionally look toward the nest, we observed that their heading direction was not noticeably improved afterwards. We assume ants must use comparison of current and stored images for corrections of their path, but suggest they are either able to chose the appropriate visual memory for comparison using an additional mechanism; or can make such comparisons without retinotopic alignment.

Keywords: ants, navigation, visual homing, insect, retinotopic, view matching

OPEN ACCESS

Edited by:
Marie Dacke,
Lund University, Sweden

Reviewed by:
Thomas Collett,
University of Sussex, UK
Paul Graham,
University of Sussex, UK

****Correspondence:***
Paul B. Ardin
p.b.ardin@staffmail.ed.ac.uk;
Barbara Webb
b.webb@ed.ac.uk

Received: *31 January 2016*
Accepted: *28 March 2016*
Published: *13 April 2016*

Citation:
Ardin PB, Mangan M and Webb B (2016) Ant Homing Ability Is Not Diminished When Traveling Backwards.
Front. Behav. Neurosci. 10:69.
doi: 10.3389/fnbeh.2016.00069

1. INTRODUCTION

Non-pheromone laying ants are expert navigators, with individuals capable of foraging for up to 1 km (Huber and Knaden, 2015) before precisely relocating their hidden nest entrance. Normally this behavior is supported by path integration (Müller and Wehner, 1988), but visual cues alone are sufficient to guide individuals home along familiar routes (Wehner et al., 1996; Kohler and Wehner, 2005; Mangan and Webb, 2012). Ants are also capable of using visual information to return from previously unvisited locations following a displacement (Wehner and Räber, 1979; Zeil, 2012). This is commonly termed "visual homing," and can be explained if there is sufficient overlap of the current scene with stored memories around the target location such that comparison between them allows an appropriate direction of movement to be obtained.

Hypothesized strategies of visual homing in insects generally adhere to a bottom-up methodology: seeking the simplest mechanism that can account for the behavior, with complexity only added when required to explain new behavioral data (Wystrach and Graham, 2012). A widespread simplifying assumption is that ants' visual memory is a retinotopic snapshot (Collett and Cartwright, 1983; Wehner et al., 1996), rather than a reconstruction of the 3D arrangement of surrounding landmarks see also discussion in Collett et al. (2013). This memory could be a single

environmental feature which has strong visual qualities and is acting as a beacon, which the ant aims to keep in the center of the field of view, or at some fixed retinal displacement, for some part of its journey (Collett, 1996). Or it could be the entire panorama (Zeil et al., 2003), or skyline (Graham and Cheng, 2009), or some parametric representation of the image projected on the retina such as the average landmark vector (Möller et al., 2001) or visual center of mass (Hafner, 2001). The assumption that the retinopic projection is important is supported by evidence that changing the distance and size of landmarks in such a way as to present the same view from a given location results in ants treating it as the same location (Wehner and Räber, 1979; Åkesson and Wehner, 2002; Narendra et al., 2007). In addition, evidence that ants do not appear to be able to transfer landmark information acquired in one eye to drive successful guidance when viewing the world with the other eye (Wehner and Müller, 1985), has been taken to support the view that this memory is "fixed relative to retinal co-ordinates" (Wehner et al., 1996) (i.e., cannot be mentally rotated, and is not stored in some rotation invariant form). Thus physical alignment of the animal to the same viewing direction as when the memory was stored must play a role in the homing process (Wehner et al., 1996).

Following such alignment, there are multiple ways the ant could use its visual memory to obtain a heading direction, either through a calculation based on the difference between memory and the current view (Cartwright and Collett, 1982; Möller et al., 2001; Vardy and Moller, 2005; Möller and Vardy, 2006), simple "move and compare" gradient descent on the translational image difference function (tIDF) (Zeil et al., 2003; Stürzl et al., 2008; Mangan, 2011; Stürzl et al., 2015), or through recovery of a "local vector"(Collett, 2010) or a motor action (Lent et al., 2009) associated to the view. The alignment itself could be based on external cues, such as the celestial compass, allowing the animal either to rotate to match a particular stored view, or to chose from multiple stored views the one which is best aligned (Collett and Cartwright, 1983; Mangan and Webb, 2009; Möller, 2012), before attempting to recover the heading. However, a parsimonious alternative is that alignment itself can be driven by view comparison (Zeil et al., 2003). Using a simple pixel-wise image difference function (IDF), as the ant rotates it will experience a minimum in the IDF when its current view is aligned to a visual memory. Moreover, if the memory was stored while the ant was facing the desired heading direction (e.g., facing the nest), then turning to face the minimum in the rotational IDF (rIDF) means the ant has recovered the required heading direction; that is, retinotopic alignment is not just necessary, but sufficient, for visual homing. The observation of "scanning" behaviors in homing ants (rotating on the spot before selecting a direction of travel) (Wystrach et al., 2014; Zeil et al., 2014) seems consistent with this explanation.

An important generalization of this idea is that the ant may be able to use the rIDF to recover the current best heading direction relative to a large set of memories, without needing to choose a specific memory for the comparison. For example, the smallest pixel-wise difference (or greatest "familiarity") between all memories and the view experienced during a physical rotation will be found for the spatially closest memory, when view and memory are aligned. The plausibility of this method is supported by neural algorithms for efficient simultaneous storage and comparison of multiple views collected along routes toward the nest (Baddeley et al., 2012; Ardin et al., 2016). Making the additional assumption that this method for recovering the heading is applied continuously by the ant, the retinotopic alignment algorithm can generate long-range route following behaviors in simulated ant environments (Baddeley et al., 2012; Ardin et al., 2016). In addition by training the same algorithm with multiple homeward facing memories, as might have been obtained on learning walks (Nicholson et al., 1999; Graham et al., 2010; Müller and Wehner, 2010), visual homing from novel locations can emerge (Wystrach et al., 2013; Dewar et al., 2014; Zeil et al., 2014; Stürzl et al., 2015). Most recently, Kodzhabashev and Mangan (2015) simplified this approach further by demonstrating that route following is possible using a continuous oscillatory algorithm driven by the instantaneous view familiarity, removing the need for scanning at every step. Some authors, including ourselves, have thus suggested that the ant could have a single mechanism for route following and homing, involving continuous realignment to obtain the best retinotopic match to memories facing the nest (Wystrach et al., 2013; Dewar et al., 2014; Ardin et al., 2016).

However, it should be noted that in some experiments, ants displaced from a familiar route to a nearby novel location do not move in the direction of the rIDF minimum but prefer the heading predicted by the lowest points of the skyline (Wystrach et al., 2012). Perhaps more crucially, ants often do not face the direction they are traveling, for example while undertaking group transport (Czaczkes and Ratnieks, 2013), when being carried by another ant (Fourcassie et al., 2000) and when they need individually to move a cumbersome food item.

In the current study we provide ants with large prey item which they can only deliver to the nest by dragging backwards, and assess their ability to home after displacement while experiencing an inverted viewpoint relative to the direction of travel. The aggressive predatory ant, *Myrmecia croslandi*, is ideal for studying navigation under challenging visual conditions as it will readily attack large prey and inhabits an environment where the both tIDF and rIDF have been shown to be consistent with the paths taken by displaced ants (Narendra et al., 2013; Stürzl et al., 2015). We find that the facing direction of ants—toward or away from the nest—has little influence on their ability to move directly home, which casts some doubt on the hypothesis that continuous retinotopic matching is a sufficient mechanism to explain homing.

2. MATERIALS AND METHODS

Experiments were conducted at the campus field station at the Australian National University (3516′49.8″ S 14906′43.9″E). A single nest of *M. croslandi* (colloquially named "Jumping Jacks" due to the frequent jumps they perform even when carrying large food items) was used for all the experiments. The foraging patterns of ants from this nest are characterized in Jayatilaka et al. (2014). Ants collect nectar from two eucalyptus trees located C.10

m South (200 degrees from north) of the nest entrance but the visual panorama is also dominated by another tree C.8 m North (320 degrees) (**Figures 1A,B**). During the morning and afternoon ants seek prey in the area a few meters around the nest which they subdue with a sting before transporting it back to the nest across rough grass and leaf litter up to 20 cm in depth (**Figure 1C**).

Outbound foragers were collected at approximately 1–1.5 m from the nest; 12 were traveling South and 8 North. Captured ants were kept in the dark for 15–30 min during which time they were fed a 10% sugar solution. Immediately prior to release, ants were offered a large live prey item (a cricket approximately 1 cm length). Individual ants were then released from a clear test tube on a level platform (50 cm × 85 cm) positioned 4 m West (275 degrees from the nest). This is distant from the familiar route to the tree (**Figure 1A**) but we cannot be certain that ants have not previously foraged in this direction. A total of 20 ants were tested, of which 8 refused the prey item and ran home unencumbered. The remaining 12 stung the prey before dragging it back to the nest.

The ant paths were recorded from above using either a Sony FDR-AX100 or Panasonic DMC-FZ200 camera mounted on a tripod, which was repositioned repeatedly to capture the path from the point the animal left the test tube all the way back to the nest, with some small gaps during camera repositioning. The position of the ant and its head-tail orientation were determined in every 25th frame (i.e., at 1 s intervals) using custom software (Matlab) with control points marked when the camera was moved. The sections of track recorded in each camera position were then aligned by matching control points and rotating the track around a fixed point (the nest). The difference between successive positions x_i is used to determine the direction of movement of the ant in each frame, and tortuosity of the path calculated as:

$$\frac{\sum (x_{i+1} - x_i)}{x_n - x_1} \quad (1)$$

i.e., the sum of euclidean distances between successive positions on the track divided by the euclidean distance between the start and end of the track.

An ant was considered as facing forwards when the head-tail orientation was within an arc ±90 degrees centered on the bearing of the nest. Using this definition, the length of segments of track facing continuously away from or toward the nest could be calculated. We note that these ants have been observed in previous studies (Zeil et al., 2014) to show substantial independent movement of the head relative to the body (which we could not resolve for the resolution in our video) which could introduce up to 30 degrees difference between the head-tail

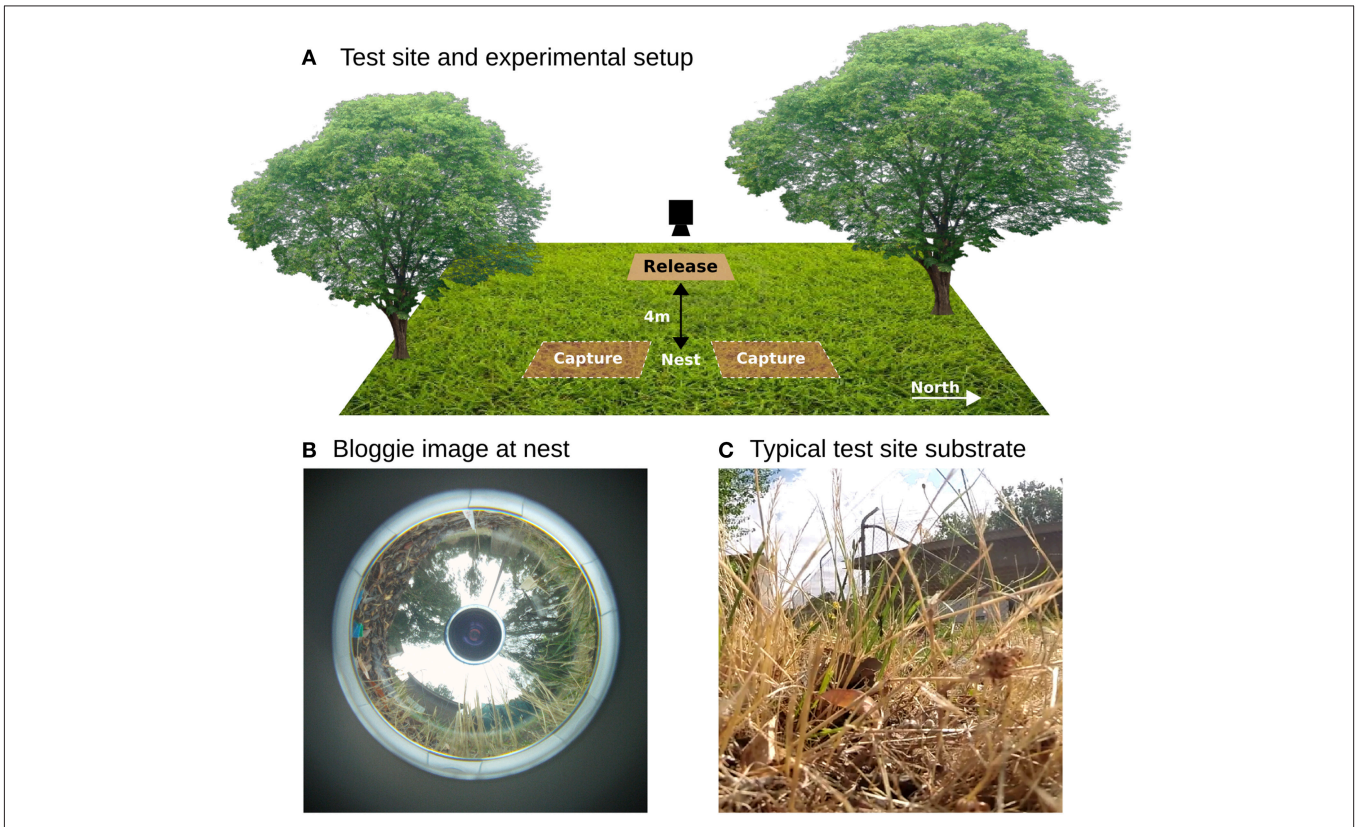

FIGURE 1 | Overview. (A) Ants were captured approximately 1–1.5 m from the nest on foraging runs towards the north and south. They were then released on a platform 4m West and the entire homeward track filmed by repositioning a camera on a tripod. **(B)** A panoramic picture taken at the nest using Sony Bloggie camera shows there is a distinctive panorama dominated by the surrounding trees. **(C)** Image from within the grassy substrate highlighting the complex 3D environment through which the ants must navigate by walking or jumping.

orientation and the actual gaze direction of the ant. Nevertheless, we can safely assume an ant with a backward orientation (more than ±90 degrees from the nest bearing) could not be gazing directly at the nest.

For one of the analyses below, we assume that ants could be gazing at the nest (i.e., obtaining retinal alignment with a image stored when facing the nest from the same direction) each time their head-tail orientation falls below ±5 degrees of the nest. We then average their direction of movement relative to the nest in the previous 3 frames (i.e., over 3 s of movement) and subsequent 3 frames. The error in this direction (i.e., the extent of deviation from 0, moving directly toward the nest) should decrease if looking forward is associated with making course corrections. Note that using different values (up to 30 degrees) for the definition of "forward looks" and different durations (1–5 frames) of averaging did not make a qualitative change to the reported results.

3. RESULTS

All 20 displaced ants returned directly to the nest irrespective of whether they were carrying food or not (**Figure 2A**). Although the ants had some path integration information, indicating the nest lay either north or south, there was no consistent deviation in their initial headings corresponding to this vector direction (**Supplementary Material 1**).

The color coding in **Figure 2A** shows the head-tail orientation relative to the nest of the ant at each point on the path. Ants without food generally faced toward the nest (yellow), but ants with large prey items still managed to travel toward the nest whilst spending significant amounts of time (percentage backward shown below each path) facing in completely the opposite direction (blue) due to the necessity to drag the food, including some long continuous segments without facing forward (**Figures 3C,E**). The ants carrying food thus had very similar mean direction of movement, despite extremely different head-tail orientation relative to the nest (**Figure 2B**). We found no statistical difference in the tortuosity of the paths of ants with and without food (no food: mean 1.42 ± 0.2, food: mean 1.58 ± 0.21, *t*-test 1.7214, $p = 0.10$, **Figure 3B**). In addition, the time taken to return to the nest is comparable for ants with and without food (control: mean 286.4 ± 87.5, experiment: mean 383.4 ± 123.6, *t*-test, 1.9144, $p = 0.0716$, **Figure 3A**). In each case the direction of difference is in favor of a faster and more direct return by ants not carrying food, and a larger N (in our experiment *N no food = 8: N with food = 12*) might have reached significance; but this could be equally due to the need to drag prey as to the higher percentage of backward movement. It remains evident that the food-dragging ants can maintain the home direction for significant distances without facing the nest. Thus continuous physical alignment toward the nest is not necessary to perform visual homing.

However, all ants show at least occasional moments of facing the nest, that is, none of them complete the full journey while facing only backwards. These nest-facing moments might provide ants with intermittent opportunities to acquire the bearing to the nest through retinotopic alignment. If this was coupled to some form of vector following or path stabilization mechanism, possibly with respect to celestial cues, it could explain the ant's ability to maintain their nestward direction when not aligned with the nest.

Previous reports have described stereotyped "stop and scan" behavior in ants (Wystrach et al., 2014; Zeil et al., 2014), particularly just after release in a novel environment. This was not obvious in our videos, where turning to face the nest occurred for a number of reasons, such as the need to manipulate the load over obstacles, or where the substrate was sufficiently smooth (such as across a leaf) to make a walk or jump forwards possible, and nestward facing periods appear to be equally distributed throughout the path (**Supplementary Material 2**). Nevertheless, some of these these moments of facing forward could be self-induced scans, or could at least provide opportunities to correct alignment through retinotopic matching or other methods. If this were the case, one might expect to see corrections in the course direction associated with these time points. However, comparison of the error in direction of ants, averaged over several seconds, before and after their forward-facing moments shows no evidence that the error has decreased after their "forward look" (**Figure 3D**). We note it is possible this analysis is not sufficiently sensitive to reveal corrections in the course. More detailed examination of the paths, or more direct experimental control over when ants can obtain view information may be needed to resolve this question.

4. DISCUSSION

We have shown that visually guided ants can travel back to their nest after displacement to a novel location with little or no impairment of efficiency irrespective of the direction they are looking. This casts doubt on some current theories of how visual navigation is undertaken.

The use of continuous heading adjustment by retinotopic alignment, either through frequent scans to find the minimum in image difference (Baddeley et al., 2012) or oscillation around the minimum (Kodzhabashev and Mangan, 2015), has been successfully applied to mimic route following in ants. In this case, the ant is assumed to have stored images along previous traversals of the route, so is likely to have stored a nearby image, facing along the route, which will provide a clear minimum (or "look familiar") when retinotopically aligned. Several papers (Graham et al., 2010; Narendra et al., 2013; Wystrach et al., 2013; Dewar et al., 2014; Zeil et al., 2014; Stürzl et al., 2015) describe how this approach could also explain visual homing behavior, if the ant is assumed to have performed learning walks to collect retinotopic views facing its nest from multiple directions around the nest. Our data suggests that this account is problematic, as ants can cover long distances toward the nest without facing the nest, and there is no apparent improvement in the directness of the approach for ants that mostly face the nest, or after the ant was "looking forward."

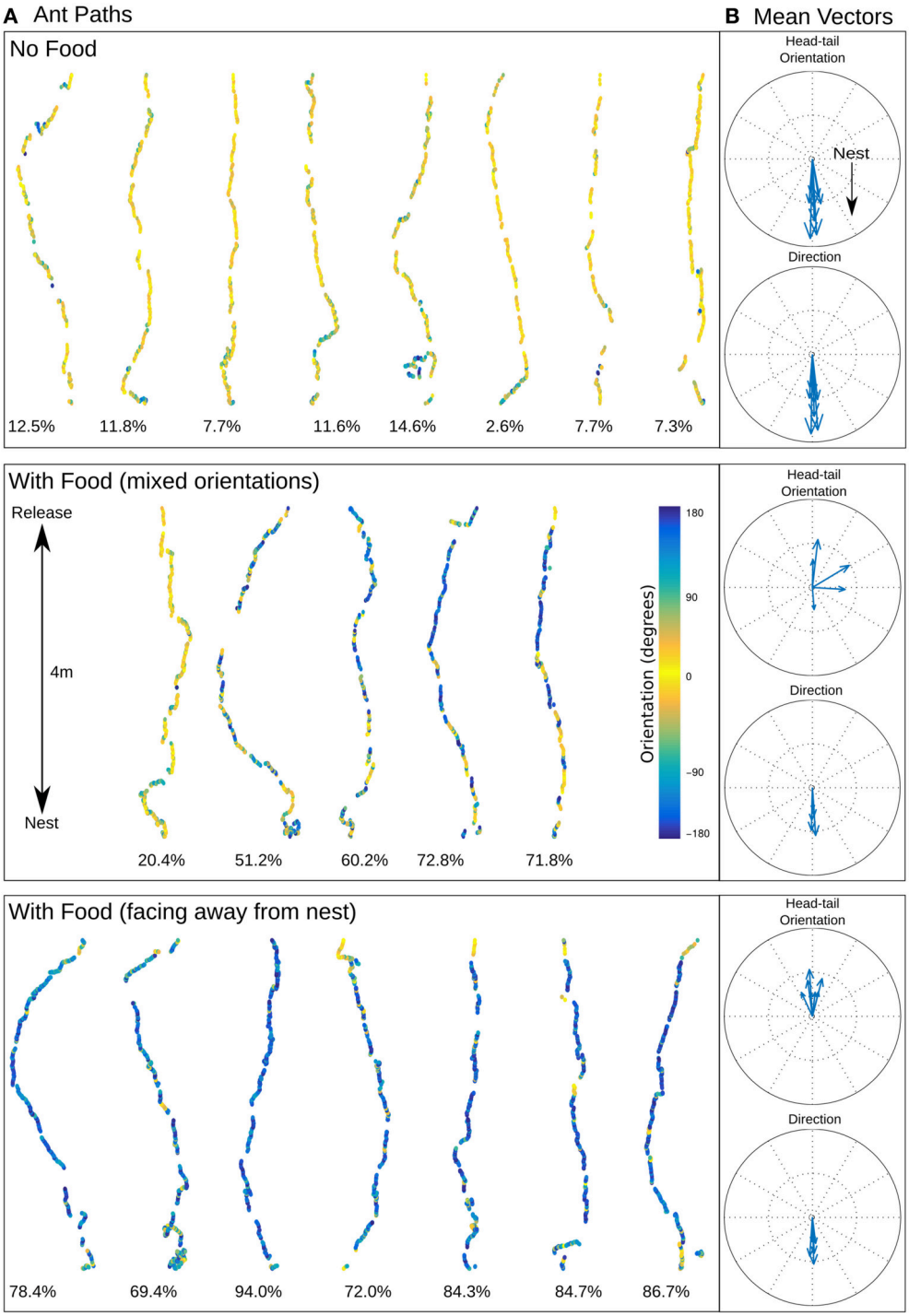

FIGURE 2 | Ant homing. (A) Recorded ant paths, with head-tail orientation shown via color-coding for ants without food (top) and ants carrying prey (middle and bottom), and **(B)** mean vectors for each path for direction of movement and head-tail orientation. The mean direction for ants with or without food is almost identical (no food: mean 0.92 ± 56.40 degrees; with food (mixed orientations): mean 1.50 ± 68.94 degrees; with food (facing away from the nest): mean 1.80 ± 61.72 degrees) but the head-tail orientation is strikingly different (no food: mean 2.11 ± 47.32 degrees; with food (mixed orientations): mean 72.62 ± 131.88 degrees; with food (facing away from the nest): mean −177.59 ± 66.17 degrees). Below each path is shown the percentage of time the ant was moving backwards.

A previous study of homing (Zeil et al., 2014), using the same ant species and a similar displacement approach to the current study, focussed on the initial movements of ants released in an unfamiliar location. These appeared consistent with the hypothesis that the ants use retinotopic alignment, at least to obtain an initial heading direction. It is thus possible that the

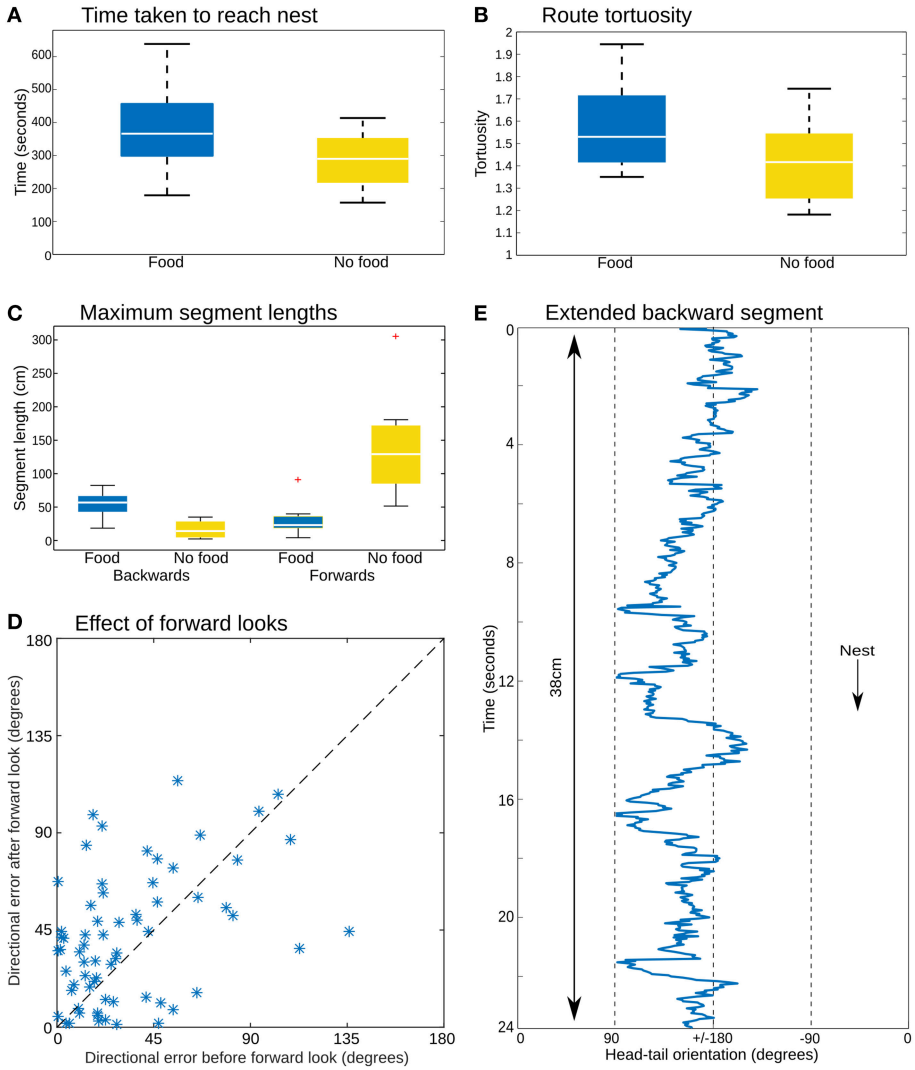

FIGURE 3 | Path analysis. (A) The time to return to the nest is similar whether or not the animals were carrying a food item. **(B)** Path tortuosity was not significantly different. **(C)** While ants without food had distinctively longer segments facing toward the nest, the ants with food managed substantial distances without facing in the nest direction. **(D)** Comparing the direction of movement for three time steps before and after the moments at which prey-carrying ants face the nest (body-tail orientation $<\pm 5$ degrees) shows no clear reduction in the error of the heading direction associated with such "forward looks," which should appear as a preponderance of points below the $x = y$ dashed line. **(E)** Head-tail orientation of a section of one ant path analyzed in every frame (25 Hz), showing an extended period of backward movement with no looks forward.

ants in our study are using a "scan and fix" strategy. By taking an initial heading based on image matching, recording the compass direction of the nest using the celestial compass, and by flipping the bearing, the compass could be used to guide the path homeward while facing backwards. Or the ant could align to the nest, turn backward, record this new view, and use this to guide its direction. It may be the case that an even simpler mechanism is being used to maintain an approximately straight course between fixes, such as directional inertia (Lent et al., 2009) or optomotor stabilization (Götz, 1971).

However, we are not certain the ant could reliably obtain even its initial heading from the rIDF in this situation, at least if we assume the release location is novel (we cannot rule out that the ants in our experiment may have experienced the world from the location of the release platform while foraging). If the ant has stored images near the nest (during learning walks) while facing from multiple directions toward the nest, and is now rotating far from the nest, there will be multiple minima in the scan as it aligns in turn with each memory (Narendra et al., 2013). The difference between these minima could be small, and potentially swamped by any noise that might be introduced by lighting changes, tilt, head-angle induced by dragging a large object, etc. The difference is dependent on the ratio of the assumed nest-learning walk distance to the nest-release point distance, as illustrated in Narendra et al. (2013), Figure 7, where 1 m "learning walk" images from 4 cardinal directions produce almost identical minima for a 10 m scan whereas 5 m images produce one with a significantly deeper minimum. The available evidence

on learning walks for these ants seems to us more consistent with the shorter distance (Jayatilaka, 2014). To date, successful use of retinotopic alignment for homing has been evaluated mostly in simulated or reconstructed environments, where noise is absent (Wystrach et al., 2013; Dewar et al., 2014; Zeil et al., 2014; Stürzl et al., 2015). The presence of this problem (i.e., lack of a single clear minima) for real images in Wystrach et al. (2012) led to the proposal that ants use different strategies when on a familiar route (rIDF retinotopic alignment) versus novel locations (skyline matching of absolutely aligned views), with the strategy selected through a visual familiarity threshold.

An alternative explanation for our results is that ants could be using the translational IDF to move toward the nest. As discussed in the introduction, this could potentially operate without physical alignment by using comparisons of the current image to a set of images stored at or around the goal in different orientations. As the ant adopts different headings, it is assumed that different images will provide a sufficiently good match such that the overall minimum should decrease as the goal is approached, and the ant could follow the gradient of this surface toward its nest. However, as the ant moves in and out of perfect alignment with one of its stored images, the surface becomes subject to local minima, surrounded by increases in the IDF when it is not so well aligned, as shown for example in Wystrach et al. (2012) where an absolute view alignment process was required for homing from novel location. Combined with other limitations of tIDF, such as the need to move through three non-colinear points to obtain sufficient gradient information to adopt an accurate direction, it is not clear that this method could account for our current data.

Following Baddeley et al. (2012), we have previously argued that simple retinotopic matching to all stored memories, through physical alignment to move in the direction that looks most familiar, can explain visual navigation in ants (Kodzhabashev and Mangan, 2015; Ardin et al., 2016). The current results suggest that a more complicated process is at work. For example, some of the described issues with the retinotopic alignment could be overcome by storing celestial compass directions to index retrieval of visual memory (Müller and Wehner, 2010). A further possibility is that the visual scene is stored in a form which is rotation and tilt invariant, which could allow IDF gradient descent despite the noise induced by uneven terrain and transport of food items (Ardin et al., 2015). At this stage it remains to be seen whether this hypothesis can explain our data, or whether an even more abstracted process, such as mental rotation, is at work in these amazing animals.

AUTHOR CONTRIBUTIONS

PA, conducted the original research, performed the majority of the analysis, authorship of paper. MM, development of argument, authorship of paper. BW, supervised research, undertook analysis, authorship and review of paper.

FUNDING

This work was supported in part by grants EP/F500385/1 and BB/F529254/1 for the University of Edinburgh School of Informatics Doctoral Training Center in Neuroinformatics and Computational Neuroscience (www.anc.ac.uk/dtc) from the UK Engineering and Physical Sciences Research Council (EPSRC), UK Biotechnology and Biological Sciences Research Council (BBSRC), and the UK Medical Research Council (MRC).

ACKNOWLEDGMENTS

The authors would like to extend their gratitude to Professor Jochen Zeil for his hospitality and assistance in undertaking this research, and both Professor Jochen Zeil and Dr Antoine Wystrach for their observations in guiding the work and comments on the draft paper. We would like to thank our reviewers for their comments and additional insights which we have incorporated into this paper.

SUPPLEMENTARY MATERIAL

The Supplementary Material for this article can be found online at: http://journal.frontiersin.org/article/10.3389/fnbeh.2016.00069

Supplementary Material 1 | Release vectors. The immediate paths taken by the animals on release was recorded while still on the platform. There is no obvious difference in the initial vector irrespective of whether the capture occurred North or South of the nest entrance. We take this as evidence that the effect of the path integration vector in our experiment was negligible.

Supplementary Material 2 | Path location and orientation. The view direction was categorized as forwards (<±90 degrees of the nest) or backwards (>±90 degrees of the nest) and collated for each of the groups used in **Figure 2A**. The relative frequency of the two categories of view direction was calculated along the path using 10cm bins. The path length was 4 m but for both groups of ants with food this was occasionally exceeded when the animal circled around the nest entrance. While there is a greater number of forward looks at the start of the path for "backwards ants" the release platform has a smooth and level surface which in some cases allows the ant to walk forwards. Therefore we believe this data does not either support or refute the possibility of ants looking forwards and taking a fix on the nest direction at the start of their path.

REFERENCES

Åkesson, S., and Wehner, R. (2002). Visual navigation in desert ants cataglyphis fortis: are snapshots coupled to a celestial system of reference? *J. Exp. Biol.* 205, 1971–1978.

Ardin, P., Mangan, M., Wystrach, A., and Webb, B. (2015). How variation in head pitch could affect image matching algorithms for ant navigation. *J. Comp. Physiol. A* 201, 585–597. doi: 10.1007/s00359-015-1005-8

Ardin, P., Peng, F., Mangan, M., Lagogiannis, K., and Webb, B. (2016). Using an insect mushroom body circuit to encode route memory in complex natural environments. *PLoS Comput. Biol.* 12:e1004683. doi: 10.1371/journal.pcbi.1004683

Baddeley, B., Graham, P., Husbands, P., and Philippides, A. (2012). A model of ant route navigation driven by scene familiarity. *PLoS Comput. Biol.* 8:e1002336. doi: 10.1371/journal.pcbi.1002336

Cartwright, B., and Collett, T. (1982). How honey bees use landmarks to guide their return to a food source. *Nature* 295, 560–564. doi: 10.1038/295560a0

Collett, M. (2010). How desert ants use a visual landmark for guidance along a habitual route. *Proc. Natl. Acad. Sci. U.S.A.* 107, 11638–11643. doi: 10.1073/pnas.1001401107

Collett, M., Chittka, L., and Collett, T. S. (2013). Spatial memory in insect navigation. *Curr. Biol.* 23, R789–R800. doi: 10.1016/j.cub.2013.07.020

Collett, T. (1996). Insect navigation en route to the goal: multiple strategies for the use of landmarks. *J. Exp. Biol.* 199, 227–235.

Collett, T., and Cartwright, B. (1983). Eidetic images in insects: their role in navigation. *Trends Neurosci.* 6, 101–105. doi: 10.1016/0166-2236(83)90048-6

Czaczkes, T. J., and Ratnieks, F. L. (2013). Cooperative transport in ants (Hymenoptera: Formicidae) and elsewhere. *Myrmecol. News* 18, 1–11.

Dewar, A. D., Philippides, A., and Graham, P. (2014). What is the relationship between visual environment and the form of ant learning-walks? An *in silico* investigation of insect navigation. *Adapt. Behav.* 22, 163–179. doi: 10.1177/1059712313516132

Fourcassie, V., Dahbi, A., and Cerdá, X. (2000). Orientation and navigation during adult transport between nests in the ant Cataglypis iberica. *Naturwissenschaften* 87, 355–359. doi: 10.1007/s001140050739

Götz, K. (1971). Principles of optomotor reactions in insects. *Bibl. Ophthalmol.* 82, 251–259.

Graham, P., and Cheng, K. (2009). Ants use the panoramic skyline as a visual cue during navigation. *Curr. Biol.* 19, R935–R937. doi: 10.1016/j.cub.2009.08.015

Graham, P., Philippides, A., and Baddeley, B. (2010). Animal cognition: multi-modal interactions in ant learning. *Curr. Biol.* 20, R639–R640. doi: 10.1016/j.cub.2010.06.018

Hafner, V. V. (2001). Adaptive homing—robotic exploration tours. *Adapt. Behav.* 9, 131–141. doi: 10.1177/10597123010093002

Huber, R., and Knaden, M. (2015). Egocentric and geocentric navigation during extremely long foraging paths of desert ants. *J. Comp. Physiol. A*, 201, 609–616. doi: 10.1007/s00359-015-0998-3

Jayatilaka, P., Raderschall, C. A., Narendra, A., and Zeil, J. (2014). Individual foraging patterns of the jack jumper ant *Myrmecia croslandi* (Hymenoptera: Formicidae). *Myrmecol. News* 19, 75–83.

Jayatilaka, P. W. A. (2014). *Individual Foraging Careers of the Jack Jumper Ant, Myrmecia croslandi*. Ph.D., thesis, The Australian National University.

Kodzhabashev, A., and Mangan, M. (2015). "Route following without scanning," in *Biomimetic and Biohybrid Systems*, eds S. P. Wilson, P. F. M. J. Verschure, A. Mura, and T. J. Prescott (Barcelona: Springer), 199–210.

Kohler, M., and Wehner, R. (2005). Idiosyncratic route-based memories in desert ants, Melophorus bagoti: how do they interact with path-integration vectors? *Neurobiol. Learn. Mem.* 83, 1–12. doi: 10.1016/j.nlm.2004.05.011

Lent, D. D., Graham, P., and Collett, T. S. (2009). A motor component to the memories of habitual foraging routes in wood ants? *Curr. Biol.* 19, 115–121. doi: 10.1016/j.cub.2008.11.060

Mangan, M. (2011). *Visual Homing in Field Crickets and Desert Ants: A Comparative Behavioural and Modelling Study*. Ph.D., thesis, The University of Edinburgh.

Mangan, M., and Webb, B. (2009). Modelling place memory in crickets. *Biol. Cybern.* 101, 307–323. doi: 10.1007/s00422-009-0338-1

Mangan, M., and Webb, B. (2012). Spontaneous formation of multiple routes in individual desert ants (Cataglyphis velox). *Behav. Ecol.* 23, 944–954. doi: 10.1093/beheco/ars051

Möller, R. (2012). A model of ant navigation based on visual prediction. *J. Theor. Biol.* 305, 118–130. doi: 10.1016/j.jtbi.2012.04.022

Möller, R., Lambrinos, D., Roggendorf, T., Pfeifer, R., and Wehner, R. (2001). "Insect strategies of visual homing in mobile robots," in *Proceedings of the Computer Vision and Mobile Robotics Workshop CVMR* (Heralikon), Vol. 98.

Möller, R., and Vardy, A. (2006). Local visual homing by matched-filter descent in image distances. *Biol. Cybern.* 95, 413–430. doi: 10.1007/s00422-006-0095-3

Müller, M., and Wehner, R. (1988). Path integration in desert ants, Cataglyphis fortis. *Proc. Natl. Acad. Sci. U.S.A.* 85, 5287–5290. doi: 10.1073/pnas.85.14.5287

Müller, M., and Wehner, R. (2010). Path integration provides a scaffold for landmark learning in desert ants. *Curr. Biol.* 20 1368–1371. doi: 10.1016/j.cub.2010.06.035

Narendra, A., Gourmaud, S., and Zeil, J. (2013). Mapping the navigational knowledge of individually foraging ants, *Myrmecia croslandi*. *Proc. R. Soc. Lond. B Biol. Sci.* 280:20130683. doi: 10.1098/rspb.2013.0683

Narendra, A., Si, A., Sulikowski, D., and Cheng, K. (2007). Learning, retention and coding of nest-associated visual cues by the australian desert ant, Melophorus bagoti. *Behav. Ecol. Sociobiol.* 61, 1543–1553. doi: 10.1007/s00265-007-0386-2

Nicholson, D., Judd, S., Cartwright, B., and Collett, T. (1999). Learning walks and landmark guidance in wood ants (Formica rufa). *J. Exp. Biol.* 202, 1831–1838.

Stürzl, W., Cheung, A., Cheng, K., and Zeil, J. (2008). The information content of panoramic images i: The rotational errors and the similarity of views in rectangular experimental arenas. *J. Exp. Psychol. Anim. Behav. Process.* 34, 1–14. doi: 10.1037/0097-7403.34.1.1

Stürzl, W., Grixa, I., Mair, E., Narendra, A., and Zeil, J. (2015). Three-dimensional models of natural environments and the mapping of navigational information. *J. Comp. Physiol. A* 201, 563–584. doi: 10.1007/s00359-015-1002-y

Vardy, A., and Moller, R. (2005). Biologically plausible visual homing methods based on optical flow techniques. *Connect. Sci.* 17, 47–89. doi: 10.1080/09540090500140958

Wehner, R., Michel, B., and Antonsen, P. (1996). Visual navigation in insects: coupling of egocentric and geocentric information. *J. Exp. Biol.* 199, 129–140.

Wehner, R., and Müller, M. (1985). Does interocular transfer occur in visual navigation by ants? *Nature* 315, 228–229. doi: 10.1038/315228a0

Wehner, R., and Räber, F. (1979). Visual spatial memory in desert ants, Cataglyphis bicolor (Hymenoptera: Formicidae). *Experientia* 35, 1569–1571. doi: 10.1007/BF01953197

Wystrach, A., Beugnon, G., and Cheng, K. (2012). Ants might use different view-matching strategies on and off the route. *J. Exp. Biol.* 215, 44–55. doi: 10.1242/jeb.059584

Wystrach, A., and Graham, P. (2012). What can we learn from studies of insect navigation? *Anim. Behav.* 84, 13–20. doi: 10.1016/j.anbehav.2012.04.017

Wystrach, A., Mangan, M., Philippides, A., and Graham, P. (2013). Snapshots in ants? new interpretations of paradigmatic experiments. *J. Exp. Biol.* 216, 1766–1770. doi: 10.1242/jeb.082941

Wystrach, A., Philippides, A., Aurejac, A., Cheng, K., and Graham, P. (2014). Visual scanning behaviours and their role in the navigation of the australian desert ant Melophorus bagoti. *J. Comp. Physiol. A* 200, 615–626. doi: 10.1007/s00359-014-0900-8

Zeil, J. (2012). Visual homing: an insect perspective. *Curr. Opin. Neurobiol.* 22, 285–293. doi: 10.1016/j.conb.2011.12.008

Zeil, J., Hofmann, M. I., and Chahl, J. S. (2003). Catchment areas of panoramic snapshots in outdoor scenes. *JOSA A* 20, 450–469. doi: 10.1364/JOSAA.20.000450

Zeil, J., Narendra, A., and Stürzl, W. (2014). Looking and homing: how displaced ants decide where to go. *Philos. Trans. R. Soc. B Biol. Sci.* 369:20130034. doi: 10.1098/rstb.2013.0034

Conflict of Interest Statement: The authors declare that the research was conducted in the absence of any commercial or financial relationships that could be construed as a potential conflict of interest.

4.2 Additional analysis

In this section additional analysis is provided which explores the characteristics of the visual environment which are relevant to models of visual navigation, and presents the results of pilot study into the role of the polarised light in backwards walking. A natural assumption is that the ant uses visual memory to select the initial heading to follow back to the nest but analysis of the rotational IDF at the release point in a simulated world and at the test site shows that if multiple snapshots are stored around the nest entrance the most familiar view at the release point may not point towards the nest. Translational IDF allows a gradient to be calculated which can allow headings to be selected when moving through the environment, however when using the images from the test site the gradient was found to contain local minima which did not correspond with the paths taken by the animals. A further hypothesis is that for both forward and backwards walking the ants select a heading and then follow this bearing by using a memory of the polarised pattern of the sky. Initial research showed that a polarising filter placed above the ants returning to the nest appeared to disrupt headings in a predictable manner suggesting that visual navigation may use heading stabilisation based on information in the sky.

4.2.1 Using rotational and translational IDF to navigate in a symmetrical environment

Visual symmetry in a scene can make getting the correct heading from nest snapshots difficult. Where the environment has visual features which do not change substantially with displacement, rotational IDF (rIDF) at any location will generate minima for every stored view of the nest creating ambiguity over the correct home direction. Based on the results from Ardin et al. (2015) during normal locomotion the variation in the attitude of the head in the environment may introduce sufficient noise to make gradient descent extremely difficult, but is a gradient available at all if the orientation of the visual field is directly away from the goal?

To analyse the visual information present in the environment a database of panoramic images was taken (Sony Bloggie MHS-PM5/V) on a 17.5cm spaced grid extending from the edge of the release platform to the nest. The camera was placed on the ground surface rather than levelled to the horizon and was always oriented in the same direction. The images were unwrapped using custom software and the response of the

green photoreceptor of the ant eye simulated by using the green channel of the image in RGB space. The image was also segmented into ground and sky using hand-tuned parameters to mimic the effect of a UV channel (Stone et al., 2014) and this was then recombined with the green channel version to give a composite image mimicking the full spectral sensitivity of the ant eye (figure 4.1.B). To more closely match the optics of *M. crosslandi* images were downsampled to approximate a 1 degree spatial resolution using the imresize function in Matlab and the field of view restricted to 300 degrees.

A bloggie panorama taken close to the nest was treated as a reference image, with images taken in 4 adjacent locations rotated to face the nest mimicking the potential snapshots stored during a learning walk (figure 4.1.A). The IDF was calculated as the sum of the root mean square (RMS) difference between each pixel in two images:

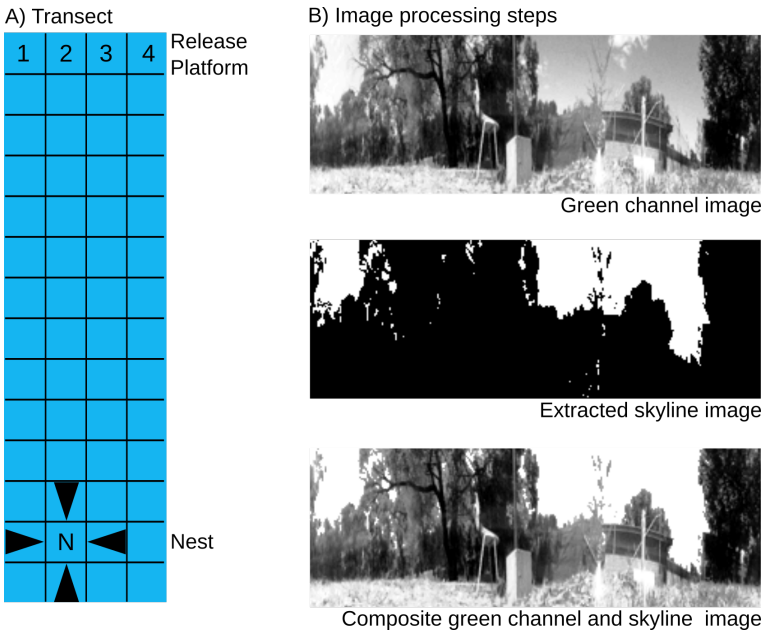

Figure 4.1: Modelling the visual content of the scene. A) The transect shows the location of the four release platform locations (1 to 4) on the 17.5cm grid relative to the nest (N). Four triangles show the position and orientation of 4 nest-facing snapshots. Only location 2 is used in the simulated world rIDF test. B) Example of the image processing steps used with the test site images. Top: images are unwrapped and the green channel selected. Middle: using hand picked variables the image is reduced to binary components of sky and ground. Bottom: the green channel and skyline extraction images are combined into a composite image.

The simulated ant environment was also used to establish the difference between

the test-site images and an ideal world in which there is absolutely no change (other than the simulated ant's position) in the environment between stored images, where a perfectly levelled, identical height, viewpoint is possible. The artificial world was based on the ant world used in previous papers (Ardin et al., 2015) modified by creating a distal panorama with an average height of 14m at a distance of 10m from a nest location with no intervening vegetation.

Could it be the case that a visual compass mechanism is used at the start, or at some points along the path, to obtain the correct heading? We first tested the ability of rIDF in simulation to select a correct heading from the 4 release points (2.8m west of the nest) when 4 reference snapshots around the goal location (from 20cm away, each facing the nest) are stored (figure 4.2.A). Note this method looks for the minima across all possible image comparisons, as the ant cannot know which of its stored memories is the right one to use. We find there is confusion between the minimum for the correct stored view (0 degrees) and the view in the opposite direction (+/-180 degrees). The results using the 4 bloggie pictures taken at the release platform in our experiment against 4 reference images in cardinal directions around the nest location are remarkably similar (figure 4.2.B). At some of the release platform points the minimum rIDF is in the wrong heading direction. Perhaps more importantly, the difference between maximum and minimum rIDF, and between potential minima is extremely small. Thus we believe it would be hard for rIDF to detect the correct minima in the presence of real-world noise such as tilt and varying lighting conditions. Previous simulations have used larger distances from the nest (e.g. 1m) for the learned views (Dewar et al., 2014; Stürzl et al., 2015) but we did not find a significant difference by doing so in our simulated results. The reported data on learning walks in this species (Jayatilaka et al., 2013) suggests trips are near the nest and predominantly in the preferred foraging directions, which would suggest ants might easily find a best minima in the wrong direction.

Alternatively, could the ant be using a visual homing method? As discussed in the introduction, these could potentially operate without physical alignment by using multiple memories. In particular, translational IDF (tIDF) could potentially produce a gradient towards the nest by taking the minima across comparisons of the current image to a set of images stored at or around the goal in different orientations. As the ant adopts different headings, different images will provide the best match, but the overall minima should decrease as the goal is approached. In our simulated world using 4 stored images at the nest and allowing the current view to be aligned either

forwards (0 degrees) or backwards (+/-180 degrees), a clear gradient is apparent which would allow direct return to the nest (figure 4.2.C). However, ants are not always so well aligned, and when the current view direction is modulated by the typical variance in orientation of the ants (+/-32 degrees, Ardin et al. (2016b)) the gradient becomes much noisier, as the effects of the rIDF swamp the effects of the tIDF. In other words, the surface becomes subject to local minima when the ant happens to be well aligned with one of its memories, surrounded by increases in the IDF when it is not so well aligned. The test-site bloggie images give similar results, although here even in the case where the images are all well aligned there is substantial noise at a local level which could lead to homing errors (figure 4.2.D). We thus suggest that unless the ant can select the appropriate stored image (e.g. through indexing its memories by the compass direction) it could not use tIDF in these conditions. Several manipulations of the images were explored (e.g. tilt correction) but no method was able to recover a gradient, although it is possible that some processing method could do so.

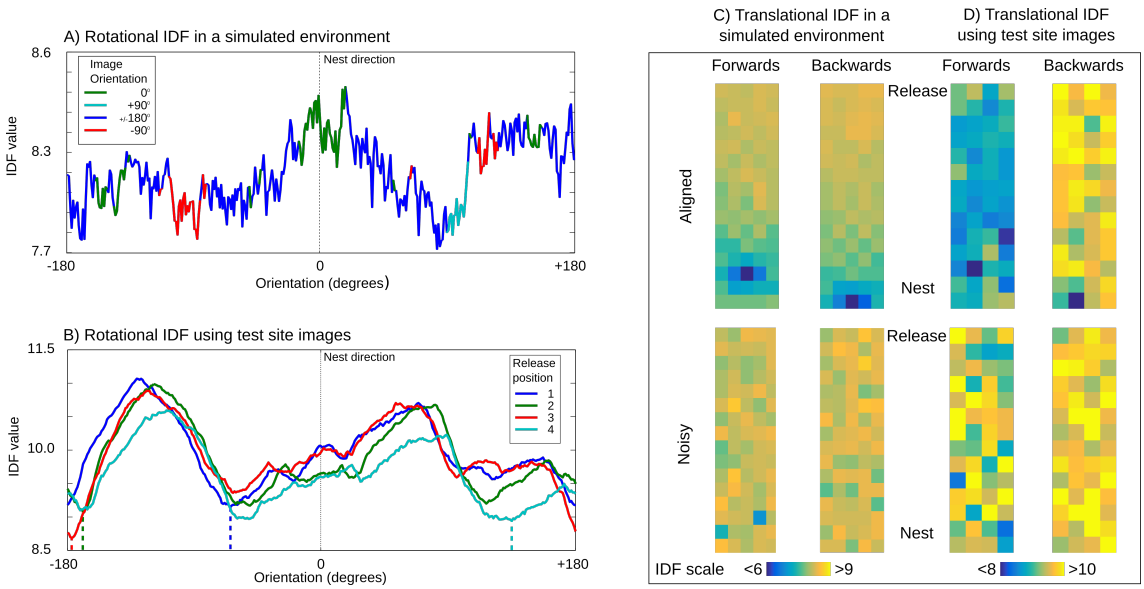

Figure 4.2: Can rotational and translational IDF be used for navigation in this experimental paradigm? A) In the simulated world at a release point 2.8m from the nest which direction would be chosen using 4 snapshots at the nest? The line shows the minimum IDF value across the reference images and the colour coding which snapshot is matched. Facing 0 degrees using the 0 degree nest snapshot (green sections) should produce the lowest IDF in order to get the correct heading but instead the minimum value is at +90 degrees. B) Undertaking the same test with field site images across the 4 release platform locations and 4 images from around the nest. At none of the locations does the rIDF minimum coincide with the nest heading; the minima are marked with drop lines to the x-axis. C) In the simulated environment a smooth tIDF using 4 nest snapshots is produced if images are aligned, but when the images are subject to +/-32 degrees of heading noise the gradient becomes indistinct. D) Using the test site images the tIDF gradient is much weaker than the simulation probably the result of using unlevelled images and the gradient is substantially disrupted with the addition of heading noise.

4.2.2 Do ants use polarised light patterns to stabilise heading directions?

While undertaking this research an experimental protocol was trialled to test whether changing the polarised pattern of the sky would introduce errors into the heading of homeward ants, with the preliminary results indicating that both forwards and backwards moving ants were affected by the intervention. Polarised light might be used

to maintain headings which have been visually selected, but this needs to be studied much more thoroughly (Reid et al., 2011).

Ants were released on the platform using the protocol of Ardin et al. (2016b) and at 1m from the release a 42 cm polarising filter (Polaroid HN22) was placed over the predicted path of the ant (figure 4.3). The filter was orientated in such a way as to attenuate the polarised light from the sky and the track of the ant filmed with the tripod-mounted camera (Sony FDR-AX100) pointed at a 45 degree angle to the ground to minimise reflections. The ant position was measured manually after the distortion by the camera alignment had been removed in software.

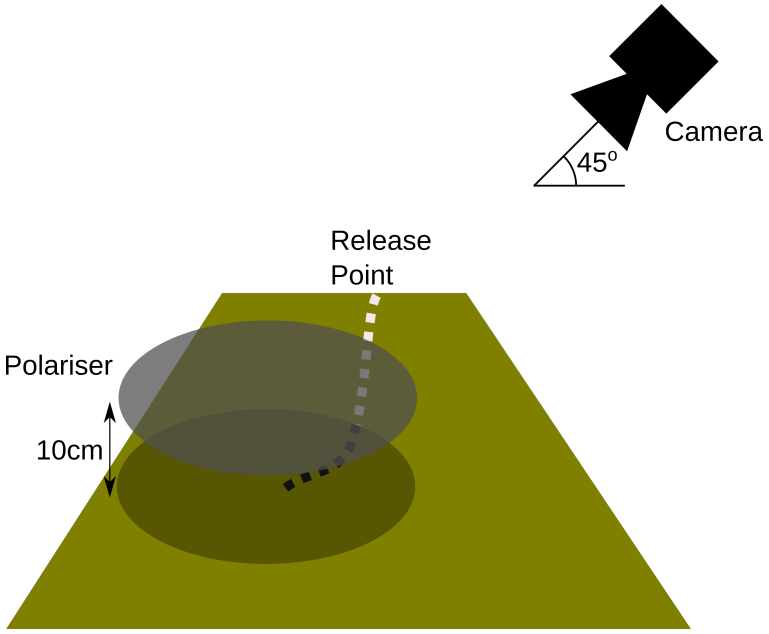

Figure 4.3: Experimental setup using polarising filter. The white dots show the ant path after release without the polarising filter. The filter was placed along the predicted path of the ant and the path recorded using a video camera angled at 45 degrees to minimise reflections from the filter surface. The black dots illustrate the path recorded under the filter.

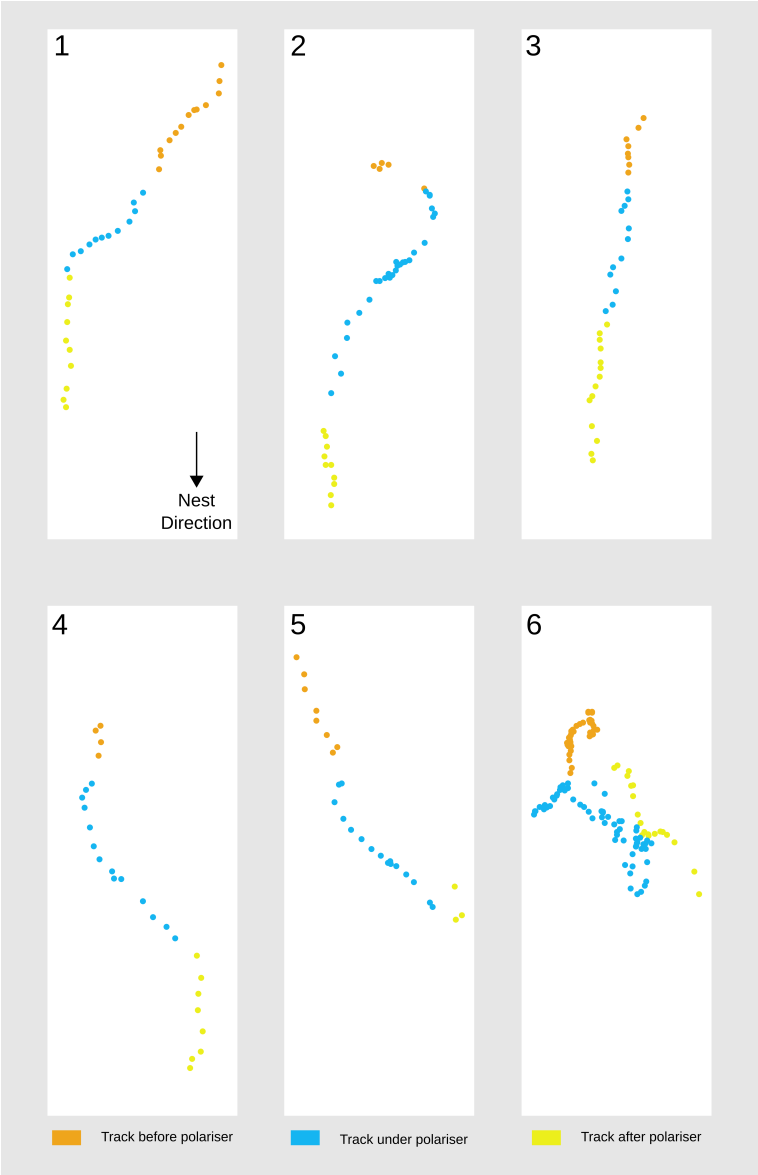

Figure 4.4: Pilot study on the effect of polarised light on heading stabilisation. Plots 1 to 6 show the tracks taken by ants heading from the release platform to the nest as they pass under a polarising filter rotated to minimise the polarised light pattern. Given the methodological constraints the results are promising and suggest that further study of the role of polarised light during zero vector visual homing could be productive.

The results from 6 ants are shown in figure 4.4, where orange dots show the ant position before heading under the polariser, blue dots the track under the polariser, and yellow dots the track after emerging from the polariser. Consistent with the results from Reid et al. (2011) the distortion of the track did not entirely match the polariser rotation but the presence of the polariser appeared to cause a change in heading. It was observed that rotating the filter over the animal could in some instances “steer”

the animal.

As an early indication of the mechanism of heading stabilisation this is promising but a number of methodological issues need to be resolved. In both this study and Reid et al. (2011) it is not clear why the rotation of the polarising filter yields a smaller turn in the animal; this could be due to the way in which the filter changes what the animal senses, that the filter is an imperfect manipulation of sky cues, or it could be indicative that other senses or mechanisms are used to keep a heading. From a technical perspective filming the ant under a dark polarising filter creates some unique technical challenges and the resulting video footage does not give as much detail as the aerial set-up.

Chapter 5

Discussion

5.1 Key Contributions

The preceding chapters have provided new insights into ant visual navigation which can be summarised as follows.

The introduction gave an overview of the scientific understanding of ant navigation and visual/UV mediated ant navigation, of what is known or can be surmised about ant vision from the relevant species (i.e. what the nature of the input into navigation must be), ant motion (in the context of how motion might affect navigation either by motion processing or the interaction of the animal and the environment) and of the models which simulate different aspects of ant navigation, culminating in the description of Ardin et al. (2016a) which is used in Chapter 2 as the basis for examining the preceding aspects of ant navigation (eye, motion and subtle aspects of behaviour). It was necessary to combine knowledge across species and within the order hymenoptera with the obvious attendant risks. In particular this thesis has used research across *cataglyphis* species alongside *Melophorous bagoti* which while they are all thermophyllic ants, inhabit different environments in different continents. Similarly the original research in this thesis used *Cataglyphis velox* and *Myrmecia crosslandi*, species which are not only from different ecologies but fill different niches in each. However such generalisation is a necessity due to the lack of research focused on a single species and we can take comfort from the behavioural similarities across the various animals to allow us to draw some conclusions. Desert ants use visual navigation which seems predominantly to use the far panorama but is also influenced by landmarks closer to the trajectory of the ant. Path integration interacts with visual navigation both by allowing the animal to build a visual memory through learning walks around the nest, and from the initial

inward routes guided by the homeward vector, but there is a more complex dynamic between the two systems on established routes which is yet to be fully understood. A simulation of ant navigation using continuous image matching will faithfully reproduce a learnt route and the case for this general family of algorithms is made more compelling by the ability to use a model of a part of the ant brain to learn and recapitulate the route. The ant visual system contains a set of adaptations starting at the optics of the eye leading through the visual pathway which are not either fully understood and therefore capable of being modelled but can be anticipated to extract features which aid critical behaviours such as central place foraging. Hence exploring the nature of the visual input into the model is a rational step to understand ant navigation further, and can either lend support to the continuous image matching hypothesis, or expose areas for further investigation.

Chapter 2 explored the effect of different types of visual processing on the Ardin et al. (2016a) model in simulation providing further evidence that a 4 degree optical resolution and 10 cm step size between training images are effective parameters.

- The tested visual processing steps do not improve over this baseline and certain types visual processing are incompatible with the model, either due to correlation of inputs, sparsity or the capacity constraints of the network.

- The route errors made by the ant in the environment suggested that the interaction of scene geometry and route are significant to the behaviour, for example that close to vegetation image correlation might make the location distinctive when correctly positioned but that changes in the retinal image over short distances reduce the tolerance to route deviation.

Having established that the untransformed retinal image provides the best input into route recapitulation the effect of normal ant motion on the visual pattern was considered in Chapter 3. Information about ant head stabilisation was acquired through a field study, the relevant data extracted and this was then applied to models.

- Small scale variations in substrate caused the ant to vary head pitch over a wide range of angles (+/-30 degrees) and head angle is principally related to body angle which means that there is little active stabilisation of the head during normal locomotion.

- When images were generated with this range of head pitch the ability to retrieve heading direction was disrupted. A variety of memory methods were then

applied to see if they could control the effect of pitch variation, including discarding cases where pitch is large during recall, averaging a number of images, and matching only against images in the vicinity of the decision point (which assumes that the ant has some knowledge of its location). In all cases large pitch still disrupted the ability to find the correct direction, and it is important to note that when using the full route memory and large pitch, the visual similarity is matched with images of similar pitch rather than place (figure 3: h,i,k,l,n, and o).

- Extending the simulation to full route recapitulation using perfect memory, there was partial success but catastrophic errors occur. The range of head pitch observed in the field when applied to the simulation can distort the untransformed retinal image sufficiently to disrupt navigation by continuous image matching .

So we can be certain that disruptions of the visual scene due to ego-motion can occur and could potentially affect navigation. With the evidence that the retinal image may not be continuously stabilised and that the degree of distortion of the image is sufficient to be detrimental to navigation by continuous image-matching we are left considering two potential hypotheses: either that the continuous image-matching hypothesis could be incorrect or that there is some form of unidentified neural processing which controls for visual effect of head motion. Further research was necessary to investigate these alternatives using a new experimental paradigm based on the observation that ants frequently drag food backwards to the nest. If ants could walk backwards to the nest when displaced, it seems highly improbable that visual navigation is a continuous process of alignment to a memorised image.

- Chapter 4 demonstrated a previously unstudied behaviour, that ants can walk backwards to the nest after displacement (i.e. without a PI vector) without the need for frequent visual checks of the goal, and that when views are taken in the direction of the goal there is no evidence that this leads to an improvement in heading. So a forward-aligned view of direction is not required for visually-mediated navigation which seems to conclusively rule out the combination of stored image matching in a continuous process in this context.

- Performing an image match against nest snapshots in a reasonably complex and realistic simulation does not necessarily lead to identification of the correct heading to a goal.

The combination of these findings may lead us in a particular direction. Visual navigation does not appear to benefit from the tested types of processing notably the elementary motion detector. In itself this does not challenge the model of continuous image matching but it is somewhat surprising given that the combination of the high speed of the animal, the presence of motion detection in the visual pathway and the algorithm's assumption of sampling at small, regular intervals seem like such a natural fit. It is more significant that the natural head motion of the ant when applied to the model is sufficient to disrupt image matching suggesting that the something is missing in the formulation of the algorithm or our knowledge of the animal. Finally the ability to return to the nest while facing away from the direction of travel for substantial periods implies that some significant modification of the continuous image matching model is required. Where then does this suggest further research is necessary?

5.2 Future Work

5.2.1 Visual processing in ant navigation simulations

It was unexpected that the simulations from Chapters 2 and 3 did not benefit from using respectively elementary motion processing or averaging in the temporal domain, but we might accept that the simplifying assumptions in both cases missed some of the critical detail of the real world. Further exploration with more elaborate visual worlds will amost certainly be illuminating.

The research in terms of the role of local and distant visual information is also contradictory: the panorama has been shown to be significant (Graham and Cheng, 2009a; Wystrach et al., 2011a) but the local structure of the environment is also important (Seidl and Wehner, 2006; Schultheiss et al., 2013). Wehner and Müller (2010) demonstrated that the approach angle to 2 landmarks at the entrance of the nest affected the search time for the nest entrance - when the sector maximised the change in the retinal image of the landmarks, then search time was reduced. As noted in the introduction we might speculate that either optic flow and motion blur may be important for objects in the near field but the rest of this thesis has been silent on this point as constructing a biologically accurate model of the eye which incorporated motion blur would in itself be complex and would also require an understanding of the response to moving stimuli in the ant which we do not yet possess. Questions remain, not the least whether the fast forward motion of the ant effectively renders near ground objects in the lateral visual

field invisible, making it possible to perceive the more distant panorama in a cluttered environment.

By building a more sophisticated 3d world (Stürzl et al., 2015) and an eye based on the anatomy of *C*. velox*t*he effect of heterogeneity in sampling could be explored more thoroughly. Stone et al. (2014) has already shown that UV can be used for skyline extraction in a simulated robot navigation task and the key issue is now the extent to which local or distal features contribute to navigation. Following the research of Dewar et al. (2014) by controlling in simulation the availability of objects by distance from the viewpoint it may be possible to determine the extent to which local or global features determine the shape of the ant routes reported by Mangan and Webb (2012). As optic flow is greatest for objects in the near visual field, if information at a short range does not contribute substantially to navigation performance this would point equally to motion processing playing a lesser role in navigation.

5.2.2 Continuous or vector-based visual navigation

A conclusion which could be drawn from this research is that desert ant navigation is not a continuous process, and in particular Chapter 4 seems to show that for a visual homing task there might be discrete steps of identification of a goal location and following a heading to reach that goal.

It could be the case that the principal role of vision in navigation is to determine headings at discontinuous locations with rotational motion and fixation a mechanism by which this achieved (Graham and Cheng, 2009b; Wystrach et al., 2014). Chapter 4 indicated that the task of heading selection using goal snapshots is not trivial in complex simulated or real world environments and further research in this area is a priority. It is perhaps co-incidental that using the formula of de Souza and Ventura (1989) and measurements of Schwarz et al. (2011b) show the calculated critical duration for *M*. bagoti*i*s 22ms, and that Wystrach et al. (2014) reports fixation periods of approximately 30ms, but it could be taken as evidence that the rotational scanning behaviour is intended to produce a small number of stabilised images from which rIDF can be calculated. Route geometry data is absent in Wystrach et al. (2014) but scanning behaviour is reported in some detail and testing how static images based on the number of fixations at each rotation and the number of rotation bouts could produce reliable headings to a goal may prove insightful.

It seems unlikely that the field of view of the eye provides sufficient overlap with

the forwards panorama to allow rotational image matching when moving backwards. Alternatively perhaps the reversing ant could identify the goal using a forward look and then once walking backwards stabilise the path by reference to the rearwards panorama it is then facing, a form of visual servoing. Such an approach would require some flexibility in the use of the visual compass as instead of the most familiar view being sought the ant would now simply be seeking to avoid significant change in the geometric relationship of the major landmarks that it can see. In addition a key step is identifying the goal and then rotating so that it is directly behind the animal, a task which cannot be performed accurately unless the visual input is a single 360 degree panorama. Finally, the video evidence shows the complex 3 dimensional path the animal follows as it navigates the obstacles in the substrate, and in Chapter 3 we have seen that even the relatively minor disruption caused by walking on a earth substrate will disrupt navigation, which makes it implausible that a constant fix is being held on the reverse view. Alternatively the behaviour is suggestive of the acquisition of a heading direction using vision and following this heading using an allocentric reference, such as the celestial compass. In the simplest case the step size during training could be increased in the simulation giving segments of uniform length which would be followed using path integration. In such a model there is no need to store vectors as the distance covered would be a relatively fixed parameter governed by step size. Repeating the experiment of Wittlinger et al. (2006) with ants under visual navigation conditions could expose whether there are systematic changes in the segment lengths on recapitulated routes.

Before discarding the continuous assumption we might wish to consider if the distortion of the visual input through ego-motion could be controlled in such a way to allow uninterrupted image-matching. A binary circular image projected on a sphere can decomposed into a set of harmonics using a fast fourier transform, and these harmonics are independent of the yaw, pitch or roll of the original image. In this way a version of the pattern falling upon the retina can be created which is independent of the physical attitude of the viewer. For a robot navigation task Stone et al. (2016) demonstrated that across angular deviations of the range +/-30 degrees the algorithm could recall locations with reasonable accuracy supporting a hypothesis that such a rotation and tilt invariant form of the cue could be used in ant navigation. Being able to completely separate the 3 dimensional structure of the environment as projected onto the retina from the orientation of a body facilitates motion in any direction. Continuous image matching may then be used without the restrictions caused by the observations in Chapters 3 and 4. Such an approach is biologically plausible (Olshausen et al.,

1996) but the demonstration in Stone et al. (2016) uses a panoramic camera with a 360 degree view of the skyline and it is not known how well the algorithm would perform with the more restricted field of view of the ant (Schwarz et al., 2011b). Observations of *M. crosslandi* in the field also suggest that the attitude of the animal in relation to the environment can be extreme and that frequently one or two eyes may have no clear view of the sky. How then would the skyline be extracted? It would be worthwhile to explore these issues in more detail first by determining the full range of motion *M. crosslandi* undergoes while returning to the nest and then applying the extraction of spherical harmonics to a continuous ant navigation model which reproduces this range of movement.

5.2.3 Integrating visual navigation and path integration

Chapter 4 indicates that visual navigation and the compass sense may compliment each other - visual navigation could select the heading which can then be used by the compass sense to maintain a bearing under motion irrespective of the animals orientation.

There is already a wealth of research exploring this relationship, most notably showing that when there is conflict in the signals a compromise direction is followed (Reid et al., 2011; Collett, 2012; Legge et al., 2014). The algorithmic basis was explored systematically by Wystrach et al. (2015) showing that the PI vector is weighted against visual cues according to the directional uncertainty which in turn is proportional to the PI vector length. On an inbound journey where the visual panorama provides a conflicting cue to the direction of the nest, the strength of this cue diminishes exponentially against the length of the PI vector. The use of PI is also implicated in learning walks around the nest, which due to the regular structure are certainly under the allothetic control (Müller and Wehner, 2010). More generally theoretical study of straight line path following has shown that it is essential for an agent to have a compass irrespective of the length of the path (Cheung et al., 2007). Taken in the context of the hypothesis of route-segment odometry (Collett and Collett, 2015) it seems we can discount what the authors describe as a 'purely visual local vector' and instead must accept either 'fixed length local vectors', 'learnt length local vectors' or perhaps vectors which are determined by the state of PI.

In Chapter 4 there was no evidence of an interaction between the PI state and visual information - the ants were captured having run over 1m from the nest but the paths betray no bias in heading between ants caught North or South of the nest. It is possible

that the short PI vector was dominated by the visual cue consistent with the results of Wystrach et al. (2015) and it would be useful to run additional experiments with ants across a range of PI home vector lengths to check whether this is indeed the case.

What is perplexing is how the backwards ants manage to run an accurate distance towards the nest. It was not entirely possible to discount that ants were using forward looks as part of their navigation repertoire and indeed by looking forwards frequently prominent landmarks may have provided waypoints which obviate the need for a sense of distance. But some ants managed to get home with little or no obvious views of the nest, and forward orientation did not improve the homeward heading, which asks for further examination of the distance the animals are covering when facing away from the goal. It is obvious that the backwards ants are not following a learnt length vector, unless there is the unlikely scenario that they had all previously learnt the route from a foraging run, and it seems equally unlikely that there is enough visual information to be able to estimate the distance. Undershooting the nest distance and reacquiring a heading certainly has an adaptive advantage and the ant routes in chapter 4 seem to have phases of re-orientation close to the nest. Repeating the experiment across a range of displacement distances would allow examination of whether these reorientations are driven by the distance travelled or the environment, although as the next section considers we may want to develop new approaches to assessing ant trajectories.

5.2.4 Analysis with more sophisticated motion metrics

The objective of this research was to assess the extent to which the navigation performance is affected by visual processing but our formal taxonomy for describing the paths the ant follows is weak. Typically animal movement can be considered to be either stochastic, that is, a random search pattern, or directed towards a goal. In both cases the pattern of motion is affected by the structure of the landscape, the perceptual discrimination of the animal, its speed or movement capability and the motivational state (With, 1994; Crist and Wiens, 1994; Lima and Zollner, 1996; Kaspari and Weiser, 1999). Clearly these factors are related as the result of evolutionary processes and it is reasonable to assume that in the case of the desert ant the relationship will hold with landscape, motion and perception acting in concert to produce a track given the behavioural state.

Methods to assess the stochastic movement of an animal remain controversial (for a discussion see Benhamou (2004)), but in the case of this research the primary in-

terest is on the goal-directed behaviour of the ant returning from a feeder location to the nest. The fractal dimension of the route calculates the length of a segment of the route as a ruler dimension varies, and thus can vary from F=1 for a straight line to F=2 for Brownian motion. It provides a scale-independent measurement of tortuosity which has been used to discriminate between different insect species interaction with the micro-structure of the landscape (With, 1994; Wiens et al., 1995). However by examining the discretization effect of the changing ruler length it is also possible to gain insight into the salient structure of the landscape. For example, animal navigation which is mediated by large landscape features, such as skyline, should show a bias towards larger ruler sizes, than navigation which is dependent on small scale features. Fractal analysis has become controversial with some evidence that it can produce incorrect results as animal tracks may not be fractal objects (Benhamou, 2004). An alternative is the multi-scale straightness index (MSSI) which at this stage lacks the pedigree of other approaches but has been shown to have promise in analysing tracking data (Postlethwaite et al., 2013). A further novel approach is to use machine learning techniques to identify prototypical subcomponents of the animal track (Braun et al., 2012) and the application of either K-means or agglomerative clustering may provide further insights. On this basis it should be possible to demonstrate whether the simulated animal and the actual movement show similar characteristics in terms of the relationship with the environment.

However some confounding issues remain. All the approaches require that data is collected at a level of detail which captures all the predictable motion of the animal and while camera recordings may offer this detail without automated processing they are time-consuming to analyse. A further environmental consideration is that ants may show preferences for particular locations within their environment which may not be the result of the combined effects of structure, perception and motion. This may then lead to differences in the tracks produced by the simulations compared to the animal data beyond what could be predicted by the model. In order to control for this it may be necessary to undertake further research on the location preferences of the animal or use surrogate data from other species. In addition, it has been shown that while substrate size is not necessarily preferred by ant species, it has a demonstrable effect on locomotion (Bernadou and Fourcassié, 2008), but this is a variable which is not readily determined.

Development of a method to formally describe the inward paths of desert ants may be possible by systematic analysis of existing datasets (Mangan and Webb, 2012) or

those which may be published in the near future. The accuracy of simulations could then be more rigorously assessed in particular how well they reproduce the degree of variability in the animal's path.

5.3 Concluding Remarks

Progress on the models of desert ant navigation inspired this work. Demonstrating that ant visual navigation could be undertaken as a continuous process using a model of a part of the insect brain was an exciting finding, and naturally lead to the hypothesis that refinement of the sensory input to more accurately replicate what the animal experiences under ego motion should lead to new findings. Chapter 2 provided these insights, but not what was expected. Closer examination of the animal's motion began to reveal new issues with the continuous model as formulated as shown in Chapter 3, and finally the field work reported in Chapter 4 confirmed that a forward continuous view was not necessary to reach a goal. This is a very satisfactory conclusion. We now know that while continuous processing or matching a static image on the retina could be part of the ant navigation system they are not used in combination. Researchers in this field can focus on alternative models and there are certain to be many surprises that the ant will disclose as we follow its tracks in the desert.

Appendix A

Glossary

A.1 Glossary

Continuous

In the context of navigation by image-matching, "continuous" means that the sampling steps between images are regular and small. This contrasts with methods of navigation where irregular distances are followed between sampling points.

Elementary motion detector (EMD)

The Hassenstein-Reichardt motion detector (Hassenstein and Reichardt, 1956) describes the sensory circuit through which motion can be detected by animals. In its simplest formulation parallel sensors detect changes in light intensity which are delayed and then compared to the adjacent signal.

Infomax

A machine-learning technique described in Bell and Sejnowski (1995) which uses a fully connected neural network to perform independent components analysis.

Lobula plate tangential cells (LPTC)

The final structure of the neuroanatomically defined visual pathway in hymenoptera.

Panorama

The 360 degree view around a particular location.

Rotational image difference function (RIDF)

The calculation of an image difference function (Zeil et al., 2003) between a sample image and those taken at different headings at the same location.

RSInfomax

A specific implementation of the Infomax algorithm to reproduce ant visual navigation. An infomax network is trained with route images for the ant's world, and route recapitulation is performed by undertaking a rotational scan where the most familiar view provided by the network gives the heading to be followed.

Translational image difference function (TIDF)

The calculation of an image difference function (Zeil et al., 2003) between a sample image and those taken at different adjacent locations using the same heading.

Zero vector ant

An ant which has returned from a feeder to the nest using path integration (i.e. on the first homeward run). At this point it no longer has a path integration vector and must rely upon other navigational senses to get to the nest if it is displaced.

Appendix B

Using an Insect Mushroom Body Circuit to Encode Route Memory in Complex Natural Environments

B.1 Introduction to the paper

The RSInfomax model (Baddeley et al., 2011, 2012) was the first complete simulation of ant visual navigation. In order to test the hypothesis that the ant visual system was specially adapted for this task it was deemed appropriate to implement RSInfomax in an accurate simulation of the ant environment, where the visual processing methodology had been developed from first principles and afforded the possibility to change various parameters. This new combination of navigation algorithm, eye model and ant world alongside the detailed routes followed by the animals (Mangan and Webb, 2012) also provided an excellent opportunity to attempt reproduction of the behaviour using an accurate simulation of the Mushroom Body, an area of the brain thought to be involved in insect learning (Wessnitzer et al., 2012). Further analysis of the Mushroom Body circuit showed that it was computationally similar to the Willshaw Net allowing the theoretical capacity of the network to be calculated (Willshaw et al., 1969). The combination of realistic simulation with the ability of a biomimetic structure (Mushroom Body model) to perform comparably to a more artificial algorithm (RSInfomax) was an exciting addition to our knowledge of the animal. The paper is included here as it provided the basis and inspiration for the subsequent research in this thesis, but as it was jointly authored it is inappropriate to submit it as a chapter in itself.

PLOS | COMPUTATIONAL BIOLOGY

RESEARCH ARTICLE

Using an Insect Mushroom Body Circuit to Encode Route Memory in Complex Natural Environments

Paul Ardin[1☯], Fei Peng[2☯], Michael Mangan[1], Konstantinos Lagogiannis[1], Barbara Webb[1]*

1 School of Informatics, University of Edinburgh, Edinburgh, United Kingdom, **2** Biological and Experimental Psychology, School of Biological and Chemical Sciences, Queen Mary University of London, London, United Kingdom

☯ These authors contributed equally to this work.
* B.Webb@ed.ac.uk

Citation: Ardin P, Peng F, Mangan M, Lagogiannis K, Webb B (2016) Using an Insect Mushroom Body Circuit to Encode Route Memory in Complex Natural Environments. PLoS Comput Biol 12(2): e1004683. doi:10.1371/journal.pcbi.1004683

Editor: Joseph Ayers, Northeastern University, UNITED STATES

Received: June 9, 2015

Accepted: November 30, 2015

Published: February 11, 2016

Data Availability Statement: All matlab code used to produce our data are available from the Dryad database: http://dx.doi.org/10.5061/dryad.pf66v.

Funding: This research was support by Biotechnology and Biological Sciences Research Council UK (www.bbsrc.ac.uk) grant BB/I014543/1; Engineering and Physical Sciences Research Council UK (www.epsrc.ac.uk) EP/F500385/1; European Commission Seventh Framework Programme (ec.europa.eu/research/fp7) 618045; China Scholarship Council (en.csc.edu.cn); Queen Mary University London. The funders had no role in

Abstract

Ants, like many other animals, use visual memory to follow extended routes through complex environments, but it is unknown how their small brains implement this capability. The mushroom body neuropils have been identified as a crucial memory circuit in the insect brain, but their function has mostly been explored for simple olfactory association tasks. We show that a spiking neural model of this circuit originally developed to describe fruitfly (*Drosophila melanogaster)* olfactory association, can also account for the ability of desert ants (*Cataglyphis velox)* to rapidly learn visual routes through complex natural environments. We further demonstrate that abstracting the key computational principles of this circuit, which include one-shot learning of sparse codes, enables the theoretical storage capacity of the ant mushroom body to be estimated at hundreds of independent images.

Author Summary

We propose a model based directly on insect neuroanatomy that is able to account for the route following capabilities of ants. We show this mushroom body circuit has the potential to store a large number of images, generated in a realistic simulation of an ant traversing a route, and to distinguish previously stored images from highly similar images generated when looking in the wrong direction. It can thus control successful recapitulation of routes under ecologically valid test conditions.

Introduction

The nature of the spatial memory that underlies navigational behaviour in insects remains a controversial issue, particularly as the neural mechanisms are largely unknown. Insects can perform path integration (PI), using a sky compass and odometer to accumulate velocity into a vector indicating the distance and direction of their start location, typically the nest or hive [1].

study design, data collection and analysis, decision to publish, or preparation of the manuscript.

Competing Interests: The authors have declared that no competing interests exist.

They are also known to be able to use landmark and/or panoramic visual memories of previously visited locations to guide their movements independently of PI [2,3]. Under normal conditions, both systems are functioning. This raises the possibility that insects additionally store PI vector information with their visual memories [4]; or link their visual memories in sequences [5] or with relative heading vectors [6], forming a topological map; or could even use the PI information to integrate their visual memories into a metric map that represents the spatial relationship of known locations [7].

However another possibility is that PI information is used to determine *which* visual memories to store, for example, the views experienced when facing the nest [8]. Subsequently, such memories can be used directly for guidance without further reference to vector information. Rotating to match the current visual experience with a stored view will give the required heading direction [9], e.g., towards the nest. Surprisingly, this navigation mechanism can exploit multiple memories without necessarily requiring recovery of the 'correct' memory for the current location. Baddeley et al [10,11] presented an algorithm by which an animal attempting to navigate home simultaneously compares the view experienced while it rotates to all memories ever stored while following a PI vector homewards. The direction in which the view looks 'most familiar', i.e., has the best match across all stored views, is generally the correct heading to take to retrace its previous path. In [11] this principle was implemented using the Infomax learning algorithm to train the weights in a two-layer network, where the input is successive images along simulated routes, and the summed activation of the output layer represents the novelty of each image. This implementation was able to replicate many features of ant route following in an agent simulation [11] and has also been shown (with some assumptions about the ant's previous experience) to produce similar search strategies to ants in visual homing paradigms [12].

Strategies of this nature, where the animal does not need to know where it is to know where to go, have been invoked as a more parsimonious explanation for experimental results presented as evidence for a cognitive maps in insects [13]. But is this explanation of navigation plausible, given realistic environmental, perceptual and neural constraints? As pointed out in a recent review [14], parsimony based on what appears simple in computational terms may not map to simplicity with respect to the underlying neural architecture. Yet so far, "nothing is known about neural implementation of navigational space in insects" [14]. In particular, Baddeley et al [11] do not claim that the Infomax implementation of their familiarity algorithm represents the actual neural processing of the ant.

Visual processing in the ant brain has not been extensively studied, but anatomically resembles that of other insects in terms of the initial sensory layers at least. Ants have typical apposition compound eyes, but the size and resolution varies substantially across species. For the desert ants *Cataglyphis* [15] and *Melaphorus bagoti* [16] each eye subtends a large visual field (estimated at 150–170 degrees horizontal extent, with a small frontal overlap) with low visual resolution (interommatidia angles between 3 and 5 degrees). Visual signals pass through the three layers of the optic lobe (lamina, medulla and lobula) maintaining a retinotopic projection but with increasing integration across the visual field [17]. Visual signals then pass directly or indirectly to several other brain regions, including the protocerebrum, the central complex, and the calyxes of the mushroom bodies [17]. The mushroom body (MB) neuropils are conspicuous central brain structures, made up from a large number of Kenyon cells (KCs), whose dendrites together form the calyx and whose axons run in parallel through the penduculus and then bifurcate to form the vertical (or α) and medial (or β) lobes [18]. The extent of visual input to the MB is significantly greater in ants and other hymenoptera than for many other insects for which the MB input is predominantly olfactory [19]. In fact there is increasing evidence that the MB may play a role in visual learning and navigation in insects. There is

evidence of expansion or reorganisation of MB at the onset of foraging in ants [20,21] and bees [22–24]. Upregulation of a learning related gene in the MB of honeybees has been linked to orientation flights in novel environments [25]. Cockroaches show impairment on a visual homing task after MB silencing [26], although the central complex rather than the MB appears essential for this task in Drosophila [27]. The MB may nevertheless play a role in some visual learning paradigms in Drosophila [28][29].

To date, the MB have been much more extensively studied in the context of olfactory associative learning, for which they appear crucial [18]. We have previously implemented a spiking neuron model of adult Drosophila MB olfactory learning [30] which used three stages of processing. Olfactory inputs produced a spatio-temporal pattern (an 'image' of the odour) in the antennal lobe (consistent with evidence in flies [31] but also observed in many other insects, including ants [32]). Divergent connectivity from the antennal lobe to the much larger number of KCs that make up the MB project this pattern onto a sparse encoding in a higher dimensional space [33–35]. Reward-dependent learning occurs in the synapses between the KC and a small number of output extrinsic neurons (ENs) [36–38], depending on the delivery at the synapse of an aminergic reward signal [39,40], such that each pattern becomes associated with a positive or negative outcome. This is a simplification of the insect MB circuit, which in reality includes significant feedback connectivity, synaptic adaptation at other levels including in the calyx [41,42] and has a substantial compartmentalisation of its inputs and outputs both between and within the lobes [40]. Nevertheless the basic feedforward architecture implemented in our model was shown to be sufficient to support learning of the association of non-elemental (configural) olfactory stimulus patterns to a reinforcement signal.

Our proposal here is that the MB of the ant allows it to similarly associate visual stimulus patterns, as viewed along a route, with the 'reinforcement' of facing, moving towards or reaching home. In fact the learnt pattern could be multimodal (e.g., including olfactory cues, see Discussion) but we focus here on demonstrating that the ecologically realistic visual learning task posed by route following could be achieved by this circuit architecture. In other words, we suggest the neural architecture of the ant MB could plausibly form the substrate for the familiarity algorithm of Baddeley et al [11]. The complexity of navigation tasks make it difficult to directly measure or manipulate neural circuits in ants under naturalistic conditions to evaluate their contribution to navigation behaviour. Instead, we take a modelling approach, and explore whether our previously developed spiking neural simulation of olfactory learning in the MB of *Drosophila* [30] could be directly applied to the complex ecological task of route memory in ants, using realistic stimuli derived directly from our field experiments.

Results

Reconstruction of the ant's task

We created a realistic reconstruction of the visual experience of ants based on ecologically relevant data from our study of route following in *Cataglyphis velox* [43]. The field site was a flat semi-arid area covered in low scrub and grass tussocks. Ants were trained to forage from a feeder 7.5m from their nest. 15 individual ants were tracked over multiple trips, each revealing an idiosyncratic route to and from the feeder, which they consistently reproduced. We mapped the tussock location and size, and used panoramic pictures taken from ground level to estimate tussock height, and to generate a corresponding virtual environment, where each tussock is a collection of triangular grass blades with a distribution of shading taken randomly from the intensity range in the panoramic pictures (Fig 1). The ground is flat and featureless, and the sky is uniform, without intensity or polarized light gradients. A simulated ant can be placed at any position, with any heading, within this environment. The simulated ant's visual input is

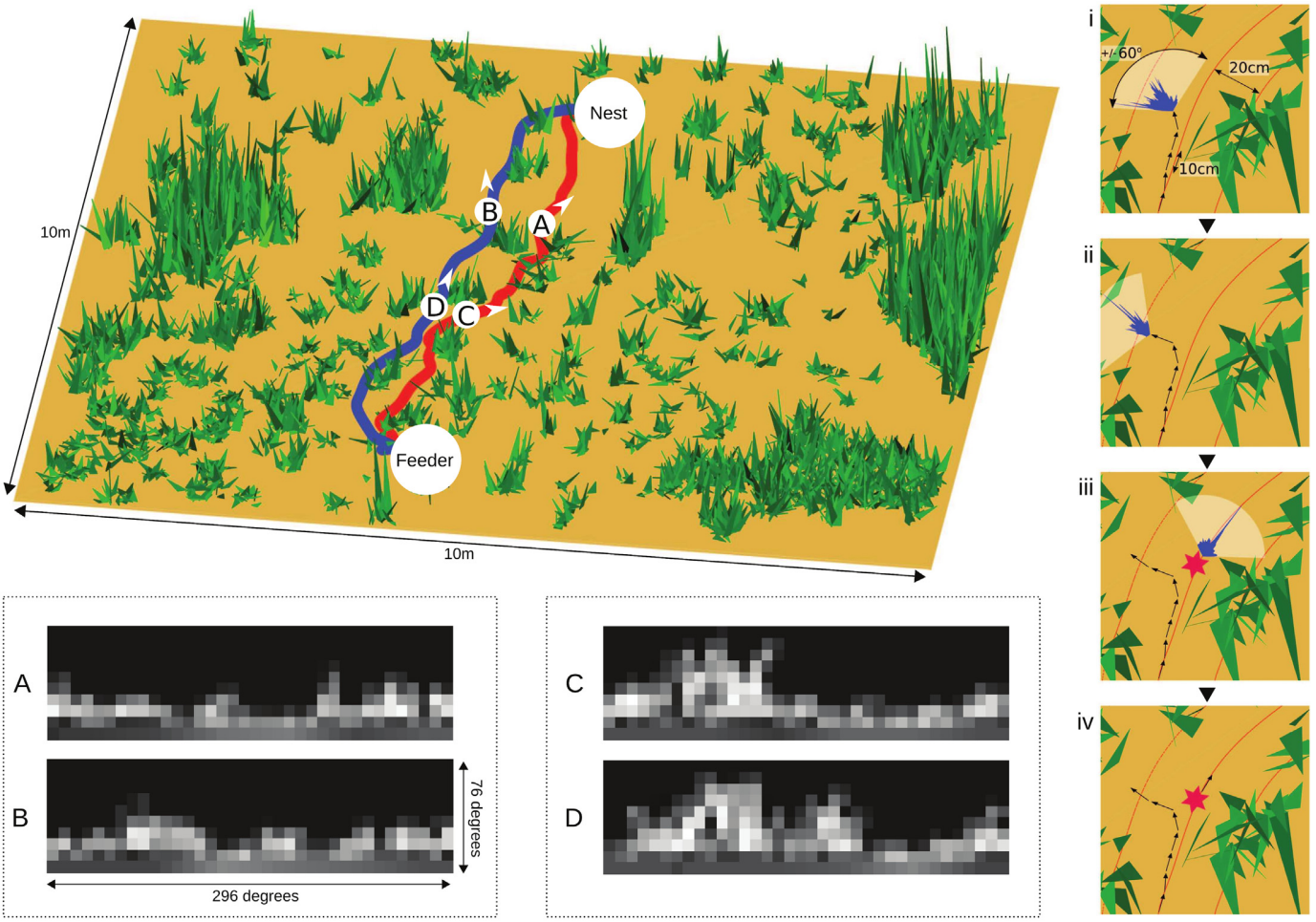

Fig 1. The ant's navigational task. Left: 3D mapping of the real ant environment, which consists of flat ground and clumps of vegetation. Two actual routes followed repeatedly by individual ants from feeder to nest are shown. From a given ground point (e.g. locations A, B, C and D as indicated), the visual input of a simulated ant facing a given direction can be reconstructed, applying a 296 degree horizontal field of view, 8 degree/pixel resolution, inversion of intensity values and histogram equalization. The task of following a specific route requires distinguishing 'familiar views', e.g. for the red route, views A and C, from 'unfamilar views' e.g. B and D from the blue route, despite their substantial similarity. Right: how route following capability is assessed. The simulated ant is trained with images taken at 10cm intervals facing along a route. To retrace the route, it scans +/-60 degrees (i), evaluating the familiarity at each angle (distribution shown in blue), then moves 10 cm in the most familiar direction (ii). Deviating more than 20cm from the route is counted as an error (iii) and the ant is replaced on the nearest point of the route to continue (iv), until home is reached.

doi:10.1371/journal.pcbi.1004683.g001

reconstructed from a point 1cm above the ground plane, with a field of view that extends horizontally for 296 degrees and vertically for 76 degrees, with 4 degree/pixel resolution [16], producing a 19x74 pixel image. The image is inverted in intensity and histogram equalized [44] and further down-sampled to 10x36 pixels (effectively 8 degree/pixel resolution) for input to the MB network.

Fig 1 shows the potential difficulty of the route following task within this environment. The ant is surrounded by relatively dense vegetation, which blocks any distant landmarks (see also supplementary S1 Fig which shows a sequence of panoramic photographs taken from ground level along an ant's route, illustrating the lack of any distant features visible throughout the route). The vegetation density is around 2 tussocks/m^2 (compared to 0.05–0.75 tussocks/m^2 used in previous simulations [11]) and ants are often observed to go directly through tussocks leading to abrupt changes in the view. As a consequence, multiple non-overlapping views need

to be stored to encode the full route, and searched when recapitulating it. The views lack unique features, especially at the ant eye's low resolution, so the potential for aliasing seems high. In particular, there is no reason to expect images seen by the ant along one route (e.g. Fig 1A and 1C) to have any common properties that could be learnt to distinguish them from non-route images (e.g. those from another ant's route, Fig 1B and 1D; or those experienced when not aligned with the route).

Mushroom body processing

We altered our mushroom body model [30] (Fig 2) only by increasing the number of neurons (staying well below estimates for the ant brain [17]), and introducing anti-Hebbian learning [39,40]. Our input layer consists of 360 visual projection neurons (vPNs), activated proportionally to the intensity of the pixels in a scaled and normalized image (Fig 1). We intentionally kept this visual pre-processing simple, as there is little evidence on which to make assumptions about the nature of the visual input to the MB in the ant. The second layer contains 20,000—KCs, each receiving input from 10 randomly selected vPNs [35,45] (note this does not preserve retinotopy), and needing coincident activation from multiple vPNs to fire. This allows decorrelation of images using a sparse code [46], i.e., only a few KCs (around 200) will be activated, and the activation patterns will be more different than the input patterns. All KC outputs converge on a single extrinsic neuron (EN) with a three-factor rule for learning [47]. This uses the relationship of presynaptic and postsynaptic spike timing to 'tag' synapses, and a global reinforcement signal to permanently decrease the strength of tagged synapses, consistent with neurophysiological evidence from the MB of locusts [39]. Thus, images that have been previously paired with reinforcement will excite KCs that no longer activate EN as these connections have been weakened.

We assume that the ant learns a homeward route by storing the views encountered as it follows its path integration home vector back to the nest. The 'reinforcement' signal could thus be generated by decreases in home vector length. In practice, we train the network by generating the images that would be seen every 10cm along the ~8m recorded route of a real ant, with the heading direction towards the next 10cm waypoint. These 80 images are each presented (statically) to the network for 40ms, followed by a transient reinforcement signal (Fig 3). The parameters in the model are set to effectively result in 'one shot' learning given this timing of presentation: i.e., a single pairing of image and reinforcement causes the relevant synaptic weights to be reduced to near zero. Such learning is not implausible as it has been shown that, for example, individual bees can acquire odour associations in one or two trials [48]. After training, the ant should be able to recover the heading direction at any point along the route by scanning and choosing the 'most familiar' direction as indicated by the minima in the activity of EN during the scan.

We compare the MB model to two alternatives. 'Perfect memory' represents the best possible performance, by assuming the ant photographically stores all 80 images and directly compares the current viewpoint with all stored images to find the highest similarity, i.e., the minimum in the sum of squared pixel intensity differences (see Methods). The Infomax algorithm, used previously for this task [11] but under less realistic environmental and perceptual processing constraints, attempts to build a generative model of the 80 views using a fully connected two layer neural network (see Methods). We note that a much higher learning rate was needed in the current study to get successful results from Infomax, and it is possibly learning by overfitting, i.e., its 'model' consists essentially of the 80 presented views. In Fig 4A–4C we show the directional choice that would be made using the output from each method for a short segment of the path, using displacements at 5cm intervals up to +/-25cm away from the

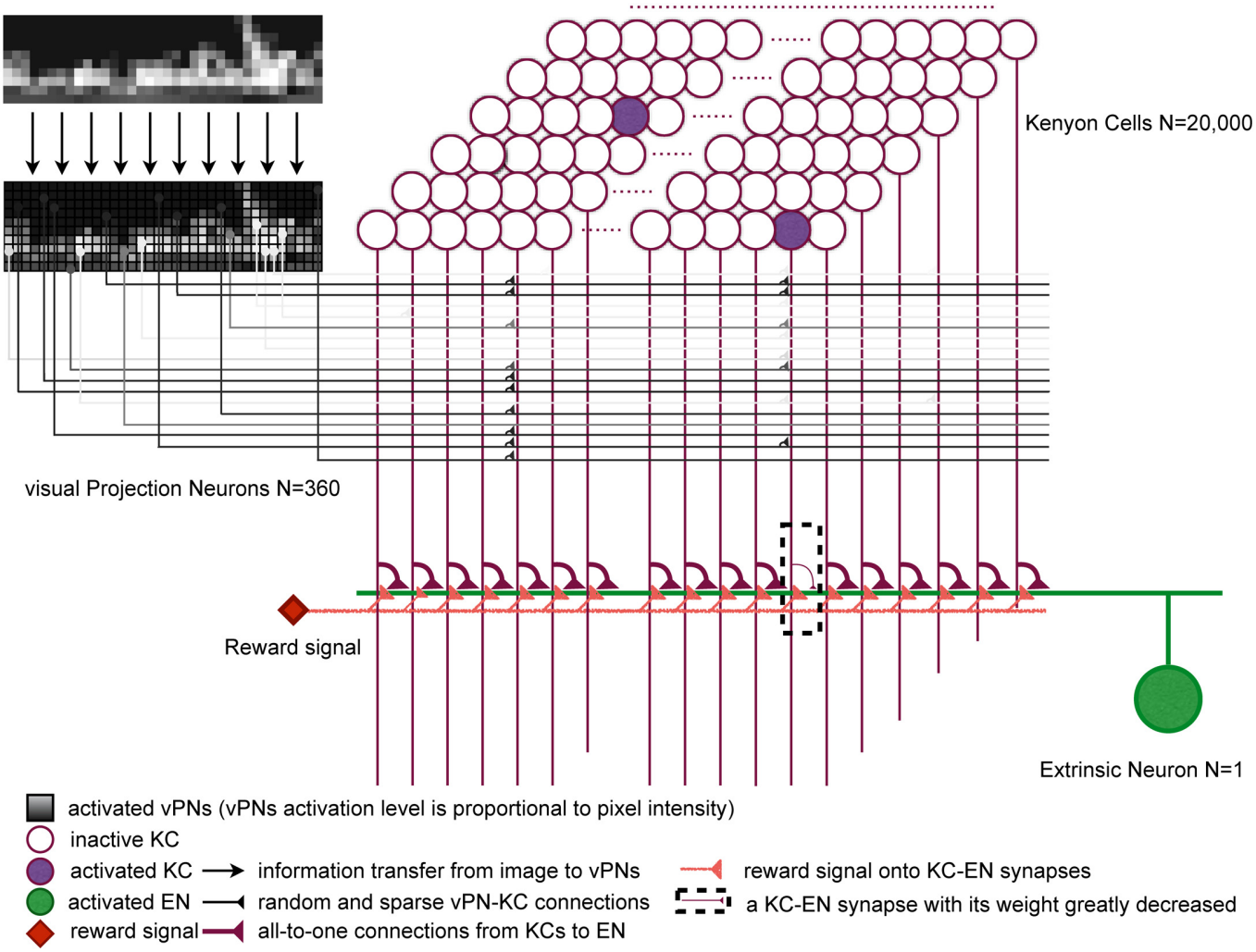

Fig 2. The architecture of the mushroom body (MB) model. Images (see Fig 1) activate the visual projection neurons (vPNs). Each Kenyon cell (KC) receives input from 10 (random) vPNs and exceeds firing threshold only for coincident activation from several vPNs, thus images are encoded as a sparse pattern of KC activation. All KCs converge on a single extrinsic neuron (EN) and if activation coincides with a reward signal, the connection strength is decreased. After training the EN output to previously rewarded (familiar) images is few or no spikes.

doi:10.1371/journal.pcbi.1004683.g002

locations at which images were stored. The MB model produces directional output of equivalent reliability to the other visual memory methods, pointing the simulated ant along the route with only a few exceptions. Note that a perfect match is possible only if the simulated ant is in exactly the same location as the memory was stored, but all the methods are quite robust for nearby locations.

Evaluating route following

We simulate retracing the route starting from the feeder, heading along the route (Fig 1, right). The next heading direction is determined by the minima in EN firing (or the equivalent choice made using Perfect Memory or Infomax) for a directional scan of ±60 degrees (reflecting a general bias to continue in the same direction). A 10cm step is taken in this direction and the process repeated until the ant reaches home. Note that it is thus possible for the simulated ant to

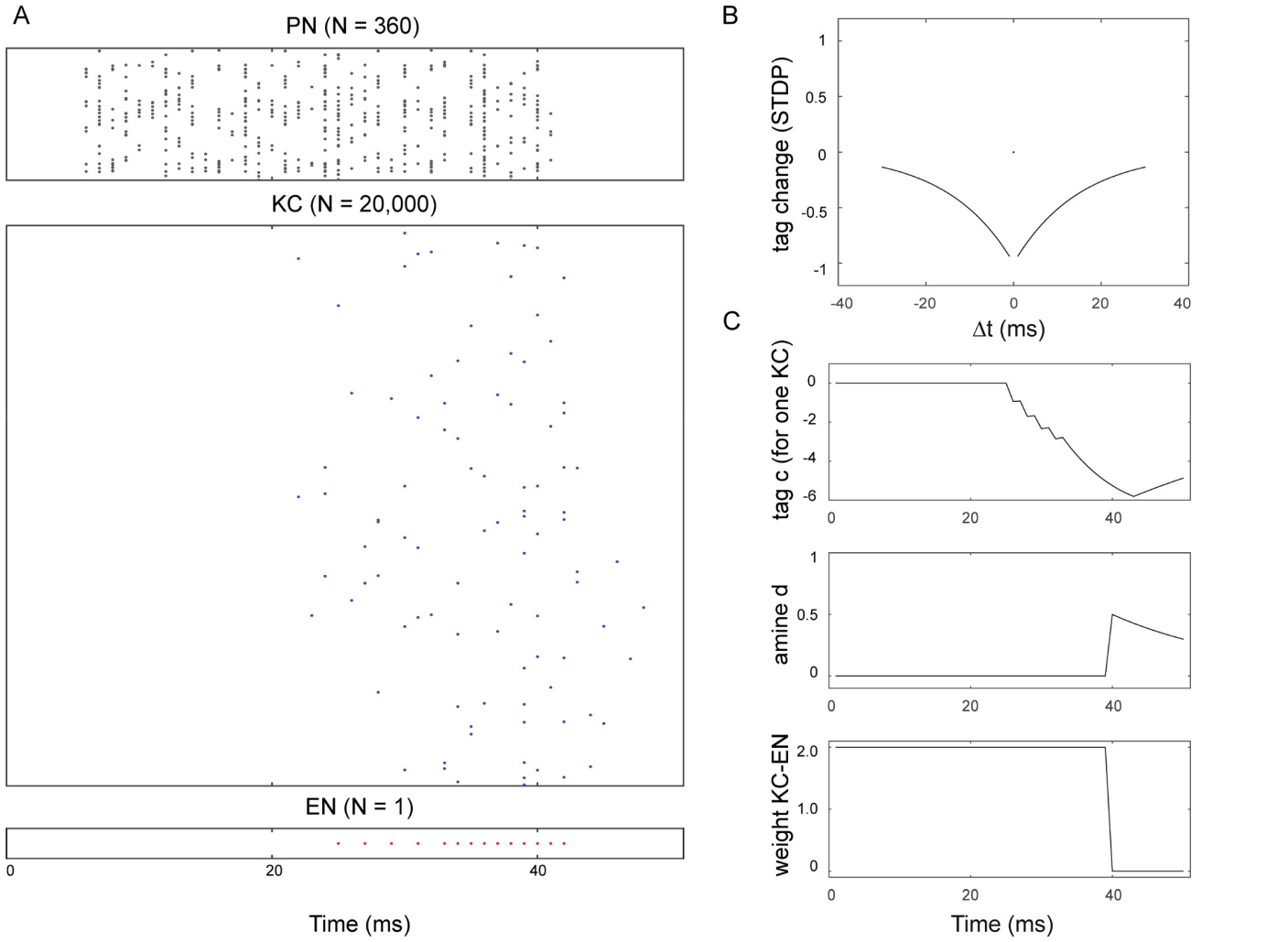

Fig 3. The response of the network during training with one image. A: The image is presented for 40ms, directly activating the vPNs which respond with a spiking rate proportional to the intensity of their input pixel. This produces sparse activation of the KC, which causes the EN to fire. B: An STDP process tags KC synapses depending on the relative timing, Δt, of their spikes to spikes in EN. C: Within 40ms, an active KC will have a strongly negative tag. An increase of amine d, representing reinforcement, will combine with the tag to greatly reduce the weight of the KC-EN synapse.

doi:10.1371/journal.pcbi.1004683.g003

be scanning from a slightly different position from where memory was stored, and hence for the wrong direction to be chosen, even for perfect memory. If successive movements lead the ant a significant distance from the route (> 20cm) then, in the cluttered environment we are testing, matches become poor and the ant will pursue a random course with little chance of recovery. Hence, if a step results in a location more than 20cm from the route, the error count is increased by one and the ant is placed back on the nearest point on route. We count the total number of such errors that occur before the ant comes within 20cm of the home position. As a baseline, we include a random control in which the visual information is ignored and the direction on each step is chosen randomly from ±60 degrees.

The performance of the model is assessed using 15 different ~8m routes, based on the observed routes of real ants recorded in our field study. The results are shown in Fig 4. Random directional choice produces a mean of 18.7 errors (standard deviation = 3.6) per route. Perfect memory has a much lower number of errors (mean 1.1, s.d. = 0.9) suggesting familiarity is an

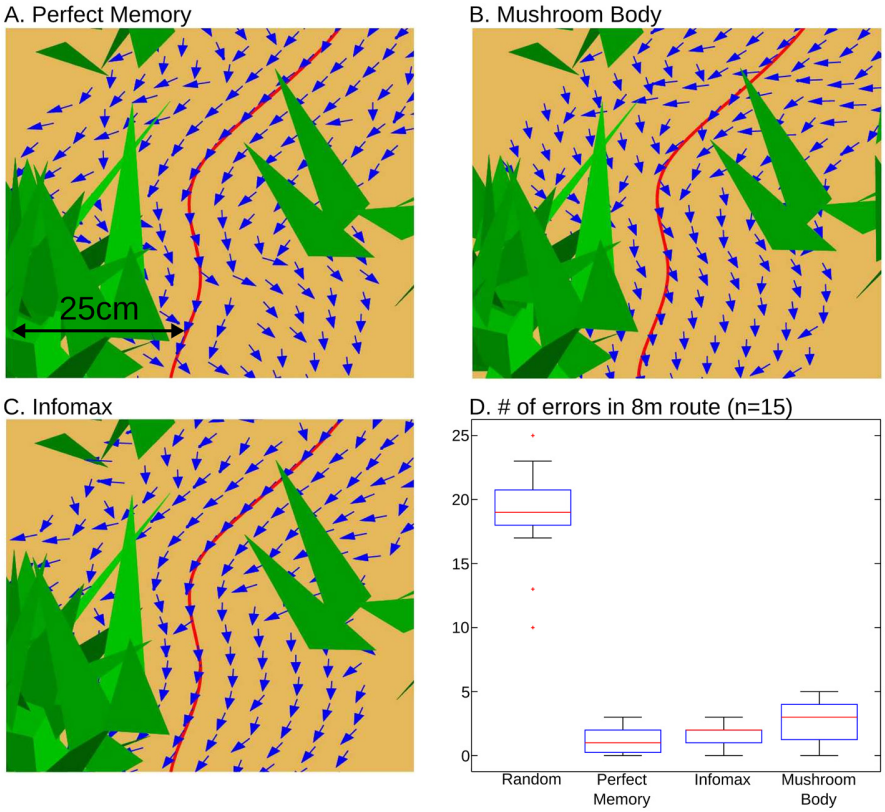

Fig 4. Performance of the familiarity algorithm. A-C: Perfect memory (A), the mushroom body (B) and infomax (C) are evaluated for a segment of the route (triangles are grass blades) after training with ~80 images along this route. For test locations in 5cm displacements up to 25cm away from the trained image locations (on red line), all three familiarity algorithms are robust, recovering directions (arrows) that enable route following, but even 'perfect' memory can produce errors when not tested at an identical location to where the image was stored. D: Comparison of number of errors made by each algorithm when retracing a route (see Fig 1), compared to random choice of direction. Boxplots show the median, interquartile range and maximum and minimum results for 15 different routes, each ~8m long, with images stored every 10cm.

doi:10.1371/journal.pcbi.1004683.g004

effective route following method. The MB model is only slightly less successful than this benchmark, with a mean of 2.6 errors (s.d. = 1.5). This is significantly worse than Perfect Memory (Bayes factor, calculated using the method in [49], is 28:1 in favour of non-equal means), but the drop in performance is small (1.5 additional errors) given the substantial reduction in computational demand – Perfect Memory requires separate comparison of the test view with every stored view for every direction in a scan, whereas MB simply uses the immediate output of the network. Infomax produces a mean of 1.5 errors (s.d. = 0.8), which is marginally better than MB (Bayes factor 2.8:1 in favour of non-equal means). But note that compared to MB, Infomax uses at least 5 times more synaptic weights, and needs to adjust every weight in the network for every training input, using a non-local rule, which is biologically less feasible. S1 Movie shows a route and images corresponding to a run in which MB produced no errors.

Analytical solution for storage capacity of the mushroom body circuit

The key properties of the MB circuit for this task are the small number of neurons activated in the KC layer (around 1% of neurons activated by each image) and fast (one-shot) learning with

no forgetting. We can abstract the spiking KCs as nodes with a binary state, representing whether or not they activated above threshold by the input pattern, and also abstract the KC-EN synaptic strength as either high (contributes to response in EN, the initial state) or low (no input to EN, the state after unidirectional, rapid learning). Because of the initially high setting (if KC is active, EN will fire), we can also simplify to a two factor learning rule: if KC activation coincides with reward, set the synapse strength permanently to low. This abstraction essentially views the learning network of the MB as a layer of binary units with outputs converging on one output unit via binary synapses that have a unidirectional plasticity rule.

Such a network is comparable to a Willshaw net [50] for which theoretical estimations of information capacity for a given number of input units N has been previously examined within a framework of fixed sparseness, binomially distributed [51]. However, the activity of each KC is not completely independent because all KCs sample from the same population of vPNs activity patterns at any given time and thus the probability distribution for the number of active KCs is not a binomial distribution [52]. Nevertheless, the expected number of active KCs is Np_{kc} (where N is the number of KCs and p_{kc} the probability of a connection between each vPN and KC) as required, while the correlation between KCs can be reduced by changing the number of vPNs sampled by each KC and thus the capacity estimation with binomial approximation may hold. Similar capacity estimations have been previously performed for networks with binary synapses and bidirectional plasticity, showing that sparseness prolongs memory lifetimes by reducing the rate of plasticity [53] and therefore the interference between new memory encoding and stored memories. Note, in our MB model, increased sparseness also influences plasticity rates and thus changes in capacity can be seen as variations in the interference of the learned patterns.

The abstracted MB allows theoretical estimation of the memory capacity m (the number of patterns that can be stored) of the mushroom body for a given size N (number of KC) and average activity p (average proportion of KC activated by each pattern). We derived (see Methods) an expression for the mean number of patterns m that can be stored before the probability of error reaches P_{error}, where error is defined as having a random unlearned pattern that activates only KC nodes that already have their KC-EN weight set low, thus producing the same EN output as a learned pattern. The resulting capacity is given by:

$$m = \frac{ln\left(\frac{1-P_{error}^{\frac{1}{N}}}{p}\right)}{ln(1-p)} \quad (1)$$

The storage capacity as a function of network size and sparsity is shown in Fig 5. Given the above assumptions, our MB model, with $N = 20{,}000$ input units, one output unit, and average KC activity $p = 0.01$ should allow around 375 random images to be stored before the probability of confusing a novel image with a stored image exceeds $P_{error} = 0.01$. We confirmed this by training our MB network with random KC patterns, and testing with 100 novel patterns. It was indeed the case that more than 350 patterns could be stored before any of the novel patterns were mistakenly classed as familiar (i.e. produced no spikes in EN, see S2 Fig). Following the same procedure for varying network size and average KC activity also produces results comparable with the theoretical predictions (Fig 5, diamonds). If memories are stored every 10cm as we have assumed, memorising 350 patterns corresponds to an ant being able to recall a route of 37.5m, or several routes of around 10m, before any confusion would occur; in uncluttered environments, memories could be more spaced (e.g. every 1m or more) and distances correspondingly increased (routes of hundreds of metres, [54]). The actual upper limit of ant route memory has not been systematically explored but these values are on the same

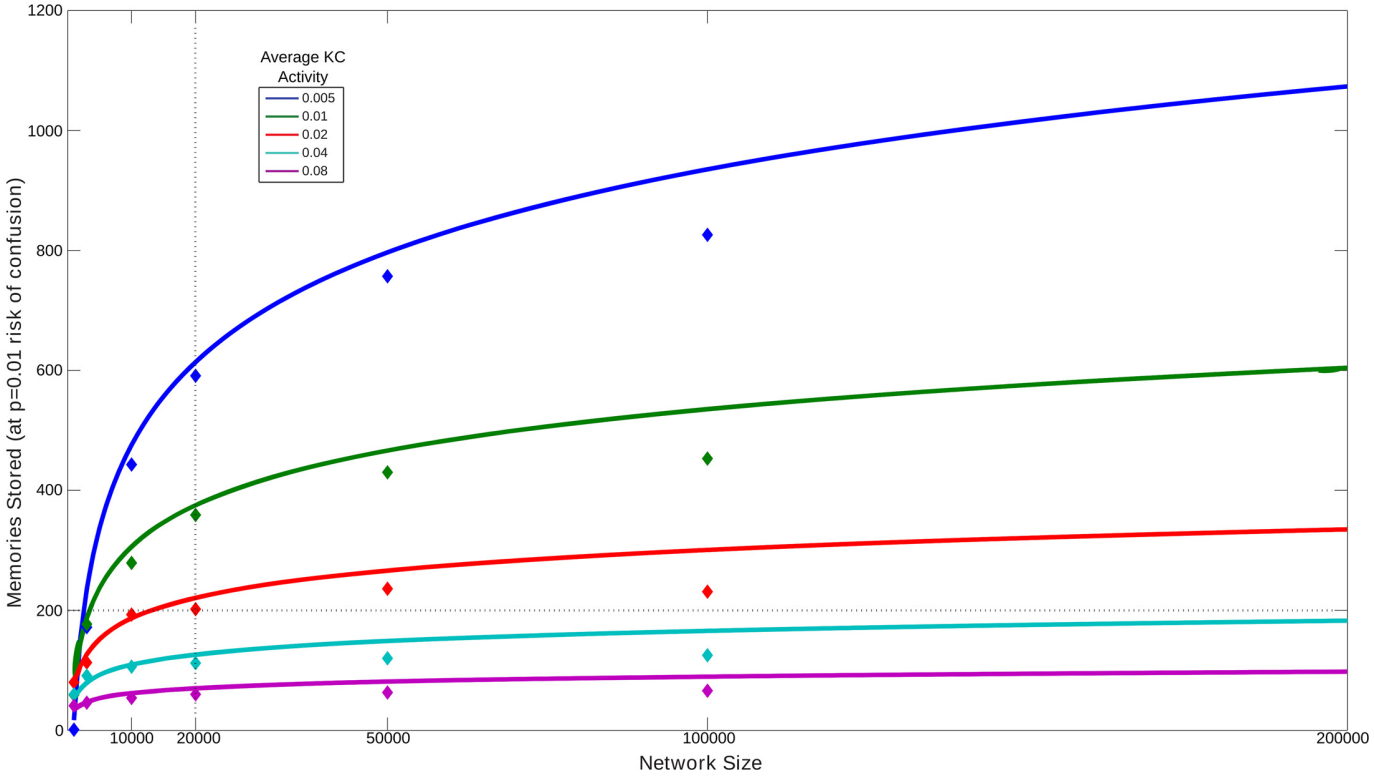

Fig 5. The number of independent images that an abstracted MB network can store before the probability of an error (producing an output of 0 for a novel image) exceeds 0.01. Lines: predictions from theoretical analysis. Diamonds: results from equivalent simulations using the full spiking model. The capacity scales logarithmically with the number of neurons, and increases if fewer KCs are activated on average by each pattern.

doi:10.1371/journal.pcbi.1004683.g005

order as those used in most experimental studies (e.g. [43,55,56]). There are also a number of plausible ways in which the capacity could be increased: e.g., having more than one EN; more states for synapses; probabilistic rather than deterministic synapse switching; or preprocessing the image data.

To compare further the capacity estimate derived from this abstraction (with independent random input patterns) to the practical performance of the MB network (with correlated input patterns from routes) we ran the following test. The MB was trained successively with each image from every route, to a total of 1200 images. After each image was added to memory, the EN response was recorded i) for that image, ii) for an image taken 5cm away and facing the same direction, iii) for an image taken from a random location in the ant environment, and iv) for a completely random image. Distinguishing i) from ii-iv) means that stored memories are not confused with new images. Distinguishing ii) from iii) is helpful for robust route following, i.e., the right direction from small displacements should still look more familiar than random locations. Distinguishing i-iii) from iv) might be expected because completely random images will rarely look like images from the environment, where sky is always above grass, which is above the ground, etc. As shown in Fig 6, the response of EN is very noisy (plotted points), hence occasional mistakes in familiarity will occur, but nevertheless the response for stored images is on average (fitted curves) clearly distinguishable from other images as it produces no EN spikes, and images from nearby locations tend to be more familiar than images from random locations, even after storing 1200 images.

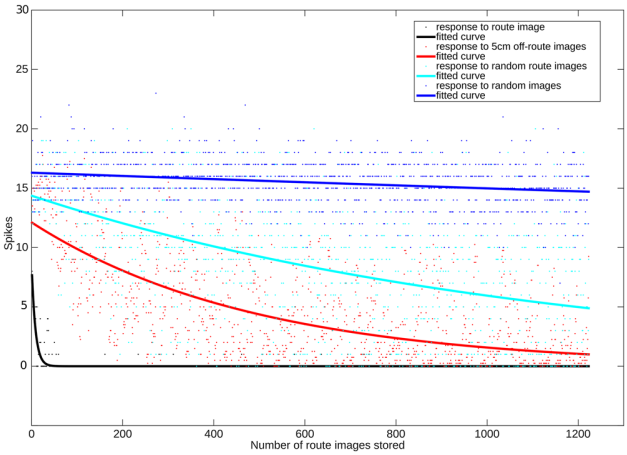

Fig 6. Testing the capacity of the MB network to distinguish familiar from novel images as additional route images are stored (x-axis). On average (fitted curves), the EN output to learned images is zero. Images from nearby locations with the same heading are more familiar (lower EN response) than those from random locations. Random images remain clearly distinguishable even with 1200 images stored.

doi:10.1371/journal.pcbi.1004683.g006

Discussion

We have shown that the neural architecture of the insect mushroom body can implement the 'familiarity' algorithm [11] for ant route following. In our simulation, the MB learns over 80 on-route images, reconstructed from real ant viewpoints in their natural habitat, and reliably distinguishes them from the highly similar images obtained when looking off-route. This is the first model of visual navigation in insects to draw such a close connection to known neural circuits, rather than appealing to abstract computational capacities; as a result we found that a simpler associative learning network (computationally equivalent to a Willshaw net [50]) than Infomax suffices for the task.

Strikingly, the network which was originally developed for modelling simple olfactory associative learning in flies required almost no modification other than increased size to perform the apparently much more complex function of supporting navigation under realistic conditions. Ants (and other navigating insects such as bees) are known to have significantly enlarged MB compared to flies [57]. Visual memory has also been localised to the central complex of the insect brain [27,58], and it remains possible that navigation, including visual memory for homing routes, is carried out entirely in the central complex and does not involve the MB. We would agree that the central complex is likely to be a key area for navigational capabilities in many insects [27,59], in particular processing polarised light [60], and potentially for path integration. However the extreme memory demands of extended route following in hymenoptera such as ants and bees may have co-opted the unique circuit properties of the MB: a divergent projection of patterns into a sparse code across a very large array of neurons, enabling separation and storage of a large number of arbitrary, similar patterns. Such an architecture appears to be unique to the MB neuropils in the insect brain, and has interesting parallels to the cerebellum in vertebrates [61].

Although we have used whole images in our simulation, we believe the approach is neutral to the issue of whether insects actually use the whole panorama, the skyline, the ground pattern, optic flow, or salient landmarks. Indeed there is no reason why the patterns stored should represent only one modality at a time. The multimodal inputs to the MB in ants [62] suggest that the KC activation pattern might combine olfactory, visual and other sensory (and possibly

proprioceptive or motivational) inputs into a gestalt experience of the current location, and alteration of any of these cues might reduce the familiarity. Manipulation of olfactory [63], wind [64] and tactile [65] cues have been shown to affect navigational memory in ants.

The network we have described simply stores patterns, rather than trying to learn an underlying generative model to classify 'on-route' vs 'off-route' memories. Nevertheless, in common with many learning problems, the ideal visual memory for route following has an over-fitting/generalization tradeoff. If the memory for individual views is too specific, then any small displacement from the route will result in no direction looking familiar and the animal being lost; and if the similar views resulting from small displacements could be stored as 'one class', the environmental range of a limited capacity memory would be increased. However, if parameters (or the learning rule) are adjusted to allow greater generalization to similar views, there will be increased aliasing and hence risk of mistaking a new view for a familiar one, which would result in moving in the wrong direction, with potentially fatal consequences. One way to deal with this problem might be to introduce more sophisticated visual processing. In particular, a more effective vPN-KC mapping than the random connectivity assumed here might be obtained by allowing self-organisation (unsupervised learning) in response to visual experience in the natural environment [66] so that only 'useful' correlations (for example features that vary strongly with rotation but not displacement [67]) are preserved. Evidence for adaptive synapses at this level of the circuit exists for bees [41] and flies [42]. More complex pre-processing might also be needed to deal with some aspects of the real performance of ants, who continue to follow a route under changing light conditions and movement of vegetation by wind, with some robustness to changing landmark information, and probably also pitch and roll of the head [68,69].

Similarly, we recognise there is likely to be more complexity to the ant's use of PI and visual memory than the algorithm presented here suggests. For example, it would be necessary to postulate a separate memory to explain the outwards routes of ants, with acquisition guided by successful progress along an outbound vector that is expected to lead to a food source. Insects also appear to acquire visual memory during learning walks and flights, by turning back to view the nest [8,70,71]. In this case we would need to assume that the reinforcement signal is under more complex control of a motor programme that maintains or generates fixations in the nest direction. Another possibility is that memory storage is triggered by significant change in the view. Interestingly, this is already inherently determined by the use of a three-factor learning rule in our MB model. If a view is already sufficiently 'familiar', the EN will not fire in response to the KC activation, so the synapses will not be tagged and learning will not occur.

The model we present provides a neurophysiological underpinning for the claim that ants can perform route navigation without requiring a map and for assessing the range over which views can provide guidance. We should be cautious to extend results from ants to other insects, particularly bees, whose sensorimotor habitat is significantly different and might thus have developed different strategies for navigation. However, although it might seem difficult to account for novel routes (or short cuts) ever being taken using the familiarity algorithm, great care is needed to distinguish a truly novel route from the behaviour that may emerge from an animal continuously orienting to make the best visual memory match possible given its current location and stored memories. This can include visual homing within a catchment area larger than that actually explored by the animal [12,72,73]. We also note that though PI is not used in route guidance in our simulations, it will normally still be active in the animal, with potential to influence the direction taken. In particular, recent results have shown that conflicting visual and PI cues often result in a compromise direction being taken by ants [73–77]. Under some circumstances, the result could appear to be a novel shortcut.

Methods

Ant data

The data on ant routes and environment comes from our previous study of route following in *Cataglyphis velox* [43]. Briefly, individual foragers were tracked over repeated journeys, by marking their location on squared paper at approximately 2 second intervals relative to a grid marked on the ground with bottle caps at 1 metre spacing. Subsequently a continuous path was reconstructed using polynomial interpolation. Mapping of tussock locations and panoramic photos from this environment were used to create the virtual environment based on the same software used in [10–11]; details and the simulated world itself are available from www.insectvision.org/walking-insects/antnavigationchallenge.

Image processing

The simulated ant's visual input, for a specific location and heading direction, is reconstructed from a point 1cm above the ground plane, with a field of view that extends horizontally for 296 degrees and vertically for 76 degrees, with 4 degree/pixel resolution, producing a 19x74 pixel image. The greyscale image values are inverted and the local contrast is enhanced using contrast-limited adaptive histogram equalisation, by applying the Matlab function *adapthisteq* [http://uk.mathworks.com/help/images/ref/adapthisteq.html] with default values. It is then further down-sampled to 10x36 pixels using the Matlab function *imresize* [http://uk.mathworks.com/help/images/ref/imresize.html] in which each output pixel is a weighted average of the pixels in the nearest 4x4 neighbourhood. For input into all models, the image is normalised by dividing each pixel value by the square root of the sum of squares of all pixel values. Matlab function *reshape* [http://uk.mathworks.com/help/matlab/ref/reshape.html] is applied to convert the normalised 2D (10x36) image into an 1D (360x1) vector used for subsequent processing.

Spiking neural network

The Mushroom Body network is essentially the same as that described in [30] except that it uses more neurons and has anti-Hebbian learning. It is composed of three layers (see Fig 2 and Tables 1–3) of 'Izhikevich' spiking neurons [78], i.e., for each neuron the change in membrane potential v(mV) is modelled as follows:

$$C\dot{v} = k(v - v_r)(v - v_t) - u + I + [\xi \sim N(0, \sigma)] \quad (2)$$

$$\dot{u} = a(b(v - v_r) - u) \quad (3)$$

The variables v (membrane potential) and u (recovery current) are reset if the membrane potential exceeds a threshold v_t:

$$\begin{cases} v \leftarrow c \\ u \leftarrow u + d \end{cases} \quad (4)$$

Table 1. Connectivity and synaptic weights.

From X to Y	Prob. of connection	Initial Weight per connection
vPN to KC	Each KC receives input from 10 randomly selected PNs	0.25 (constant)
KC to EN	1 (all KCs connect to the EN)	2.0 (subject to learning)

doi:10.1371/journal.pcbi.1004683.t001

Table 2. Parameters for each neuron type.

Parameter	PN	KC	EN
Neuron Number	360	20000	1
Scaling factor	5250	N/A	N/A
C	100	4	100
a	0.3	0.01	0.3
b	-0.2	-0.3	-0.2
c	-65	-65	-65
d	8	8	8
k	2	0.035	2
v_r	-60	-85	-60
v_t	-40	-25	-40
ξ	$N(0, 0.05)$	$N(0, 0.05)$	$N(0, 0.05)$

Neuron Number is the number of neurons in each type. Scaling factor is specifically for visual Projection Neurons: the input signal without scaling is the result from normalisation of grayscale images, thus in the range of [0, 1]. The scaling factor amplifies the signal so that any image will activate about half of the vPNs. The parameters from C to v_t in the first column are Izhikevich spiking neuronal model parameters. ξ defines Gaussian random noise current injected into each neuron.

doi:10.1371/journal.pcbi.1004683.t002

The parameter C is the membrane capacitance, v_r is the resting membrane potential, I is the input current, $\xi \sim N(0, \sigma)$ is noise with a Gaussian distribution, and a, b, c, d and k are model parameters (see Table 2) which determine the characteristic response of the neuron.

Synaptic input to the first layer, which consists of 360 visual projection neurons (vPNs), is given as an input current proportional to the corresponding pixel in the normalised image 1D vector (360x1) described above:

$$PN\ \ input = \ \ scaling\ \ factor \times Vector$$

The normalization and choice of scaling factor ensures that approximately half the vPNs are activated by each image. The subsequent layers consist of 20,000 Kenyon cells (KC), each receiving input from 10 randomly selected vPNs, and a single extrinsic neuron (EN) receiving input from all KC, and their synaptic input is modelled by:

$$I = gS(v_{rev} - v) \tag{5}$$

Table 3. Parameters for each synapse type.

Parameter	PN to KC	KC to EN
τ_{syn}	3.0	8.0
ϕ	0.93	8.0
g	0.25	[0, 2.0]
τ_c	N/A	40ms
τ_d	N/A	20ms

The parameter τ_{syn} is the time constant for synapses, ϕ represents the quantity of neurotransmitter released per synapse, and g is the weight per synapse. Note that the weights of connections from vPN to KC are fixed whereas the weights from KC to EN are bounded to the range of 0 to 2.0. The parameter τ_c is the time constant for Izhikevich type synaptic eligibility trace in KC-EN synapses, and τ_d is the Biogenic Amine concentration time constant.

doi:10.1371/journal.pcbi.1004683.t003

where g (nS) is the maximal synaptic conductance (the synaptic 'weight'), $v_{rev} = 0$ is the reversal potential of the synapses, and S is the amount of active neurotransmitter which is updated as follows:

$$\dot{S} = \frac{-S}{\tau_{syn}} + \phi\delta(t - t_{pre}) \tag{6}$$

where the parameter ϕ is a quantile of the amount of neurotransmitters released when a pre-synaptic spike occurred, τ_{syn} is the synaptic time constant, t_{pre} is the time at which the presynaptic spike occurred and δ is the Dirac delta function. See Table 3 for synapse parameter values. The weights from vPN to KC are fixed. The weights g from KC to EN are altered by learning using a modification of the three-factor rule from [79]:

$$\dot{g} = cd \tag{7}$$

where g is the synaptic conductance, c is a synaptic 'tag' which maintains an eligibility trace over short periods of time, signalling which KC was involved in activating EN (see below); and d is the extracellular concentration of a biogenic amine, modelled by:

$$\dot{d} = \frac{-d}{\tau_d} + BA(t) \tag{8}$$

where $BA(t)$ is the amount of biogenic amine released at time t, which depends on the presence of the reinforcement signal [30] (see training procedure below) and τ_d is a time constant for the decay of concentration d.

The synaptic tag c is modified using spike timing dependent plasticity (STDP):

$$\dot{c} = \frac{-c}{\tau_c} + STDP(t_{pre} - t_{post})\delta[(t - t_{pre}) * (t - t_{post})] \tag{9}$$

where $\delta(t)$ is the Dirac delta function, t_{pre} is the time of a pre-synaptic spike, t_{post} is the time of a post-synaptic spike, and τ_c is a time constant for decay of the tag c. Thus, either pre- or post-synaptic neuronal firing will change variable c by the amount STDP, defined as:

$$STDP(t_{pre} - t_{post}) = \begin{cases} A_+ e^{\frac{t_{pre} - t_{post}}{\tau_+}}, & if\, t_{pre} - t_{post} < 0 \\ 0, & if\ \ t_{pre} - t_{post} = 0 \\ A_- e^{\frac{t_{pre} - t_{post}}{\tau_-}}, & if\ \ t_{pre} - t_{post} > 0 \end{cases} \tag{10}$$

A_+ and A_- are the amplitudes, and τ_+/τ_- are the time constants. However we use an anti-Hebbian form of this rule, such that the tag is always negative:

$$\begin{aligned} A_+ = A_- &= -1.0 \\ \tau_+ = \tau_- &= 15 \end{aligned} \tag{11}$$

Network geometry

Training procedure

We assume that an ant learns a route while running home (following a home vector) and avoiding obstacles. This gives rise to a unique set of visual experiences which it memorises, so that subsequent traversals of the same route can be made without a home vector, and starting

from any point along it. In practice, we take each recorded route of a real ant (of average length 8m) and use it to train the spiking neural network as follows. From nest to home, every 10cm along the route, we use the simulated environment to generate an image facing the next 10cm waypoint. After pre-processing as described above, the normalised image pixel values are given as input to the first layer (vPNs) of the network every 1ms for 40ms. Then a reinforcement signal is presented for one time-step (BA(t) = 0.5, for t = 40ms from image onset) and a further 10ms of simulation time (with no image or reinforcement signal presented) allowed to elapse, during which any synaptic weight changes will occur. Given the parameters below, this presentation results in rapid, 'one-shot' learning of the presented image, with weights between any active KC and EN decreasing rapidly to zero (see Fig 3). To save computation time, we do not explicitly model network activity during the lapse of time until the next image to be learnt would be encountered (during which the ant moves 10cm further along the route). Instead we simply reset the membrane potentials, synaptic tags and amine levels in the network to their initial state, and then present the new image for 40ms, followed by reinforcement, etc., until all the images for that route (around 80 for an 8m route) have been presented. Subsequently the spiking rate output of EN will indicate the novelty of any image presented to the network.

Perfect memory

As a benchmark for the difficulty of the navigation task, we determine the performance of a simulated ant which has a perfect memory, i.e., it simply stores the complete set of training images, and uses direct pixel-by-pixel image differencing to compare images [9]. When recapitulating a route, novelty of the current view I with respect to all stored images is calculated as:

$$Novelty(I) = \min_i \left(\sum_{x,y} (I(x,y) - V_i(x,y))^2 \right) \quad (12)$$

Where V_i is each of the stored images, and x,y define the individual pixels.

Infomax

For comparison, we also implemented the Infomax algorithm, a continuous 2-layer network, closely following the method described in [11], except with a much higher learning rate. The input layer has $N = 360$ units and the normalized intensities of the 36x10 image pixels are mapped row by row onto the input layer to provide the activation level of each unit, x_i. The output layer also has 360 units and is fully connected to the input layer. The activation of each unit of the output layer, h_i, is given by:

$$h_i = \sum_{j=1}^{N} w_{ij} x_j \quad (13)$$

Where w_{ij} is the weight of the connection from the *jth* input unit to the *ith* output unit. The output y_i is then given by:

$$y_i = \tanh(h_i) \quad (14)$$

Each image is learnt in turn by adjusting all the weights (initialized with random values) by:

$$\Delta w_{ij} = \frac{\eta}{N} (w_{ij} - (y_i + h_i) \sum_{k=1}^{N} h_k w_{kj}) \quad (15)$$

Where $\eta = 1.1$ is the learning rate.

Subsequently the novelty of an image is given by the summed activation of the output layer:

$$d(\vec{x}) = \sum_{i=1}^{M} \mid h_i \mid \tag{16}$$

Capacity

For this analysis we simplify the MB model by assuming the KC have a binary state (activated if input is above threshold, otherwise not active) and learning will alter the state of the respective KC-EN synapse by setting it to zero when KC activity coincides with reward. We can analyse the storage capacity of a network with N input nodes and average activity p by deriving an expression for the probability of error P_{error}, defined as the probability that a random unlearned pattern activates only KC nodes that already have their weight set to 0, producing the same EN output as a learned pattern (i.e. 0). We assume the number of neurons k coding a pattern is drawn from the binomial distribution with probability p. After learning m random patterns:

$$P(w_i = 0) = 1 - (1-p)^m \tag{17}$$

The probability that a new pattern activates only neurons with $w_i = 0$ is given by:

$$P_{error} = \sum_K \binom{N}{k} (p(1-(1-p)^m))^k (1-p)^{N-k} \tag{18}$$

That is, the sum of possible arrangements of k active units that all have weights set to 0. This can be written as:

$$\begin{aligned} P_{error} &= (1-p)^N \sum_k \binom{N}{k} \left(\frac{p(1-(1-p)^m)}{1-p}\right)^k \\ &= (1-p)^N \left(1 + \frac{p(1-(1-p)^m)}{(1-p)}\right)^N \\ &= (1-p(1-p)^m)^N \end{aligned} \tag{19}$$

For a given acceptable error rate P_{error}, we can solve for the number of patterns m that can be stored before that error rate will be exceeded:

$$\mathrm{m} = \frac{\ln\left(\frac{1-P_{error}{}^{1/N}}{p}\right)}{\ln(1-p)} \tag{20}$$

Fig 5 shows how the capacity m of the network changes with the number of neurons N and average activity p, for $P_{error} = 0.01$.

To confirm this analysis is consistent with the behaviour of the full spiking network, we carried out an equivalent capacity testing process using the simulation. For a network of a given size, we generated random activation of the KC neurons at different levels of average activity. Patterns were learned as before, i.e., by applying a reward signal after 40ms, resulting in altered KC-EN weights. After each successive pattern was learned, we tested the network with 100 random patterns, to see if any produced a spiking response as low as that of the learned patterns, i.e., would potentially be confused with a learnt pattern (see S2 Fig for the result with N = 20000, p = 0.01). We noted how many patterns could be learnt before $P_{error} = 0.01$, i.e. where ≥ 1 out of 100 new patterns would start to be confused with a learnt pattern.

Note however this analysis and simulation assumes both learned and tested KC patterns are independent and random, which is not strictly true in the navigation task. We also tested the

spiking network (with N = 20000, p = 0.01) by continuously storing additional patterns generated by real route images, and counting the spikes produced by EN for the learnt image, for an image taken from a 5cm displacement facing the same way, for an image taken at a random location in the ant environment, and for a random image. The results are shown in Fig 6.

External database

The virtual ant world is available from: www.insectvision.org/walking-insects/antnavigationchallenge.

Supporting Information

S1 Movie. This movie shows the result of a route re-capitulation by a simulated ant using the mushroom body model, and the corresponding visual information from the ant's point of view that is used as input to the model. The direction of each 10cm step along the route is chosen by scanning (the scanning movement is not shown) ±60 degrees and choosing the direction producing the fewest spikes from the extrinsic neuron output. The simulated ant never departs far enough from the trained route to get lost, and successfully returns home over 8 meters in the complex environment.
(ZIP)

S1 Fig. A. Distant view of the study site on the outskirts of Seville, Spain with the approximate nest position indicated by the arrow. The nest is surrounded by grass shrub blocking the view of distant objects such as trees. B. Close up view of the field site with the ant nest and experimental feeder marked. C. An example route followed by an ant through the environment shown in blue from an overhead perspective. D. Panoramic images sampled along the route are shown which clearly demonstrate that distant objects were not visible to homing ants.
(EPS)

S2 Fig. Capacity of a MB network with N = 20000 and p = 0.01. From Fig 5, the abstracted model provides the estimate that around 375 random images can be stored (KC weights set to 0) before the probability of an error (a new random image activates only KCs that have already had weights set to 0) exceeds 0.01. Using the full spiking network and the three factor learning rule, we train successively with 500 random KC activation patterns. After each additional pattern is stored, we test the network with 100 random patterns to see how many produce an error (have an EN output of 0 spikes, indicating a familiar pattern). More than 350 patterns could be stored before $>$ 1/100 errors occur. The same method is used to generate data points for other values of N and p plotted in Fig 5.
(EPS)

Acknowledgments

Bart Baddeley introduced us to the familiarity and 3D world recreation approaches, Saran Lertpredit helped with the visual image generation, Jan Wessnitzer & Jonas Klein developed the original spiking MB neural network, and Shang Zhao first explored it for navigation. Lars Chittka, Paul Graham and Antoine Wystrach commented on earlier versions of the manuscript.

Author Contributions

Conceived and designed the experiments: BW MM PA FP. Performed the experiments: PA FP MM. Analyzed the data: PA FP MM KL BW. Wrote the paper: BW PA FP MM KL.

References

1. Wehner R. The architecture of the desert ant's navigational toolkit (Hymenoptera: Formicidae). Myrmecological News. 2009; 12:85–96.
2. Collett TS, Graham P, Harris RA. Novel landmark-guided routes in ants. J. Exp. Biol. 2007; 210:2025–32. PMID: 17562876
3. Zeil J. Visual homing: An insect perspective. Curr. Opin. Neurobiol. 2012; 22:285–93. doi: 10.1016/j.conb.2011.12.008 PMID: 22221863
4. Cruse H, Wehner R. No need for a cognitive map: Decentralized memory for insect navigation. PLoS Comput. Biol. 2011; 7:e1002009. doi: 10.1371/journal.pcbi.1002009 PMID: 21445233
5. Wehner R. Desert ant navigation: How miniature brains solve complex tasks. J. Comp. Physiol. A Neuroethol. Sensory, Neural, Behav. Physiol. 2003; 189:579–88.
6. Collett TS, Collett M. Memory use in insect visual navigation. Nat. Rev. Neurosci. 2002; 3:542–52. PMID: 12094210
7. Menzel R, Greggers U, Smith A, Berger S, Brandt R, Brunke S, et al. Honey bees navigate according to a map-like spatial memory. Proc. Natl. Acad. Sci. U. S. A. 2005; 102:3040–5. PMID: 15710880
8. Müller M, Wehner R. Path integration provides a scaffold for landmark learning in desert ants. Curr. Biol. 2010; 20:1368–71. doi: 10.1016/j.cub.2010.06.035 PMID: 20619653
9. Zeil J, Hofmann MI, Chahl JS. Catchment areas of panoramic snapshots in outdoor scenes. J. Opt. Soc. Am. A. Opt. Image Sci. Vis. 2003; 20:450–69. PMID: 12630831
10. Baddeley B, Graham P, Philippides A, Husbands P. Holistic visual encoding of ant-like routes: Navigation without waypoints. Adapt. Behav. 2011; 19:3–15.
11. Baddeley B, Graham P, Husbands P, Philippides A. A Model of Ant Route Navigation Driven by Scene Familiarity. PLoS Comput. Biol. 2012; 8:e1002336. doi: 10.1371/journal.pcbi.1002336 PMID: 22241975
12. Wystrach A, Mangan M, Philippides A, Graham P. Snapshots in ants? New interpretations of paradigmatic experiments. J. Exp. Biol. 2013; 216:1766–70. doi: 10.1242/jeb.082941 PMID: 23348949
13. Cheung A, Collett M, Collett TS, Dewar A, Dyer F, Graham P, et al. Still no convincing evidence for cognitive map use by honeybees: Proc. Natl. Acad. Sci. 2014; 111:E4396–7. doi: 10.1073/pnas.1413581111 PMID: 25277972
14. Menzel R, Greggers U. The memory structure of navigation in honeybees. J. Comp. Physiol. A. 2015;1–15.
15. Zollikofer C, Wehner R, Fukushi T. Optical scaling in conspecific Cataglyphis ants. J. Exp. Biol. 1995; 198:1637–46. PMID: 9319542
16. Schwarz S, Narendra A, Zeil J. The properties of the visual system in the Australian desert ant Melophorus bagoti. Arthropod Struct. Dev. 2011; 40:128–34. doi: 10.1016/j.asd.2010.10.003 PMID: 21044895
17. Ehmer B, Gronenberg W. Mushroom Body Volumes and Visual Interneurons in Ants: Comparison between Sexes and Castes. J. Comp. Neurol. 2004; 469:198–213. PMID: 14694534
18. Heisenberg M. Mushroom body memoir: from maps to models. Nat. Rev. Neurosci. 2003; 4:266–75. PMID: 12671643
19. Fahrbach SE. Structure of the mushroom bodies of the insect brain.Ann, Rev. Entomology 2006; 51:209–232.
20. Stieb SM, Muenz TS, Wehner R, Rössler W. Visual experience and age affect synaptic organization in the mushroom bodies of the desert ant Cataglyphis fortis. Dev. Neurobiol. 2010; 70:408–23. doi: 10.1002/dneu.20785 PMID: 20131320
21. Kühn-Bühlmann S, Wehner R. Age-dependent and task-related volume changes in the mushroom bodies of visually guided desert ants, Cataglyphis bicolor. J. Neurobiol. 2006; 66:511–21. PMID: 16555240
22. Fahrbach SE, Giray T, Farris SM, Robinson GE. Expansion of the neuropil of the mushroom bodies in male honey bees is coincident with initiation of flight. Neurosci. Lett. 1997; 236:135–8. PMID: 9406755
23. Durst C, Eichmüller S, Menzel R. Development and experience lead to increased volume of subcompartments of the honeybee mushroom body. Behav. Neural Biol. 1994; 62:259–63. PMID: 7857249
24. Withers GS, Fahrbach SE, Robinson GE. Effects of experience and juvenile hormone on the organization of the mushroom bodies of honey bees. J. Neurobiol. 1995; 26:130–44. PMID: 7714522
25. Lutz CC, Robinson GE. Activity-dependent gene expression in honey bee mushroom bodies in response to orientation flight. J. Exp. Biol. 2013; 216:2031–8. doi: 10.1242/jeb.084905 PMID: 23678099

26. Mizunami M, Weibrecht JM, Strausfeld NJ. Mushroom bodies of the cockroach: Their participation in place memory. J. Comp. Neurol. 1998; 402:520–37. PMID: 9862324

27. Ofstad T a, Zuker CS, Reiser MB. Visual place learning in Drosophila melanogaster. Nature. 2011; 474:204–7. doi: 10.1038/nature10131 PMID: 21654803

28. Liu L, Wolf R, Ernst R, Heisenberg M. Context generalization in Drosophila visual learning requires the mushroom bodies. Nature. 1999; 400:753–6. PMID: 10466722

29. Vogt K, Schnaitmann C, Dylla KV, Knapek S, Aso Y, Rubin GM, et al. Shared mushroom body circuits operate visual and olfactory memories in Drosophila. Elife. 2014; 3:1–22.

30. Wessnitzer J, Young JM, Armstrong JD, Webb B. A model of non-elemental olfactory learning in Drosophila. J. Comput. Neurosci. 2012; 32:197–212. doi: 10.1007/s10827-011-0348-6 PMID: 21698405

31. Wang JW, Wong AM, Flores J, Vosshall LB, Axel R. Two-photon calcium imaging reveals an odor-evoked map of activity in the fly brain. Cell. 2003; 112:271–82. PMID: 12553914

32. Galizia CG, Menzel R, Hölldobler B. Optical imaging of odor-evoked glomerular activity patterns in the antennal lobes of the ant Camponotus rufipes. Naturwissenschaften. 1999; 86:533–7. PMID: 10551948

33. Honegger KS, Campbell RA, Turner GC. Cellular-resolution population imaging reveals robust sparse coding in the Drosophila mushroom body. J. Neurosci. 2011; 31:11772–85. doi: 10.1523/JNEUROSCI.1099-11.2011 PMID: 21849538

34. Perez-Orive J, Mazor O, Turner GC, Cassenaer S, Wilson RI, Laurent G. Oscillations and sparsening of odor representations in the mushroom body. Science. 2002; 297:359–65. PMID: 12130775

35. Szyszka P, Ditzen M, Galkin A, Galizia CG, Menzel R. Sparsening and temporal sharpening of olfactory representations in the honeybee mushroom bodies. J. Neurophysiol. 2005; 94:3303–13. PMID: 16014792

36. Gerber B, Tanimoto H, Heisenberg M. An engram found? Evaluating the evidence from fruit flies. Curr. Opin. Neurobiol. 2004; 14:737–44. PMID: 15582377

37. Menzel R, Manz G. Neural plasticity of mushroom body-extrinsic neurons in the honeybee brain. J. Exp. Biol. 2005; 208:4317–32. PMID: 16272254

38. Strube-Bloss MF, Nawrot MP, Menzel R. Mushroom body output neurons encode odor-reward associations. J. Neurosci. 2011; 31:3129–40. doi: 10.1523/JNEUROSCI.2583-10.2011 PMID: 21414933

39. Cassenaer S, Laurent G. Conditional modulation of spike-timing-dependent plasticity for olfactory learning. Nature. 2012; 482:47–52. doi: 10.1038/nature10776 PMID: 22278062

40. Aso Y, Hattori D, Yu Y, Johnston RM, Iyer NA, Ngo T-T, et al. The neuronal architecture of the mushroom body provides a logic for associative learning. Elife. 2014; 3:e04577. doi: 10.7554/eLife.04577 PMID: 25535793

41. Szyszka P, Galkin A, Menzel R. Associative and non-associative plasticity in Kenyon cells of the honeybee mushroom body. Front. Syst. Neurosci. 2008; 2:3. doi: 10.3389/neuro.06.003.2008 PMID: 18958247

42. Hourcade B, Muenz TS, Sandoz J-C, Rössler W, Devaud J-M. Long-term memory leads to synaptic reorganization in the mushroom bodies: a memory trace in the insect brain? J. Neurosci. 2010; 30:6461–5. doi: 10.1523/JNEUROSCI.0841-10.2010 PMID: 20445072

43. Mangan M, Webb B. Spontaneous formation of multiple routes in individual desert ants (Cataglyphis velox). Behav. Ecol. 2012; 23:944–54.

44. Laughlin S. A simple coding procedure enhances a neuron's information capacity. Z. Naturforsch. C. 1981; 36:910–2. PMID: 7303823

45. Caron SJC, Ruta V, Abbott LF, Axel R. Random convergence of olfactory inputs in the Drosophila mushroom body. Nature. 2013; 497:113–7. doi: 10.1038/nature12063 PMID: 23615618

46. Laurent G. Olfactory network dynamics and the coding of multidimensional signals. Nat. Rev. Neurosci. 2002; 3:884–95. PMID: 12415296

47. Izhikevich EM. Simple model of spiking neurons. IEEE Trans. Neural Networks. 2003; 14:1569–72. doi: 10.1109/TNN.2003.820440 PMID: 18244602

48. Pamir E, Chakroborty NK, Stollhoff N, Gehring KB, Antemann V, Morgenstern L, et al. Average group behavior does not represent individual behavior in classical conditioning of the honeybee. Learn. Mem. 2011; 18:733–41. doi: 10.1101/lm.2232711 PMID: 22042602

49. Rouder JN, Speckman PL, Sun D, Morey RD, Iverson G. Bayesian t tests for accepting and rejecting the null hypothesis. Psychon. Bull. Rev. 2009; 16:225–37. doi: 10.3758/PBR.16.2.225 PMID: 19293088

50. Willshaw DJ, Buneman OP, Longuet-Higgins HC. Non-holographic associative memory. Nature. 1969; 222:960–2. PMID: 5789326

51. Barrett AB, Van Rossum MCW. Optimal learning rules for discrete synapses. PLoS Comput. Biol. 2008; 4(11):e1000230. doi: 10.1371/journal.pcbi.1000230 PMID: 19043540

52. Huerta R, Nowotny T. Fast and robust learning by reinforcement signals: explorations in the insect brain. Neural Comput. 2009; 21:2123–51. doi: 10.1162/neco.2009.03-08-733 PMID: 19538091

53. Tsodyks MV. Associative Memory in Neural Networks With Binary Synapses. Mod. Phys. Lett. B. 1990; 04:713–6.

54. Huber R, Egocentric and geocentric navigation during extremely long foraging paths of desert ants. J. Comp.Physiol.A; 201:609–616.

55. Kohler M, Wehner R. Idiosyncratic route-based memories in desert ants, Melophorus bagoti: How do they interact with path-integration vectors? Neurobiol. Learn. Mem. 2005; 83:1–12. PMID: 15607683

56. Wystrach A, Schwarz S, Schultheiss P, Beugnon G, Cheng K. Views, landmarks, and routes: How do desert ants negotiate an obstacle course? J. Comp. Physiol. A Neuroethol. Sensory, Neural, Behav. Physiol. 2011; 197:167–79.

57. Gronenberg W. Subdivisions of hymenopteran mushroom body calyces by their afferent supply. J. Comp. Neurol. 2001; 435:474–89. PMID: 11406827

58. Liu G, Seiler H, Wen A, Zars T, Ito K, Wolf R, et al. Distinct memory traces for two visual features in the Drosophila brain. Nature. 2006; 439:551–6. PMID: 16452971

59. Seelig JD, Jayaraman V. Neural dynamics for landmark orientation and angular path integration. Nature. 2015; 521:186–91. doi: 10.1038/nature14446 PMID: 25971509

60. Heinze S, Homberg U. Maplike representation of celestial E-vector orientations in the brain of an insect. Science. 2007; 315:995–7. PMID: 17303756

61. Farris SM. Are mushroom bodies cerebellum-like structures? Arthropod Struct. Dev. 2011; 40:368–79. doi: 10.1016/j.asd.2011.02.004 PMID: 21371566

62. Gronenberg W. Structure and function of ant (Hymenoptera: Formicidae) brains: strength in numbers. Myrmecological News. 2008; 11:25–36.

63. Steck K. Just follow your nose: Homing by olfactory cues in ants. Curr. Opin. Neurobiol. 2012; 22:231–5. doi: 10.1016/j.conb.2011.10.011 PMID: 22137100

64. Wolf H, Wehner R. Pinpointing food sources: olfactory and anemotactic orientation in desert ants, Cataglyphis fortis. J. Exp. Biol. 2000; 203:857–68. PMID: 10667968

65. Seidl T, Wehner R. Visual and tactile learning of ground structures in desert ants. J. Exp. Biol. 2006; 209:3336–44. PMID: 16916970

66. Rao RPN, Fuentes O. Hierarchical Learning of Navigational Behaviors in an Autonomous Robot using a Predictive Sparse Distributed Memory. Mach. Learn. 1998; 31:87–113.

67. Stürzl W, Zeil J. Depth, contrast and view-based homing in outdoor scenes. Biol. Cybern. 2007; 96:519–31. PMID: 17443340

68. Ardin P, Mangan M, Wystrach A, Webb B. How variation in head pitch could affect image matching algorithms for ant navigation. J. Comp. Physiol. A. 2015; 201:585–97.

69. Raderschall C, Narendra A, Zeil J. Balancing act: Head stabilisation in Myrmecia ants during twilight. Int. Union Study Soc. Insects. 2014. p. P192.

70. von Frish K. The dance language and orientation of bees. London: Oxford University Press; 1967.

71. Nicholson D, Judd S, Cartwright B, Collett T. Learning walks and landmark guidance in wood ants (Formica rufa). J. Exp. Biol. 1999; 202 (Pt 13:1831–8. PMID: 10359685

72. Stürzl W, Grixa I, Mair E, Narendra A, Zeil J. Three-dimensional models of natural environments and the mapping of navigational information. J. Comp. Physiol. A. 2015; 201:563–84.

73. Narendra A, Gourmaud S, Zeil J. Mapping the navigational knowledge of individually foraging ants, Myrmecia croslandi. Proc. R. Soc. B Biol. Sci. 2013; 280:20130683.

74. Wystrach A, Mangan M, Webb B. Optimal cue integration in ants. Proc. R. Soc. B Biol. Sci. 2015;

75. Legge ELG, Wystrach a., Spetch ML, Cheng K. Combining sky and earth: desert ants (Melophorus bagoti) show weighted integration of celestial and terrestrial cues. J. Exp. Biol. 2014; 217:4159–66. doi: 10.1242/jeb.107862 PMID: 25324340

76. Collett M. How navigational guidance systems are combined in a desert ant. Curr. Biol. Elsevier; 2012; 22:927–32.

77. Reid SF, Narendra A, Hemmi JM, Zeil J. Polarised skylight and the landmark panorama provide night-active bull ants with compass information during route following. J. Exp. Biol. 2011; 214:363–70. doi: 10.1242/jeb.049338 PMID: 21228195

78. Izhikevich EM. Which model to use for cortical spiking neurons? IEEE Trans. Neural Networks. 2004; 15:1063–70. PMID: 15484883

79. Izhikevich EM. Solving the distal reward problem through linkage of STDP and dopamine signaling. Cereb. Cortex. 2007; 17:2443–52. PMID: 17220510

Bibliography

Åkesson, S. and Wehner, R. (2002). Visual navigation in desert ants cataglyphis fortis: are snapshots coupled to a celestial system of reference? *Journal of Experimental Biology*, 205(14):1971–1978.

Ardin, P., Mangan, M., Wystrach, A., and Webb, B. (2015). How variation in head pitch could affect image matching algorithms for ant navigation. *Journal of Comparative Physiology A*, 201(6):585–597.

Ardin, P., Peng, F., Mangan, M., Lagogiannis, K., and Webb, B. (2016a). Using an insect mushroom body circuit to encode route memory in complex natural environments. *PLOS Comput Biol*, 12(2):e1004683.

Ardin, P. B., Mangan, M., and Webb, B. (2016b). Ant homing ability is not diminished when traveling backwards. *Frontiers in behavioral neuroscience*, 10.

Aso, Y., Hattori, D., Yu, Y., Johnston, R. M., Iyer, N. A., Ngo, T.-T., Dionne, H., Abbott, L., Axel, R., Tanimoto, H., et al. (2014). The neuronal architecture of the mushroom body provides a logic for associative learning. *Elife*, 3:e04577.

Baddeley, B., Graham, P., Husbands, P., and Philippides, A. (2012). A model of ant route navigation driven by scene familiarity. *PLoS Comput Biol*, 8(1):e1002336.

Baddeley, B., Graham, P., Philippides, A., and Husbands, P. (2011). Holistic visual encoding of ant-like routes: Navigation without waypoints. *Adaptive Behavior*, 19(1):3–15.

Barrett, A. B. and van Rossum, M. C. (2008). Optimal learning rules for discrete synapses. *PLoS Comput Biol*, 4(11):e1000230.

Barta, A. and Horváth, G. (2004). Why is it advantageous for animals to detect celestial polarization in the ultraviolet? skylight polarization under clouds and canopies is strongest in the uv. *Journal of theoretical biology*, 226(4):429–437.

Basten, K. and Mallot, H. A. (2010). Simulated visual homing in desert ant natural environments: efficiency of skyline cues. *Biological cybernetics*, 102(5):413–425.

Bell, A. J. and Sejnowski, T. J. (1995). An information-maximization approach to blind separation and blind deconvolution. *Neural computation*, 7(6):1129–1159.

Bell, A. J. and Sejnowski, T. J. (1997). The independent components of natural scenes are edge filters. *Vision research*, 37(23):3327–3338.

Benhamou, S. (2004). How to reliably estimate the tortuosity of an animal's path:: straightness, sinuosity, or fractal dimension? *Journal of theoretical biology*, 229(2):209–220.

Benhamou, S., Sauvé, J.-P., and Bovet, P. (1990). Spatial memory in large scale movements: efficiency and limitation of the egocentric coding process. *Journal of Theoretical Biology*, 145(1):1–12.

Bernadou, A. and Fourcassié, V. (2008). Does substrate coarseness matter for foraging ants? an experiment with lasius niger (hymenoptera; formicidae). *Journal of insect physiology*, 54(3):534–542.

Bogacz, R. and Brown, M. W. (2003). Comparison of computational models of familiarity discrimination in the perirhinal cortex. *Hippocampus*, 13(4):494–524.

Borst, A. and Egelhaaf, M. (1989). Principles of visual motion detection. *Trends in neurosciences*, 12(8):297–306.

Borst, A., Haag, J., and Reiff, D. F. (2010). Fly motion vision. *Annual review of neuroscience*, 33:49–70.

Braitenberg, V. (1986). *Vehicles: Experiments in synthetic psychology*. MIT press.

Braun, E., Dittmar, L., Boeddeker, N., and Egelhaaf, M. (2012). Prototypical components of honeybee homing flight behavior depend on the visual appearance of objects surrounding the goal. *Frontiers in behavioral neuroscience*, 6:1.

Buehlmann, C., Graham, P., Hansson, B. S., and Knaden, M. (2015). Desert ants use olfactory scenes for navigation. *Animal Behaviour*, 106:99–105.

Buehlmann, C., Hansson, B. S., and Knaden, M. (2012). Desert ants learn vibration and magnetic landmarks. *PLoS One*, 7(3):e33117.

Buehlmann, C., Hansson, B. S., and Knaden, M. (2013). Flexible weighing of olfactory and vector information in the desert ant cataglyphis fortis. *Biology letters*, 9(3):20130070.

Bühlmann, C., Cheng, K., and Wehner, R. (2011). Vector-based and landmark-guided navigation in desert ants inhabiting landmark-free and landmark-rich environments. *Journal of Experimental Biology*, 214(17):2845–2853.

Cammaerts, M.-C. (2004). Some characteristics of the visual perception of the ant myrmica sabuleti. *Physiological Entomology*, 29(5):472–482.

Cammaerts, M.-C. (2012). The visual perception of the ant myrmica ruginodis (hymenoptera: Formicidae). *Biologia*, 67(6):1165–1174.

Caron, S. J., Ruta, V., Abbott, L., and Axel, R. (2013). Random convergence of olfactory inputs in the drosophila mushroom body. *Nature*, 497(7447):113–117.

Cartwright, B. and Collett, T. (1982). How honey bees use landmarks to guide their return to a food source. *Nature*, pages 560–564.

Cartwright, B. and Collett, T. S. (1983). Landmark learning in bees. *Journal of comparative physiology*, 151(4):521–543.

Cassenaer, S. and Laurent, G. (2012). Conditional modulation of spike-timing-dependent plasticity for olfactory learning. *Nature*, 482(7383):47–52.

Cerdá, X. and Retana, J. (1997). Links between worker polymorphism and thermal biology in a thermophilic ant species. *Oikos*, pages 467–474.

Cerdá, X., Retana, J., and Cros, S. (1998). Critical thermal limits in mediterranean ant species: trade-off between mortality risk and foraging performance. *Functional Ecology*, 12(1):45–55.

Chameron, S., Schatz, B., Pastergue-Ruiz, I., Beugnon, G., and Collett, T. S. (1998). The learning of a sequence of visual patterns by the ant cataglyphis cursor. *Proceedings of the Royal Society of London B: Biological Sciences*, 265(1412):2309–2313.

Cheng, K., Narendra, A., Sommer, S., and Wehner, R. (2009). Traveling in clutter: navigation in the central australian desert ant melophorus bagoti. *Behavioural processes*, 80(3):261–268.

Cheng, K., Shettleworth, S. J., Huttenlocher, J., and Rieser, J. J. (2007). Bayesian integration of spatial information. *Psychological bulletin*, 133(4):625.

Cheung, A., Collett, M., Collett, T. S., Dewar, A., Dyer, F., Graham, P., Mangan, M., Narendra, A., Philippides, A., Stürzl, W., et al. (2014). Still no convincing evidence for cognitive map use by honeybees. *Proceedings of the National Academy of Sciences*, 111(42):E4396–E4397.

Cheung, A., Zhang, S., Stricker, C., and Srinivasan, M. V. (2007). Animal navigation: the difficulty of moving in a straight line. *Biological Cybernetics*, 97(1):47–61.

Collett, M. (2010). How desert ants use a visual landmark for guidance along a habitual route. *Proceedings of the National Academy of Sciences*, 107(25):11638–11643.

Collett, M. (2012). How navigational guidance systems are combined in a desert ant. *Current Biology*, 22(10):927–932.

Collett, M., Chittka, L., and Collett, T. S. (2013). Spatial memory in insect navigation. *Current Biology*, 23(17):R789–R800.

Collett, M. and Collett, T. S. (2009). The learning and maintenance of local vectors in desert ant navigation. *Journal of Experimental Biology*, 212(7):895–900.

Collett, M., Collett, T. S., Bisch, S., and Wehner, R. (1998). Local and global vectors in desert ant navigation. *Nature*, 394(6690):269–272.

Collett, T. (1978). Short communication: Peering-a locust behaviour pattern for obtaining motion parallax information. *Journal of experimental Biology*, 76(1):237–241.

Collett, T. (1992). Landmark learning and guidance in insects. *Philosophical Transactions of the Royal Society of London B: Biological Sciences*, 337(1281):295–303.

Collett, T. (1996). Insect navigation en route to the goal: multiple strategies for the use of landmarks. *Journal of Experimental Biology*, 199:227–235.

Collett, T. and Cartwright, B. (1983). Eidetic images in insects: Their role in navigation. *Trends in Neuroscience*, 6:101–105.

Collett, T., Dillmann, E., Giger, A., and Wehner, R. (1992). Visual landmarks and route following in desert ants. *Journal of Comparative Physiology A*, 170(4):435–442.

Collett, T., Graham, P., and Harris, R. (2007). Novel landmark-guided routes in ants. *Journal of Experimental Biology*, 210(12):2025–2032.

Collett, T. S. and Collett, M. (2002). Memory use in insect visual navigation. *Nature Reviews Neuroscience*, 3(7):542–552.

Collett, T. S. and Collett, M. (2015). Route-segment odometry and its interactions with global path-integration. *Journal of Comparative Physiology A*, 201(6):617–630.

Crist, T. O. and Wiens, J. A. (1994). Scale effects of vegetation on forager movement and seed harvesting by ants. *Oikos*, pages 37–46.

Cruse, H. and Wehner, R. (2011). No need for a cognitive map: decentralized memory for insect navigation. *PLoS Comput Biol*, 7(3):e1002009–e1002009.

Czaczkes, T. J. and Ratnieks, F. L. (2013). Cooperative transport in ants (Hymenoptera: Formicidae) and elsewhere. *Myrmecol. News*, 18:1–11.

de Ibarra, N. H., Philippides, A., Riabinina, O., and Collett, T. S. (2009). Preferred viewing directions of bumblebees (bombus terrestris l.) when learning and approaching their nest site. *Journal of Experimental Biology*, 212(20):3193–3204.

de Souza, J. M. and Ventura, D. F. (1989). Comparative study of temporal summation and response form in hymenopteran photoreceptors. *Journal of Comparative Physiology A: Neuroethology, Sensory, Neural, and Behavioral Physiology*, 165(2):237–245.

Dennett, D. C. (1978). Why not the whole iguana? *Behavioral and Brain Sciences*, 1(1):103.

Dewar, A. D., Philippides, A., and Graham, P. (2014). What is the relationship between visual environment and the form of ant learning-walks? an in silico investigation of insect navigation. *Adaptive Behavior*, 22(3):163–179.

Dittmar, L., Stürzl, W., Baird, E., Boeddeker, N., and Egelhaaf, M. (2010). Goal seeking in honeybees: matching of optic flow snapshots? *Journal of Experimental Biology*, 213(17):2913–2923.

Duelli, P. (1975). A fovea for e-vector orientation in the eye ofcataglyphis bicolor (formicidae, hymenoptera). *Journal of comparative physiology*, 102(1):43–56.

Durst, C., Eichmüller, S., and Menzel, R. (1994). Development and experience lead to increased volume of subcompartments of the honeybee mushroom body. *Behavioral and neural biology*, 62(3):259–263.

Ehmer, B. and Gronenberg, W. (2004). Mushroom body volumes and visual interneurons in ants: comparison between sexes and castes. *Journal of Comparative Neurology*, 469(2):198–213.

Eichner, H., Joesch, M., Schnell, B., Reiff, D. F., and Borst, A. (2011). Internal structure of the fly elementary motion detector. *Neuron*, 70(6):1155–1164.

Fahrbach, S. E. (2006). Structure of the mushroom bodies of the insect brain. *Annu. Rev. Entomol.*, 51:209–232.

Fahrbach, S. E., Giray, T., Farris, S. M., and Robinson, G. E. (1997). Expansion of the neuropil of the mushroom bodies in male honey bees is coincident with initiation of flight. *Neuroscience letters*, 236(3):135–138.

Farris, S. M. (2011). Are mushroom bodies cerebellum-like structures? *Arthropod structure & development*, 40(4):368–379.

Fent, K. and Wehner, R. (1985). Oceili: A celestial compass in the desert ant cataglyphis. *Science*, 228(4696):192–194.

Fischbach, K.-F. and Dittrich, A. (1989). The optic lobe of drosophila melanogaster. i. a golgi analysis of wild-type structure. *Cell and tissue research*, 258(3):441–475.

Fourcassie, V., Dahbi, A., and Cerdá, X. (2000). Orientation and navigation during adult transport between nests in the ant Cataglypis iberica. *Naturwissenschaften*, 87(8):355–359.

Franz, M. O. and Krapp, H. G. (2000). Wide-field, motion-sensitive neurons and matched filters for optic flow fields. *Biological cybernetics*, 83(3):185–197.

Franz, M. O., Schölkopf, B., Mallot, H. A., and Bülthoff, H. H. (1998). Where did i take that snapshot? scene-based homing by image matching. *Biological Cybernetics*, 79(3):191–202.

Galizia, C. G., Menzel, R., and Hölldobler, B. (1999). Optical imaging of odor-evoked glomerular activity patterns in the antennal lobes of the ant camponotus rufipes. *Naturwissenschaften*, 86(11):533–537.

Gerber, B., Tanimoto, H., and Heisenberg, M. (2004). An engram found? evaluating the evidence from fruit flies. *Current opinion in neurobiology*, 14(6):737–744.

Gibson, J. J. (2014). *The ecological approach to visual perception: classic edition*. Psychology Press.

Götz, K. (1971). Principles of optomotor reactions in insects. *Bibliotheca Ophthalmologica: supplementa ad ophthalmologica*, 82:251–259.

Graham, P. and Cheng, K. (2009a). Ants use the panoramic skyline as a visual cue during navigation. *Current Biology*, 19(20):R935–R937.

Graham, P. and Cheng, K. (2009b). Which portion of the natural panorama is used for view-based navigation in the australian desert ant? *Journal of Comparative Physiology A*, 195(7):681–689.

Graham, P. and Collett, T. S. (2002). View-based navigation in insects: how wood ants (formica rufa l.) look at and are guided by extended landmarks. *Journal of Experimental Biology*, 205(16):2499–2509.

Graham, P., Philippides, A., and Baddeley, B. (2010). Animal cognition: Multi-modal interactions in ant learning. *Current Biology*, 20(15):R639–R640.

Gronenberg, W. (2001). Subdivisions of hymenopteran mushroom body calyces by their afferent supply. *Journal of Comparative Neurology*, 435(4):474–489.

Gronenberg, W. (2008). Structure and function of ant (hymenoptera: Formicidae) brains: strength in numbers. *Myrmecological News*, 11:25–36.

Gronenberg, W. and Hölldobler, B. (1999). Morphologic representation of visual and antennal information in the ant brain. *Journal of Comparative Neurology*, 412(2):229–240.

Hafner, V. V. (2001). Adaptive homing—robotic exploration tours. *Adaptive Behavior*, 9(3-4):131–141.

Harris, R. A., de Ibarra, N. H., Graham, P., and Collett, T. S. (2005). Ant navigation: Priming of visual route memories. *Nature*, 438(7066):302–302.

Harrison, J. F., Fewell, J. H., Stiller, T. M., and Breed, M. D. (1989). Effects of experience on use of orientation cues in the giant tropical ant. *Animal behaviour*, 37:869–871.

Hassenstein, B. and Reichardt, W. (1956). Systemtheoretische analyse der zeit-, reihenfolgen-und vorzeichenauswertung bei der bewegungsperzeption des rüsselkäfers chlorophanus. *Zeitschrift für Naturforschung B*, 11(9-10):513–524.

Heinze, S. and Homberg, U. (2007). Maplike representation of celestial e-vector orientations in the brain of an insect. *Science*, 315(5814):995–997.

Heisenberg, M. (2003). Mushroom body memoir: from maps to models. *Nature Reviews Neuroscience*, 4(4):266–275.

Heusser, D. and Wehner, R. (2002). The visual centring response in desert ants, cataglyphis fortis. *Journal of experimental biology*, 205(5):585–590.

Higgins, C. M., Douglass, J. K., and Strausfeld, N. J. (2004). The computational basis of an identified neuronal circuit for elementary motion detection in dipterous insects. *Visual Neuroscience*, 21(04):567–586.

Honegger, K. S., Campbell, R. A., and Turner, G. C. (2011). Cellular-resolution population imaging reveals robust sparse coding in the drosophila mushroom body. *The Journal of Neuroscience*, 31(33):11772–11785.

Hourcade, B., Muenz, T. S., Sandoz, J.-C., Rössler, W., and Devaud, J.-M. (2010). Long-term memory leads to synaptic reorganization in the mushroom bodies: a memory trace in the insect brain? *The Journal of Neuroscience*, 30(18):6461–6465.

Huber, R. and Knaden, M. (2015). Egocentric and geocentric navigation during extremely long foraging paths of desert ants. *Journal of Comparative Physiology A*, 201(6):609–616.

Huerta, R. and Nowotny, T. (2009). Fast and robust learning by reinforcement signals: explorations in the insect brain. *Neural computation*, 21(8):2123–2151.

Izhikevich, E. M. (2003). Simple model of spiking neurons. *IEEE Transactions on neural networks*, 14(6):1569–1572.

Izhikevich, E. M. (2004). Which model to use for cortical spiking neurons? *IEEE transactions on neural networks*, 15(5):1063–1070.

Izhikevich, E. M. (2007). Solving the distal reward problem through linkage of stdp and dopamine signaling. *Cerebral cortex*, 17(10):2443–2452.

Jayatilaka, P., Raderschall, C., Zeil, J., and Narendra, A. (2013). Learning to forage: the learning walks of australian jack jumper ants. In *Front. Physiol. Conf. Abstract: Int. Conf. Invertebrate Vision*.

Jayatilaka, P., Raderschall, C. A., Narendra, A., and Zeil, J. (2014). Individual foraging patterns of the jack jumper ant Myrmecia croslandi (Hymenoptera: Formicidae). *Myrmecol. News*, 19:75–83.

Jayatilaka, P. W. A. (2014). *Individual foraging careers of the Jack Jumper ant, Myrmecia croslandi*. PhD thesis, The Australian National University.

Joesch, M., Schnell, B., Raghu, S. V., Reiff, D. F., and Borst, A. (2010). On and off pathways in drosophila motion vision. *Nature*, 468(7321):300–304.

Judd, S. and Collett, T. (1998). Multiple stored views and landmark guidance in ants. *Nature*, 392(6677):710–714.

Kaspari, M. and Weiser, M. (1999). The size–grain hypothesis and interspecific scaling in ants. *Functional Ecology*, 13(4):530–538.

Kien, J. and Menzel, R. (1977). Chromatic properties of interneurons in the optic lobes of the bee. *Journal of comparative physiology*, 113(1):17–34.

Knaden, M. and Wehner, R. (2006). Ant navigation: resetting the path integrator. *Journal of Experimental Biology*, 209(1):26–31.

Kodzhabashev, A. and Mangan, M. (2015). Route following without scanning. In *Biomimetic and Biohybrid Systems*, pages 199–210. Springer.

Kohler, M. and Wehner, R. (2005). Idiosyncratic route-based memories in desert ants, Melophorus bagoti: how do they interact with path-integration vectors? *Neurobiology of Learning and Memory*, 83(1):1–12.

Krapp, H. G., Hengstenberg, B., and Hengstenberg, R. (1998). Dendritic structure and receptive-field organization of optic flow processing interneurons in the fly. *Journal of Neurophysiology*, 79(4):1902–1917.

Kretz, R. (1979). A behavioural analysis of colour vision in the antcataglyphis bicolor (formicidae, hymenoptera). *Journal of comparative physiology*, 131(3):217–233.

Kühn-Bühlmann, S. and Wehner, R. (2006). Age-dependent and task-related volume changes in the mushroom bodies of visually guided desert ants, cataglyphis bicolor. *Journal of neurobiology*, 66(6):511–521.

Labhart, T. (1986). The electrophysiology of photoreceptors in different eye regions of the desert ant, cataglyphis bicolor. *Journal of Comparative Physiology A: Neuroethology, Sensory, Neural, and Behavioral Physiology*, 158(1):1–7.

Lambrinos, D., Möller, R., Labhart, T., Pfeifer, R., and Wehner, R. (2000). A mobile robot employing insect strategies for navigation. *Robotics and Autonomous systems*, 30(1):39–64.

Land, M. F. (1997). Visual acuity in insects. *Annual review of entomology*, 42(1):147–177.

Land, M. F. and Nilsson, D.-E. (2012). *Animal eyes*. Oxford University Press.

Laughlin, S. (1981). A simple coding procedure enhances a neuron's information capacity. *Zeitschrift für Naturforschung c*, 36(9-10):910–912.

Laurent, G. (2002). Olfactory network dynamics and the coding of multidimensional signals. *Nature reviews neuroscience*, 3(11):884–895.

Legge, E. L., Spetch, M. L., and Cheng, K. (2010). Not using the obvious: desert ants, melophorus bagoti, learn local vectors but not beacons in an arena. *Animal cognition*, 13(6):849–860.

Legge, E. L., Wystrach, A., Spetch, M. L., and Cheng, K. (2014). Combining sky and earth: desert ants (melophorus bagoti) show weighted integration of celestial and terrestrial cues. *Journal of Experimental Biology*, 217(23):4159–4166.

Lehrer, M., Srinivasan, M. V., Zhang, S.-W., and Horridge, G. A. (1988). Motion cues provide the bee's visual world with a third dimension. *Nature*, 332(6162):356–357.

Lent, D. D., Graham, P., and Collett, T. S. (2009). A motor component to the memories of habitual foraging routes in wood ants? *Current Biology*, 19(2):115–121.

Lent, D. D., Graham, P., and Collett, T. S. (2010). Image-matching during ant navigation occurs through saccade-like body turns controlled by learned visual features. *Proceedings of the National Academy of Sciences*, 107(37):16348–16353.

Lima, S. L. and Zollner, P. A. (1996). Towards a behavioral ecology of ecological landscapes. *Trends in Ecology & Evolution*, 11(3):131–135.

Liu, G., Seiler, H., Wen, A., Zars, T., Ito, K., Wolf, R., Heisenberg, M., and Liu, L. (2006). Distinct memory traces for two visual features in the drosophila brain. *Nature*, 439(7076):551–556.

Liu, L., Wolf, R., Ernst, R., and Heisenberg, M. (1999). Context generalization in drosophila visual learning requires the mushroom bodies. *Nature*, 400(6746):753–756.

Lulham, A., Bogacz, R., Vogt, S., and Brown, M. W. (2011). An infomax algorithm can perform both familiarity discrimination and feature extraction in a single network. *Neural computation*, 23(4):909–926.

Lutz, C. C. and Robinson, G. E. (2013). Activity-dependent gene expression in honey bee mushroom bodies in response to orientation flight. *Journal of Experimental Biology*, 216(11):2031–2038.

Mangan, M. (2011). *Visual homing in field crickets and desert ants: A comparative behavioural and modelling study*. PhD thesis, The University of Edinburgh.

Mangan, M. and Webb, B. (2009). Modelling place memory in crickets. *Biological Cybernetics*, 101(4):307–323.

Mangan, M. and Webb, B. (2012). Spontaneous formation of multiple routes in individual desert ants (Cataglyphis velox). *Behavioral Ecology*, 23(5):944–954.

Matin, L. (1968). Critical duration, the differential luminance threshold, critical flicker frequency, and visual adaptation: A theoretical treatment. *JOSA*, 58(3):404–415.

Menzel, R. (2012). The honeybee as a model for understanding the basis of cognition. *Nature Reviews Neuroscience*, 13(11):758–768.

Menzel, R. and Greggers, U. (2015). The memory structure of navigation in honeybees. *Journal of Comparative Physiology A*, 201(6):547–561.

Menzel, R., Greggers, U., Smith, A., Berger, S., Brandt, R., Brunke, S., Bundrock, G., Hülse, S., Plümpe, T., Schaupp, F., et al. (2005). Honey bees navigate according to a map-like spatial memory. *Proceedings of the National Academy of Sciences of the United States of America*, 102(8):3040–3045.

Menzel, R. and Manz, G. (2005). Neural plasticity of mushroom body-extrinsic neurons in the honeybee brain. *Journal of Experimental Biology*, 208(22):4317–4332.

Merkle, T., Knaden, M., and Wehner, R. (2006). Uncertainty about nest position influences systematic search strategies in desert ants. *Journal of Experimental Biology*, 209(18):3545–3549.

Mizunami, M., Weibrecht, J. M., and Strausfeld, N. J. (1998). Mushroom bodies of the cockroach: their participation in place memory. *Journal of Comparative Neurology*, 402(4):520–537.

Moll, K., Roces, F., and Federle, W. (2010). Foraging grass-cutting ants (atta vollenweideri) maintain stability by balancing their loads with controlled head movements. *Journal of Comparative Physiology A*, 196(7):471–480.

Möller, R. (2001). Do insects use templates or parameters for landmark navigation? *Journal of Theoretical Biology*, 210(1):33–45.

Möller, R. (2002). Insects could exploit uv–green contrast for landmark navigation. *Journal of theoretical biology*, 214(4):619–631.

Möller, R. (2012). A model of ant navigation based on visual prediction. *Journal of Theoretical Biology*, 305:118–130.

Möller, R., Lambrinos, D., Roggendorf, T., Pfeifer, R., and Wehner, R. (2001). Insect strategies of visual homing in mobile robots. In *Proceedings of the Computer Vision and Mobile Robotics Workshop CVMR*, volume 98.

Möller, R. and Vardy, A. (2006). Local visual homing by matched-filter descent in image distances. *Biological Cybernetics*, 95(5):413–430.

Mote, M. I. and Wehner, R. (1980). Functional characteristics of photoreceptors in the compound eye and ocellus of the desert ant, cataglyphis bicolor. *Journal of comparative physiology*, 137(1):63–71.

Müller, M. and Wehner, R. (1988). Path integration in desert ants, Cataglyphis fortis. *Proceedings of the National Academy of Sciences*, 85(14):5287–5290.

Müller, M. and Wehner, R. (1994). The hidden spiral: systematic search and path integration in desert ants, cataglyphis fortis. *Journal of Comparative Physiology A*, 175(5):525–530.

Müller, M. and Wehner, R. (2007). Wind and sky as compass cues in desert ant navigation. *Naturwissenschaften*, 94(7):589–594.

Müller, M. and Wehner, R. (2010). Path integration provides a scaffold for landmark learning in desert ants. *Current Biology*, 20(15):1368–1371.

Nachtigall, W. and Roth, W. (1983). Correlations between stationary measurable parameters of wing movement and aerodynamic force production in the blowfly (calliphora vicina r.-d.). *Journal of comparative physiology*, 150(2):251–260.

Nalbach, H.-O. (1989). Three temporal frequency channels constitute the dynamics of the optokinetic system of the crab, carcinus maenas (l.). *Biological Cybernetics*, 61(1):59–70.

Narendra, A. (2007a). Homing strategies of the australian desert ant melophorus bagoti i. proportional path-integration takes the ant half-way home. *Journal of Experimental Biology*, 210(10):1798–1803.

Narendra, A. (2007b). Homing strategies of the australian desert ant melophorus bagoti ii. interaction of the path integrator with visual cue information. *Journal of Experimental Biology*, 210(10):1804–1812.

Narendra, A., Gourmaud, S., and Zeil, J. (2013). Mapping the navigational knowledge of individually foraging ants, Myrmecia croslandi. *Proceedings of the Royal Society of London B: Biological Sciences*, 280(1765):20130683.

Narendra, A., Reid, S. F., Greiner, B., Peters, R. A., Hemmi, J. M., Ribi, W. A., and Zeil, J. (2010). Caste-specific visual adaptations to distinct daily activity schedules in australian myrmecia ants. *Proceedings of the Royal Society of London B: Biological Sciences*, page rspb20101378.

Narendra, A., Si, A., Sulikowski, D., and Cheng, K. (2007). Learning, retention and coding of nest-associated visual cues by the australian desert ant, Melophorus bagoti. *Behavioral Ecology and Sociobiology*, 61(10):1543–1553.

Nicholson, D., Judd, S., Cartwright, B., and Collett, T. (1999). Learning walks and landmark guidance in wood ants (Formica rufa). *Journal of Experimental Biology*, 202(13):1831–1838.

O'Carroll, D. C. and Warrant, E. J. (2011). Computational models for spatiotemporal filtering strategies in insect motion vision at low light levels. In *Intelligent Sensors, Sensor Networks and Information Processing (ISSNIP), 2011 Seventh International Conference on*, pages 119–124. IEEE.

Ofstad, T. A., Zuker, C. S., and Reiser, M. B. (2011). Visual place learning in drosophila melanogaster. *Nature*, 474(7350):204–207.

Olberg, R. M. (2012). Visual control of prey-capture flight in dragonflies. *Current opinion in neurobiology*, 22(2):267–271.

Olshausen, B. A. et al. (1996). Emergence of simple-cell receptive field properties by learning a sparse code for natural images. *Nature*, 381(6583):607–609.

Pamir, E., Chakroborty, N. K., Stollhoff, N., Gehring, K. B., Antemann, V., Morgenstern, L., Felsenberg, J., Eisenhardt, D., Menzel, R., and Nawrot, M. P. (2011). Average group behavior does not represent individual behavior in classical conditioning of the honeybee. *Learning & Memory*, 18(11):733–741.

Paulk, A. C., Dacks, A. M., Phillips-Portillo, J., Fellous, J.-M., and Gronenberg, W. (2009). Visual processing in the central bee brain. *The Journal of Neuroscience*, 29(32):9987–9999.

Perez-Orive, J., Mazor, O., Turner, G. C., Cassenaer, S., Wilson, R. I., and Laurent, G. (2002). Oscillations and sparsening of odor representations in the mushroom body. *Science*, 297(5580):359–365.

Pfeffer, S. E. and Wittlinger, M. (2016). How to find home backwards? navigation during rearward homing of cataglyphis fortis desert ants. *Journal of Experimental Biology*, 219(14):2119–2126.

Philippides, A., Baddeley, B., Cheng, K., and Graham, P. (2011). How might ants use panoramic views for route navigation? *The Journal of Experimental Biology*, 214(3):445–451.

Postlethwaite, C. M., Brown, P., and Dennis, T. E. (2013). A new multi-scale measure for analysing animal movement data. *Journal of theoretical biology*, 317:175–185.

Raderschall, C., Narendra, A., and Zeil, J. (2014). Balancing act: Head stabilisation in myrmecia ants during twilight. In *17th Congress of the International Union for the Study of Social Insects (IUSSI)*. IUSSI.

Raderschall, C. A., Narendra, A., and Zeil, J. (2016). Head roll stabilisation in the nocturnal bull ant myrmecia pyriformis: implications for visual navigation. *Journal of Experimental Biology*, 219(10):1449–1457.

Rao, R. P. and Fuentes, O. (1998). Hierarchical learning of navigational behaviors in an autonomous robot using a predictive sparse distributed memory. *Autonomous Robots*, 5(3-4):297–316.

Reid, S. F., Narendra, A., Hemmi, J. M., and Zeil, J. (2011). Polarised skylight and the landmark panorama provide night-active bull ants with compass information during route following. *The Journal of experimental biology*, 214(3):363–370.

Reinhardt, L. and Blickhan, R. (2014). Ultra-miniature force plate for measuring triaxial forces in the micronewton range. *Journal of Experimental Biology*, 217(5):704–710.

Ronacher, B. (2008). Path integration as the basic navigation mechanism of the desert ant cataglyphis fortis (forel, 1902)(hymenoptera: Formicidae). *Myrmecological News*, 11:53–62.

Ronacher, B. and Wehner, R. (1995). Desert ants cataglyphis fortis use self-induced optic flow to measure distances travelled. *Journal of Comparative Physiology A*, 177(1):21–27.

Ronacher, B., Westwig, E., and Wehner, R. (2006). Integrating two-dimensional paths: do desert ants process distance information in the absence of celestial compass cues? *Journal of Experimental Biology*, 209(17):3301–3308.

Rouder, J. N., Speckman, P. L., Sun, D., Morey, R. D., and Iverson, G. (2009). Bayesian t tests for accepting and rejecting the null hypothesis. *Psychonomic bulletin & review*, 16(2):225–237.

Russakoff, D. B., Tomasi, C., Rohlfing, T., and Maurer Jr, C. R. (2004). Image similarity using mutual information of regions. In *European Conference on Computer Vision*, pages 596–607. Springer.

Schöne, H. (1996). Optokinetic speed control and estimation of travel distance in walking honeybees. *Journal of Comparative Physiology A*, 179(4):587–592.

Schultheiss, P. and Cheng, K. (2011). Finding the nest: inbound searching behaviour in the australian desert ant, melophorus bagoti. *Animal behaviour*, 81(5):1031–1038.

Schultheiss, P. and Nooten, S. S. (2013). Foraging patterns and strategies in an australian desert ant. *Austral Ecology*, 38(8):942–951.

Schultheiss, P., Stannard, T., Pereira, S., Reynolds, A. M., Wehner, R., and Cheng, K. (2016a). Similarities and differences in path integration and search in two species of desert ants inhabiting a visually rich and a visually barren habitat. *Behavioral Ecology and Sociobiology*, pages 1–11.

Schultheiss, P., Wystrach, A., Legge, E. L., and Cheng, K. (2013). Information content of visual scenes influences systematic search of desert ants. *Journal of Experimental Biology*, 216(4):742–749.

Schultheiss, P., Wystrach, A., Schwarz, S., Tack, A., Delor, J., Nooten, S. S., Bibost, A.-L., Freas, C. A., and Cheng, K. (2016b). Crucial role of ultraviolet light for desert ants in determining direction from the terrestrial panorama. *Animal Behaviour*, 115:19–28.

Schwarz, S., Albert, L., Wystrach, A., and Cheng, K. (2011a). Ocelli contribute to the encoding of celestial compass information in the australian desert ant melophorus bagoti. *Journal of Experimental Biology*, 214(6):901–906.

Schwarz, S., Narendra, A., and Zeil, J. (2011b). The properties of the visual system in the australian desert ant melophorus bagoti. *Arthropod Structure & Development*, 40(2):128–134.

Seelig, J. D. and Jayaraman, V. (2015). Neural dynamics for landmark orientation and angular path integration. *Nature*, 521(7551):186–191.

Seidl, T. and Wehner, R. (2006). Visual and tactile learning of ground structures in desert ants. *Journal of Experimental Biology*, 209(17):3336–3344.

Seidl, T. and Wehner, R. (2008). Walking on inclines: how do desert ants monitor slope and step length. *Frontiers in zoology*, 5(1):1.

Smith, L., Philippides, A., Graham, P., Baddeley, B., and Husbands, P. (2007). Linked local navigation for visual route guidance. *Adaptive Behavior*, 15(3):257–271.

Srinivasan, M. V. and Gregory, R. (1992). How bees exploit optic flow: behavioural experiments and neural models [and discussion]. *Philosophical Transactions of the Royal Society of London B: Biological Sciences*, 337(1281):253–259.

Stavenga, D. (2003). Angular and spectral sensitivity of fly photoreceptors. i. integrated facet lens and rhabdomere optics. *Journal of Comparative Physiology A*, 189(1):1–17.

Steck, K. (2012). Just follow your nose: homing by olfactory cues in ants. *Current opinion in neurobiology*, 22(2):231–235.

Steck, K., Knaden, M., and Hansson, B. S. (2010). Do desert ants smell the scenery in stereo? *Animal Behaviour*, 79(4):939–945.

Steck, K., Wittlinger, M., and Wolf, H. (2009). Estimation of homing distance in desert ants, cataglyphis fortis, remains unaffected by disturbance of walking behaviour. *Journal of Experimental Biology*, 212(18):2893–2901.

Stieb, S. M., Muenz, T. S., Wehner, R., and Rössler, W. (2010). Visual experience and age affect synaptic organization in the mushroom bodies of the desert ant cataglyphis fortis. *Developmental neurobiology*, 70(6):408–423.

Stone, T., Differt, D., Milford, M., and Webb, B. (2016). Skyline-based localisation for aggressively manoeuvring robots using uv sensors and spherical harmonics. In *2016 IEEE International Conference on Robotics and Automation (ICRA)*, pages 5615–5622. IEEE.

Stone, T., Mangan, M., Ardin, P., and Webb, B. (2014). Sky segmentation with ultraviolet images can be used for navigation. In *Proceedings Robotics: Science and Systems*.

Strube-Bloss, M. F., Nawrot, M. P., and Menzel, R. (2011). Mushroom body output neurons encode odor–reward associations. *The Journal of neuroscience*, 31(8):3129–3140.

Stürzl, W., Cheung, A., Cheng, K., and Zeil, J. (2008). The information content of panoramic images i: The rotational errors and the similarity of views in rectangular experimental arenas. *Journal of Experimental Psychology: Animal Behavior Processes*, 34(1):1–14.

Stürzl, W., Grixa, I., Mair, E., Narendra, A., and Zeil, J. (2015). Three-dimensional models of natural environments and the mapping of navigational information. *Journal of Comparative Physiology A*, 201(6):563–584.

Stürzl, W. and Mallot, H. A. (2006). Efficient visual homing based on fourier transformed panoramic images. *Robotics and Autonomous Systems*, 54(4):300–313.

Stürzl, W. and Zeil, J. (2007). Depth, contrast and view-based homing in outdoor scenes. *Biological cybernetics*, 96(5):519–531.

Szyszka, P., Ditzen, M., Galkin, A., Galizia, C. G., and Menzel, R. (2005). Sparsening and temporal sharpening of olfactory representations in the honeybee mushroom bodies. *Journal of neurophysiology*, 94(5):3303–3313.

Szyszka, P., Galkin, A., and Menzel, R. (2008). Associative and non-associative plasticity in kenyon cells of the honeybee mushroom body. *Frontiers in systems neuroscience*, 2:3.

Takemura, S.-Y., Lu, Z., and Meinertzhagen, I. A. (2008). Synaptic circuits of the drosophila optic lobe: the input terminals to the medulla. *Journal of Comparative Neurology*, 509(5):493–513.

Taylor, C. P. (1981). Contribution of compound eyes and ocelli to steering of locusts in flight: I. behavioural analysis. *Journal of Experimental Biology*, 93(1):1–18.

Tsodyks, M. (1990). Associative memory in neural networks with binary synapses. *Modern Physics Letters B*, 4(11):713–716.

Van Oudenhove, L., Boulay, R., Lenoir, A., Bernstein, C., and Cerda, X. (2012). Substrate temperature constrains recruitment and trail following behavior in ants. *Journal of chemical ecology*, 38(6):802–809.

Vardy, A. and Moller, R. (2005). Biologically plausible visual homing methods based on optical flow techniques. *Connection Science*, 17(1-2):47–89.

Vogt, K., Schnaitmann, C., Dylla, K. V., Knapek, S., Aso, Y., Rubin, G. M., and Tanimoto, H. (2014). Shared mushroom body circuits underlie visual and olfactory memories in drosophila. *Elife*, 3:e02395.

Von Frisch, K. (1967). *The dance language and orientation of bees.* Harvard University Press.

Wang, J. W., Wong, A. M., Flores, J., Vosshall, L. B., and Axel, R. (2003). Two-photon calcium imaging reveals an odor-evoked map of activity in the fly brain. *Cell*, 112(2):271–282.

Webb, B. (2002). Robots in invertebrate neuroscience. *Nature*, 417(6886):359–363.

Webb, B. and Wystrach, A. (2016). Neural mechanisms of insect navigation. *Current Opinion in Insect Science*, 15:27–39.

Wehner, R. (2003). Desert ant navigation: how miniature brains solve complex tasks. *Journal of Comparative Physiology A*, 189(8):579–588.

Wehner, R. (2009). The architecture of the desert ants navigational toolkit (hymenoptera: Formicidae). *Myrmecol News*, 12:85–96.

Wehner, R., Boyer, M., Loertscher, F., Sommer, S., and Menzi, U. (2006). Ant navigation: one-way routes rather than maps. *Current Biology*, 16(1):75–79.

Wehner, R., Cheng, K., Cruse, H., et al. (2014). Visual navigation strategies in insects: lessons from desert ants. *The new visual neurosciences. MIT Press, Cambridge*, pages 1153–1164.

Wehner, R., Marsh, A., and Wehner, S. (1992). Desert ants on a thermal tightrope. *Nature*, 357(6379):586–587.

Wehner, R., Michel, B., and Antonsen, P. (1996). Visual navigation in insects: coupling of egocentric and geocentric information. *The Journal of Experimental Biology*, 199(1):129–140.

Wehner, R. and Müller, M. (1985). Does interocular transfer occur in visual navigation by ants? *Nature*, 315:228–229.

Wehner, R. and Müller, M. (2010). Piloting in desert ants: pinpointing the goal by discrete landmarks. *Journal of Experimental Biology*, 213(24):4174–4179.

Wehner, R. and Räber, F. (1979). Visual spatial memory in desert ants, Cataglyphis bicolor (Hymenoptera: Formicidae). *Experientia*, 35(12):1569–1571.

Weihmann, T. and Blickhan, R. (2009). Comparing inclined locomotion in a ground-living and a climbing ant species: sagittal plane kinematics. *Journal of comparative physiology A*, 195(11):1011–1020.

Wessnitzer, J., Young, J. M., Armstrong, J. D., and Webb, B. (2012). A model of non-elemental olfactory learning in drosophila. *Journal of computational neuroscience*, 32(2):197–212.

Wiens, J. A., Crist, T. O., With, K. A., and Milne, B. T. (1995). Fractal patterns of insect movement in microlandscape mosaics. *Ecology*, 76(2):663–666.

Willshaw, D. J., Buneman, O. P., and Longuet-Higgins, H. C. (1969). Non-holographic associative memory. *Nature*.

With, K. A. (1994). Using fractal analysis to assess how species perceive landscape structure. *Landscape Ecology*, 9:25–36.

Withers, G., Fahrbach, S., and Robinson, G. (1995). Effects of experience and juvenile hormone on the organization of the mushroom bodies of honey bees. *Journal of neurobiology*, 26(1):130–144.

Wittlinger, M., Wehner, R., and Wolf, H. (2006). The ant odometer: stepping on stilts and stumps. *Science*, 312(5782):1965–1967.

Wittlinger, M., Wehner, R., and Wolf, H. (2007). The desert ant odometer: a stride integrator that accounts for stride length and walking speed. *Journal of experimental Biology*, 210(2):198–207.

Wittlinger, M. and Wolf, H. (2013). Homing distance in desert ants, cataglyphis fortis, remains unaffected by disturbance of walking behaviour and visual input. *Journal of Physiology-Paris*, 107(1):130–136.

Wohlgemuth, S., Ronacher, B., and Wehner, R. (2002). Distance estimation in the third dimension in desert ants. *Journal of Comparative Physiology A*, 188(4):273–281.

Wolf, H. and Wehner, R. (2000). Pinpointing food sources: olfactory and anemotactic orientation in desert ants, cataglyphis fortis. *Journal of Experimental Biology*, 203(5):857–868.

Wystrach, A., Beugnon, G., and Cheng, K. (2011a). Landmarks or panoramas: what do navigating ants attend to for guidance? *Frontiers in zoology*, 8(1):1.

Wystrach, A., Beugnon, G., and Cheng, K. (2012). Ants might use different view-matching strategies on and off the route. *The Journal of Experimental Biology*, 215(1):44–55.

Wystrach, A., Dewar, A., Philippides, A., and Graham, P. (2016). How do field of view and resolution affect the information content of panoramic scenes for visual navigation? a computational investigation. *Journal of Comparative Physiology A*, 202(2):87–95.

Wystrach, A. and Graham, P. (2012). What can we learn from studies of insect navigation? *Animal Behaviour*, 84(1):13–20.

Wystrach, A., Mangan, M., Philippides, A., and Graham, P. (2013a). Snapshots in ants? new interpretations of paradigmatic experiments. *The Journal of Experimental Biology*, 216(10):1766–1770.

Wystrach, A., Mangan, M., and Webb, B. (2015). Optimal cue integration in ants. In *Proc. R. Soc. B*, volume 282, page 20151484. The Royal Society.

Wystrach, A., Philippides, A., Aurejac, A., Cheng, K., and Graham, P. (2014). Visual scanning behaviours and their role in the navigation of the australian desert ant Melophorus bagoti. *Journal of Comparative Physiology A*, 200(7):615–626.

Wystrach, A. and Schwarz, S. (2013). Ants use a predictive mechanism to compensate for passive displacements by wind. *Current Biology*, 23(24):R1083–R1085.

Wystrach, A., Schwarz, S., Baniel, A., and Cheng, K. (2013b). Backtracking behaviour in lost ants: an additional strategy in their navigational toolkit. *Proceedings of the Royal Society of London B: Biological Sciences*, 280(1769):20131677.

Wystrach, A., Schwarz, S., Schultheiss, P., Beugnon, G., and Cheng, K. (2011b). Views, landmarks, and routes: how do desert ants negotiate an obstacle course? *Journal of Comparative Physiology A*, 197(2):167–179.

Zeil, J. (2012). Visual homing: an insect perspective. *Current Opinion in Neurobiology*, 22(2):285–293.

Zeil, J., Hofmann, M. I., and Chahl, J. S. (2003). Catchment areas of panoramic snapshots in outdoor scenes. *JOSA A*, 20(3):450–469.

Zeil, J., Narendra, A., and Stürzl, W. (2014). Looking and homing: how displaced ants decide where to go. *Philosophical Transactions of the Royal Society B: Biological Sciences*, 369(1636):20130034.

Zollikofer, C., Wehner, R., and Fukushi, T. (1995). Optical scaling in conspecific cataglyphis ants. *Journal of Experimental Biology*, 198(8):1637–1646.